# EFFECTS OF CHOLINERGIC RECEPTOR NICOTINIC ALPHA 5 (CHRNA5) RNAi ON APOPTOSIS, DNA DAMAGE RESPONSE, DRUG SENSITIVITY, AND HSA-MIR-495-3P OVEREXPRESSION IN BREAST CANCER

**A DISSERTATION SUBMITTED TO**

**THE GRADUATE SCHOOL OF ENGINEERING AND SCIENCE**

**OF BILKENT UNIVERSITY**

**IN PARTIAL FULFILLMENT OF THE REQUIREMENTS**

**FOR THE DEGREE OF**

**DOCTOR OF PHILOSOPHY**

**IN MOLECULAR BIOLOGY AND GENETICS**

**By**

**ŞAHİKA CINGIR KÖKER**

**December, 2018**

EFFECTS OF CHOLINERGIC RECEPTOR NICOTINIC ALPHA 5 (CHRNA5) RNAi ON APOPTOSIS, DNA DAMAGE RESPONSE, DRUG SENSITIVITY, AND HSA-MIR-495-3P OVEREXPRESSION IN BREAST CANCER

By Şahika Cıngır Köker
December, 2018

We certify that we have read this dissertation and that in our opinion it is fully adequate, in scope and in quality, as a thesis for the degree of Doctor of Philosophy.

_____

Özlen Konu Karakayalı (Advisor)

_____

Ayşe Elif Erson Bensan

_____

Özgür Şahin

_____

Işık Yuluğ

_____

Sreeparna Banerjee

Approved for the Graduate School of Engineering and Science:

_____

Ezhan Karaşan

**Director of the Graduate School**

# ABSTRACT

## EFFECTS OF CHOLINERGIC RECEPTOR NICOTINIC ALPHA 5 (CHRNA5) RNAi ON APOPTOSIS, DNA DAMAGE RESPONSE, DRUG SENSITIVITY, AND HSA-MIR-495-3P OVEREXPRESSION IN BREAST CANCER

**Şahika Cıngır Köker**

**Ph.D. in Molecular Biology and Genetics**

**Supervisor: Özlen Konu Karakayalı**

**December 2018**

Cholinergic Receptor Nicotinic Alpha 5 (CHRNA5) is associated with nicotine addiction and it has an important role in the prognosis of lung cancer. Despite its important cellular functions, its role in breast cancer remains to be elucidated. In this thesis, I aimed to identify the alterations in the important cancer signaling pathways occurring upon CHRNA5 depletion.

Drug resistance is one of the major obstacles in breast cancer therapy. Heterogeneous nature of breast cancer necessitates identification of more biomarkers which aid in precise diagnosis and hence development of proper treatment options. In this study, by using more than one cell line which is representative of different subtypes of breast cancer, I showed the alterations occurred in cancer signaling pathways such as cell cycle and apoptosis upon CHRNA5 depletion, which could serve as a novel biomarker in breast cancer subtyping. Depending on mutation status of TP53, which is the gatekeeper protein during G1/S checkpoint, CHRNA5 depletion mostly exerted its effects over decreasing the levels of total CHEK1 and pCHEK1 (S345) which significantly altered the response of MCF7 cells to topoisomerase inhibitors in terms of enhanced drug sensitivity. Increases in apoptotic markers, such as BAX/BCL2 ratio along with increased FAS levels, further confirmed that this sensitization of MCF7 cells upon CHRNA5 depletion might have ended with apoptosis.

So far in the literature, there is no study examining the regulation of CHRNA5 by small endogenous molecules such as miRNAs. Due to the predictive binding sites in 3'UTR of CHRNA5 and the importance of participating in tamoxifen resistance in breast cancer; I also examined the interplay between miR-15a family and CHRNA5 in MCF7 cells. I showed significant decrease in CHRNA5 levels upon using miR-15a mimic while demonstrating similar activity of miR-15a family mimics with CHRNA5 depletion using RT-qPCR.

Another important implication of CHRNA5 depletion in MCF7 cells was the global change in miRNA expression prolife which was verified with independent microRNA arrays. Based on these *in silico* results, hsa-miR-495-3p appeared as the most downregulated miRNA which is known as a tumor suppressor miRNA. As stated in the literature, the role of miR-495 differs depending on the tumor type. Therefore, I tried to restore its expression by mimicking along with CHRNA5 depletion. The transcriptomic changes observed with CHRNA5 depletion was boosted with the restoration of miR-495 levels.

**Keywords:** Breast cancer, cholinergic signaling, CHRNA5, RNAi, DNA damage, drug sensitivity, apoptosis, microRNAs

# ÖZET

## KOLİNERJİK RESEPTÖR NİKOTİNİK ALFA 5 (CHRNA5) RNAi UYGULAMASININ, MEME KANSERİNDE APOPTOZ, DNA HASARI YANITI, İLAÇ DUYARLILIĞI VE HSA-MIR-495-3P'NİN YÜKSEK İFADESİNE ETKİSİ

**Şahika Cıngır Köker**

**Moleküler Biyoloji ve Genetik Doktora Programı**

**Tez Danışmanı: Özlen Konu Karakayalı**

**Aralık 2018**

Kolinerjik Reseptör Nikotinik Alfa 5 (CHRNA5), nikotin bağımlılığıyla ilişkilidir ve akciğer kanseri prognozunda önemli bir role sahiptir. Önemli hücresel işlevlerine rağmen, bu molekülün meme kanserindeki rolü henüz bilinmemektedir. Bu tezde, CHRNA5 deplesyonu yapıldığında önemli kanser sinyal yolaklarında meydana gelen değişikliklerin belirlenmesini amaçladım.

İlaca karşı direnç, meme kanseri tedavisi önündeki en büyük engellerden biridir. Meme kanserinin heterojen doğası, kesin tanı konulmasına ve dolayısıyla doğru tedavi seçeneklerinin belirlenmesine yardımcı olabilecek daha çok biyobelirtecin bulunmasını gerektirmektedir. Bu çalışmada, meme kanserinin farklı alt tiplerini temsilen birden fazla hücre hattı kullanarak, meme kanseri alt tiplerinin ortaya çıkarılmasında yeni bir biyobelirteç görevi görebilecek olan CHRNA5'in deplesyonu yapıldığında hücre döngüsü ve apoptoz gibi yaygın sinyal yolaklarında meydana gelen değişiklikleri gösterdim. Hücre döngüsünde G1/S noktasında denetleyici görevi gören TP53 proteinin mutasyon durumuna bağlı olarak, CHRNA5 deplesyonu, etkilerini ağırlıklı olarak hem total CHEK1 hem de pCHEK1 (S345) seviyelerinde azalmaya neden olarak göstermiş ve bu da, MCF7 hücrelerinin Topoizomeraz inhibitörlerine yanıtlarını önemli ölçüde değiştirerek ilaca duyarlılıkta artışa neden olmuştur. Artan FAS seviyelerinin yanında, BAX/BCL2 oranı gibi

apoptoz belirteçlerde de artış görülmesi, CHRNA5 deplesyonunu takiben MCF7 hücrelerinde gelişen duyarlılığın apoptozla sonuçlanabileceğini göstermiştir.

Literatürde şimdiye kadar miRNA'lar gibi küçük endojen moleküllerle CHRNA5 regülasyonunu inceleyen bir çalışma yapılmamıştır. CHRNA5'in 3'UTR'sindeki potansiyel miR-15a bağlanma bölgeleri ve miR-15a'nın meme kanserinde tamoksifen direncinde yer alması nedeniyle; bu çalışmada miR-15a ailesi ve CHRNA5 arasındaki etkileşimi MCF7 hücrelerinde araştırdım. RT-qPCR metodu ile, miR-15a mimikleri kullanarak CHRNA5 seviyesinde ciddi bir azalma gözlemledim, aynı şekilde bu aileye ait miRNA mimikleri ile de CHRNA5 RNAi'nin etkilerine de benzerlikler gözlemledim.

MCF7 hücrelerinde CHRNA5 deplesyonunun bir diğer önemli sonucu ise, bağımsız microRNA dizilimleriyle de doğrulanan, miRNA ifade profilindeki global değişikliklerdir. Bu in silico sonuçlara dayanarak, tümör baskılayıcı miRNA olarak bilinen hsa-miR-495-3p, ifadesi en çok azalan miRNA olarak belirlenmiştir. Literatürde de belirtildiği gibi, miR-495'in rolü tümörün türüne göre değişmektedir. Bu nedenle, CHRNA5 deplesyonunun yanında, miR-495'in ifadesini de mimik uygulaması ile eski seviyesine çıkarılmaya çalışılmıştır. CHRNA5 deplesyonu ile gözlemlenen transkriptomik değişiklikler, miR-495'in yüksek ifade edilmesiyle daha da arttırılmıştır.

**Anahtar Sözcükler:** Meme kanseri, kolinerjik sinyal yolağı, CHRNA5, RNAi, DNA hasarı, ilaç hassasiyeti, apoptoz, mikroRNAlar.

***To my precious family….***

## ACKNOWLEDGEMENTS

First and foremost, I would like to express my gratitude to my supervisor Assoc. Prof. Özlen Konu, not only for her guidance and scientific contributions throughout my PhD study but also for her patience and sincerity. Thanks to her tolerance, I succeeded to become a scientist and a mom at the same time. She always kept believing in me and never let me give up in any situation.

I would also like to express my deepest thanks to my committee members; Prof. Dr. Ayşe Elif Erson and Assist. Prof. Özgür Şahin for their fruitful discussions and for sharing their academic knowledge with me during my committee meetings. Moreover, I am very thankful to Assoc. Prof. Işık Yuluğ both for accepting to become my jury member and for providing me with her groups' bench and letting me use reagents/equipment and culture hood. I would like to also express my thanks to Prof. Dr. Sreerparna Baneerje for accepting to become my jury member and sharing the antibodies with us.

I would like to thank Prof. Dr. İhsan Gürsel and his group for helping me with PI staining and letting me use the tools in their lab whenever I needed. I also would like to thank Şahin group for sharing their knowledge and experiences.

Konu lab members have always been supportive especially during tough times. I would like to especially thank Ayşe Gökçe Keşküş, not only for her friendship, but also for her contributions to the manuscript. I am also thankful to her for her contributions to statistics study as well. Without her hard work, this task might last longer. I am also thankful to Ermira Jahja and Huma Shehwana for their great contributions to the manuscript. I also would like to thank Said Tiryaki for his nice friendship and his contributions to miRNA studies. Başak Özgürsoy and Mehtap Yılmaz Tezcan also contributed a lot to miRNA studies so I am also thankful to them. I am also thankful to the present members of Konu lab especially to Seniye and Damla for their support, help and friendships.

My sincere thanks go to past and present members of MBG family. Özge Saatçi has been a great friend and a collaborator; moreover, whenever I needed, she always helped me.

I was very lucky to have my dear friends Ece Akhan Güzelcan, Damla Gözen, Deniz Cansen Kahraman, Seçil Demirkol Canlı and Derya Cavga. They never stopped supporting me even there existed distances between us. I would like to also thank Eda Süer both for her scientific advices and for being such a cool friend.

I would also like to extend my appreciation to Pelin Makas and Seda Birkan. They made the lab environment as convenient as possible to support our work. They were also among the great friends that I have had in MBG. I would like to also thank Ümmühan Çolak and Abdullah Ünnü for their efforts to make our lives easier in the lab and also for their warm greeting every in the morning. I want to also thank Füsun Elvan and Yıldız Kahyaoğlu for their help whenever I asked them.

My greatest gratitude goes to Hande Mertoğlu. She was always more than a friend to me since METU years. She was always with me during my hard times and joyful moments. I would like extend my special thanks to one of my oldest friends, Esra Çopuroğlu. She was present in my life since my high school years, and she never stopped helping me in every condition.

Last but not the least; I would like to express my special thanks to my precious family. My mother, Ayşe Cıngır and my father Ramazan Cıngır, had never ever stop believing me and supporting me. It is their belief which made me determined to finish this study. I am very grateful and lucky for sharing my life with Yasin Köker. Not only during my PhD study, starting from my master's study, he kept supporting me and never let me down. I am very thankful for his unconditional love and support. My precious daughter Ayşe İdil Köker also deserved the greatest thanks due to her patience during my PhD study despite her age. Her presence made me stronger and forced me to accomplish my PhD study. My mother in love, Songül Köker and my father in love, Mürsel Köker greatly sacrificed their lives whenever I needed their help. I am also thankful to them. My sisters, Duygu Balkan and Selva Kaya have never stop believing and supporting me. They are always co-mother to me all the time. I owe many things to their presence.

I am also thankful to Bilkent University Department of Molecular Biology and Genetics for giving me support for obtaining a PhD degree. This work was supported by TÜBİTAK (The Scientific and Technological Research Council of Turkey) with the research grants (to OK) 111T316 (Results 3.1-3.8) and COST BM1406-114S367 (Results 3.9-3.15 and and Appendix A) from which I received PhD scholarships.

**CONTENTS**

List of Tables

# CHAPTER 1: INTRODUCTION

## 1.1 Breast cancer

### 1.1.1 General background of the disease and the breast tissue

Among women, breast cancer is the most common cancer type worldwide [1]. According to Cancer Statistics 2018 held in USA, out of 878.980 cancer cases, it is estimated that 266.120 of woman will be diagnosed with breast cancer which accounts for 30% of the top 10 cancer types in woman. Among diagnosed women, 40.920 estimated deaths will occur in 2018.

Apart from pediatric cancers, cancer is generally defined as the disease of the old [2]. Generally, without an obvious genetic background, sporadic cancers occur later in life [3], however the ones having a hereditary background may occur earlier in life implying the importance of genetic contribution [4].

Similar to the other types of cancer, due to its heterogeneous nature, breast cancer has varying prognoses and treatment options for breast cancer patients [1]. Prognosis of the cancer patients is important, since it estimates the risk of recurrence at early stages and also helps define the patients who could benefit from a specific therapy or not [5]. In the case of breast cancer, which exhibit high intra-tumor as well as inter-tumor heterogeneity [6], prognosis of a patient is highly dependent on the successful classification of the cancer subtype and hence proper therapy to be received.

The two main components of mammary gland are parenchyma, which performs the specific function of the organ, and the stroma, which is the connective tissue providing both the framework of the organ as well as the environment where parenchyma can work and grow [7]. The parenchyma is composed of alveoli, where milk is produced and stored, and the branching ducts from where the milk is carried to the nipples [8]. The branching ducts are composed of two types of cells, namely, inner bilayer epithelial cells where the

milk is produced, and the outer surrounding layer of myoepithelial cells, which contacts with basement membrane [9].

This relatively basic structure of the mammary gland actually has more complex order of cellular functions which appears during carcinogenesis leading to the high level of heterogeneity of breast cancers [10]. It is this intra- and inter-tumor heterogeneity of the breast tissue that can lead to many subtypes of this disease.

Breast cancer develops from normal tissue to invasive ductal carcinoma (IDC) with stepwise progression involving many genetic and epigenetic alterations (Figure1). This starts with over production of normal looking cells called hyperplasia which is then followed by atypical hyperplasia where the cells divide on top of each other and some of them have the necessary alterations to turn into a cancerous tissue [11]. Atypical hyperplasia is then followed by noninvasive ductal carcinoma *in situ* (DCIS). DCIS is known to be non-invasive, but it can vary between the low-grade and high-grade lesions that can have alterations for invasiveness leading to invasive ductal carcinoma (IDC) [2]. Although it is speculative whether DCIS is the necessary step for the invasive breast cancer progression or not, many invasive cancer lesions occur together with adjacent DCIS during diagnosis. Moreover, recently, similar genetic alterations were identified between DCIS and invasive breast cancer suggesting that DCIS may act as a precursor for the invasive breast cancer in the absence of intervention [12].

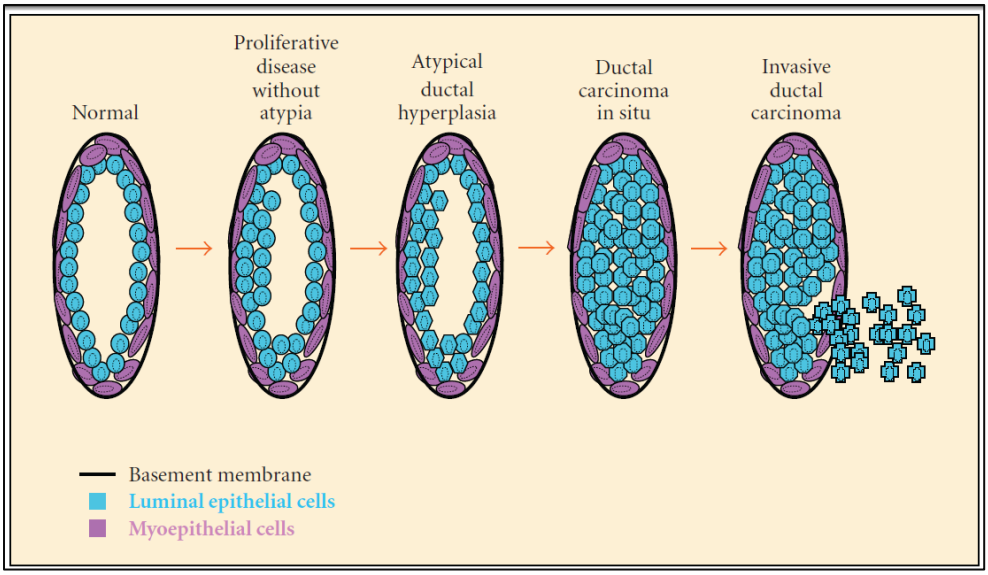


**Figure 1.1: Progression of invasive ductal carcinoma.** Progression of breast cancer tumorigenesis starting from epithelial hyperplasia to invasive ductal carcinoma. *Adapted from Myal Y. et al.,2010. Journal of Biomedicine and Biothecnology* [13].

### 1.1.2 Subtypes of breast cancer and current treatment strategies

The subtyping of breast cancer is important since it helps to determine the course of therapy as well as gives information about the tumor progression [10].

The histological and molecular characteristics of breast cancer lead to emergence of many subtypes of the disease. The traditional histopathological and immunochemical classification of breast cancer was recently replaced with molecular subtyping since it is based on gene expression profiling and hence has the potential to combine clinical outcome and disease mechanism by giving better prognosis [6]. Actually, as stated by Perez EA (2011), breast cancer is among the few types of cancers where the molecular subtyping works best and increases the rate of disease free survival with individualized targeted therapy [14].

Based on gene expression profiling of large patient cohorts, currently six molecular subtypes of breast cancer were identified as follows (Figure 1.2):

- *Luminal A* and *Luminal B Breast Cancers* are characterized by their ER positivity (ER+). Luminal A is the most common subtype and has a favorable prognosis among the other types of the breast cancers [15]. Together with ER positivity, Luminal B is also characterized by its Her2 overexpression [16], and hence the drugs such as trastuzumab which targets Her2 has increased the survival of this group of patients [17]. In addition to Her2 status, one of the major differences between these two subtypes is the expression pattern of the genes related with proliferation [18], [19]. In addition to the ER and Her2 status, Luminal A subtype of breast cancers express PR, whereas Luminal B type of breast cancers may or may not express PR. Compared to Luminal B breast cancers, Luminal A breast cancers give better prognosis [20] but altogether, these two subtypes of breast cancers still have better prognosis compared to the ER (-) subtype since they can respond to targeted anti-estrogen treatments like tamoxifen [2].

- *Her2+ Breast Cancers* are associated with their over expression of HER2/neu proliferation related genes. HER2 is one of the epidermal growth factor receptor family, and in cancers, it behaves as an oncogene [21]. Since this subtype is frequently negative for ER status, therapy does not include anti-estrogenic hormone therapy [2]. Despite these, Her2 (+) subtype of breast cancers have poorer prognosis compared to luminal ones [20], yet combined targeted therapies such as trastuzumab (anti-Her2 antibody) and lapatinib (tyrosine kinase inhibitor), improved the survival of these patients [22], [23].

- *Basal Like Breast Cancers* comprises 15% of invasive ductal carcinomas. Since this subtype of breast cancers shares high number of genes with basal epithelial cells, they are called as '*Basal like breast cancers'*. Since they do not express any of the ER, PR and Her2/neu receptors, they are so called 'Triple negative breast cancers' (TNBC) [5]. Since they are negative for all three receptors (which

could be otherwise targeted for either hormone or Her2 targeted therapy), and they also have high proliferation rate, they have very poor prognosis [20]. Most of the TNBC patients have mutations in BRCA1/2 gene which is one of the most important components of DNA repair machinery [24]. Therefore, using agents inducing DNA damage such as platinum for the treatment of TNBC patients is considered as an alternative treatment strategy [25].

- *Claudin-low Breast cancers* are associated with the high expression levels of the genes involved in epithelial to mesenchymal transition (EMT), stem cell related genes, and the ones associated with tumor initiation [26]. Patients with Claudin low breast cancers could be treated with chemotherapeutic agents however the prognosis is poor. Since they do not express hormone receptors and Her2, they are not sensitive to conventional chemotherapy [26].

- *Normal Like* breast cancers are so called since they reside closely to the normal breast epithelium based on microarray gene expression studies. They express ER and PR however do not express Her2 [27]. It is still speculative that whether this subtype of breast cancer represents a distinct subtype, or they are just outside of the other subtypes due to contamination of normal epithelium [27].

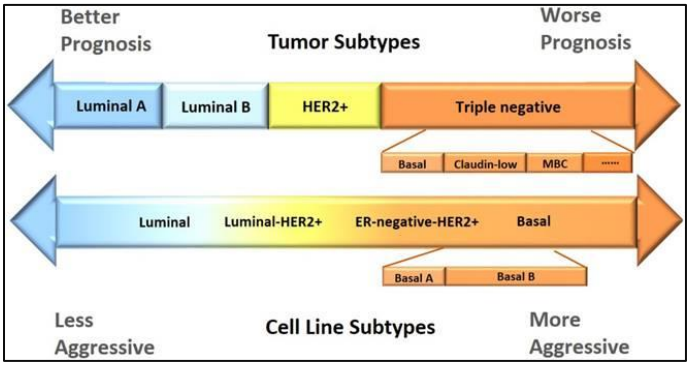


**Figure 1.2: Breast cancer subtypes.** The classification of breast cancer according to hormonal receptor status. Breast tumors and cell lines are compatible with each other. *Figure adapted from Dai X. et al., 2017. Journal of Cancer* [28].

## 1.2 Chemotherapy and drug resistance mechanisms in cancer

Chemotherapy constitutes one of the most important components of primary cancer treatment for both survival and better prognosis of the cancer patients [29]. However, one of the biggest challenges throughout the chemotherapy is the occurrence of drug resistance [30], [31]; in other terms tumor cells fail to respond to the actions of cytotoxic drugs. Drug resistance can be present intrinsically even before encountering the chemotherapeutic drugs or can be acquired during the therapy [31] such as by activating an alternative compensatory pathway which is intended to be targeted or by mutations which result in increased expression of targeted molecule [32]. In addition to these, resistance could also develop by the group of the cells which gains drug induced resistance and have a selective advantage over the other cell populations due to the heterogeneous nature of the tumor [33].

Drug resistance, either it is acquired or inherited, can occur via many different mechanisms. Among them alterations in drug metabolism is the most studied one [30]. This includes changes in uptake, efflux and activation/inactivation of the drug. The nature of the drug determines the way how it will enter to the cell. It may enter via transporters or it may exert its function by just binding to the receptors and transmit the effects without entering the cell. At this point, mutations in transporters and receptors, or changes in the expression levels of them may lead to drug resistance [30]. Another way which cancer cells gain drug resistance is the excessive efflux of the chemotherapeutic agent and promoting expression levels of the transmembrane proteins which efflux the drugs, such as multidrug resistance protein 1 (MDR1) [34].Inactivation of drug or lack of drug activation are the other ways of mechanisms for the development of drug resistance [34]. Mutations or downregulation of the enzymes required for the activation of the drug or overexpression of drug metabolizing enzymes such as CYP450 can lead to drug inactivation and hence drug resistance eventually [30]. Cancer cells have great tendency to be addicted to oncogenic mutations which give them growth advantage and resistance to various apoptotic stimuli [34]. In this case, targeting one protein may be ineffective since another alternative pathway may support the survival of the cancer cells, which is

termed as ‘synthetic lethal relationship’, making the cancer cells resistant to the chemotherapeutic agent [35]. Another way, which cancer cells resist chemotherapeutic agents inducing DNA damage directly or indirectly, is the promotion of DNA repair pathway. Upon treatment with drugs inducing DNA damage such as platinum-based drugs or topoisomerase inhibitors, cancer cells activate cell cycle arrest in order to gain time to repair their DNA and escape from apoptosis [34]. Thus using the drugs targeting the repair pathways in cancer cells together with DNA damage inducing agents is important to prevent cancer cells escape from apoptosis [34].

### 1.2.1 Topoisomerase inhibitors

During DNA replication, transcription or recombination, there occur topological restrictions such as introduction of supercoils due the double helix structure of the DNA [36]. To preserve the integrity of DNA, enzymes called ‘DNA topoisomerases’ solve such problems by introducing a temporary cleavage to one or both strand of the DNA [37]. In the case of topoisomerase class I enzymes, one cleavage is introduced to one strand, and then it is passed through the other strand of the helix. In the case of topoisomerase class II enzymes, both strands are cleaved and passed through the other helix [36]. At the end, cleavage sites are resealed to the backbone of the DNA. During this cleavage event, a temporary covalent bond between DNA and topoisomerases occurs which is called as ‘trappable complexes or cleavable complexes’. It is these sites where topo-active anti-cancer agents act [38] on. Topoisomerase (TOPO) inhibitors interfere with the bond between the DNA strand and topoisomerase by creating a permanent DNA breakage. Since the DNA cannot be repaired, replication fork collapses leading to cell death [39].

There two types of topoisomerase inhibitors, topoisomerase I inhibitors and topoisomerase II inhibitors which are explained as follows.

### 1.2.2 Cytotoxic effects of topoisomerase I inhibitors

This class of inhibitors includes camptothecin (CPT) and non-camptothecin compounds; such as topotecan, irinotecan and indolocarbazoles, indenoisoquinolines, dibenzonaphthyridinones, respectively [40]. Camptothecin is a plant alkaloid which has an anti-tumor activity against many solid tumors [41]. These highly selective TOP1 inhibitors exert their cytotoxic effects neither by binding to the enzyme nor to the DNA but by interfering with the enzyme-DNA complex leading to the formation of non-productive complex [42]. When DNA replication or transcription machinery collides with this bulky DNA lesion, it leads to the double stranded break (DSB) which is called as 'replication fork run off' [43]. Upon DSB, DNA damage response (DDR) signaling pathway steps in by the activation of ATM (ataxia telangiectasia mutated) and ATR (ataxia telangiectasia and Rad-3-related) kinases, H2AX phosphorylation and p53 stabilization. It is important to note that, not the inhibition of TOP1 itself, but the formation of TOP1-cleaveable complex and the following DSB are the major requirements for the cytotoxic effect of CPTs. Cell types, proliferation status, expression levels of TOP1 are also important factors for determining the cytotoxic effects of CPTs [44].

### 1.2.3 Cytotoxic effects of topoisomerase II inhibitors

TOP2 inhibitors are categorized into two classes and the first one is called as 'TOP2 poisons' including doxorubicin, etoposide and mitoxantrone. The TOP2 poisons exert their cytotoxic effect by increasing the levels of TOP2-DNA covalent complexes. This includes DNA strand breaks as well as protein accumulation bound to DNA, which eventually blocks transcription and replication [45]. As a result, TOP2 poisons rapidly result in enzyme mediated DNA damage which steps in DDR by the activation of ATM and downstream signaling pathways [46]. Among TOP2 poisons, anthracycline doxorubicin is one of the most studied chemotherapeutic drugs since it is also accepted as one of the most potent FDA approved chemotherapeutic agents [47]. Doxorubicin intercalates the DNA's double helix hence resulting in DNA damage. When the attempt to repair the DNA fails, cellular growth is inhibited, as a result apoptosis is triggered [48].

The second class of TOP2 inhibitors is named as TOP2 catalytic inhibitors since they do not generate the DNA-enzyme complex rather they inhibit the catalytic activity of the enzyme [45]. Some of the TOP2 catalytic inhibitors are novobiocin, merbarone and the anthracycline aclarubicin [49] .

## 1.3 Role of nicotinic cholinergic receptors in cancer

### 1.3.1 Nicotine and its connection with cancer

There is an increasing evidence that consumption of nicotine, which is the major component of tobacco [50], is associated with many cancer types [51] such as lung, gastric, liver, colon, breast and kidney cancers as well as other diseases including heart diseases and stroke [52].

In order for tumorigenesis to develop, there should be a constant exposure to the agent, which is easily achieved in the case of smoking due to the addictive nature of nicotine [53]. In addition to cotinine, which is produced by the conversion nicotine in the tissues, the other two tobacco nitrosamines; *N'*-nitrosonornicotine (NNN) and 4-(methylnitrosamino)-1-(3-pyridyl)-1-butanone (NNK) are the carcinogens which have higher affinity for binding to nicotinic acetylcholine receptors (nAChRs) than the natural ligand acetylcholine (Ach) in non-neural cells [51]. Furthermore, nicotine also results in upregulation of nAChRs in cancer cells resulting in increased signaling of nAChRs [51] .

Most of the nicotine is absorbed by gastrointestinal tract and converted to cotinine which exerts its carcinogenic effects by increasing the formation of DNA adducts, promoting proliferation and evasion of apoptosis [54]. Moreover, these carcinogens result in mutations in vital genes such as KRAS, Rb and p53 which also contribute to DNA adduct formation [55]. In addition to cotinine, other nicotine metabolite NNN is also carcinogenic which induces tumorigenesis as well [56]. Genotoxic effects of nicotine also occur with the production of high levels of reactive oxygen species (ROS) by the stimulation nAChRNs, which eventually results in DNA damage [51] (Figure 1.3). Moreover, in one

study, it was shown that nicotine resulted in upregulation of anti-apoptotic protein BCL-2 (B-Cell Lymphoma2) levels in highly malignant MDA-MB-231 breast cancer cell lines showing the interplay between nicotine and cancer cell survival in breast cancer [57]. In another study, it was also shown that cigarette smoke extract (CSE) exposed MCF7 breast cancer cell line showed metastasis in the lungs of the mice, whereas no metastasis was observed in mice injected with unexposed MCF7 cells suggesting the metastasis promoting feature of cigarette smoking hence nicotine exposure [58]. Moreover, an *in vivo* study with mouse model of lung cancer showed that nicotine resulted in increased number and size of the tumor, and promoted metastasis [59].

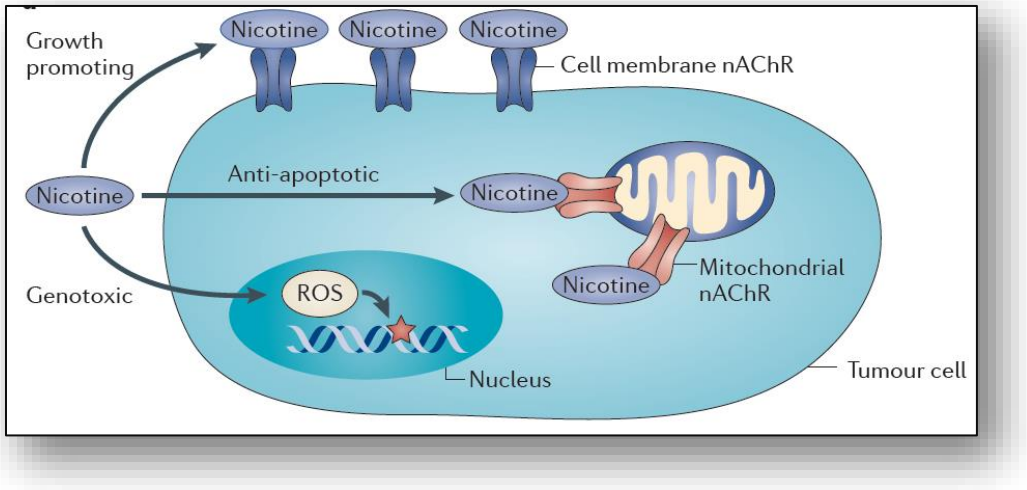


**Figure 1.3: Effect of nicotine.** Nicotine exerts its effect through binding to nAChRs resulting in transcriptional and post-transcriptional modifications. *Adapted from Grando A. S., 2014. Nature Reviews Cancer* [51]*. (License Number 4487160216099).*

### 1.3.2 Nicotinic acetylcholine receptors (nAChRs)

Nicotinic acetylcholine receptors are integral transmembrane proteins [60] which are expressed both in neuronal and non-neuronal tissues [61]. Depending on their pharmacological properties and the relative affinities to the certain molecules, they are classified into two categories: metabotropic muscarinic AChRs (mAChRs) and ionotropic nAChRs. As the name implies mAChRs are responsive to muscarine and natural agonist Ach and mostly found in skeletal muscles where they participate in mediating

neuromuscular transmission [62]. mAChRs are ligand gated ion channels and they are composed of different combinations of 5 subunits including two α1, one β1, one δ and γ (or ε depending on the developmental stage). Similarly, nAChRs are also ligand gated ion channels and found both in neuronal and non-neuronal tissues which are responsive to nicotine besides Ach [63]. In neuromuscular junctions, upon stimulation, they result in release of neurotransmitters like γ-aminobutyric acid (GABA), serotonin and dopamine and that's the actual reason why these receptors are associated with nicotine addiction [64]. nAChRs are composed of either homomeric or heteromeric combinations of 5 subunits which includes 9 alternative α subunits (α2- α10) and 3 alternative β subunits (β2- β4) [60], [65], [66]. Homomeric pentamer channels are only composed of one of identical α7, α8 (not in humans) or α9 subunits (Figure 1.4).

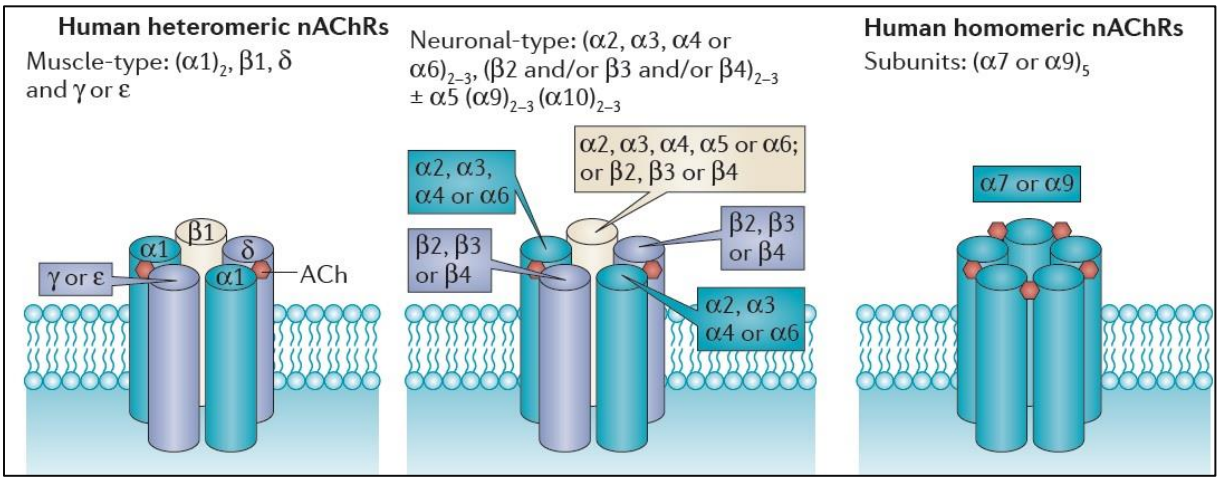


**Figure 1.4: Structure of nicotinic acetylcholine receptors family**. Homomeric and heteromeric structure of nAChRs. *Adapted from Grando A. S., 2014. Nature Reviews Cancer* [51]. *(License Number 4487160216099)*

In a study done by Schuller H. M., (1989), the involvement of nAChRs in tumorigenesis has been shown for the first time [67]. Moreover, through other researches it is also shown that nAChRs are involved in various cancer signaling pathways in cell type specific manner such as angiogenesis [68], metastasis [69], apoptosis [70].

Among the cholinergic receptors, homomeric pentamer composed of only α7 subunits, are mainly implicated in nicotine and NNK induced proliferation [71]. Through the stimulation of Akt and ERK pathways, α7 nAChRNs contributes to the progression, metastasis and angiogenesis of lung, bladder and gastrointestinal cancers [59]. Since the antagonists of α7 nAChRNs like α-Bungorotoxin result in deactivation of these receptors, downregulation of these receptors such as by using siRNAs represents an alternative approach for cancer therapy [72].

### 1.3.3 Role of nicotinic acetylcholine receptors (nAChR) in cancer signaling pathways

Acetylcholine, which is the natural agonist of nAChRs, acts like an autocrine growth factor both at systematic and cellular levels [73]. It participates in many biological signaling pathways in neuronal as well as non-neuronal cells such as learning, memory, sleep cycle regulation [61] and proliferation, apoptosis, differentiation, migration [74], respectively. Ach is synthesized from choline and acetyl coenzyme A by choline acetyltransferase (ChAT) and hydrolyzed by acetylcholinesterase (AchE) [51].

Upon binding of Ach or nicotine to the α subunit of nAChRs, it results in a conformational change in the receptor and hence leads to Ca+ and Na+ influx from extracellular side to the intracellular side of the cell and efflux of K+ ions [75]. Increase in Ca+ levels ends up with thedepolarization of the membrane and this further propagates the opening of the voltage-operated calcium channels (VOCC). Hence more and more Ca+ enters to the cell triggering the release of growth factors which activates various downstream signaling pathways such as proliferation, apoptosis, angiogenesis, migration and differentiation depending on the cell type.

One of the important pathways involved in upon nAChRs stimulation is proliferation and regulation of the genes involved in proliferation. B-arrestin, which is a scaffolding protein, is recruited to the nAChRs upon one of the agonists of it (nicotine or other nicotine derived metabolites or Ach) binds to the receptor [76] (Figure 1.5). With the downstream activation

of Src and Raf pathway, Retinoblastoma protein (Rb) is bound by Raf leading to Rb inactivation. Subsequent release of E2F from inhibitory binding of Rb, leads to CDK-cyclin activation which results in transcriptional activation of E2F initiated transcription of the G1-S transition genes [71] (Figure 1.5). Therefore, we can say that Rb-E2F pathway is one of the major players upon stimulation of nAChRs [76].

Another pathway involved in nAChR-stimulated proliferation is JAK-STAT pathway. STAT3 promotes the cell cycle progression through overexpression of cyclin-D1 [77]. In one study, chemotherapy sensitivity was restored with the depletion of STAT3 showing the impact of nAChR mediated stimulation of cell cycle progression [71].

Beside modulations of cell proliferation pathways, nAChR signaling also participate in resistance against apoptotic signals through PI3K-AKT signaling [78] (Figure 1.5). Akt is known to regulate anti-apoptotic protein BCL-2 and pro-apoptotic BAX, BAD proteins by phosphorylating them [79],[78]. Moreover, this signaling cascade also upregulates survivin and x-linked inhibitor of apoptosis (XIAP) which are the inhibitors of apoptosis [80]. Together with the modulations of pro-survival and anti-apoptotic signaling cascades, nAChRs have great impact on chemoresistance and hence the cancer patients who smoke have worse prognosis and poor response to chemotherapy compared to their non-smoking counterparts [81],[82],[83].

During tumor progression, the needs of oxygen and nutrients for cancer cells exceed beyond the simple diffusion. Therefore they develop ways to induce angiogenesis which stands for ‘development new blood vessels’ [84]. The developmental stages of angiogenesis start with recruitment of endothelial cells by secreting cytokine or angiogenesis inducing stimuli such as hypoxia. Following these inductions, endothelial cells degrade the basement membrane and move towards to the stimuli via VEGF (vascular growth factor) mediated mechanism [85], [86]. Similar to the cancer cells, vascular endothelial cells express nAChRs, hence Ach, as well as nicotine and its metabolites can act as in an autocrine or paracrine fashion to induce vascularization via VEGF signaling [87],[88]. Moreover, in a study done by Jarzynka MJ et al, estradiol in

combination with nicotine, enhanced the growth of lung cancer xenograft through VEGF mediated mechanism [89].

Another important biological process highly modulated in cancer cells is EMT which is the crucial step for metastasis and invasion [59]. β-catenin and E-cadherin are the two important epithelial markers are downregulated followed by the upregulation of mesenchymal markers like fibronectin and vimentin occurs upon nicotine induction [59], [90]. Implication of nAChRs in metastasis and invasion was identified in many cancers including lungs, pancreas and breasts [90].

Taking into account the interplay between nAChRs and various cancer signaling pathways, nicotine and its metabolites confer important factors for the tumor progression. Different subtypes of nAChRs may become prominent in one specific type of cancers such as the implication of α7 nAChRs in lung cancer and α9 nAChRs in breast cancer tumorigenesis [91].

Since most of the drugs targeting nAChRs are not subtype-specific [92], it is important to reveal the precise connection between the deregulated signaling pathway in cancer type specific manner.

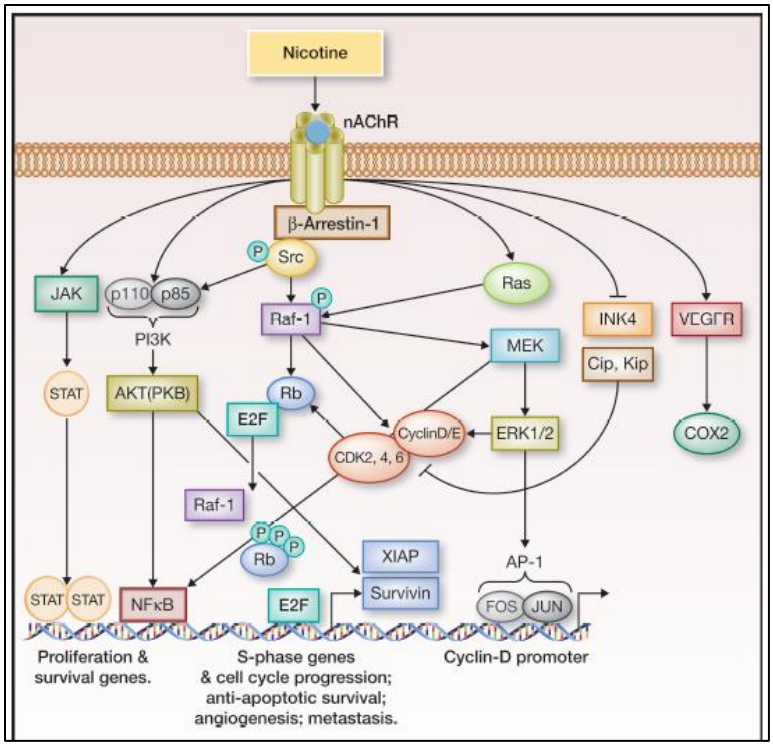


**Figure 1.5: Signaling cascade upon nAChRs activation**. Binding of nicotine to nAChR activates common cancer signaling pathways via recruitment of β-arrestin which in turn recurits Src kinase. This leads to activation of PI3K/AKT signalling, Ras/Raf/MAPK signalling pathways. *Adapted from Schall C. et al., 2014. Molecular Cancer Research* [71]*. (License Number 4487160885032).*

## 1.3.4 Implication of CHRNA5 in cancer

The chromosomal locus 15q25.1 locus is home for *CHRN* genes encoding for nAChRα3, nAChRα5, nAChRβ4 [93],[94] which are highly associated with nicotine addiction, smoking behavior and hence predisposition for the development of lung cancer [95].

Moreover, the non-synonymous single nucleotide polymorphism in CHRNA5 which causes an amino acid change in aspartic acid to asparagine at the position of 398 (D398N) [96], (Figure 1.6), contributes to the nicotine addiction and hence strongly associated with risk of lung cancer development [97].

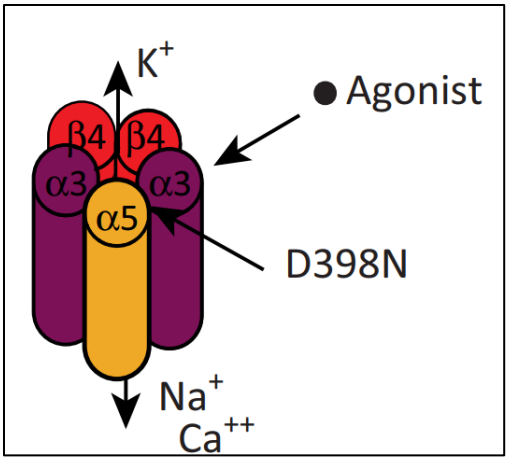


**Figure 1.6: Cholinergic Receptor Nicotinic Alpha-5.** Subunit composition of CHRNA5. *Adapted from Lassi G. et al., 2016. Trends in Neuroscience* [98].

In a study done by Ramirez et al, the authors demonstrated the importance of α5 subunit for the formation and the lining of functional receptor complex. Depletion of α5 subunit with anti-sense oligonucleotides resulted in selective deletion of the highest conductance channel from the cholinergic receptor [97].

## 1.4 Cell cycle and DNA damage response

### 1.4.1 Cell cycle regulation in cancer cells

The process where the cell replicates all its components and partitions it to the daughter cells termed as cell division cycle [99]. It is composed of four sequential steps; where in the S phase DNA is replicated, in M phase, two daughter cells are generated with cell division. In between S and M phases, there are two gaps named as G1 and G2 [100]. The first gap, G1, plays an important role for the cell to decide whether or not to initiate DNA replication [101]. Moreover, in G1 phase, cell is sensitive to both positive and negative signals [100]. The second gap called G2, is in between S and M phases, where the cell prepares to enter mitosis. In the case of high cell density or deprivation of positive signals for the promotion of cell division, cells are reversibly withdrawn from this cycle and stay in a state termed as ‘G0’ [102].

Cell cycle progression is propelled by the proteins termed as ‘cyclin-dependent kinases’ (CDKs) which are serine/threonine kinases. As the name implies, their activation depends on the other proteins called ‘cyclins’ whose levels change throughout out the cell cycle [103]. Cyclin D-CDK4, cyclin D- CDK6 and cyclin E-CDK2 complexes are responsible for G1 to S phase transition [104], whereas S phase is initiated by cyclin A-CDK2. Followed by S phase, cyclin B-CDK1 complexes are responsible for the transition from G2 phase to mitosis [105].

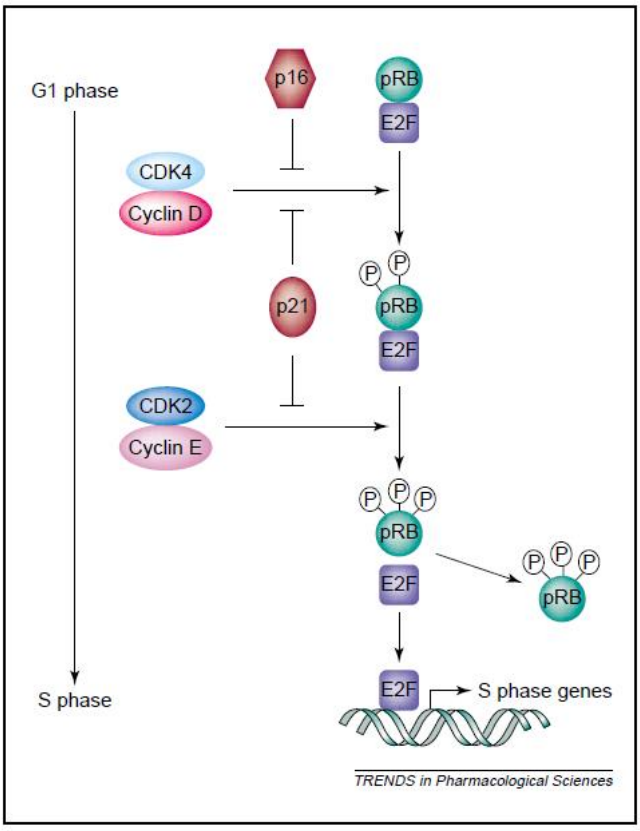


**Figure 1.7: G1-S progression.** RB is phosphorylated by the activated cyclin-D-CDK4 and cyclin-D-CDK2 complexes, which in turn releases E2F transcription factors. E2F transcribes the genes necessary for S phase transition. *Adapted from Stewart A. Z. , et al., 2003. Trends in Pharmacological Sciences* [104]. *(License Number 4490711193264).*

The retinoblastoma (RB) protein, which is known as a tumor suppressor protein since it negatively regulates cell cycle progression [106], is the substrate for the activated cyclin-CDK complexes during G1 phase. Moreover, it is responsible for G1 checkpoint, determining either entry to S phase or blocking the growth [106] depending on its phosphorylation level by cyclin-D-CDK4,6 and cyclin-E-CDK2 [104]. Hypophosphorylated RB does not dissociate from E2F member of transcription factors and hence inactivates them. Since E2F member transcription factors are needed for the transcription of the genes required for S phase transition, cells arrested at G1-S phase [104]. Therefore, for the activation of E2F, RB should be hyperphosphorylated by cyclin-CDK complexes for S phase entry [106].

Cyclin-B-CDK1 complexes regulate the transition from G2 to M phase [104], and are activated by CDC25C phosphatase which is responsible for removing the inhibitory phosphate group from CDK1 [107]. Followed by this, cells enter mitosis after the ubiquitination and degradation of cyclin-B by the anaphase-promoting complex (APC), which in turn deactivates CDK1 [108].

The complex series of this cell cycle phases are regulated by another pathway called as cell-cycle checkpoints [109]. Upon recognition of aberrant or incomplete cell cycle event, checkpoint elements signal this problem to the effectors to induce cell cycle arrest until the problem is solved. If the problem cannot be solved, then the checkpoint signaling can activate the pathways inducing programmed cell death.

Dysregulation of cell cycle is the hallmark in cancer cells [104]. For example, the dysregulation of pRB occurs through alterations in the upstream molecules such as cyclins and CDKs in most of the cancer types including lung and breast [110]. This can occur by increased levels of cyclin D and cyclin E as well as upregulation of the genes encoding CDK4 and CDK6 or deletion of the negative regulator of these CDKs, p16 [110]. Another protein altered in many of the tumors is p53 which acts as a tumor suppressor gene [111]. Alterations in p53 can occur as a germline mutation as well as its regulation

can be altered such that the amplification of MDM2, the negative regulator of p53, can result in inactivation of p53 [112].

### 1.4.2 DNA damage response in cancer cells

Endogenous and exogenous agents can induce DNA damage which in turn evokes cells' DNA damage response (DDR) machinery [113]. The major functions of DDR are to sustain genomic integrity as well as to prevent tumor formation. DDR involves three main components one of which is the sensors such as pH2AX, RAD51 and MRN (Mre11-Rad50-Nbc1) complex [113]. The sensors then recruit the mediators like ATM (ataxia-telangiectasia mutated) and the ATR (ATM and Rad3 related) which are the key serine/threonine protein kinases. These mediators in turn phosphorylate various effector molecules such as CHEK1, CHEK2, p53, Wee1 and the others [114].

There are three important consequences of DDR; first by activation of checkpoint proteins controlling the regulation of cell cycle which gives time to cells to repair the damage. Second is the activation of DNA repair mechanism. And finally, the induction of apoptosis in the case of damage is too extended to be repaired [113].

Checkpoint kinase 1 (CHEK1) and checkpoint kinase 2 (CHEK2) are the important substrates of ATR and ATM kinases, respectively [113]. In the case double strand breaks (DSB), the sensors, MRE11/NBS1/RAD50 activate ATM which in turn activates CHEK2 pathway to induce S arrest and p53 dependent G1-S checkpoint [115] (Figure 1.8). On the contrary, ATR is activated upon the accumulation of replication protein A (RPA) on the sites of single-stranded DNA (ssDNA) which occurs due to DNA damage .The ATR's binding partner ATR-interacting protein (ATRIP) is also recruited to ssDNA [116]. The key downstream molecule of ATR pathway is CHEK1 is activated by phosphorylation at Ser-317 and Ser-345. This also leads the rapid autophosphorylation of CHEK1 at Ser-296. These phosphorylations create binding sites for the CDC25 family phosphatases [113]. Similarly, the sequential phosphorylation of CHEK2 also creates binding sites for these phosphatases. In normal cells, the common mission of CDC25 phosphatases is to

remove the inhibitory phosphate groups of CDK proteins to let them pursue the cell cycle progression. In the case of DDR context, CHEK1/CHEK2 phosphorylates CDC25 proteins leading them to proteasomal degradation. Hence, this abolishes either CDK2/cyclinE complexation to lead G1/S arrest [117] or proteasomal degradation of CDK1/cyclin B kinases leading G2/M arrest [118].

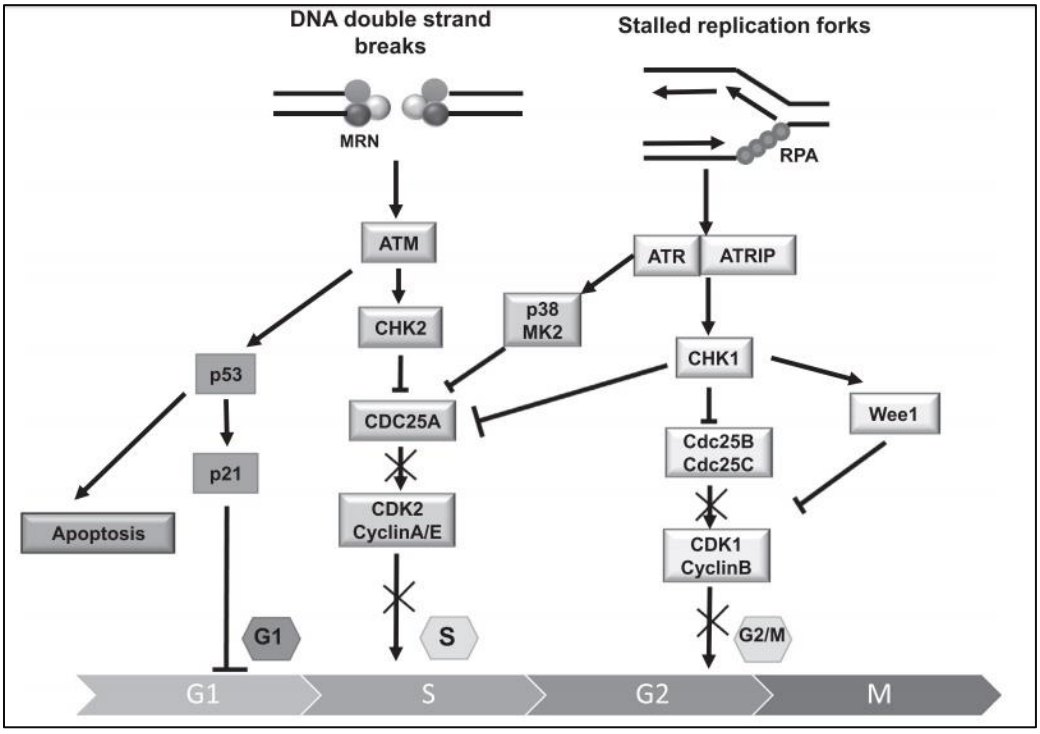


**Figure 1.8: Activated checkpoints upon DNA damage.** DNA double strand breaks lead ATM activation, whereas single strand breaks together with stalled replication forks activate ATR. These in turn activates checkpoint kinases resulting in either cell cycle arrest or apoptosis. *Adapted from Qiu Z. et al., 2018. Radiotherapy and Oncology* [119]*. (License Number 4490720913271).*

Alterations in DDR mechanism resulting in both activation and inactivation of the pathway, are found in many of the sporadic cancers [120]. For example, increased autophosphorylation of ATM and CHEK2 are found in early stage tumors [121] representing a barrier to the progression of tumor. Moreover, in late stage breast cancer tumors, hyper activation of ATM is also recorded which implies that it participates in metastasis and tumor progression as well [122]. In addition to these, overexpression of

the proteins such as RAD51, BRCA1, PARP1, CHEK1, CDC25A are also observed in various cancers which also contribute to the resistance of cancers to chemotherapy [123], [124], [125].

On the other hand, inactivation of the proteins participating in DDR mechanism is also widely observed in cancers. One of them is the mutations in p53 gene, which is known as the guardian of the genome due to its tumor suppressor function [126]. Inactivation of p53 can occur via different genetic alteration such as deletion, loss of heterozygosity or decreased expression levels [127]. Moreover, decreased expression levels of ATM, the MRN complex, CHEK2 and RAD51 together with the inactivation of molecules serving as DNA damage sensors, mediators and effectors are widely observed in many of the cancers [128], [129], [130], [131].

### 1.4.3 Role of CHEK1 and CHEK1 inhibitors in cancer cells

One of the major mediators and signal transducers of DDR mechanism is CHEK1. As mentioned above, in normal cells, it regulates the checkpoints and is required for the transition from S phase to mitotic entry. On the other hand, in the case of aberrant DNA replication, it induces G1/S arrest via phosphorylating and subsequent degradation of Cdc25A [132].

In one study it was shown that, deletion of CHEK1 in mammary cells in mice caused increased levels of Cdc25A accumulation. This resulted in increased number of cells at S phase and accumulation of DNA damage which eventually ends up with premature mitotic entry followed by cell death [133].

In cancer, the mutations or loss of CHEK1 is rare since its role in proliferation, survival and cell cycle regulation. On the other hand, partial abolishment of CHEK1 favors tumor formation [134] such that in stomach, colorectal and endometrial cancers loss of function CHEK1 mutations are detected [135], [136], [137]. Similar to this, it was reported that, complete loss of CHEK1 resulted in suppression of carcinogenesis induced by chemicals

whereas its partial deletion leads formation of benign malignancy [138]. Moreover, it was found that triple negative breast cancers express high levels of CHEK1 and is highly associated with poor prognosis suggesting that CHEK1 have important roles for cell proliferation [139].

In the light of these, CHEK1 inhibitors have gained enormous importance for cancer therapy [140]. These are used either alone or in combination with DNA damaging agents [141]. Inhibition of CHEK1 together with chemotherapeutics which creates genotoxic stress results in abrogation of checkpoints, abolishment of DDR and promotion of cell death [142]. Therefore usage of small molecules targeting CHEK1 increases the anti-tumor activity of cytotoxic chemotherapeutics by sparing the normal cells [143].

Topoisomerase I inhibitors (topotecan, camptothecin and irinotecan) result in single strand breaks which then lead the cells arrested at G1/S transition. In the literature it was shown that, CHEK1 inhibitors increased the potency of topoisomerase I inhibitors [144], which was also supported by CHEK1 siRNA [145] usage as well. Moreover, in MDA-MB-435 breast cancer xenografts, it was shown that the selective CHEK1-inhibitor, CHIR-124 increased the potency of anti-tumor effects of irinotecan, which was supported by TUNEL assay showing the enriched number of cells in apoptosis [146]. Also, the effect of irinotecan was increased with the usage of another CHEK1-inhibitor, SAR-020106 in colon cancer xenografts which was supported by the decreased levels of pSer296 CHEK1 levels in tumor [147]. The same CHEK-1 inhibitor also increased the potency of topoisomerase II inhibitor, doxorubicin in HT29 cells [147].

All together these suggest that CHEK1 inhibitors when used together with other cytotoxic agents can result in enhancement of chemotherapy efficiency [148].

## 1.5 Apoptosis in cancer cells

### 1.5.1 Regulation of apoptosis

Apoptosis, which is also named as programmed cell death (PCD), is the way for multicellular organisms to eliminate the damaged or infected cells which otherwise may

cause uncontrolled division of aberrant cells [149]. Defects in apoptosis may promote cancer as well as neurodegenerative diseases [150].

Apoptosis can occur in two commonly identified pathways; extrinsic and intrinsic pathways [151]. In the extrinsic pathway, activation of the Tumor Necrosis Factor Receptor (TNFR) superfamily, which includes TNFR, Fas and TRAIL, results in activation and hence recruitment of initiator caspase 8 and 10, which are the proteolytic enzymes controlling cell death and inflammation by cleaving the substrates from specific cleavage sites [152]. This process results in the formation of death inducing complex (DISC) which further activates the executioner caspases such as caspase 3 and caspase 7. These caspases cleave the substrates which eventually lead to DNA fragmentation, cell shrinkage, membrane blebbing and many other changes associated with apoptosis [153].

The intrinsic pathway is largely modulated by mitochondria. It starts with the release of cytochrome c, resulting in the formation of apoptosome [154] which is composed of Apaf-1 like molecules [155]. Followed by apoptosome formation, initiator caspases are activated which in turn activates executioner caspases. At this point, intrinsic pathway also converges to the same response as extrinsic pathway. Moreover, the pro-apoptotic Bcl-2 family proteins (BAX and BAK), are activated and trigger the release of cytochrome c from mitochondria. In addition to cytochrome c, other pro-apoptotic proteins also released from mitochondria such as Smac/Diablo [156]. Mitochondrial pathway can also be activated by extrinsic pathway via the truncation of pro-apoptotic protein Bid (tBid) by the caspase 8 [157].

Alterations in apoptosis lead tumor progression since these allow cancer cells to survive more than the normal lifespan of a cell, and also provide protection from non-optimal conditions such as hypoxia which gives time to cells to accumulate more and more genetic alterations [150]. This further gives opportunity to the cancer cells to alter cell survival mechanisms as well as to promote angiogenesis and metastasis throughout tumor progression [158]. Taken together, development of an anti-apoptotic phenotype is one of the most important hallmarks of cancer cells [159], [160], [161].

The anti-apoptotic protein BCL-2 is termed as an oncogene since it is overexpressed in most of the lymphomas due to the reciprocal chromosomal translocation (t14; 18) [162]. It is not because it promotes proliferation, rather it prevents cell death in spite of the different stress conditions [163]. As opposed to this, downregulation of pro-apoptotic proteins, including BAX, was also detected in many of the cancer types [160].

The most common way which the cancer cells evade apoptosis is upregulating the genes which act anti-apoptotically. In addition to BCL-2, heat shock proteins, chaperones and the ones encoding for the scavengers of reactive oxygen species (ROS) among the ones which are up-regulated to escape from apoptotic stimuli [164], [165], [166]. Identification of the upregulated anti-apoptotic genes is important for the development pharmacological interference which in turn enhances current therapeutics [167], [168].

### 1.5.2 Implication of BAX/BCL-2 ratio

The ratio between the pro-apoptotic protein BAX and the anti-apoptotic BCL-2 is important, since a shift in this ratio will determine the fate of a cell [48] since they play a role in the permeabilization of the mitochondrial membrane [158]. The pro-apoptotic members of BCl-2 family, such as BAX, BAK, participate in the dysfunction of the mitochondria by inducing the release of cytochrome c from the mitochondria. On the other hand, the members of anti-apoptotic members of BCL-2 family such as BAX, BAD protect the outer membrane of mitochondria along with inhibiting the release of cytochrome c [169]. Therefore, it is the balance between the pro-apoptotic and the anti-apoptotic proteins rather than their individual expression levels; in other words the ratio of BAX/BCL2 which determines the fate of a cell in terms of survival or induction of death [170].

In a study done by Lee et al., they observed that increased levels of BAX/BCL2 ratio at protein levels by western blotting and this was associated with the cellular radiosensitivity of some cells in pancreatic cancer [170]. Similar to this, immunohistochemical analysis of

BAX/BCL2 ratio was observed to be associated with the response to chemoradiotherapy in bladder cancer patients [171]. In another study, they revealed the contribution of high BCL-2/BAX ratio in the pathogenesis of leukemic cells in the clinical course of CLL [172].

### 1.5.3 Importance of cleaved caspase-7 as an apoptotic marker

One of the key players of apoptosis is caspases which are the class of aspartate specific cysteine proteases [173]. They cleave the targeted proteins next to an aspartate residue. Caspases produced as an inactive form as latent zymogens to prevent unprogrammed cell death. Caspase signaling occurs in two steps. In the first step, 'initiator caspases' which are caspase-1, -8, -9, are autoactivated. In the second step, these caspases activate the 'executioner caspases' which are caspase-3, -7 by cleaving the inhibitory domain. As followed by this, executioner caspases cleave various proteins which contribute to the typical apoptotic biochemical and morphological features such as cell shrinkage, DNA fragmentation and so on [174].

In between the executioner caspases, caspase-7 was thought to be functionally redundant with caspase-3, however later it was revealed that caspase-7 also has non-redundant functions in apoptosis and in inflammation [175] as well. The redundancy between caspases-3, -6 and -7 was observed in PARP cleavage by the removal of any of the caspases. But in another study, with mouse embryonic fibroblasts (MEFs) deficient of caspase-7, upon apoptosis stimuli, they observed mild survival advantage in capsase-7 deficient MEFs over the normal MEFs [176]. Moreover, in the same study, it was also shown that, despite caspase-3 was mostly responsible for the morphologic changes occurred during apoptosis as well as DNA fragmentation; capase-7 seemed to be more involved in the loss of viability.

Taken into the fact that MCF7 cells lack capase-3 [177], the desired effects of executioner caspases are mostly and slowly achieved via cleaved-caspase-7 in those cells.

### 1.5.4 Association between nAChRs and apoptosis

As mentioned in the section 1.3.3, nAChRs, depending on their subunit composition, are involved in a variety of cellular signaling pathways such as proliferation, differentiation, and apoptosis so on. For example, in neurons, stimulation of α7 containing nicotinic receptor activates anti-apoptotic kinase AKT through PI3K signaling [178], implying that this signaling can also have a protective role for neurons from cell death [179]. Moreover, in another study, it has been shown that, α7 subtype of nAChRs can result in mobilization of $Ca^{2+}$ from ryanodine-sensitive intracellular stores which in turn promotes cellular survival. The increased $Ca^{2+}$ levels can result in neuroprotection via induction of Cdk5 through increased BCL-2 expression [180].

The agonist of nAChRs, nicotine, is found to participate in the regulation of BCL-2 family proteins [181]. In one study, they have shown that, nicotine induces phosphorylation of BCL-2 and hence exhibiting a protective role for NSCLC from cisplatin induced apoptosis [79]. Moreover, in another study, they have shown the role of α3 and α4 containing nAChRs exhibiting apoptotic activity though Akt activation in bronchial epithelial cells [91]. In A549 NSCLC cells, nicotine's protective action has been revealed which occurred upon upregulation of anti-apoptotic XIAP and survivin with the activation of α3 containing nAChR [80].

Since there also exist discrepancies in the literature in terms of nicotine's effect on apoptosis, it should be also noted that, anti-apoptotic effects of nicotine occur depending on the composition of nAChRs as well as depending on the tissue type. Therefore, together with the subunit composition of nAChRs and their involvement in apoptosis should be further investigated [182].

## 1.6 microRNAs

### 1.6.1 Biogenesis of microRNAs

MicroRNAs (Microribonucleic acids,miRNAs) are small non coding nucleotides composed of around 20-23 nucleotide in length [183]. They have important roles in the regulation of many cellular functions such as proliferation, EMT, apoptosis, and development [184], [185], [186]. They exert their functions either by degradation or inhibition of translation of the mRNAs that they target [187].

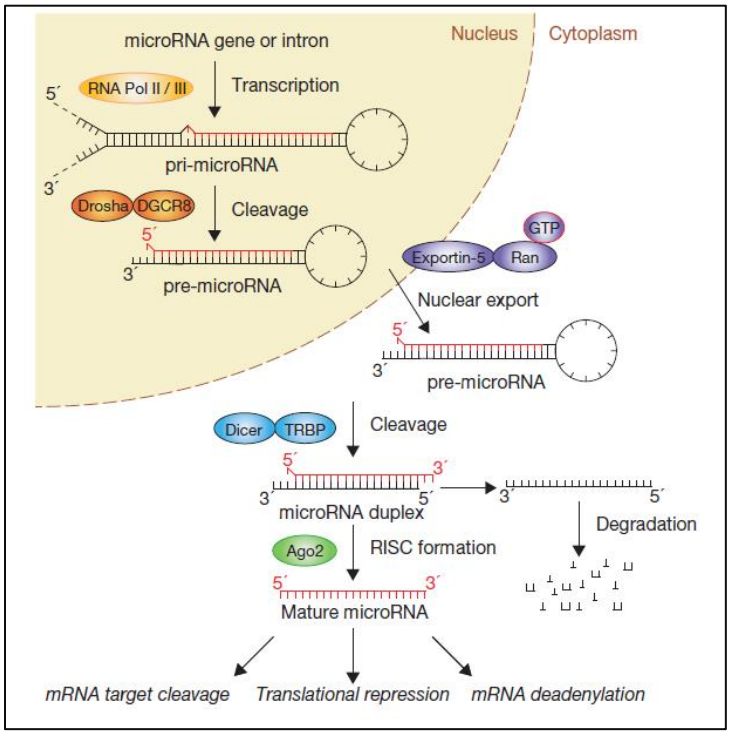


**Figure 1.9: Biogenesis of microRNAs.** *Adapted from Winter J. et al., 2009. Nature Cell Biology* [187] *. (License Number 4487170124632).*

As illustrated in the figure 1.9, miRNAs are transcribed from either intergenic or intragenic regions of the genome. RNA polymerase II or III are responsible for miRNA transcription. After the generation of 60-70nt length pri-miRNA, it is cleaved by RNase III enzyme DROSHA to create pre-miRNA. Then, for the generation of mature miRNA by dicer in the cytoplasm, it is exported through exportin-5 to cytoplasm [188], (Figure 1.9).

### 1.6.2 microRNAs that are targeting CHRNA5 through prediction and validation

miR-15 family microRNAs include miR-15a, miR-15b, miR-16-1, miR-16-2, miR-195 and miR-497 [189]. Deletions or low expression levels of miR-15a family is highly associated with drug sensitivity in cancer such as tamoxifen [190].

Figure1.10 illustrates the predictive binding sites of miR-15 family miRNas which were obtained from microrna.org [191].

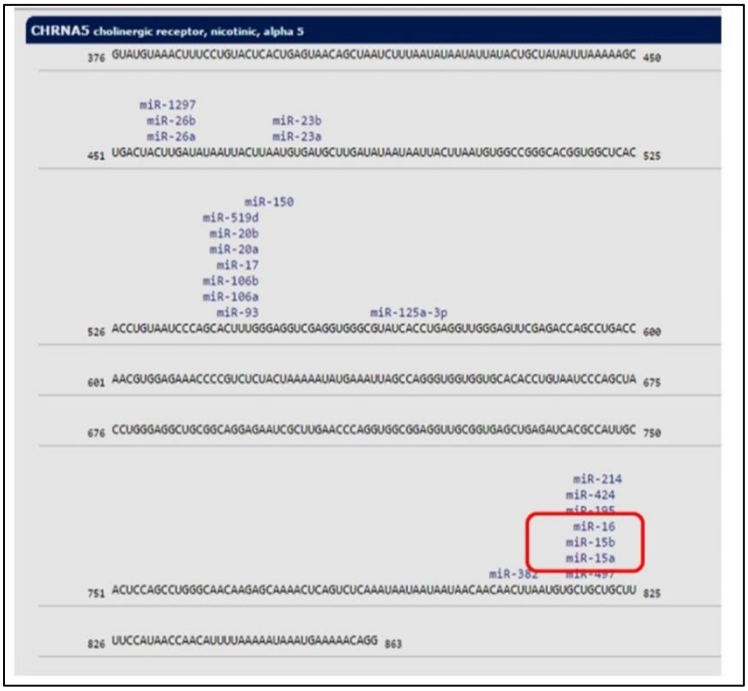


**Figure 1.10: Predictive binding sites of miR-15a family in 3'UTR of CHRNA5.**

### 1.6.4. miR15/16 family in cancer and cancer related signaling pathways

Tumor suppressive role of miR15/16 family through induction of apoptosis or inhibition of cell proliferation has been shown in different cancers. BCL2 was found to be a target of miR-15a through mimic studies; and due to its role in apoptosis this makes miR-15a a tumor suppressor by increasing rate of apoptosis [192]. miR-15a was known to inhibit

genes related with cancer including BCL2 in colon cancer [193]. In HPV-positive hypopharyngeal squamous cell carcinoma miR-15a mimic could lead to apoptosis through reduction of BCL2L2 and BCL2 expression levels [194]. BCL2 was also found to be target of miR-15b in liver cancer cell HepG2. The effect of miR-15b was cell cycle inhibitory as expected while miR-15b inhibitor could lead to tumor formation [195]. Mesothelioma cells expressed less miR-15/16 and increasing the amount of miR-16 resulted in reduced BCL2 and CCND1 levels and reduced cell proliferation while resulting in drug sensitization [196].

miR-16 levels were found to be dependent on Ago2 levels; in the overexpression of Ago2 miR-16 levels were increased and Bcl2 was again found to be a target of miR-16 [197]. Post-transcriptional control of CDKN2B by miR-15a-5p also was shown by mimic studies [198]. miR-15a and miR-16-1, found in chromosome 13q14.3 which is deleted in chronic lymphocytic leukemia, can be overexpressed to reduce tumor size while inhibitors of these microRNAs acted in the opposite manner [199]. In melanoma, miR-15a mimic expression resulted in decreases in proliferation [200]. Effects of plant derived chemicals were tested on miR-15b expression levels and cell proliferation in glioma cells and these antiproliferative effects were verified by using mimic exposure of the miR-15b [201]. CCNE1 was targeted by miR-15b mimic leading to decreased expression while the miR-15b inhibitor resulted in the opposite action. This was validated by 3'UTR luciferase assay in osteoblastic cells [202]. miR-15a-3p also was found to be inducing apoptosis by activating caspase-3/7 and inhibit cell proliferation in different cancer cell lines [203]. Antiproliferative and apoptosis inducing effects of miR-15a mimics also were seen in nasopharyngeal carcinoma cells through induction of BAX, pro-caspase and active caspase 3 [204]. An important target of miR-15b emerged as Cyclin D1 in glioma tissues resulting in inhibition of proliferation and apoptosis [205]. In AD models on the other hand miR-16 mimic has led to decreased apoptosis while inhibitor of miR-16 increased apoptosis as opposed to cancer cell lines [195].

### 1.6.4.1 Mimic studies of miR-15/16 Family

Cancer related cellular signaling pathways have been studied using miR15/16 mimics. The relationship between miR-15a/16 family and TGFβ signaling also has been investigated. miR-15a/16 mimics resulted in reduced TGF-β and VEGF in retinal endothelial cells grown in high glucose and this was supported also *in vivo* [206]. In ARPE19 cells miR-16 mimic resulted in reduced VEGF levels [207]. VEGF-A was among the targets of miR-16 in endometrial cells [208]. A recent study performed with miR-16 mimics provided insight into the relationship between this microRNA and autophagy in lung cancer cells (A549). miR-16 mimic resulted in formation of autophagasomes, which were inhibited by TGF-β signaling. The authors suggested that TGBF-beta induced EMT could be inhibited by overexpression of miR-16 [209].

Another validated target of miR-15b has been found to be IGF1R through studies performed in glioblastoma cell lines U87 and U251. The reduction in cell viability caused by miR-15b mimics resulted in reduced tumor progression [210]. In addition, miR-15b/16 was found to target Rictor and mTOR in Dicer (-/-) CD4+ T cells demonstrating regulation of Tregs via modulation of microRNAs [211]. miR-16 is also known to downregulate MEK1. The authors tested whether it targeted FGFR1 mediated ERK1 activity and found that the effects of FGFR1 and miR-16 were similar in fibroblasts [212]. In endometrial cells mimic miR-15a-5p reduced expression of genes involved in cell proliferation as well as wnt3a expression thus wnt signaling [213]. MEK1, putative target of miR-16, was also validated by using miR-16 mimic in HP75 cells, and the result was suppression of MEK1 and downstream pathway including Cyclin D1 [214].

Mimics studies also shown a role for miR15/16 family in drug sensitization. In breast cancer, expression of miR-15 family was found to be sensitive to gamma irradiation and mimics were able to sensitize the irradiated cells [215]. Studies with miR-15b also focused on validation of target genes, one of which is, Wee1, which is important in drug resistance. miR-15b mimic application was found to sensitize cells to doxorubicin and resulted in cell death in osteosarcoma [216]. Tamoxifen resistant breast cancer cells could be made

more sensitive upon exposure to miR-15a/16 mimics via inhibition of CCNE1 and BCL2 while E2F7 was found to negatively regulate the miR-15a/16 gene cluster expression [190].

The role of miR15/16 family in cancer cell migration and differentiation was studied in different cancers. In cholangiocarcinoma miR-15a was reduced in expression while miR-15a mimic was shown to inhibit cell migration [217]. Another evidence for the tumor suppressor and anti-migratory role of miR-15a comes from liver cancer cells in which miR-15a mimic inhibits migratory behavior of liver cancer cells through suppression of cMyB [218]. In head and neck carcinomas decreased levels of miR-15a were related with lymph node invasion [219]. Differentiation and angiogenesis studies are less but emerging. The relationship between c-myc and miR-15a has been functionally shown by luciferase assay in K562 myeloid leukemia cells which were overexpressing miR-15a and negatively correlated in differentiating blood cells [220]. The tumor suppressive role of miR-15b was also studied in the context of inhibition of metastasis in xenograft studies and mimic exposure was found to sensitize cells to chemotherapy and reversed formation of EMT in tongue cancer cell lines [221]. By mimic and inhibitor studies and luciferase assays, Smurf1 were found to be a validated target of miR-15b; Smurf1 was suggested to regulate the level of Runx2 and lead to differentiation of osteoblasts [222].

The effects of miR-15a on inflammatory signaling were shown in retinal endothelial cells in vitro and with vascular tissue specific knockout of miR-15a/16 in mouse [223]. The role of miR15a/b in inflammatory response has been also shown in sepsis [224]. Another validated target of miR-16 was found to be PDCD4, which is a mediator of apoptosis. Mimic of miR-16 led to reduced pro-inflammatory signals and increased anti-inflammatory ones. These results were confirmed with PDCD4 siRNA suggesting that they act on these pathways [225]. COX-2 mRNA was downregulated by miR-16 in monocytes and miR-16 could bind to COX-2 3’UTR [226]. Downregulation of expression in target genes when exposed to miR-15a/16 mimics were tested for PD-L1, which was upregulated in multiple cancers [227]. miR-15a depletion also increased TLR4 [228].

Other areas of research include studies in metabolism. miR-15a's role was also shown in metabolism such that mimics of miR-15a could reduce UCP-2 protein by reducing also the energy metabolism [229]. Lipid content of mammary epithelial cells was found to be regulated by miR-15b such that miR-15b mimic could decrease it while its inhibitor increases it. This study also shows that miR-15b levels were reduced by E2 and Progesterone and led to increases in lipid levels [230]. miR-15b/16 also was found to modulate insulin resistance through TNFα and SOCS signaling [231].

The potential importance of miR-15a intervertebral disc regeneration was also shown through mimic studies as well [232]. The role of miR-16 in liver fibrosis was also studied [233].

On the other hand, conflicting studies also exist such that increased miR-15b was found to be a marker for NSCLC via possible inhibition of TIMP2 [234]. Therefore, it gains importance to investigate the effects of miRNAs in tumor specific manner.

## 1.7 Hsa-miR-495-3p

### 1.7.1 In cancer

miR-495 is one of the miRNAs encoded from 14q32.31 gene cluster which is an imprinted region of the human genome [235]. Similar to the other miRNAs encoded from this cluster, miR-495 participates in both development of normal tissues and also apoptosis, chemosensitivity and metastasis of cancer cells [236].

miR-495 levels have been altered in many tumor types. For example, in medullablastoma, which is a brain tumor seen in children, recorded to have low levels of miR-495 compared to cerebellum. In a study done by Ce Wang, they found that miR-495 as a predictor marker in medullablastoma [237]. Moreover they also stated that, patients having low miR-495 levels had decreased survival rate.

Despite miR-495 is mostly known as a tumor suppressor miRNA in most of the solid tumors [236], in the literature there exist also conflicting studies about the role of miR-495 in cancer. For example, in hepatocellular carcinoma (HCC), the levels of miR-495 is high and negatively regulates MAT1A (Methionine adenosyltrasnferase) gene expression which is normally expressed in adult liver tissue [238] tissue .On the contrary in NSCLC, prostate, gastric cancers exhibit be low levels of miR-495 [239], [126], [235], [241], [242].

### 1.7.2 Review of mir-495 mimic or inhibitor studies in cancer or other contexts

In one of the first studies performed with miR-495 overexpression in breast cancer, CDH1 inhibition was found to be prominent upon overexpression of miR-495 suggesting that miR-495 could be oncogenic [243]. Future studies also shown tumor suppressive activity of miR-495 in breast cancer. miR-495 was shown to regulate JAM-A; the interaction was shown using overexpression of miR-495 followed by rescue with the overexpression of JAM-A, which inhibited breast cancer migration in breast cancer cell lines [244]. The effects of miR-495 stable overexpression were tested also in different breast cancer cell lines showing that Bmi-1 was a target of miR-495 in breast cancer [245]. Tumor suppressive effects of miR-495 were stated through G1-S arrest by overexpressing it [237]. In breast cancer, miR-495 together with miR-195-5p was also studied for diagnosis of breast cancer and exhibited high discriminative power for early detection [246]. In breast cancer, STAT3 was found to be a direct target of miR-495; and in addition, miR-495 was responsive to 5-AZA treatment leading to target gene downregulation. Silencing of miR-495 promoter could be abrogated by demethylation [247].

miR-495 and its overexpression was studied widely in other cancers as well and different targets of miR-495 were validated by means of different strategies. In medulloblastoma miR-495 targeted GFI1, a factor modulating survival of patients [237]. miR-495 was shown to target FOXC1 in endometrial cancer cells inhibiting cell proliferation [248]. However, conflicting evidence also is available. For example, in bladder cancer miR-495 was found to be oncogenic through inhibition of PTEN and hence reinstitution of PTEN

resulted in decreased cell proliferation and invasion initiated by overexpression of miR-495 [249]. The relationship between a long noncoding RNA UCA1 and miR-495 has also been shown through suppression of CDKN1A expression; UCA1 was found to be downregulated by miR-495 in renal cell carcinomas [250]. In osteosarcoma miR-495 was shown to target HMGN5 while it also inhibited Cyclin B1 and BCL2 leading to inhibition of cell proliferation and induction of apoptosis [251]. Role of miR-495 in epigenetic control of loci, such that depletion of miR-495 results in induction of oncogenic epigenetic modifiers, has also been shown in gastric cancer. DNA methylation inhibitor 5-AZA treatment resulted in increased expression of miR-495-3p and this suggested regulation of this microRNA by DNMT1 [252]. miR-495 is often downregulated in melanoma and hepatocellular cancer (HCC). A study performed with miR-495 mimic demonstrated the anti-tumorigenic effects of this microRNA in melanoma cells A375 and MeWo. The effects of miR-495 could be driven through PBX3, whose silencing also resulted in inhibition of cell proliferation [253]. Ye et al. (2018) studied overexpression of miR-495 leading to tumor suppression in HCC and suggested different players in connection with this miRNA such as PKB and IGF1R signaling [254].

Another cancer type in which miR-495 levels are relatively lower than normal is colorectal cancer. The authors identified Annexin 3 as a target of miR-495 and shown that downregulation of Annexin 3 and induction of TP53 pathway induced EMT [255]. Another study in colorectal cancer supported the role of miR-495 as a tumor suppressor and identified FAM83D as a target of this microRNA. Rescue of FA84D reversed the effects of miR-495 [256]. Other than colorectal cancer, miR-495 was also involved in other diseases of colon such as ulcerative colitis in which miR-495 levels were reduced. Overexpression of miR-495 was found to help reinstate the barrier function in the intestinal mucosa through modulations in JAK/STAT3 pathway [257].

miR-495 has been studied in combination with other microRNAs or used for reversal of phenotype by overexpression of mRNAs along with its overexpression. For example, RUNX3 was found to be another target of miR-495 and its synergistic inhibition by miR-495 and miR-130a resulted in inhibition of apoptosis and downregulation of RUNX3

mediated transcriptional regulation, e.g., (CDKN1A and BIM) [258]. Another target of miR-495 was found to be SAT1B in renal carcinoma. This was shown by demonstrating the cell cycle inhibitor effects of overexpression of miR-495 rescued by overexpression of SAT1B [259]. Other evidence for the tumor suppressive role of miR-495 comes from glioma since overexpression of miR-495 results in inhibition of cell proliferation and invasion through targeting MYB [260]. miR-495 and HMGA2 were found to interact based on validation studies while miR-495 mimic resulted in decreased invasion and cell migration by affecting EMT relevant genes such as CHD1, VIM and ACTA2 in gastric cancer cells [261].

In addition to cell cycle modulatory effects, miR-495 was also associated with inhibition of authophagy, a result of starvation or mTOR inhibition. This is through targeting and blocking of ATG3, an important molecule in regulation of autophagy. Inhibition of miR-495 restored autophagy. This study was important showing that under conditions of starvation or mTOR inhibition miR-495 increased survival of cells and could have important impact on cancer cell death [262]. The role of tumor suppressive miR-495 in regulation of Akt1 and mTOR pathways was also supported by studies performed in prostate cancer cell lines [263]. In esophageal squamous carcinoma the role of miR-495 also was found to be tumor suppression since its overexpression resulted in reduced Akt1 and resulted in cell cycle inhibition [264].

Modulation of drug resistance is another effect miR-495 has been associated with. miR-495 was found to target TSPAN12, a known chemoresistance factor in SCLC [265]. Another study showed that miR-495 could lead to decreased chemo-resistance to drugs in SCLC by decreasing EMT due to decreases in Etk/BMX and thus levels of Zeb-2, Twist, and Vim [266]. The role of miR-495 in restoring drug sensitivity was shown by using a miR-495 mimic in SGC7901R and A2780DX cells by suppression of MDR1 [267].

## 1.8 siRNA and siRNA + miRNA as a treatment modality

RNAi based therapy has been studied for a long time, and some of the phase I study of clinical trials have also been completed. Moreover, by 2018, FDA approved the first RNAi based drug called ‘Patisirian’ [268] which inhibits the hepatic production of transthyretin. This kind of approach illustrates the importance of treating the main cause of the disease by preventing the mRNA translation which produces disease causing protein.

Due to the fact that some of the cancers cannot be druggable, trails in RNAi based therapies gain more importance [269]. Since most of the cancers have aberrant gene expression levels which contribute to abnormal growth or pathogenesis of the tumor, silencing of those genes is an alternative way for the treatment of cancer [270]. Silencing of those genes can be achieved with antisense oligonucleotides (ASOs), short interfering RNAs (siRNAs), microRNAs (miRNAs), and so on. Basically, siRNAs and miRNAs are processed by ribonuclease III-like enzyme called as DICER; which then leads them to interact with RNA-induced silencing complex (RISC) to target and block the translation of mRNA [271], [272]. Compared to siRNA, miRNAs can have more than one mRNA target; similarly, mRNAs can also be targeted more than one miRNA [273].

Systemic administration of siRNAs in cancer treatment has the advantage of targeting both localized and metastasized tumors [274]. Among the other advantages using siRNAs as a treatment modality, it gives the opportunity to target any gene. In addition to this, specificity of targeting can be increased with the chemical modifications and sequence specific designs which prevent the off-target possibility [275]. Moreover, more than one gene can be targeted one at a time. As an example, three siRNA molecules targeting KRAS, PIK3CA and PIK3CB were encapsulated by nanoparticles and delivered to tumor xenografts. This approach increased the efficiency without inducing any toxicity [276].

Despite the effectiveness of siRNA usage as a therapy option, there also exist several challenges in terms of the stability of siRNAs due to the enzymatic degradation by nucleases [277]. One possible solution to this problem was suggested as to use various

carriers such as small molecules (i.e. cholesterol, bile acids), polymers, nanocarriers or antibodies [278] .

In addition to mRNA targeting with siRNA molecules, miRNAs are also in the center of RNAi based therapy since their deregulation are common in human diseases makes them attractive therapeutic targets as well [279]. Due to their location in the fragile sites of the human genome, miRNAs are generally aberrantly expressed in most of the cancers [280]. They participate in many biological pathways such as survival, apoptosis, angiogenesis and metastasis [281]. They can be identified as oncomiRs if they target the tumor suppressor genes; or they can be identified as tumor suppressor miRNAs if they target oncogenes [282] .

One of the most important advantages of using miRNA-based therapy is due to their multiple targeting effects. First miRNA based therapy has already been in phase I clinical trials which targets MRX34 gene by miR-34a mimics in advanced hepatocellular carcinoma patients [283]. On the other hand the upregulated miR-122 was targeted with antimiRs in the treatments of hepatitis also has reached to phase II trials [282].

Taken together the advantages of using siRNA and miRNA based strategies, the combination of miRNA and siRNAs are also widely used in the literature to improve the total anticancer effect [283] as also described with the examples in sections1.6.4.1 and 1.7.2.

## 1.9. Aims and rationale

We previously in Konu lab have shown by using a microarray study for mRNA expression that CHRNA5 downregulated several categories such as DNA replication but mainly all categories of DNA damage came out to be downregulated (Ermira Jahja, PhD Thesis). In addition, PI analysis has shown an increase in subG1 that indicates apoptosis. *In silico* analysis of siRNA microarray results in mirnet also suggested that there is similarity

between doxo and cpt signatures and there could be a set of microRNAs were expected to be modulated by CHRNA5 (Ermira Jahja, PhD thesis).

microRNAs regulate expression of many genes. Among the predicted targets of mir15/16 family is CHRNA5. However, no study exists in this respect in the literature. Furthermore, microRNA mimics are new models of cancer therapy along with siRNA molecules. Therefore, it is interesting to investigate whether mimic of a microRNA downregulated by CHRNA5 RNAi can modulate the CHRNA5 siRNA action when used together with it.

In the present study I have the following hypotheses/questions/aims:

1. Does CHRNA5 RNAi result in increased BAX and decreased BCL2 expression at the mRNA and protein levels in MCF7 cells?
2. Does CHRNA5 RNAi result in apoptosis evidenced by caspase activation?
3. Does CHRNA5 RNAi modulate CHEK1 levels whose inhibition modulates DDR and drug sensitivity using western blotting?
4. Does CHRNA5 RNAi in combination or alone modulate drug sensitivity using MTT analyses?
5. Does CHRNA5 expression levels are downregulated, upregulated or unchanged when tested in the presence of mir-15a, mir-15-b, and mir-16 mimics?
6. Does CHRNA5 RNAi affect microRNA expression profile and what is one of the most downregulated microRNA by CHRNA5 based on microRNA array statistical analysis?
7. Does use of CHRNA5 RNAi or mimic mir-495 alone or together with each other affect a) cell viability using MTT; b) pRb1 levels as a proxy of cell cycle inhibition; and c) p21 levels as proxy for p53 signaling?
8. Does use of CHRNA5 RNAi or mimic mir-495 alone or together with each other alter cell cycle distributions using FACS?
9. Does transcriptional profile of CHRNA5 RNAi correlate with that of mimic mir-495 based on comparative transcriptomics plots (log fold change vs. log fold change)?

10. What are the additively and oppositely affected genes with CHRNA5 siRNA-mimic mir-495 based on microarray analysis and can they be validated by qPCR and/or IPA?

Based on the above questions I aim to answer the role of CHRNA5 in apoptosis, DNA damage response, drug sensitivity in breast cancer as well as its interactions with microRNAs and their outcome using breast cancer cells which we already have an existing CHRNA5 RNAi model.

# CHAPTER 2: MATERIALS AND METHODS

## 2.1 Materials

### 2.1.1 General laboratory chemicals, reagents and kits

General laboratory chemicals, reagents and kits with their catalog number and company information are listed in table 2.1.

**Table 2-1**: Kits, Reagents, General Chemicals

| **Product name** | **Catalog Number** | **Company (Country)** |
|---|---|---|
| Water, molecular biology grade, nuclease free | SH30538.01 | HyClone (USA) |
| LightCycler® 480 SYBR Green I Master | 4887352001 | Roche (Switzerland) |
| LightCycler 480 Multiwell Plate 96, White | 4729692001 | Roche (Switzerland) |
| RNase-Free DNase Set (50) | 79254 | Qiagen (Germany) |
| RevertAid First Strand cDNA Synthesis Kit | K1622 | Fermentas (Canada) |
| miRscript RT Kit | 218160 | Qiagen (Germany) |
| RNeasy Mini Kit | 74104 | Qiagen (Germany) |
| miRneasy Mini Kit | 217004 | Qiagen (Germany) |
| miScript syber green kit | 218073 | Qiagen, Germany |
| NucleoBond® Xtra Midi Prep | 740412 | MN |
| Nucleospin Plasmid | 740588.50 | MN |
| QIAzol lysis reagent | 79306 | Qiagen, Germany |
| Attractene Transfection Reagent | 301007 | Qiagen, Germany |
| HiPerfect | 301704 | Qiagen, Germany |
| GeneRuler 100 bp DNA Ladder | SM0241 | Thermo Scientific (USA) |
| GeneRuler 1 kb DNA Ladder | SM0312 | Thermo Scientific (USA) |
| NaCl | 31434 | Sigma-Aldrich (Germany) |
| KCl | 12636 | Sigma-Aldrich (Germany) |
| Dimethyl sulfoxide (DMSO) | A1584 | Applichem (Germany) |
| EDTA | A3562 | Applichem (Germany) |
| Glycerol | 15524 | Sigma-Aldrich (Germany) |
| Agarose | BHE500 | Prona (Spain) |
| Ethidium bromide | 17898 | Thermo Scientific (USA) |

| | | |
|---|---|---|
| 2-mercaptoethanol | M3148 | Sigma-Aldrich (Germany) |
| Glacial acetic acid | 27225 | Sigma-Aldrich (Germany) |
| EtOH | B2221 | Sigma-Aldrich (Germany) |
| S-(+)-Camptothecin (100mg) | C9911-100MG | Sigma-Aldrich (Germany) |
| Doxorubicin | 5927S | Cell Signaling (USA) |
| SDS | 71725 | Sigma-Aldrich (Germany) |
| HCl | 7102 | Sigma-Aldrich (Germany) |
| NaOH | 6203 | Sigma-Aldrich (Germany) |
| MetOH | 24229 | Sigma-Aldrich (Germany) |
| Tween-20 | 822184 | Merck (USA) |
| Propidium iodide solution | P4864 | Sigma-Aldrich (Germany) |
| RNase A | 34388 | Serva (Germany) |
| Triton X-100 | T8787 | Sigma-Aldrich (Germany) |
| Trisma HCl | T3253 | Sigma-Aldrich (Germany) |
| Trisma Base | T1503 | Sigma-Aldrich (Germany) |
| Bacto-tryptone | 1612 | Conda (Spain) |
| Yeast Extract | 1702 | Conda (Spain) |
| Agar (microbiology grade) | 5039 | Sigma-Aldrich (Germany) |
| MTT | M6494 | Invitrogen |
| Glycine | G8898 | Sigma-Aldrich (Germany) |
| Ammonium persulfate | A3678 | Sigma-Aldrich (Germany) |
| TEMED | A11480100 | Applichem (Germany) |
| NP-40 | A16940250 | Applichem (Germany) |
| cOmplete, EDTA-free | 11873580001 | Roche (Switzerland) |
| TGX Stain-Free™ FastCast™ Acrylamide Kit, 10% | 1610183 | BIORAD |
| PageRuler Prestained Protein Ladder | 26616 | Thermo Scientific (USA) |
| PVDF membrane | 3010040 | Roche (Switzerland) |
| ECL Plus Western Blotting Detection System | RPN 2232 | GE Healthcare (UK) |
| MXBE-Film | 771 0783 | Carestream (USA) |
| Amersham ECL Prime Western Blotting Detection Reagent | RPN2232 | sigma |
| Phosstop Easypack phosphatase inhibitor cocktail tablets | 4906845001 | Roche |
| Kodak Medical X-ray Film General Purpose Blue/E 18x24 cm | 8143059 | Carestream |

| | | |
|---|---|---|
| BCA Protein Assay kit | 23227 | Thermo Scientific, USA |
| Ponceau S solution | P-7170 | Sigma Aldrich, USA |
| 4X Laemmli Sample Buffer | 161-0747 | Bio-Rad |
| BSA | A7905 | Sigma Aldrich, USA |
| 6-Aminocaproic acid | A2504 | Sigma-Aldrich (Germany) |

## 2.1.2 Nucleic Acids used in the Experiments

The information of nucleic acids of the three siRNA molecules, miRNA primers miRNA mimics which are all obtained from Qiagen, together with plasmids obtained from Addgene are listed in table 2.2.

**Table 2-2:** List of Nucleic Acids

| **Name of the Nucleic Acids** | **Catalog Number** | **Description** |
|---|---|---|
| Hs_CHRNA5_5 FlexiTube siRNA | SI03051111 | siRNA-1 |
| Hs_CHRNA5_7 FlexiTube siRNA | SI03099453 | siRNA-2 |
| Hs_CHRNA5_6 FlexiTube siRNA | SI03096940 | siRNA-3 |
| AllStars Negative Control siRNA | SI03650318 | siRNA-CN |
| Syn-hsa-miR-495-3p miScript miRNA Mimic | MSY0002817 | MIMAT0002817: 5'AAACAAACAUGGUGCACUUCUU |
| Hs_miR-495_1 miScript Primer Assay | MS00004347 | MIMAT0002817: 5'AAACAAACAUGGUGCACUUCUU |
| Hs_RNU6-2_11 miScript Primer Assay | MS00033740 | Reference gene for miRNA study |
| Hs_miR-15a_1 miScript Primer Assay | MS00003178 | MIMAT0000068: 5'UAGCAGCACAUAAUGGUUUGUG |
| Hs_miR-15b_2 miScript Primer Assay | MS00008792 | MIMAT0000417: 5'UAGCAGCACAUCAUGGUUUACA |
| Hs_miR-16_2 miScript Primer Assay | MS00031493 | MIMAT0000069: 5'UAGCAGCACGUAAAUAUUGGCG |

| | | |
|---|---|---|
| mEGFP-N1 | Addgene Plasmid# 54767 | Empthy Backbone ;Excitation: 488, Emission: 507 |
| EBFP2-N1 | Addgene Plasmid #54595 | Empthy Backbone;Excitation: 383, Emission: 448 |

### 2.1.3 PCR primers

The sequence, amplicon size and efficiencies of PCR primers used in this study are listed in table 2.3. (#Primers and related parameters that have been previously reported in PhD Thesis of Ermira Jahja (2017)).

**Table 2-3:** Primer Pairs

| | | | |
|---|---|---|---|
| **Name** | **Primer sequence (5'-3')** | **Size of amplicon (bp)** | **Amplification efficiency** |
| CHRNA5_v1# | F: AGATGGAACCCTGATGACTATGGT | 104 | 1.87 |
| | R: AAACGTCCATCTGCATTATCAAAC | | |
| CHRNA5_v2# | F: GGAAACTGAGAGTGGTAGTGGA | 122 | 1.95 |
| | R: CTTCAACAACCTCACGGACA | | |
| CHRNA5_v3# | F: CATCAGGTGTTGAAGATTGGAAAT | 101 | 1.92 |
| | R: AAAAAGCCCAAGAGATCCAACAAT | | |
| CHRNA5_iso2 * | F: TGGAGAATGGGAGATTGTGAGTGCA | 78 | 1.97 |
| | R: CCAATCTTCAACAACCAGCAACAGC | | |
| CHRNA5_iso3 * | F: TGGAGAATGGGAGATTGTGAGTGCA | 84 | 1.96 |
| | R: CCAATCTTCAACAACGGATACCAGC | | |
| MAP1B# | F: GTTGGAAGGAAAGGCTCAGT | 110 | 1.81 |
| | R: CTTGCTGTTTCTCATGGGTC | | |
| CLDN1# | F: CTGTCATTGGGGGTGCGATA | 118 | 1.88 |
| | R: CTGGCATTGACTGGGGTCAT | | |
| WDHD1# | F: AGCAGCCAAGGACGAGTAAA | 192 | 1.95 |
| | R: CTTCGGCTTTGGAATCAGAG | | |
| ANLN# | F: TAAAGCAGGTGATTGTTCGG | 180 | 1.97 |
| | R: GTTCTTCATCAACACAGCAG | | |

| | | | |
|---|---|---|---|
| BIRC5[#] | F: GTTGCGCTTTCCTTTCTGTC | 141 | 1.92 |
| | R: TCTCCGCAGTTTCCTCAAAT | | |
| CDKN1A[#] | F: GTCACTGTCTTGTACCCTTGTG | 129 | 1.82 |
| | R: CGGCGTTTGGAGTGGTAGAA | | |
| GPNMB[#] | F: TGCTGACTGTGAGACGAACC | 204 | 1.92 |
| | R: ACACCAAGAGGGAGATCACAG | | |
| GJA1[#] | F: TCTGAGTGCCTGAACTTGCC | 171 | 2 |
| | R:CCCTCCAGCAGTTGAGTAGG | | |
| GADD45A[#] | F:TCTCGGCTGGAGAGCAGAAGAC | 121 | 1.96 |
| | R:AGCTTGGCCGCTTCGTACAC | | |
| BAX | F:GGGTTGTCGCCCTTTTCTAC | 198 | 2.09 |
| | R:CTGGAGACAGGGACATCAGT | | |
| BCL2 | F:TGAACTGGGGGAGGATTGTG | 183 | 2.04 |
| | R:CGTACAGTTCCACAAAGGCA | | |
| FAS | F:AATAAACTGCACCCGGACCC | 192 | 2.06 |
| | R:AGAAGACAAAGCCACCCCAA | | |
| CCND1 | F:CTGCGAAGTGGAAACCATCC | 199 | 1.97 |
| | R:GCACTTCTGTTCCTCGCAGA | | |
| CCNE2 | F:GTAGCTGGTCTGGCGAGGTTT | 83 | 2.08 |
| | R:GGGCTGCTGCTTAGCTTGTAA | | |
| CHEK1 | F:TGGTCACAGGAGAGAAGGCA | 151 | 1.72 |
| | R:CAGATAAACCACCCCTGCCA | | |
| TPT1[#] | F:GATCGCGGACGGGTTGT | 100 | 1.95 |
| | R:TTCAGCGGAGGCATTTCC | | |
| SDHA[#] | F: TGGGAACAAGAGGGCATCTG | 86 | 2.01 |
| | R: CCACCACTGCATCAAATTCATG | | |

### 2.1.4 Antibodies used in western blot

The primary and the secondary antibody information used in western blot experiments are listed in table 2.4.

**Table 2-4:** Antibody Information

| **Antibody Information** | **catalog No:** | **Company** |
|---|---|---|
| CHRNA5 [EPR5395] | ab157470 | ABCAM |
| GAPDH | sc-47724 | SantaCruz |
| BAX | #5023 | Cell signalling |
| BCL2 | #2870 | Cell Signalling |
| Total -CHEK1 | sc-8408 | SantaCruz |
| pCHEK1[Ser345] | #2348 | Cell Signalling |
| Phospho-RB1[Ser807/811]* | #9308 | Cell Signaling |
| γH2AX [Ser139]* | #9718 | Cell Signaling |
| Total-Caspase-7** | #9492 | Cell Signaling |
| cleaved caspase-7 * | #8438 | Cell Signaling |
| Anti-rabbit IgG, HRP-linked | #7074 | Cell Signaling |
| Anti-mouse IgG, HRP-linked | #7076 | Cell Signaling |
| | | |
| (*) Kind gifts from Dr.Özgür Şahin | | |
| (**) Kind gift from Prof.Dr İhsan Gürsel | | |

## 2.1.5 Equipment used in the study

Names and company information of the devices and machines used in this study are listed in table 2.5.

**Table 2-5:** List of Equipment

| **Name of the instrument** | **Company** |
|---|---|
| LightCycler 480 Instrument | Roche (Sweitzerland) |
| µQuant elisa reader | Biotek (USA) |
| Thermal cycler TC-512 | Techne (UK) |
| BD Accuri C6 | BD Biosciences (USA) |
| PCR Thermal Cycler 2720 | Applied Biosystems (USA) |
| Hyperprocessor (x-ray) | Amersham (Mexico) |
| NanoDrop ND-1000 | Thermo Scientific (USA) |

| | |
|---|---|
| DIC Microscope | Leica (DMi8) |
| Amersham (TM) Imager 600 | GE Healthcare Life Sciences(USA) |

## 2.2 Solutions and media

### 2.2.1 Common solutions

Common solutions and buffers used in this study are listed in table 2.6.

**Table 2-6:** General Buffers and Solutions

| Solution | Content |
|---|---|
| TE buffer(pH8.0 10mM) | 1ml 1M Tris-HCL(pH: 8), 0.2ml 0,5M EDTA(pH:8) 98.8ml dd$H_2O$ |
| MTT | 0,01g MTT,2ml Streile 1X PBS |
| SDS-HCL solution | 2 g SDS, 16µL HCl, 20mL dd$H_2O$ |
| PI solution | 5 µl 1mg/ml PI, 5 µl 100% Triton-X, 100 µl RNase A, NF-$H_2O$ upto 10mL |
| L-agar | 5 g tryptone, 2,5 g yeast extract, 5g NaCl ,7,5 g Bacto agar dd$H_2O$ upto 500mL |
| L-broth | 5 g tryptone, 2,5 g yeast extract, 5g NaCl dd$H_2O$ upto 500mL |
| 50x TAE buffer | 242 g Trisma base, 18.6 g EDTA, 57.1 ml glacial acetic acid, d$H_2O$ upto 1L |
| 1.5% Agarose gel | 1.5 g agarose, 100mL (1X)TAE buffer, 3 µl 1mg/ml EtBr |

### 2.2.3 Cell culture solutions and media preparations

Chemicals, reagents and media which are needed for handling of cell lines are listed in table 2.7.

**Table 2-7:** Cell Culture Solutions

| Products | Catalog No | Company |
|---|---|---|
| DMEM w/1.0 g/L glucose w/o L-Glut | BE12-707F | Lonza |
| DMEM, low glucose, pyruvate, no glutamine, no phenol red | 11880028 | GIBCO |
| PBS-1X w/o Ca, Mg | BE17-516F | Lonza |
| FBS | S181G-500 | Biowest |
| NEAA 100X | BE13-114E | Lonza |
| Sodium Pyruvate Solution 100 mM | BE13-115E | Lonza |
| Pen/strep stock | DE17-602E | Lonza |

| | | |
|---|---|---|
| L-glutamine 200 mM | BE17-605E | Lonza |
| Trypsin-Versene(EDTA) Mix(1X) | BE17-161E | Lonza |

## 2.2.4 Solutions used in western-blot

Buffers, chemicals and solutions used during western blot experiments are listed in table 2.8 and the composition of 10% SDS-PAGE used in this study is shown in table 2.9.

**Table 2-8:** Western Blot Reagents and Solutions

| **Reagent/Solution** | **Content** |
|---|---|
| PI (25X) | 2 tablets in 840µL dd$H_2O$ |
| PhosStop(20X) | 2 tablets in 1mLdd$H_2O$ |
| 4X SDS Loading Dye | 100uL 2-mercaptoethanol , 900 µl BioRad Laemmli Buffer |
| RIPA buffer | 75 µl 2M NaCl, 50 µl 1M Tris-HCl, 10 µl 10% SDS, 40 µl 25x proteinase inhibitor, 40 µl 20X PhoStop,775 µl dd$H_2O$ (for 1mL) |
| 10x Running buffer | 30.3 g Trisbase, 144.1 glycine, 100 ml 10% SDS, dd$H_2O$ upto 1L |
| Anode I buffer | 18.15g Trisbase, 100ml 100%MetoH, dd$H_2O$ upto 500mL |
| Anode II buffer | 1.5g Trisbase,100ml 100%MetoH, dd$H_2O$ upto 500mL |
| Cathode buffer | 2.62 g aminocaparoic acid, 100ml 100%ethanol, dd$H_2O$ upto 500mL |
| Blocking solution (5%) | 5 g BSA, 100 mL TBS-T(2%) |
| 10% APS | 0,5 APS, 5mL dd$H_2O$ |
| 10X TBS | 24 g Tris, 88 g NaCl dissolve in 900 ml dd$H_2O$. PH adjusted to 7.6, volume bring up to 1000ml. |
| 1X TBS-T (Tween 0.2%) | 100ml from 10X TBS, 900 ml dd$H_2O$, 2ml Tween-20. |
| 10X Running Buffer | 10.08 g SDS, 30.3 g Trismabase, 144g Glycine, volume up to 1000ml with ddH2O. |
| Mild Stripping Buffer | 1.5g Glycine, 0.1g SDS, 1ml Tween-20 volume up to 50 ml; adjust pH 2.2, complete volume to 100mL |

**Table 2-9:** Composition of 10% SDS-PAGE

| Solutions | Resolver Gel | Stacking Gel |
|---|---|---|
| Solution A (ml) | 4 | 1,5 |
| Solution B (ml) | 4 | 1,5 |
| 10% APS (µl) | 40 | 15 |
| TEMED (µl) | 4 | 3 |

# 2.3 Methods

## 2.3.1 General maintenance and handling of cell lines

Cells were kept in cryo-vials which were then preserved in liquid nitrogen tanks. Upon needed, cells were thawed in water bath at 37$^{o}$C and immediately resuspended with complete DMEM, and briefly centrifuged for 3 min at 1500 rpm in order to remove the freezing medium. Then, obtained pellet was resuspended with complete DMEM and cells were transferred to T-25 tissue culture flasks and left in 5% $CO_2$, 37$^{o}$C incubator for one day. In the following day, after the removal of media, cells were washed with 1X sterile PBS, and then trypsinized with 0.25% Trypsin /EDTA for 5 min. Cells were resuspended with complete DMEM and centrifuged for 3 min to obtain cell pellets. After the removal of supernatant, cells were transferred to T75 tissue culture flasks in order to let them expand. Depending on the growth rate of the cells, if they reach 80-90% confluency, cells were passaged as follows: after the removal of media, cells were washed with 1X sterile PBS, and then trypsinized with 0.25% Trypsin/EDTA for 5 min. Cells were collected with fresh DMEM and split into the flasks with appropriate dilutions depending on the growth rate of the cells. When cells reached to 80-90% of confluency, they were again split into 1:2 or 1:5 depending on the growth rate of the cells.

The day before a specific experimental treatment, a culture plate having a specific number of cells (i.e. 2000 cells/ well for 96 well plate, and 200 000 cells/ well for 6 well plate throughout the study) was prepared.10µl of cell suspension was taken and cells were counted with a glass hematocytometer under inverted light microscopy. Average number of cells was multiplied with $10^4$ giving the number of cells in 1 ml. According to this, required number of cells was calculated and taken from cell suspension and then the volume was completed with fresh DMEM to a final volume required to be distributed evenly between the wells/plates.

For the continuity of the cell lines, at early passages, cells were frozen with appropriate freezing medium (90 % sterile filtered FBS and 10% DMSO for MCF7 and MDA-MB-231 cells; 80% complete media, 10% DMSO for BT-20 cells). After obtaining the cell pellets as explained above, they were resuspended in 2ml freezing media and transferred into cryo-vials to be kept at -20 $^{o}$C for 1h followed by overnight incubation at -80 $^{o}$C. Next day, the cryo-vials were transferred to liquid nitrogen tanks.

### 2.3.2 Transfection and co-transfection with siRNA and miRNA mimics

For CHRNA5 silencing, 3 siRNA molecules, which were optimized at different concentrations, were complexed with Hiperfect Transfection Reagent (Qiagen) at a ratio of 1:12 (µl), (nucleic acid: transfection reagent) (Ermira Jahja, PhD Thesis, August, 2017). Effective silencing of CHRNA5 in MCF7 cells was achieved with siRNA-1 (Flexitube SI0305111) at a final concentration of 10 nM; with siRNA-2 (Flexitube SI03099453) or siRNA-3 (Flexitube SI03096940) at a final concentration of 50nM. For each siRNA treatment, a negative siRNA-control (siRNA-CN) (AllStars Negative control siRNA 1027281) was used at a corresponding siRNA concentration. For co-transfection experiments, 10nM of Syn-hsa-miR-495-3p miRNA mimic (MSY0002817) was used; alone or in combination with siRNA-1 and/or siRNA-CN molecules.

For BT-20 and MDA-MB-231 cells, effective silencing of CHRNA5 was achieved with siRNA-1 at a concentration of 10nM and 50nM, respectively.

The day before transfection, 200.000 cells/well for 6 well plate and 2.000 cells/well for 96 well plates, were seeded and at the day of transfection or co-transfection, media were replenished with fresh DMEM. In each reaction tube, first 12 µl transfection reagent was added and then required volume of siRNA molecules and/ or miRNA mimic were added which were then left at room temperature for 10 min to let complex formation. Transfection complexes were added to the cells as dropwise and plates were placed in incubator at 37$^{o}$C. For 120 h of treatments, at the end of 48$^{th}$ h an additional transfection was performed. At the end of the incubation period, the cells treated with only siRNA or siRNA-CN were collected and after snap-freezing, pellets were kept at -80 $^{o}$C for RNA isolation. For co-transfected cells with siRNA-1/siRNA-CN and miRNA mimic, cells were collected with Qiazol lysis reagent, and after snap freezing, they were also kept at -80 $^{o}$C for miRNA and RNA isolations. Each treatment was performed in duplicates.

### 2.3.4 RNA and miRNA isolations

For RNA isolation, cell pellets were placed on ice and RNA was isolated with RNeasy Mini Kit (Qiagen) by following the kit's instructions. At the end of isolation, RNA was eluted with 35µl RNase/DNase free water, and concentration was measured with Nanodrop spectrophotometer (ThermoScientific).

In miRNA study, cells which were collected with Qiazol lysis reagent, were placed on the bench and thawed for 5 minutes. Then, after the chloroform addition at a ratio of 1:5 (choloroform : Qiazol), isolation was done using miRNeasy Kit (Qiagen) by following the instructions. At the end of the protocol, RNAs were eluted with 35µl RNase/DNase free water, and concentration was measured with Nanodrop spectrophotometer.

### 2.3.5 cDNA synthesis of mRNAs and miRNAs

In order to check mRNA levels of the samples treated siRNA molecules, 1µg of total RNA was taken and cDNA synthesis was obtained with RevertAid first strand cDNA synthesis kit (Fermentas) by following the kit's instructions.

To check miRNA levels of the samples treated with siRNA molecules together with miRNA mimic, 800µg of total RNA was taken, and by using HiSpec Buffer coming with the miRscript RT II kit (Qiagen) cDNA synthesis was performed. Diluted cDNAs were kept at -20 $^{o}$C; and undiluted stocks were kept at -80 $^{o}$C for further use.

### 2.3.6 Primer design and primer efficiency

Primers for checking the gene expression levels were designed by using 'Primer-Blast' tool from National Centre for Biotechnology Information (NCBI) online software (http://www.ncbi.nlm.nih.gov). In between the primer pair options the ones giving a product at maximum 200bp, were picked which at the same time are spanning an exon-exon junction, or spanning at least one long intronic region. The selected primer pairs then tested *in silico* by using the 'In silico PCR' tool of UCSC Genome Bioinformatics website (http://www.genome.ucsc.edu).

Primer efficiencies were calculated for only the primers designed (see Table for all primer sequences, amplicon sizes, and efficiencies) and done by using either 5 fold dilution series (1:5, 1:25, 1:125,1:625) or 2 fold dilution series (1:2,1:4,1:8,1:16) of cDNA. Linear graph was plotted by using $Log_{10}$ (cDNA dilution) against related Ct values. To obtain the average amplification efficiency of each primer pair, the slope of the graph was used in this formula: ***Eq (1):*** $Effciency = 10^{-1/slope}$. Ermira Jahja, Sıla Özdemir and Ilgın Cağnan contributed to the efficiency studies.
For detection of miRNA levels, forward and reverse primers were purchased from Qiagen and hence efficiencies of these primers were assumed as 2.

### 2.3.7 Real-time PCR and expression analysis

Gene expression levels were detected by using LightCycler® 480 Instrument (Roche, Ref:04 887 352 001). PCR reaction volume was reduced to 10µl composing of 1µl forward primer (10µM), 1µl Reverse primer (10µM), 5µl 2X SYBR Green I Master mix (04707516001), 1µl Nuclease free water and 2µl cDNA. The PCR conditions were adjusted according to Table 2.10. For only siRNA related part of the study, SDHA was used as a reference gene for the normalization of gene expression level.

**Table 2-10:** RT-qPCR conditions for the detection of gene expression levels

| Step | Hold Temperature(°C) | Hold Time (seconds) | Number of cycles |
|---|---|---|---|
| **Pre-incubation** | 95 | 5 | 1 |
| **Denaturation** | 95 | 10 | - |
| **Annealing** | 58-60 | 20 | 40-50 |
| **Extention** | 72 | 20 | - |
| | 95 | 5 | |
| **Acquisition** | 55 | 60 | 1 |
| | 95 | Continuous | |
| **Final Extention** | 40 | 30 | 1 |

miRNA levels were detected by using LightCycler® 480Instrument. PCR reaction mixture was composed of 1 µl miRNA specific miScript Primer Assay, 1 µl reverse primer (Universal Primer, Qiagen), 5 µl 2x QuantiTect SYBR Green PCR Master Mix (218073), 1µl Nuclease free water and 2µl cDNA which was synthesized with miRscript RT II kit. Reaction condition was adjusted as indicated in Table 2.11. miRNA expression levels were normalized with snRNA RNU6B (RNU6-2) expression levels. In this miRNA-siRNA part of the study, gene expression levels were again detected with the same protocol as mentioned above but as the reference gene, TPT1 was used.

**Table 2-11**:RT-qPCR conditions for the detection miRNA expression levels

| Step | Time | Tempertature (ºC) |
|---|---|---|
| **PCR initial Activation** | 15min | 95 |
| **3 –step cycling:** | | |
| **Denaturation** | 15sec | 94 |
| **Annealing** | 30sec | 55 |
| **Extention** | 30sec | 70 |
| **Cycle Number** | 40 cycles | |

During RT-qPCR studies, Ct (cycle threshold) values were obtained from the average of two of the technical replicates. By using the efficiency values of each primer as stated in Table 2.3, expression levels of the genes were calculated according to 'Eq (2)'. Final conclusion about expression levels of genes was achieved with log(2) transformation of $\Delta\Delta Ct$ values.

$$\boldsymbol{Eq\ (2)}: Relative\ Expression(\Delta\Delta Ct) = Eff^{\Delta CtTarget(control-treatment)} \Big/ \Delta CtRef(control-treatment)$$

## 2.3.8 Toxicity detection of siRNA and miRNA mimics (alone or in combination) with MTT Assay

The day before treatment, 2.000 cells/well were seeded in 96 well plates. Same transfection conditions and protocol were used as mentioned in Section 2.3.2. At the end of 72h, MTT ((3-(4,5-Dimethylthiazol-2-yl)-2,5-Diphenyltetrazolium Bromide) reagent was prepared by dissolving 0,01g MTT with 2ml 1X sterile PBS, vortexed thoroughly and sterile filtered. Each of the experimental wells received 100 µl of fresh phenol free DMEM mixed with 10 µl of sterile filtered MTT reagent. It is important to use phenol free DMEM at this stage, which otherwise interferes with absorbance values. After the addition of MTT mixture, the plate was left in the incubator (37 ºC) for 4 h. At the end of 4 h, freshly prepared SDS- HCL solution (100 µl), which was prepared by dissolving 2gr SDS in 20ml water along with16 µl of HCL, was distributed as 100 µl to each well. The plate was left in

the incubator (37 $^{o}$C) maximum for 18 h and absorbance values were obtained at a wavelength of 570 nm by using Microplate Spectrophotometer (μQuant, Biotek). Results were analyzed by using One-Way ANOVA and multiple t-test comparisons (Tukey HSD test).

### 2.3.9 Drug sensitivity MTT assays in combination with siRNA molecules

Dose response of camptothecin and doxorubicin were first carried out within the range of 0-2μM (Ermira Jahja, PhD Thesis, August 2017) for MCF7 cells. In the present study, in order to test whether CHRNA5 depletion increase the sensitivity of cancer cells for these drugs, cells were exposed to lower doses of these two drugs (0.25μM, 0.125 μM, 0.06 μM, 0.03 μM, 0.015μM) in combination with siRNA molecules (siRNA-1, siRNA-2 and siRNA-CN). In the case of MDA-MB-231, only for camptothecin, a different range of dose was used (0.03μM -0,001875μM). Since these drugs were dissolved in DMSO, a group of control having the same percentage of DMSO in the presence or absence of siRNA-1 or -2 and siRNA-CN, was also included in the study. All treatment groups had at least three replicas.

In order to assess the effects of CHRNA5 depletion together with miRNA mimic exposures on cell viability, similar MTT assays carried out as mentioned above. The day before the treatments 2.000 cells/well were seeded in 96 well plates. On the day of the treatment, firstly the media change was done according to the volumes explained above. Then, the transfections were done by using the same transfection protocol (1:12 ratio for siRNA molecule: transfection reagent). At the end of 72h of incubation, the experiment was ended by the addition of MTT and SDS-HCL as explained above. Results were analyzed by using One-Way ANOVA and multiple t-test comparisons (Tukey HSD test).

### 2.3.10 Analysis of DNA replication with PI staining and 7-AAD/Brdu staining

In order to observe the combinatorial effect of siRNA and miRNA mimics on cell cycle distributions, Propidium Iodide (PI) staining and 7-AAD/BrDu staining were performed. The treatment groups were determined similar to the mRNA and protein studies as duplicates which are indicated in Table 2.12:

**Table 2-12**: Experimental Groups

| | |
|---|---|
| Only Transfection Reagent | siRNA-CN (20nM) |
| siRNA-CN (10nM) + siRNA-1 (10nM) | siRNA-CN (10nM) + miRNA mimic 495(10nM) |
| siRNA-1 (10nM) + miRNA mimic 495 (10nM) | siRNA-1(20nM) |

The day before treatment 200.000 MCF7 cells/ well seeded in 6-well plates. On the day of the treatment, the same transfection protocol was carried out after media replenishment. At the end of 72h of incubation, the media inside the wells were transferred into the separate tubes, in order not to lose detached cells. Cells attached to the wells firstly washed with 1X cold PBS and this rinse was not discarded as well, instead it was transferred to the corresponding tubes having the detached cells floating in the media which were collected one step before. After this rinse, 500 µl trypsin was added to each well, and the detached cells were collected with 2 mL DMEM which was transferred to the corresponding tubes having the cell suspension and PBS rinse before. Complete detachment of the cells from each other was provided by pipetting up and down (~40X). After observing the detachment of the cells under the microscope, cells were centrifuged at 1500 rpm for 3 min and pellet was washed with 1.5 ml cold 1X PBS. This was repeated for three times. At the end, supernatant was discarded and after the addition of 1X cold PBS on top of the tubes placed on ice, cells were fixed with the dropwise addition of 3.5ml cold 100% EtOH. After centrifugation at 1500 rpm for 4 min, pellet was washed with PBS twice. At the end of last washing, supernatant was discarded and 500 µl PI solution (50µg/ml PI, 0,1mg/ml RNase A, 0.05% Triton X-100 in PBS) was added. Stained cells

were incubated at 4 $^{o}$C for 40 min in dark, and then analysis of cell cycle distribution was carried out with FACS (BD Accuri C6).

To further get insight about the cell cycle progression of MCF7 cells upon CHRNA5 depletion along with miRNA mimic application, 7-AAD/BrDU staining was also performed. Treatments groups were kept same as mentioned above. At the end of 72h of treatments, in order to stain the DNA, BrDU(10µM) solution was added to each well and the plates were left in dark at 37 $^{o}$C for 1.5h. After the media was removed, cells were washed with 1X PBS, and then 0.5ml/well trypsin was added. When the cells detached, they were collected with the addition of 1ml fresh media into the FACS tubes which were then centrifuged 5min at 1200rpm. Next, the supernatant was removed, and the pellet was resuspended with 1ml PBS. Tubes were centrifuged as before, and at the supernatant was removed. This washing step was repeated one more time. To fix the cells, 100µl Cytofix/Cytoperm buffer was added and the tubes were left on ice for 15-30min. At the end of the incubation, cells were washed with 1ml 1X Perm/Wash buffer. Tubes were centrifuged as before, and the supernatant was removed. The obtained pellets were resuspended with 100 µl BD CytoPerm permalization plus buffer and incubated for 10 min on ice. Again, the cells were washed 1ml 1X Perm/Wash buffer and centrifuged as before. After the removal of the supernatant, DNase was added at a working concentration of 300µg/ml for each sample and incubated at 37 $^{o}$C for 1h in the dark. At the end, cells were washed with 1X Perm/Wash buffer and centrifuged as before. After the removal of supernatant, cells were resuspended with 50 µl FITC-anti BrDU antibody solution (1 µl antibody + 49 µl Perm/Wash buffer). Then the cells were incubated for 20min at RT by protecting from the light. At the end, cells were washed with 1X Perm/Wash buffer and centrifuged as before. The pellet then resuspended with 7-AADsolution (5 µl 7-AAD+95 µl staining buffer [3%FBS-PBS]). Tubes were incubated for 10 min at RT by protecting from light. Finally, 200 µl staining buffer was added and FACS analysis was performed.

### 2.3.11 Total protein extraction

As described previously, 72h or 120 h of siRNA-1, and 72h of siRNA-2 and siRNA-3 treatments were performed. At the end of incubation time, when necessary, dead cells were also collected with centrifugation at 4500-5000 rpm for 5 min. This pellet was combined with the pellet obtained with scraping procedure where the cells first washed with cold PBS and then scraped with freshly prepared RIPA buffer (Table 2.8) on ice. This mixture left on ice for 30 min and every 5 min they were vortexed thoroughly. At the end of 30 min, samples were centrifuged at 13000 rpm for at least 20 min. Next, supernatant, which had the proteins, was taken carefully without touching the pellet to be stored at -80 $^{o}$C.

### 2.3.12 BCA assay and protein quantification

Total protein concentration was measured by using BCA Protein Assay Reagent Kit (Thermo Scientific, USA, 23227) according to the manufacturer's protocol with triplicates. After getting the absorbance values, a standard curve was plotted which gave the equation '***y=ax+b'*** where the y stands for the absorbance and x stands for the concentration of the unknown sample. More importantly, the dilution factor (volume of standard/volume of measured sample) was also taken into account while reaching the final concentration of the unknown sample by multiplying the value obtained from the equation.

According to the desired concentration of protein (10µg for siRNA study, 15µg for siRNA+miRNA study; unless otherwise stated), the required volume of sample was taken, and after the addition of 4X SDS Loading dye (Biorad, USA, 161-0747), the final volume of protein mixes equalized by using RIPA buffer. Just before loading, proteins were denatured at 95 $^{o}$C for 5 min. The remaining proteins were kept at -80 $^{o}$C.

## 2.3.13 SDS-PAGE preparation and western blot

In this study, separation of proteins was carried out with 10% SDS-PAGE (161-0183, Bio-Rad Acrylamide Kit) which was prepared according to the Table 2.9. After loading of the samples and 4µl of page ladder, proteins were run at 80V; and by the time they passed from the stacking part to the resolving part, they were run at 120V. At the end of running, proteins were transferred to PVDF membrane (3010040, Roche) and semi- dry transfer for 55min (up to 1.3A, 25V) was carried out. The buffers used for running and transfer protocols were listed at Table 2.8. Membranes were stained with Ponceu Red for 5 min at RT on the shaker. Photos of Ponceu stained membranes were taken and then they were washed with distilled water to get rid of the Ponceu Red. Membranes were blocked with 5% BSA in TBS-T (0.2%) for 1h at RT and then left at 4 $^{o}$C on the shaker with the specific primary antibody for overnight incubation. The information about the antibodies used throughout this study can be found in Table 2.4. Next day, membranes were washed 3X with 1X TBST for 10 min at RT. Unless otherwise stated, secondary antibodies were prepared at a dilution of 1:5000 for all of the proteins, except 1:10000 for GAPDH, with 5% BSA and left at RT at least 1h.At the end of secondary antibody incubation, membranes were washed 3X with 1X TBST for 10min. Detection of proteins were carried out with ECL Plus Western Blotting Detection System (RPN 2232, GE Healthcare) either by capturing with MXBE-Film (771 0783, Carestream) and /or using Amersham (TM) Imager 600.

## 2.3.14 Mild stripping Protocol

In order to check more than one protein in the same membrane or to get rid of the background resulted from secondary antibody incubation; mild stripping protocol was carried out. Buffers were prepared according to Table 2.8 and all steps were done at RT. Membranes were first covered with freshly prepared stripping buffer and left for 10 min on the shaker, this was done twice. Then, they were washed with 1X TBS for 5 min, twice. After that, they were washed with 1X TBS-T two times. In the end, after they were blocked

with 5% BSA for 1h, specific primary antibodies were put and membranes were left at 4$^{o}$C for overnight incubation.

## 2.3.15 Microarray studies

### 2.3.15.1 Affymetrix microRNA microarray sample preparation and hybridization for CHRNA5 siRNA treated cells vs scrambled controls

RNAs were isolated as explained in section 2.3.4 from siRNA-1(10nm) and siRNA-CN (10nM) treated MCF7 cells (in collaboration with Başak Özgürsoy and Mehtap Yilmaz Tezcan). RIN (RNA Integrity Number) values were measured with Agilent and the ones above 9 over 10 were chosen for studying miRNA microarray (two biological replicates for each treatments). Affymetrix miRNA 4_0 platform was used (AYKA Ltd.). RMA normalization was done with R Bioconductor pakage and differential expression was obtained by *limma* package which were performed by Huma Shehwana and Başak Özgürsoy.

### 2.3.15.2 Affymetrix microRNA microarray statistical analysis and selection of mir-495 as the candidate microRNA

mRNA microarrays, obtained with CHRNA5 depleted samples and their corresponding control samples (GSE89333, Ermira Jahja, PhD Thesis), was analyzed together with miRNA microarray experiments mentioned above. When the expression of the miRNAs sorted from the most downregulated to the least, top ten significantly downregulated miRNAs got the attention to be further analyzed. Among them, hsa-miR-495-3p came in the first rank therefore for this study hsa-miR-495-3p was chosen.

#### 2.3.15.3 Affymetrix mRNA microarray sample preparation and hybridization for mir-495 mimic, mir-495 mimic+CHRNA5 siRNA, and scrambled siRNA exposure

In order to observe the changes of global mRNA expression profile upon siRNA-1 and siRNA-1 + mimic miR-495 exposures, transfection protocol was carried out as explained in section 2.3.2. After isolation, total quality of RNAs was measured with Agilent and the samples having RIN values 9 over 10 were chosen to be further studied with Affymetrix HGU Plus2 mRNA platform (AY-KA Ltd.). Quality control, RMA normalization and statistical analysis were done in collaboration with Ayşe Gökçe Keşküs.

#### 2.3.15.4 Scatterplot and correlation analysis of CHRNA5 siRNA profile with that of mir-495 mimic, mir-495 mimic_CHRNA5 siRNA profiles

mRNA microarray results obtained with CHRNA5 depleted samples and their corresponding control samples (GSE89333, Ermira Jahja, PhD Thesis) was analyzed together with siRNA-1 + mimic miR-495 microarray. Log fold changes obtained from the two microarrays were compared.

### 2.3.16 *Ingenuity Pathway Analysis (IPA)* of the gene lists affected by mimic mir-495 and mimic miR-495 +CHRNA5 siRNA-1

Normalized mRNA and microRNA microarray log fold change results were merged on excel and uploaded on IPA (Qiagan Inc) program (in collaboration with Said Tiryaki). During all analyses, ‘Core Analysis’ option was chosen and only the genes exhibiting a log fold change higher than 0.5 over log2 were taken into account. The most significant and prominent biological pathways/functions were analyzed further.

### 2.3.17 Cell morphology detection with 3-D Imaging

Transfected 6 well plates were visualized with DIC microscope (Leica DMi8). Images of the wells were taken randomly by using 10X and 40X objectives.

### 2.3.18 Preliminary studies for generation of stably EGFP & EBFP or shCHRNA5 expressing MCF7 cells

In this study, in order to obtain MCF7 cells stably expressing EGFP or EBFP, firstly polyclonal cells were obtained, later from these polyclonal cells, monoclonal cells were obtained by Said Tiryaki (Ms Thesis, 2018).The related information about polyclonal cells can be found in appendix-A. Also, in order to obtain prolonged silencing of CHRNA5, shRNA against CHRNA5 studies were initiated was well and the preliminary result can be found in appendix B.

#### 2.3.18.1 EGFP and EBFP expressing plasmid DNA isolation

Plasmids were arrived in bacterial stab. Sterilized iron loop dipped inside, and streaks were done on agar plates having the appropriate antibiotics. Next day, one single colony was picked up, and put inside the LB having the appropriate antibiotics. Tubes left at $37^0$C inside the shaker for overnight. Next day, before plasmid isolation, glycerol stocks were also done. For this (1:1) LB and glycerol mixed thoroughly and filtered. Then equal amount of LB-glyerol was mixed with LB-bacteria which were kept at -80 $^o$C for further usage. From the remaining LB-bacteria mix, plasmid isolation was done with Nucleospin Plasmid kit according to the manufacturer's protocol. Plasmid DNAs were eluted with water and concentrations were measured with nanodrop, then they were kept at -20 $^o$C.

### 2.3.18.2 Optimization of transfection conditions for EGFP and EBFP plasmids

MCF7 cells were transfected with mEGFP and EBFP plasmids according to these three steps:
Firstly, plasmid DNAs were given to MCF7 cells after complexed with Attractane Transfection reagent (301005, Qiagen) with three different volume (1µL,1.5µL,3µL) and with two different DNA concentrations (0,4µg and 0.6µg). This experiment clearly showed that more than 1.5µL Attractane Transfection reagent and more than 0.4 µg DNA resulted in toxicity in MCF7 cells.

Secondly, in addition to Attractane transfection reagent, transfection agents Lipofectamine (2000) (11668027, Thermo scientific) and PEI were also tried using different DNA concentrations.

### 2.3.18.3 Kill curve For Determination of Geneticin Concentration

Since mEGFP and EBFP cells had resistance to Geneticin (G418), determining the optimum concentration of G418 was important to have only the cells having these plasmids hence expressing either GFP or BFP. After transfecting the cells as mentioned above, different doses of G418 between 1500µg/ml -50 µg/ml were given to these cells. Plate was observed for 7 days, and the concentration resulting in toxicity at day 7 was determined as minimum concentration which was 500 µg/ml. Continuity of MCF7 cells either expressing EGFP or EBFP was carried out by providing 500 µg/ml G418 to the media.

### 2.3.18.4 shCHRNA5 plasmid isolation

The shRNA molecules were purchased from Qiagen and 5 lyophlized tubes having 4 clones targeting CHRNA5, along with the negative control were first centrifuged and transformed into DH5α competent cells. Briefly, 2µl of each plasmid was taken and dipped into 50µl competent cells which were left on ice for 30min. Next, at 42$^{o}$C heat-shock was

performed by dipping the tubes into 45ºC water. Then the tubes were immediately removed on ice for 2min. After the addition of 200 µl of LB without antibiotics, the tubes were incubated in the shaker at 37ºC for 1h at 220rpm. Next, 150 µl from each LB-bacteria mix were taken and streaked on agar plates having ampicilline (50 µg/ml) and left in the incubator at upside down position at 37ºC for overnight incubation. Next day, single colonies were taken and inoculated in LB (~3mL) having ampicilline (50 µg/ml) for 7-8 h in the shaker at 3 ºC. To get larger amounts of plasmid, at the end of 7-8 h of incubation, LB was poured into 200mL LB having ampicilline (50 µg/ml) and left for overnight incubation. In the following day, midi prep was performed with NucleoBond® Xtra Midi Prep (Macherey Nage, 740412) according to the manufacturer's protocol to get the DNAs. At the end, DNA concentrations were measured with nanodrop.

#### 2.3.18.5 shCHRNA5 transfection and RNA isolation

The day before transfections, 250.000 cells/well were seeded in 6-well plates. On the day of transfections, first media were refreshed, and 600ng DNA was diluted with culture medium without serum in a final volume of 100µl. Then 4.5µl Attractene transfection reagent (Qiagen, 3010005) was added and mixed by vortexing. The mixture was incubated at RT for 10-15min for the formation of transfection complexes. Then the complexes were added drop-wise onto the cells. Plates were left in the incubator. Next day the medium was changed in order to prevent the toxicity that might result from DNA or transfection reagent. At the end of 72h of incubations, cell pellets were collected and stored at -80ºC.

For RNA isolation, cell pellets were thawed on ice and 1ml Trizol was added. After pipetting up and down, 200µl chloroform was added and the tubes were shaked vigorously for 15 sec. Then the tubes were left at RT for 3min. Next, the samples were centrifuged at 13200 rpm for 17min at 4 ºC. Then, the aqueous phase, which was taken carefully by not touching the interphase, was mixed with 500µl isopropanol by inverting the tubes 5 times and the tubes were left at RT for 10min. Next, the samples were centrifuged at 13200rpm for 12min at 4ºC. The supernatants were discarded and1ml

sterile filtered 75% EtOH was added and the pellet was dissolved by flicking the tubes. The samples were centrifuged again at 8000 rpm for 8 min at 4$^{o}$C. Then the supernatant was discarded and 1ml sterile filtered 100%EtOH was added. The samples were centrifuged again at 8000 rpm for 8 min at 4$^{o}$C. The pellets were dried in the upside down position under the hood. Later, the pellets were dissolved with 25µl RNase/DNase free water and the concentrations were measured with nanodrop.

### 2.3.19 Statistical analysis:

Statistical analysis was done with GraphPad Prism® 6.0. RT-qPCR and MTT results were analyzed with One-Way ANOVA and multiple test comparisons (Tukey HSD test). Western blot densitometry measurements were done in collaboration with Ayşe Gökçe Keşküş. Depending on the experimental group, appropriate control was used followed by Student's t-test, One way or Two-Way ANOVA's with uncorrected Fisher's LSD tests. Here, while the main effect was drug treatments, the simple effects were siRNA treatments.

# CHAPTER 3: RESULTS

## 3.1 Downregulation of CHRNA5 using siRNA-1, -2, and -3 and validation of microarray results in siRNA-2 and siRNA-3 treated MCF7 cells.

CHRNA5 has been investigated in Konu Lab by using different breast cancer cell lines and its detailed splice variants are well presented in Sıla Özdemir's Master Thesis (2014). Briefly, CHRNA5 has 6 exons, 5$^{th}$ one being alternatively spliced resulting in 3 different splice variants (*CHRNA5_V1*, *CHRNA5_V2* and *CHRNA5_V3*). In addition to these 3 splice variants 2 isoforms (*iso2* and *iso3*) published by Falvella et al. (2013) have also been included in our studies. Specificity of primers for 3 spliced variants has been confirmed with sequencing after RT-PCR and gel extraction protocols (Ermira Jahja, PhD Thesis, 2017).

Based on previous results, downregulation of CHRNA5 variants was achieved at the end of 72 h with 3 different siRNA molecules at different doses in MCF7 cells, optimized by Ermira Jahja (PhD thesis, August 2017). While 10nM was optimal dose for siRNA-1 and for non-targeting corresponding control (Allstars Negative siRNA control stated as siRNA-CN); 50nM was optimal for siRNA-2 and siRNA-3 hence for their corresponding non-targeting control in MCF7 cells. siRNA molecules were given to the cells after complexed with 12µl Hiperfect transfection reagent as explained in materials and methods chapter. Downregulation of each of these 5 variants of CHRNA5 with siRNA-1 molecule was shown previously (Figure 3.5B; Ermira Jahja's PhD thesis).

In the present study, I showed downregulation of the same series of CHRNA5 variants with siRNA-2 and siRNA-3 molecules at mRNA levels and along with siRNA-1 at protein levels (Figure 3.1A-B) at 72 h of exposure together with densitometry analysis (Figure 3.1C-D). Complementing the previously shown phalloidin staining results (Figures 3.14,

3.15 and 3.16 of Ermira Jahja, PhD Thesis, 2017), in the present study, I showed the phenotypical changes upon CHRNA5 depletion with DIC microscopy as well (Figure 3.1E, F, G, H and I). Accordingly, MCF7 cells lost their typical spherical structure and some cells exhibited a more branched as well as sparse appearance in the presence of siRNA molecules at the end of 72 h of treatments.

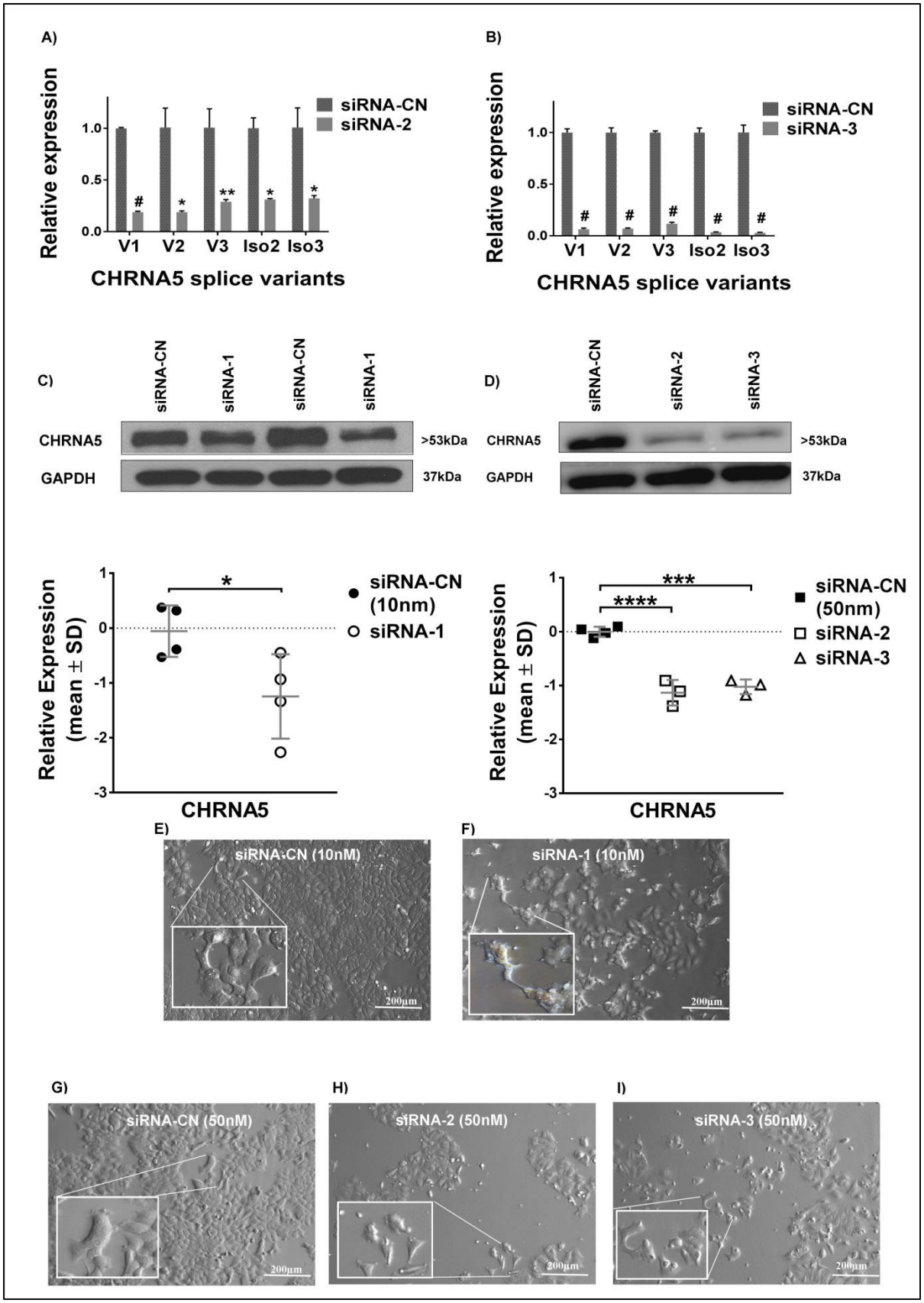
A)
Relative expression
siRNA-CN
siRNA-2
1.0
0.5
0.0
#
*
**
*
*
V1
V2
V3
Iso2
Iso3
CHRNA5 splice variants
B)
Relative expression
siRNA-CN
siRNA-3
1.0
0.5
0.0
#
#
#
#
#
V1
V2
V3
Iso2
Iso3
CHRNA5 splice variants
C)
siRNA-CN
siRNA-1
siRNA-CN
siRNA-1
CHRNA5
>53kDa
GAPDH
37kDa
D)
siRNA-CN
siRNA-2
siRNA-3
CHRNA5
>53kDa
GAPDH
37kDa
Relative Expression
(mean ± SD)
1
0
-1
-2
-3
*
siRNA-CN
(10nm)
siRNA-1
CHRNA5
Relative Expression
(mean ± SD)
1
0
-1
-2
-3
***
****
siRNA-CN
(50nm)
siRNA-2
siRNA-3
CHRNA5
E)
siRNA-CN (10nM)
200μm
F)
siRNA-1 (10nM)
200μm
G)
siRNA-CN (50nM)
200μm
H)
siRNA-2 (50nM)
200μm
I)
siRNA-3 (50nM)
200μm

**Figure 3.1: Downregulation of CHRNA5 expression with RNAi**. Downregulation of CHRNA5 isoforms at mRNA levels treated with 72 h of siRNA-2 **(A)**, with siRNA-3 **(B)** (n=2 per group). Downregulation of CHRNA5 at protein level with siRNA-1 **(C)** (n=4 per group), with siRNA-2 and siRNA-3 **(D)** along with their densitometry analyses (n=4 for siRNA-CN, n=3 for siRNA-2 and siRNA-3).DIC microscopy images of MCF7 cells treated with 72 h of siRNA-CN (10nm) (**E**), siRNA-1(10nm) (**F**), siRNA-CN (50nm) (**G**), siRNA-2 (50nm) (**H**), siRNA-3 (50nm) (**I**). One-Way ANOVA followed by Tukey's HSD tests for RT-qPCR and Student's t-test for densitometry analysis were used, (*:p<0.05; **:p<0.01; ***,#:p<0.001; ****p<0.0001).

To observe the global transcriptional changes upon siRNA-1 exposure, a microarray study was performed with 72 h siRNA-1 treated MCF7 cells in comparison with control siRNA treated cells (Figure 3.8 A, Ermira Jahja, PhD Thesis, 2017). Moreover, expressions of the selected genes were validated with RT-qPCR studies (Figure 3.8A; Ermira Jahja, PhD Thesis, 2017).

In the present study, these findings were also supported with 72h treatment of siRNA-2 and siRNA-3 in MCF7 cells by RT-qPCR (Figure 3.2). While the depletion of CHRNA5 resulted in upregulation of cytoskeletal (MAP1B, CLDN1 and GJA1) and p53 pathway (GADD45A, GPNMB, CDKN1A) related genes, it also resulted in downregulation of cell cycle associated genes (ANLN, BIRC5 and WDHD1).

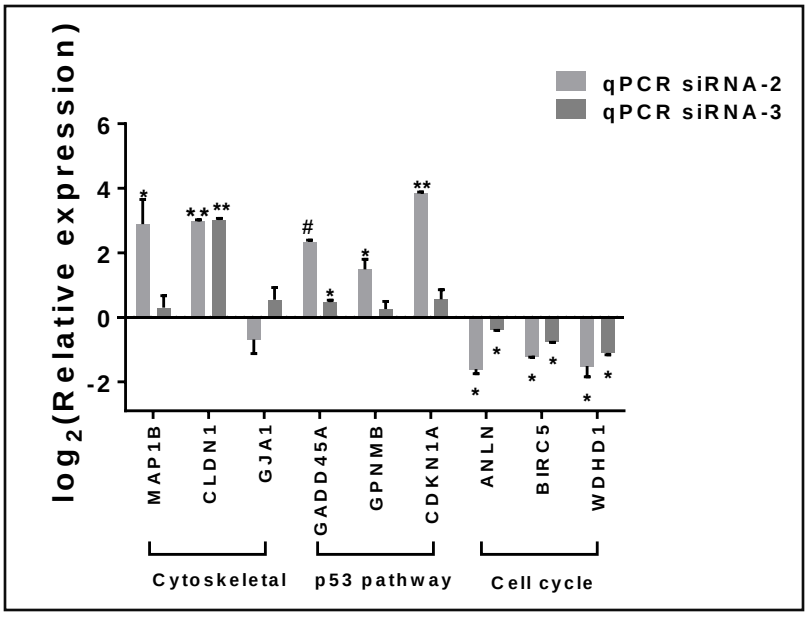


**Figure 3.2: RT-qPCR validation of CHRNA5 RNAi microarray data**. Validation of microarray findings with RT-qPCR of selected genes by using 72 h of independent siRNA-2 and siRNA-3 exposure studies (n=2 per group). Student's t-tests in comparison with their corresponding siRNA-CN group was performed, (*: $p<0.05$; **: $p<0.01$, #: $p<0.001$).

## 3.2 Validation of effects of CHRNA5 depletion on cell viability using multiple siRNA molecules

Since transcriptional results and microscopic findings indicated reduced cell viability in the presence of siRNA-1, an MTT assay was performed with 3 siRNA molecules at 72h in MCF7 cells. Each siRNA molecule significantly reduced cell viability when compared to their controls (Figure 3.3).

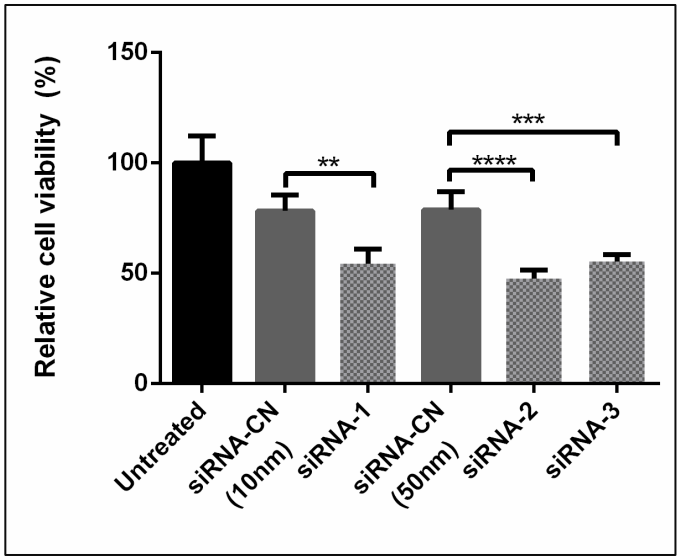


**Figure 3.3: The Effects of CHRNA5 depletion on cell viability in MCF7 cells**. Relative cell viabilities of MCF7 cells upon 72h of siNRA-1 (10nM), siRNA-2 (50nM) and siRNA-3 (50nM) transfections (n=3 per group). One-Way ANOVA followed by Tukey's HSD tests was used. (**: p<0.01; ***: p<0.001; ****: p<0.0001).

## 3.3 Effects of CHRNA5 RNAi on apoptosis and DNA damage in MCF7 cells

Based on the above-mentioned results obtained with MTT and reduced DNA synthesis rates based on BrDU incorporation assay (Ermira Jahja, PhD Thesis, 2017) the key regulators of cell cycle were investigated with Western blotting and RT-qPCR in order to reveal the mechanisms behind G1-S arrest measured by PI staining (Ermira Jahja, PhD Thesis, 2017) upon CHRNA5 depletion. One of the key points during cell cycle progression is the phosphorylation status of RB (Retinoblastoma) protein. Despite there was not a change in RB mRNA levels upon CHRNA5 depletion (i.e., log FC -0.077, p=0.37), decreased pRB (S807/811) levels with all three CHRNA5 targeting siRNA molecules were observed (Figure 3.4A, B and C) which further supported that MCF7 cells were arrested during G1-S transition. Reduction in cell viability, enrichment of cells at G1 phase together with the floating cells that were observed with DIC microscopy further prompted me to check whether the end point of these events could be apoptosis. One of the most important apoptotic marker cleaved-CASP7 was significantly increased upon

72h of siRNA-1 treatment (Figure 3A). Consistent with this, the decreased levels of total CASP7 levels and hence increased levels of cleaved CASP7/total CASP7 ratio also further supported this finding (Figure 3.4G). However, this significant alteration in cleaved CASP7 level could not be observed with siRNA-2 and siRNA-3 treatments (Figure 3B and G). However, significant increases in pro-apoptotic protein BAX and decreases in anti-apoptotic protein BCL2 levels with 72h of siRNA-1 and siRNA-2 levels, which were also reflected as increased BAX/BCL2 ratio, further supported apoptosis was taking place upon CHRNA5 depletion (Figure 3.4A, B and D). Despite being not significant, 72h of siRNA-3 treatment also exhibited the same trend with siRNA-1 and siRNA-2 (Figure 3.4B and G).

Based on the GSEA enrichment analysis of microarray data (in collaboration with Huma Shehwana and Ayse Gokce Keskus), DNA Damage Response (DDR) appeared as one of the most significantly altered pathways upon CHRNA5 depletion. This observation was further supported with significant decreases of total CHEK1 and pCHEK1 (S345) at protein levels with 72h siRNA-1 and siRNA-2 of treatments. 72h of siRNA-3 treatment significantly decreased the levels of total CHEK1 (Figure 3.4E). Although pCHEK1 level exhibited a decreased trend with 72h of siRNA-3 treatment, this was not found significant (Figure 3.4F).

Previous studies with breast as well as other cancer types such as leukemia and lymphoma have shown the association between the inhibition of CHEK1 and increased levels of pH2AX (319) levels [284], [285], [286]. Although there was an increasing trend upon 72h of siRNA-1 treatment, the results obtained with three different siRNAs were not consistent, since pH2AX exhibited labile expression levels (Figure 3.4A, B and H).

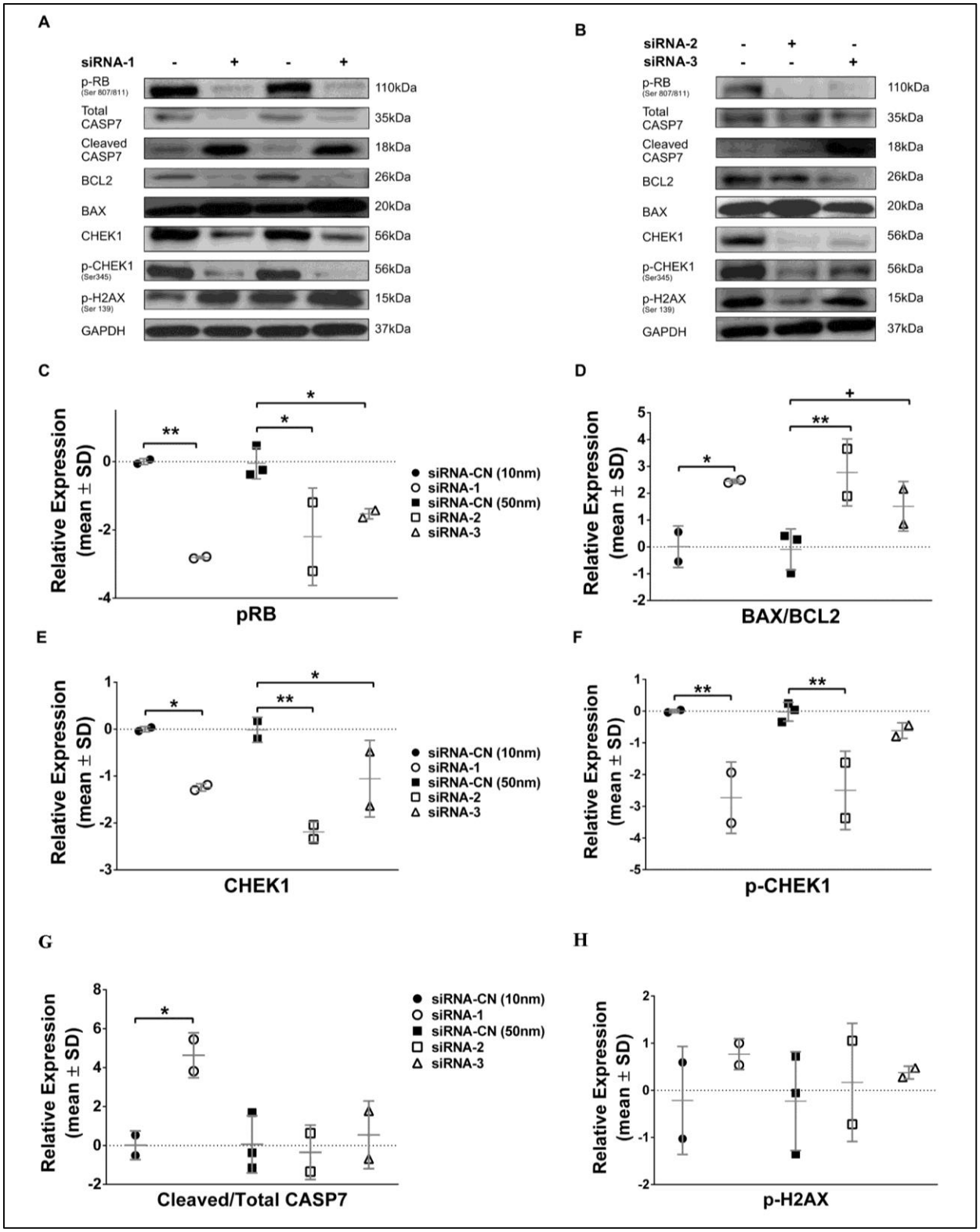
A
siRNA-1 - + - +
p-RB (Ser 807/811) 110kDa
Total CASP7 35kDa
Cleaved CASP7 18kDa
BCL2 26kDa
BAX 20kDa
CHEK1 56kDa
p-CHEK1 (Ser345) 56kDa
p-H2AX (Ser 139) 15kDa
GAPDH 37kDa
B
siRNA-2 - + -
siRNA-3 - - +
p-RB (Ser 807/811) 110kDa
Total CASP7 35kDa
Cleaved CASP7 18kDa
BCL2 26kDa
BAX 20kDa
CHEK1 56kDa
p-CHEK1 (Ser345) 56kDa
p-H2AX (Ser 139) 15kDa
GAPDH 37kDa
C
Relative Expression (mean ± SD)
pRB
siRNA-CN (10nm)
siRNA-1
siRNA-CN (50nm)
siRNA-2
siRNA-3
D
Relative Expression (mean ± SD)
BAX/BCL2
E
Relative Expression (mean ± SD)
CHEK1
siRNA-CN (10nm)
siRNA-1
siRNA-CN (50nm)
siRNA-2
siRNA-3
F
Relative Expression (mean ± SD)
p-CHEK1
G
Relative Expression (mean ± SD)
Cleaved/Total CASP7
siRNA-CN (10nm)
siRNA-1
siRNA-CN (50nm)
siRNA-2
siRNA-3
H
Relative Expression (mean ± SD)
p-H2AX

**Figure 3.4: Effects of CHRNA5 depletion apoptosis, cell cycle and DDR pathways in MCF7 cells.** Western blot results for pRB (S807/811), total CASP7, Cleaved CASP7-7, BCL2, BAX, total CHEK1, p-CHEK1 (S345), pH2AX(Ser139) in 72 h siRNA-1 treated MCF7 cells **(A)**; and 72 h siRNA-2 and siRNA-3 treated MCF7 cells (**B**). Densitometry measurements of pRB (**C**), BAX/BCL2 (**D**), total CHEK1 (**E**) and pCHEK1 (**F**), cleaved CASP7/total CASP7 ratio (**G**) and pH2AX (**H**). One-Way ANOVA was used in comparison with corresponding control groups, siRNA-CN (10nM) vs siRNA-1 and siRNA-CN (50nM) vs siRNA-2 and siRNA-3. (n=2 per group for siRNA-CN (10nM) and siRNA-1; n=3 per group for siRNA-CN (50nM) and siRNA-2 and siRNA-3), (+ :p <0.1, *: p< 0.05,**:p<0.01).

The molecules contributing to the cell cycle inhibition, apoptosis and DDR were studied at the mRNA level as well. Among these, CCND1, making a complex with CDK4/6 which in turn phosphorylates RB, was found to be decreased with siRNA-2 and siRNA-3 molecules but not with siRNA-1 (Figure 3.5A). Most importantly, CCNE2 levels were also significantly decreased with three of the siRNA molecules. Consistent decreased levels of CCNE2 could be a direct result of decreased pRB (Figure 3.4A, B and C) and E2F (microarray result: log FC =-0.43, p=0.004) levels which in turn resulting in decreased E2F regulated transcription (Figure 3.5A). In addition to cell cycle related genes, well-known genes participating in apoptotic pathway was checked with RT-qPCR by using samples treated either one of the three siRNA molecules. Expression level of FAS (Fas Cell surface Death Receptor), playing a major role during apoptosis, was increased upon CHRNA5 depletion; and this increase in expression was consistently observed with all three of the siRNA molecules (Figure 3.5A). One of the important indicators of apoptosis is increased BAX/BCL2 ratio. The expression of the pro-apoptotic BAX was also increased in siRNA-1, siRNA-2 treatments validating microarray results while the expression of the anti-apoptotic protein BCL2 was decreased in all siRNA treatments (Figure 3.5A). The decreased level of BAX with siRNA-3 was not observed at protein level suggesting that it could be transient. Increased BAX/BCL2 ratio at protein level with three siRNA molecules (Figure 3.4D) was also further supported at mRNA levels as well (Figure 3.5B). CHEK1 was also significantly downregulated at mRNA levels with three of the siRNA molecules which was also supported with microarray data (Figure 3.5B). This also further supported the notion that CHRNA5 depletion had led significant alterations in DDR.

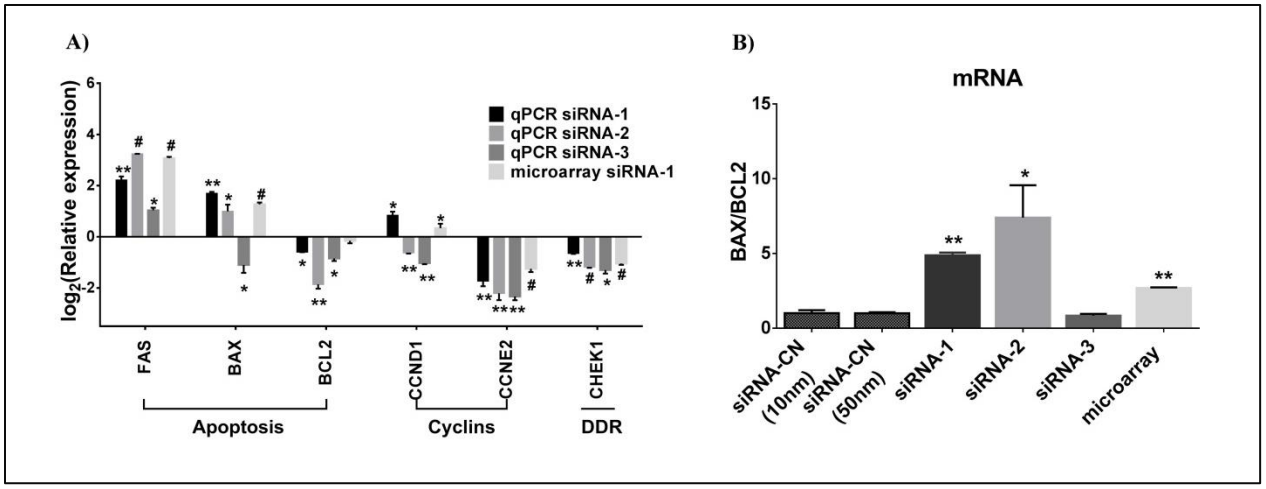


**Figure 3.5: Effects of CHRNA5 depletion on genes related with apoptosis**. **A)** RT-qPCR and microarray results of FAS, BAX, BCL2, CCND1, CCNE2 and CHEK1 in 72h of siRNA-1-3 treated MCF7 cells (n=2 per group). **B)** BAX/BCL2 ratio from RT-qPCR results (n=2 per group). One-Way ANOVA followed by Tukey's multiple test correction is used. (*: $p<0.05$, **: $p<0.01$, #: $p<0.001$)

In order to observe the effects of prolonged CHRNA5 depletion, siRNA-1 (10nM) treatment was also performed for a period of 120h. Significant downregulation of CHRNA5 was achieved at mRNA and at protein levels as well (Figure 3.6A and B, respectively). Moreover, the genes related with cytoskeletal (MAP1B, CLDN1, GJA), the genes related with p53 pathway (GADD45A, GPNMB, CDKN1A) and the ones related with cell cycle progression (ANLN, BIRC5, WDHD1) also exhibited the same results that were observed with 72h of siRNA-1 treatment (Ermira Jahja, PhD Thesis, 2017). Moreover, the proteins that were investigated upon 72h of three siRNA treatments were also investigated with 120h of siRNA-1 treatment (Figure 3.6C). Upon 120h of siRNA-1 treatment, pRB and pCHEK1 levels significantly decreased which were consistent with 72h siRNA-1 treatment results. Despite significant decreases of pCHEK1, this was not supported with total CHEK1 levels due to high variability of the samples. Significant increases in pH2AX levels (Figure 3.6D) were also consistent with pCHEK1 inhibited cellular profile, despite this was not observed with 72h of treatments. The significant increases in cleaved CASP7/ total CASP7 ratio further implied the end point of CHRNA5 depletion was apoptosis (Figure 3.6D). Despite BAX/BCL2 ratio was not significant, it had marginally increased levels in comparison to the control group (Figure 3.6D).

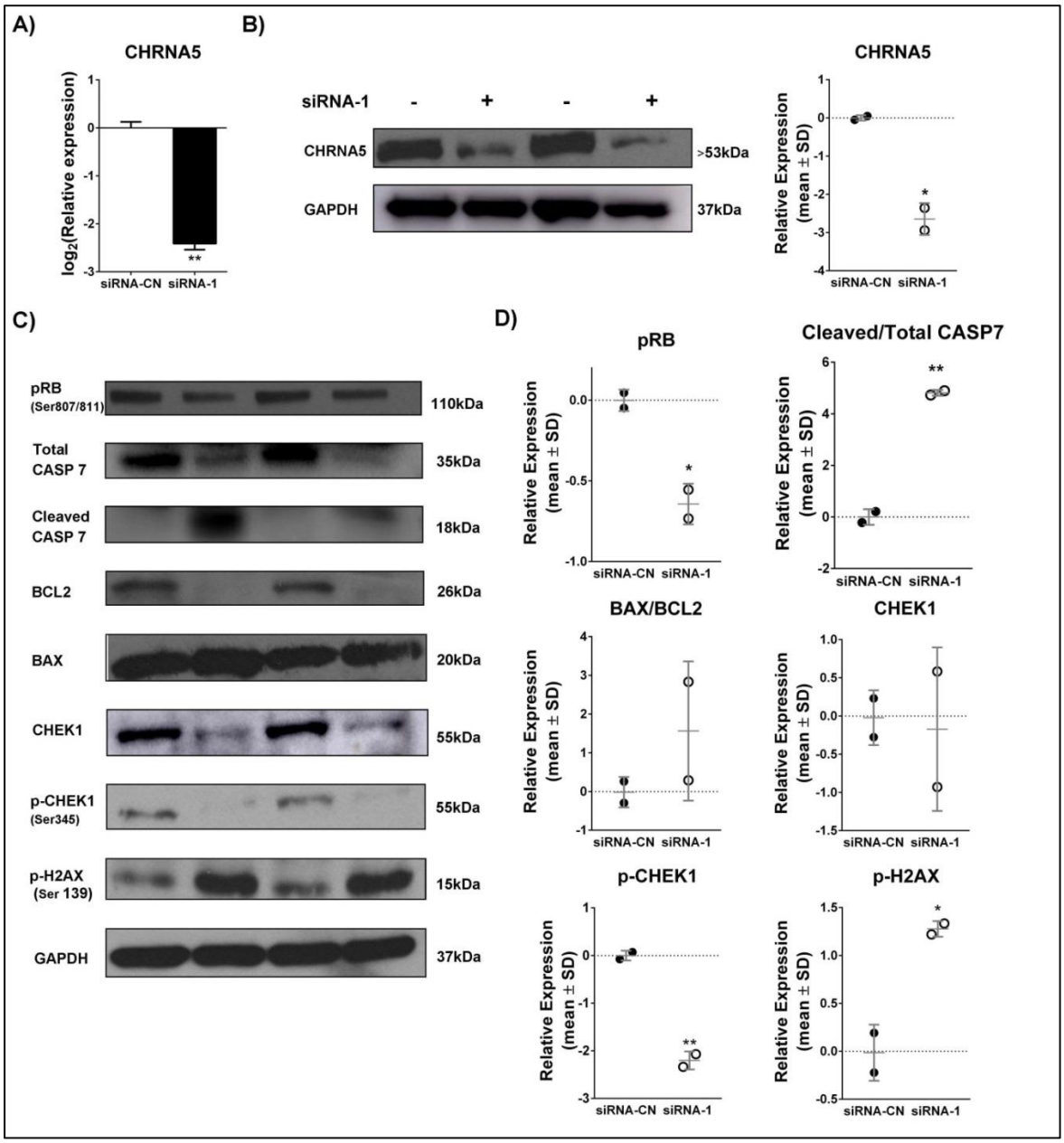


**Figure 3.6: Effects of prolonged depletion of CHRNA5.** 120h siRNA-1 treatment in MCF7 cells at mRNA **(A)** and at protein levels together with densitometry analysis **(B).** Western blot results for pRB, Total CASP7, cleaved CASP7, BCL2, BAX, CHEK1, pCHEK1 and pH2AX **(C)**; together with their densitometry analyses **(D)**, (n=2 per group). Student's t-test was applied, (*: $p<0.05$; **: $p<0.01$).

## 3.4 Effects of CHRNA5 RNAi on apoptosis and DNA damage in BT20 and MDA-MB-231

Compared to MCF7 cell line which is ER+ and TP53 wildtype, ER- and TP53 mutant BT20 and MDA-MB-231 cells were investigated in the context of CHRNA5 RNAi study. 72h of siRNA-1 treatment resulted in CHRNA5 depletion at mRNA levels in BT-20 cells ($p<0.05$) and MDA-MB-231 cells ($p=0.06$), (Ermira Jahja, PhD Thesis, 2017). These cell lines also had tendency to exhibit decreased cell viability upon CHRNA5 depletion yet depending on seeding density (Ermira Jahja, PhD Thesis, 2017).

The genes investigated in MCF7 cells with respect to apoptosis and cell cycle arrest were also checked with 72h siRNA-1 treated BT-20 and MDA-MB-231 cells. The cyclin genes, CCND1 and CCNE2 were downregulated upon CHRNA5 depletion in MDA-MB-231 cells but did not change in BT-20 cells (Figure 3.7 A). Changes in FAS levels was downregulation in MDA-MB-231 cells and no change was observed in BT-20 cells (Figure 3.7A) Similarly, no difference was observed with siRNA-1 treatment in BAX/BCL2 ratio in these two cell lines (Figure 3.7B). Therefore, unlike MCF7 cells, it is not possible to claim that CHRNA5 depletion can result in neither G1-S arrest nor apoptosis in these cell lines through BAX/BCL and FAS pathways.

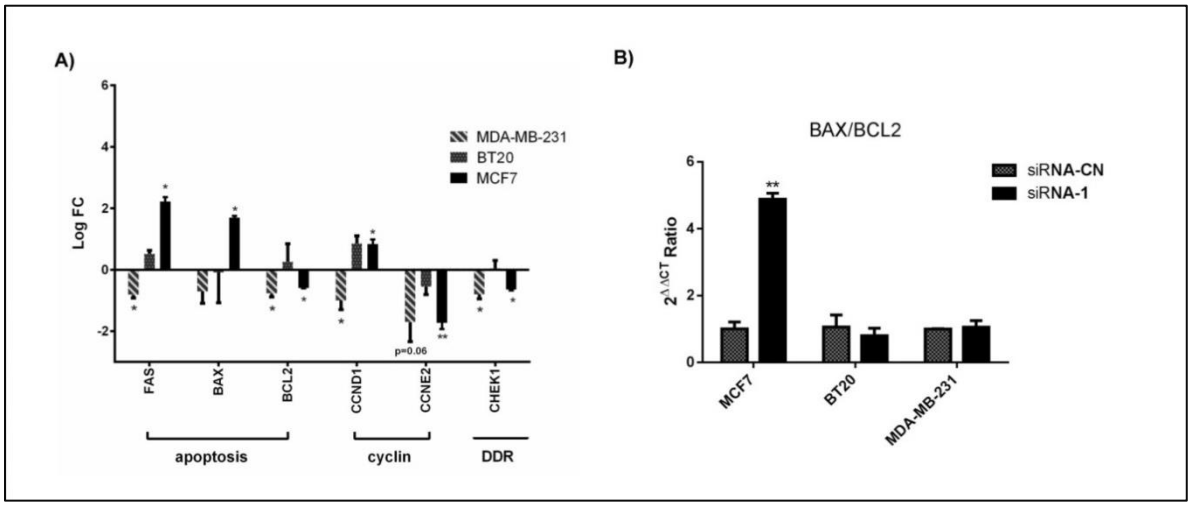

**Figure 3.7: Effects of CHRNA5 RNAi on apoptosis, cell cycle and DDR in BT20 and MDA-MB-231 cells.** Selected genes were checked with RT-qPCR **(A)**. BAX/BCL2 ratio in BT20 and MDA-MB-231 cells treated with 72 h of siRNA-1 molecules **(B)**, (n=2 per group). One-Way ANOVA followed by Tukey's multiple test correction was used). (+:p <0.1, *: p< 0.05, **: p<0.01).

## 3.5 Effects of CHRNA5 RNAi alone or in combination with doxorubicin (DOXO) or camptothecin (CPT) on cellular viability.

CHRNA5 RNAi microarray study has revealed that a cluster of genes affected by CHRNA5 depletion belonged to the DNA replication machinery and DDR. Since reduced DDR can make cancer cells more prone to chemotherapeutic [287] agents, the log-fold expression changes in affected genes from CHRNA5 RNAi microarray study were analyzed along with topoisomerase inhibitors in MCF7 cells (GSE19638, in collaboration with Huma Shehwana, data not shown). This analysis revealed that there could be similarities between the genes altered upon CHRNA5 depletion and those altered with topoisomerase inhibitors. Moreover, the shared genes between two treatments were enriched within TP53 targets suggesting a TP53 dependent activation.

In order to test the drug sensitizing potential of CHRNA5 depletion, MTT assays were carried out with variable doses of CPT and DOXO alone or together with siRNA molecules in TP53 wild type MCF7 cells as well as TP53 mutant BT-20 and MDA-MB-231 cells. Previous studies suggested optimum doses of CPT and DOXO treatment in MCF7 cells (Ermira Jahja, PhD Thesis, 2017) and additionally I have found that cell viability of MCF7 cells decreased more than 50% in the presence of siRNA CHRNA5 molecules at all doses including the lowest one *(0,015μM)* when compared to controls having CPT or DOXO with or without siRNA-CN (Figure 3.8A-B). This experiment, which was further supported with another siRNA molecule against CHRNA5 (siRNA-2), suggested that depletion of CHRNA5 sensitized TP53 wild type MCF7 cells to topoisomerase inhibitors (Figure 3.8C-D).

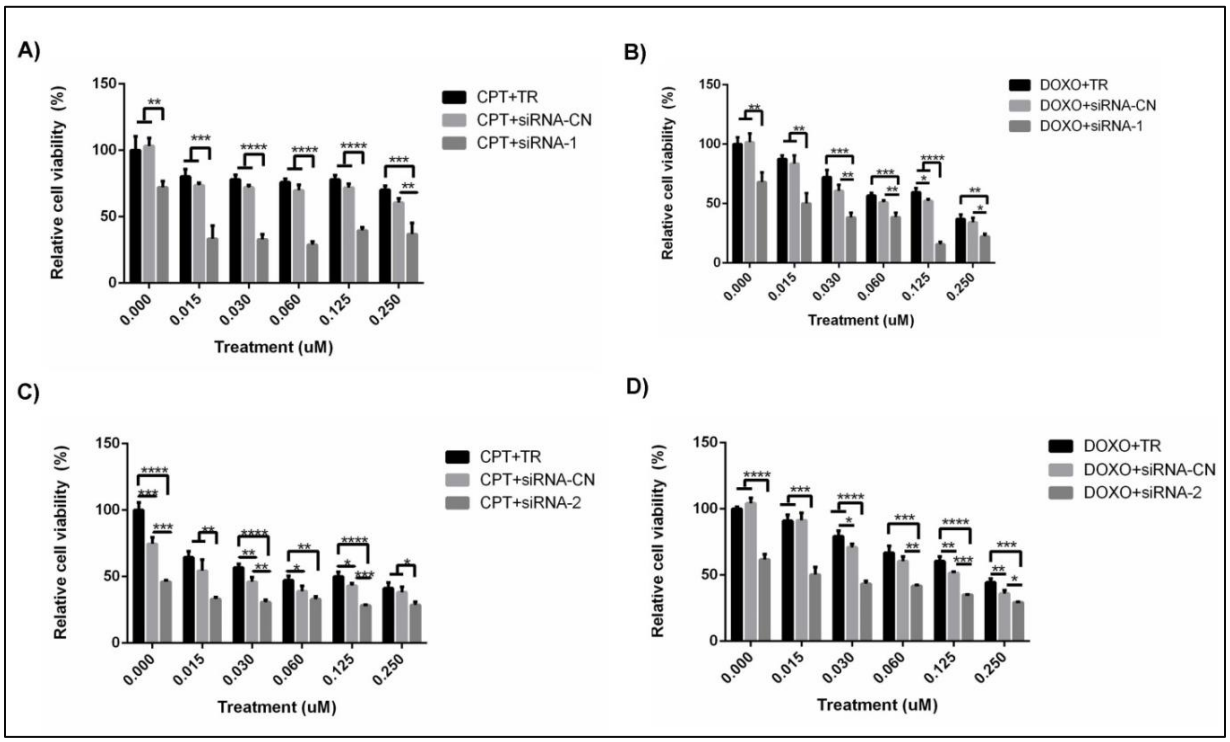


**Figure 3.8: Effects of CHRNA5 depletion on drug sensitivity in MCF7 cells**. MTT analyses of different doses of CPT **(A)** and DOXO **(B)** along with 72h of siRNA-1 treatments or CPT **(C)** and DOXO **(D)** along with72h of siRNA-2 treatments in MCF7 cells, (n=3 per group). One-Way ANOVA followed by Tukey's multiple test correction were used for statistical analysis. (*: $p<0.05$, **: $p<0.01$; ***: $p<0.001$; ****: $p<0.0001$).

To further clarify the relationship between CHRNA5 depletion and TP53 status on drug sensitization in breast cancer cells, the same MTT set up was carried out with TP53 mutant BT-20 and MDA-MB-231 cells. In MCF7 cells the synergistic anti-proliferative actions of CPT and DOXO along with siRNA molecules were observed at much lower doses compared to BT20 cells, i.e, 0.125μM CPT (Figure 3.9A). For DOXO treatments in BT20 cells, siRNA treatments were not significantly different than the corresponding siRNA-CN groups suggesting no synergism (Figure 3.9B). Unlike MCF7 cells, cell viability of MDA-MB-231 cells was above 50% and no synergism with CHRNA5 siRNA was observed with CPT treatments (Figure 3.9C). For DOXO treatments in MDA-MB-231 cells, a synergism between siRNA-1 and DOXO could only be observed after 0.06μM (Figure 3.9D).

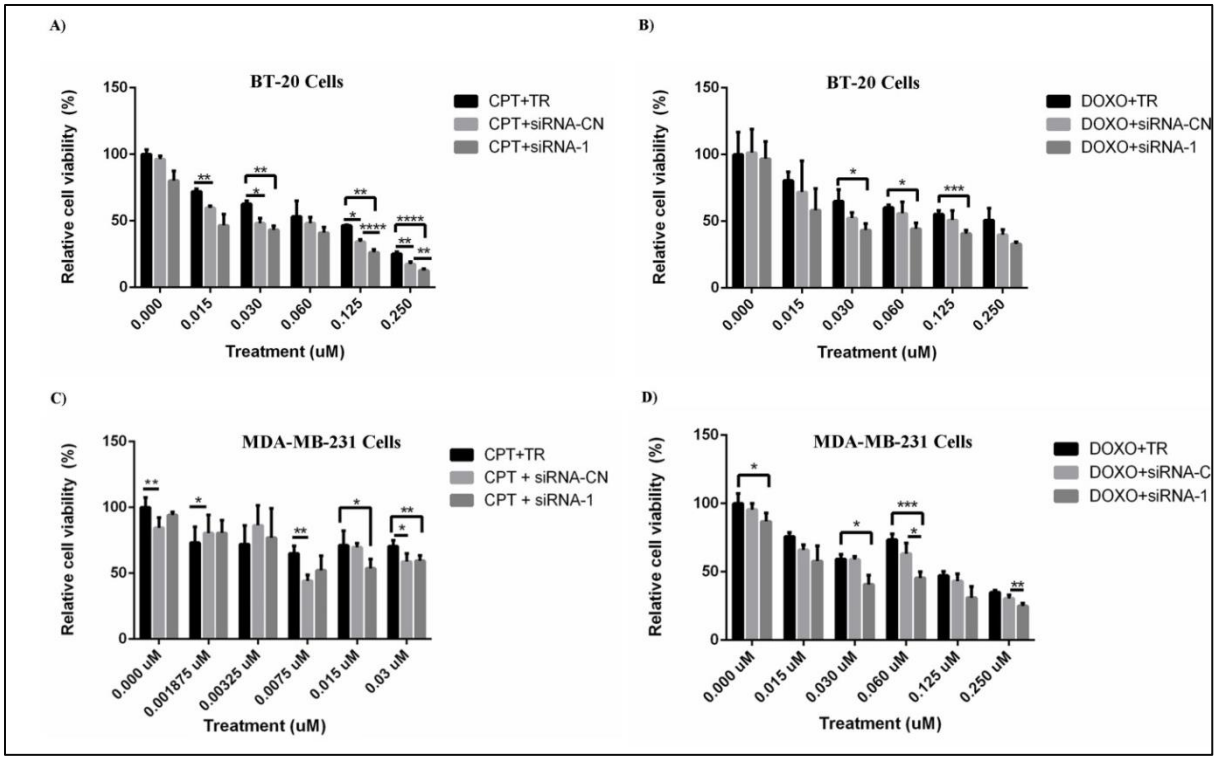


**Figure 3.9: Effects of CHRNA5 depletion on drug sensitivity in BT20 (A and B) and in MDA-MB-231 cells (C and D).** MTT analyses of different doses of CPT **(A)** and DOXO **(B)** with 72h of siRNA-1 treatment in BT20 and CPT **(C)** and DOXO **(D)** with 72h of siRNA-1treatment in MDA-MB-231 cells, (n=3 per group). One-Way ANOVA followed by Tukey's multiple test correction were used for statistical analysis. (*: $p<0.05$, **: $p<0.01$; ***: $p<0.001$; ****: $p<0.0001$).

## 3.6 Effects of CHRNA5 RNAi treatment with or without CPT and DOXO on apoptotic and DDR proteins in MCF7 cells

In order to reveal the mechanism behind the drug sensitization of CHRNA5 depletion, western blotting was carried out. Based on the microarray and RT-qPCR findings, proteins participating DDR and apoptotic pathways were examined. Before the lysate collection at the end of 72 h of treatments, cells were visualized with DIC microscopy. Compared to the control groups (DMSO+TR and DMSO+siRNA-CN), MCF7 cells lost their spherical structure and became more lunate in morphology with CPT and DOXO treatments together with all three siRNA molecules (Figure 3.10A, B and C).

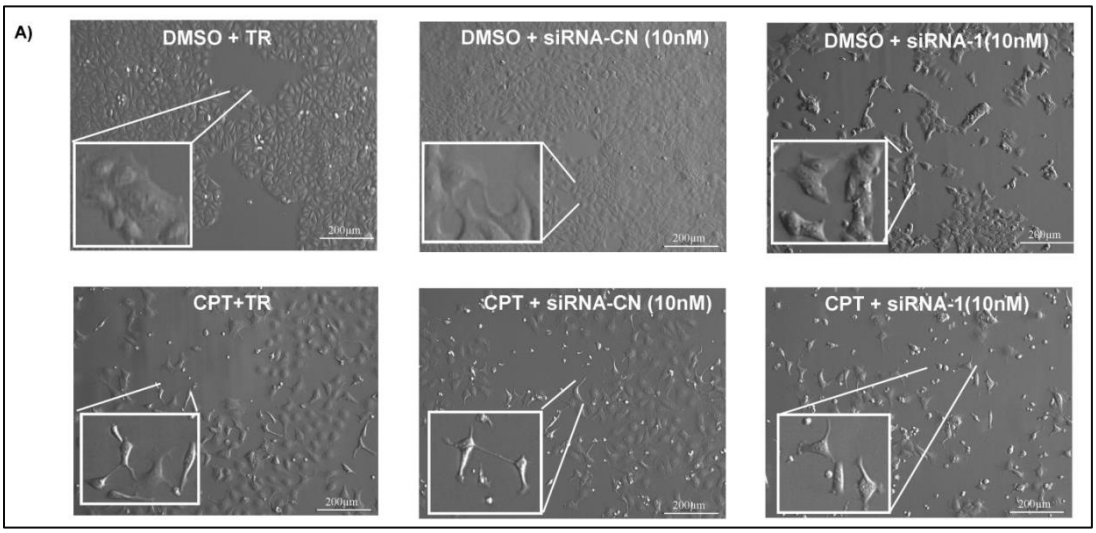
A)
DMSO + TR
DMSO + siRNA-CN (10nM)
DMSO + siRNA-1(10nM)
CPT+TR
CPT + siRNA-CN (10nM)
CPT + siRNA-1(10nM)
200μm

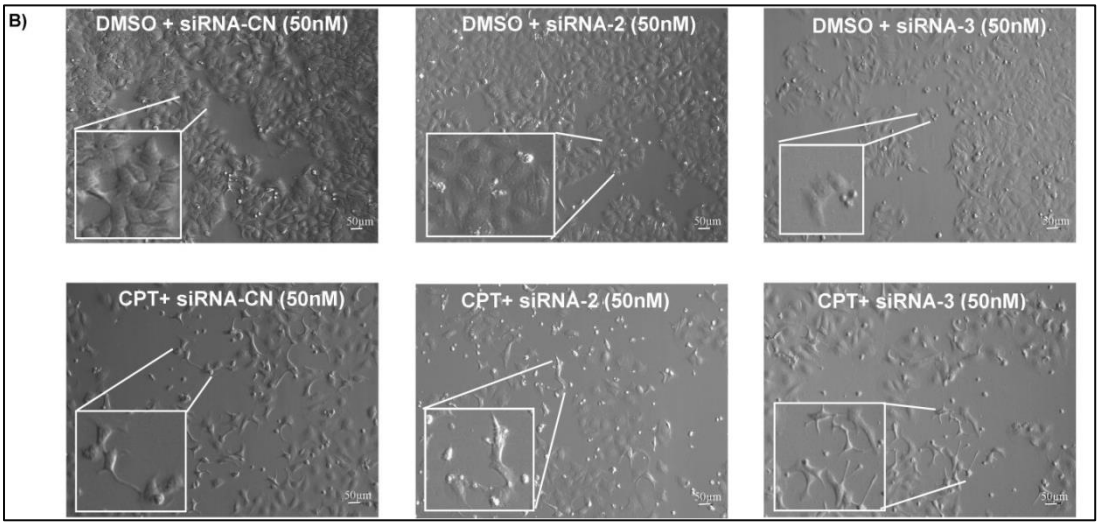
B)
DMSO + siRNA-CN (50nM)
DMSO + siRNA-2 (50nM)
DMSO + siRNA-3 (50nM)
CPT+ siRNA-CN (50nM)
CPT+ siRNA-2 (50nM)
CPT+ siRNA-3 (50nM)
50μm

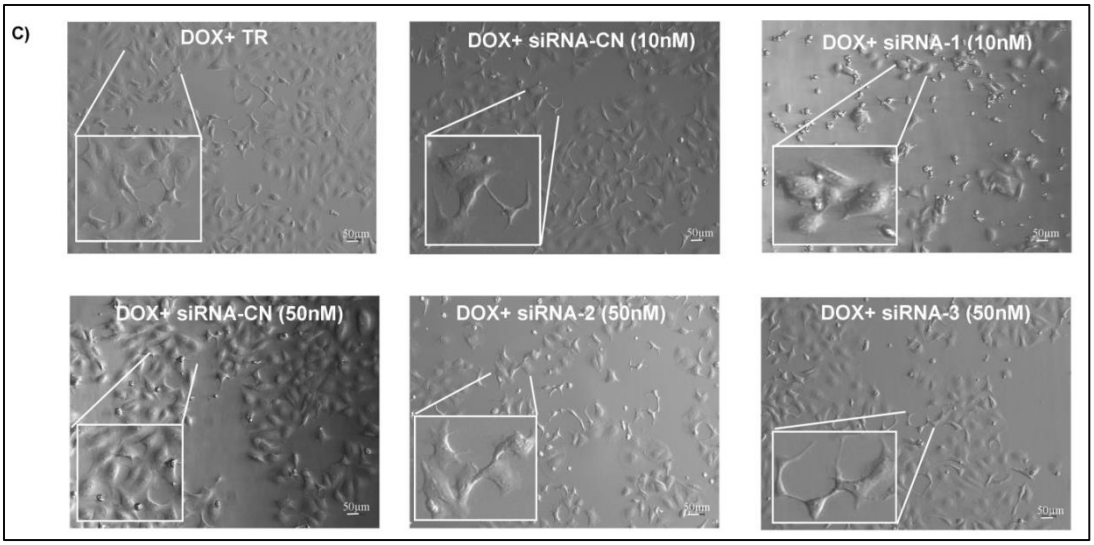


**Figure 3.10: Phenotypic changes in MCF7 cells upon siRNA or siRNA-CN treatments with or without TOPO inhibitors**. Microscopy images of MCF7 cells at the end of 72 h treatment with siRNA-CN (10nm) and siRNA-1 (10nm) with 0.125μM CPT or DMSO **(A);** treatment with siRNA-CN (50nM), siRNA-2 (50nM) and siRNA-3 (50nM) with 0.125μM CPT or DMSO **(B);** treatment with siRNA-CN (10nM), siRNA-1 (10nM), siRNA-CN (50nM), siRNA-2 (50nM) and siRNA-3 (50nM) with 0.125μM DOXO or DMSO **(C).**

The proteins investigated in the context of CHRNA5 depletion study, were also examined in the presence of TOPO inhibitors as well (except pRB) (Figure 3.11A, B and C). CHRNA5 was significantly downregulated only by siRNA-2 in DMSO control group yet with siRNA-1 it marginally decreased ($p<0.1$) (Figure 3.11D). In terms of the effects of TOPO inhibitors, DOXO treatment further caused significant downregulation of CHRNA5 regardless siRNA molecules compared to DMSO group (Figure 3.11D). Although siRNA-1 and siRNA-2 had tendency to downregulate CHRNA5 levels in the CPT treated group, when analyzed together they did not differ significantly from DMSO control group (Figure 3.11D). The BAX/BCL2 ratio was significantly increased by siRNA-1 and siRNA2 in DMSO group (Figure 3.11E) which was shown before as well (Figure 3.4D). Despite CPT and DOXO treatments significantly increased BAX/BCL2 ratio compared to DMSO control group, siRNA molecules did not exhibit any additional effect on BAX/BCL2 ratio in drug treated groups (Figure 3.11D). Decreased levels of total CHEK1 upon siRNA treatments (Figure 3.4E) were supported here as well, such that three of the siRNA molecules

resulted in significantly decreased levels of total CHEK1 (Figure 3.11F). Moreover, CPT and DOXO treatments significantly downregulated overall total CHEK1 levels compared to DMSO group (Figure 3.11F). Despite siRNA-1 significantly downregulated total CHEK1 levels in CPT and DOXO treated groups; siRNA-2 and siRNA-3 could not exhibit any additional effect (Figure 3.11F). p-CHEK1 levels were effectively downregulated by three of the siRNA molecules in both DMSO and DOXO groups (Figure 3.11G). CPT itself also resulted in significant reductions in pCHEK1 levels compared to DMSO group and within CPT treatment, only siRNA-3 also additionally downregulated pCHEK1 levels ($p<0.1$) (Figure 3.11G). The ratio of cleaved CASP7/total CASP7 ratio both increased significantly upon CPT and DOXO treatments regardless of the presence of siRNA molecules (Figure 3.11H). Similarly, due to the high variability in the expression levels of pH2AX, there was not a significant further change in pH2AX levels due to presence of siRNA molecules. However, pH2AX levels were significantly increased upon DOXO treatment compared to DMSO control group.

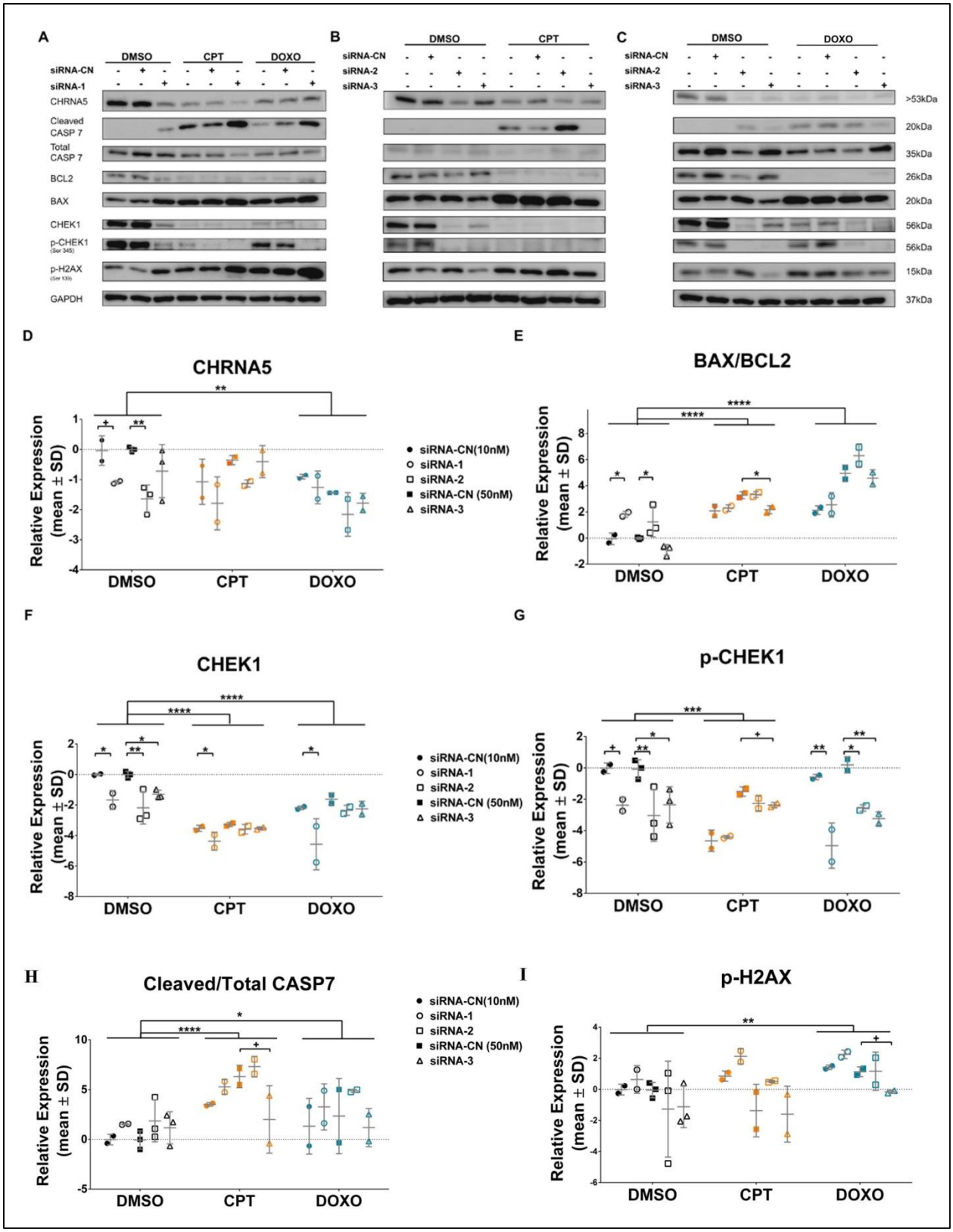


**Figure 3.11: The effects of CHRNA5 depletion in drug sensitivity in MCF7 cells**. (**A-C**) The representative western blot images treated with DMSO, CPT and DOXO (all 0.125μM) along with

siRNA-1 **(A)** or siRNA-2 and siRNA-3 **(B** and **C)**. The densitometry analysis of CHRNA5 **(D)**, BAX/BCL2 (**E**), total CHEK1 (**F**), pCHEK1 (**G**), cleaved CASP7/total CASP7 (**H**), pH2AX (**I**). Two-Way ANOVA was used. (n=3 for DMSO siRNA-CN (50nM), siRNA-2 and siRNA-3; n=2 for other groups). (+:p <0.1, *: p< 0.05, **: p<0.01, ***:p<0.001, ****:p<0.0001).

## 3.7 Effects of CHRNA5 RNAi treatment with or without CPT and DOXO on DDR proteins in BT20 and MDA-MB-231 cells

In order to reveal how the depletion of CHRNA5 affected TP53 mutant BT-20 and MDA-MB-231 cells in terms of apoptosis and anti-proliferation, similar experimental set up was performed with CPT and DOXO in the presence or absence of siRNA-1 in these cell lines as well. Again, just before collection of the cell lysates cells were visualized with DIC microscopy at the end of 72 h treatments. In BT-20 cells, CHRNA5 depletion did not result in phenotypical changes which were observed in the case of MCF7 cells. As expectedly, only the addition of TOPO inhibitors resulted in cell death in both of the cell lines regardless of the presence of siRNA-1 (Figure 3.12 A and B).

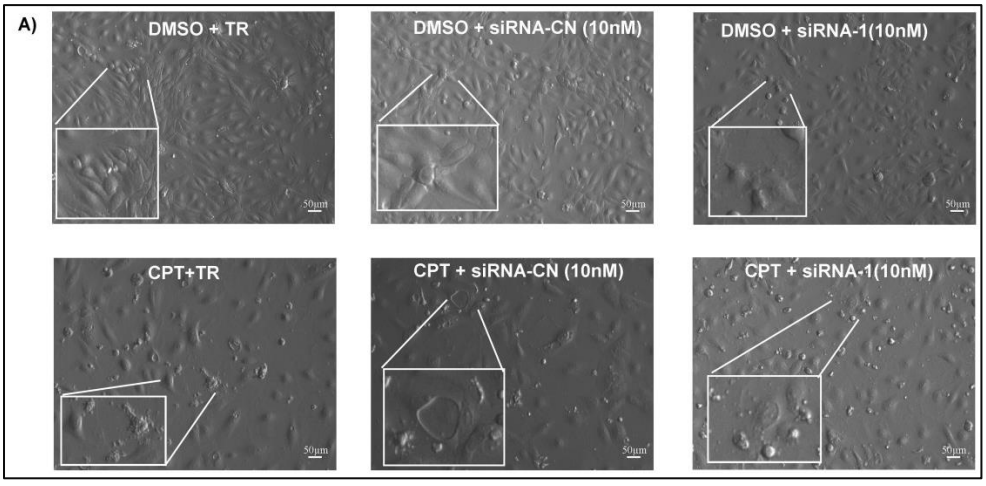

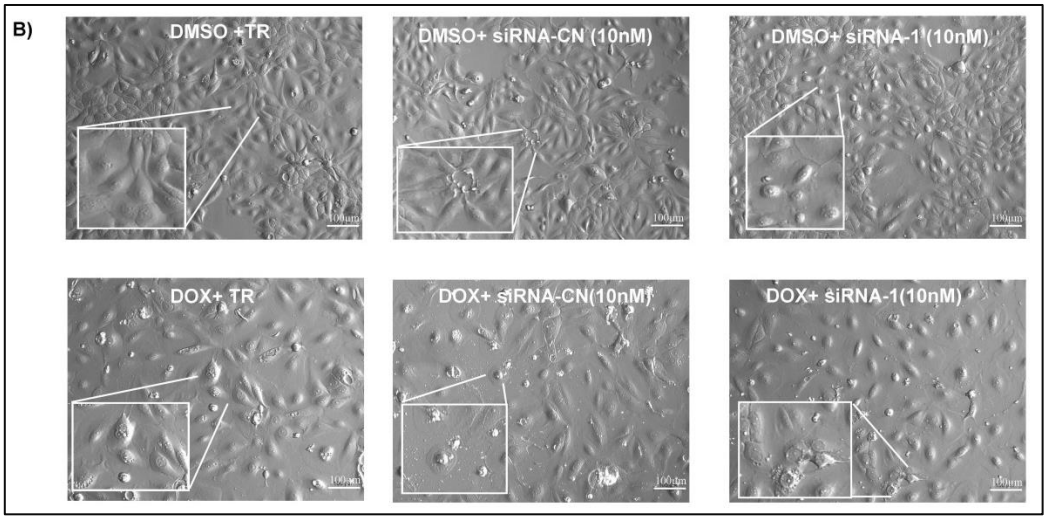


**Figure 3.12: Microscopy images of BT-20. A)** Effect of CPT (0.125μM) along with siRNA-1 (10nM) in comparison to their corresponding control groups on BT-20 cells' phenotype. **B)** Effect of DOXO (0.125μM) along with siRNA-1(10nM) in comparison to their corresponding control groups in BT-20 cells.

With Western Blotting the proteins involved in DDR mechanism were examined in the presence of TOPO inhibitors along with siRNA molecules in BT-20 cells (Figure 3.13A-D). Despite CHRNA5 was marginally downregulated in DMSO group, with the addition of CPT (0.125μM), it remained unchanged. Opposite of what was observed in MCF7 cells (Figure 3.11F and G), both total CHEK1 and pCHEK1 levels were significantly upregulated with the addition of CPT regardless of siRNA-1 presence (Figure 3.13C). pH2AX levels were labile in DMSO and CPT groups making it hard to conclude. Similar to CPT results, DOXO (0.125 μM) treatments also did not change CHRNA5 levels, and as observed with CPT treatment, DOXO treatment alone also increased the levels of total CHEK1 levels ($p<0.1$) (Figure 3.13D). In consistent with this, pCHEK1 levels were also increased significantly with the addition of DOXO, but siRNA-1 treatment did not exhibit any additional effect (Figure 3.13D). pH2AX level was significantly downregulated in the presence of DOXO and siRNA-1 (Figure 3.13D).

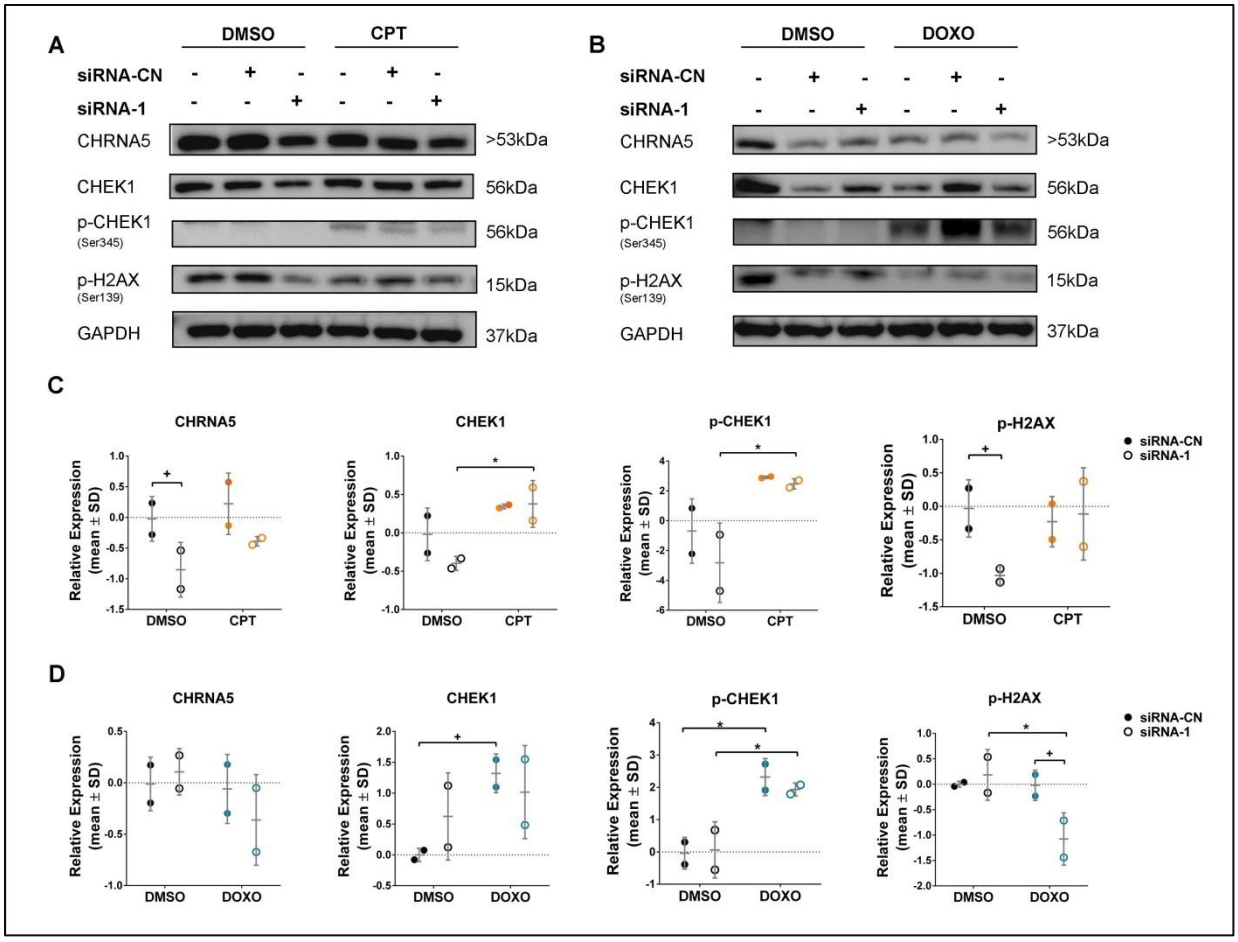


**Figure 3.13: Effects of CHRNA5 RNAi along with TOPO inhibitors on DDR proteins in BT-20 cells**. Western Blot results of BT-20 cells with CPT (0.125μM) **(A)** and DOXO (0.125μM) **(B)** treatments along with siRNA-1(10nM) and siRNA-CN (10nM). Densitometry results with statistical analysis of CPT (**C**) and DOXO (**D**) with or without siRNA-1. (n=2 per group), Two-Way ANOVA was used, (+ :p<0.1, * :p< 0.05).

Similar experimental set up and examination of the same proteins with Western blotting were also held for MDA-MB-231 cells. Again, before protein collection, cells were visualized under DIC microscopy (Figure 3.14 A and B). Similar to BT-20 cells, CHRNA5 depletion itself did not result in phenotypic changes unlike MCF7 cells. Again, addition of TOPO inhibitors resulted in cell death and changes in morphology apart from siRNA presence.

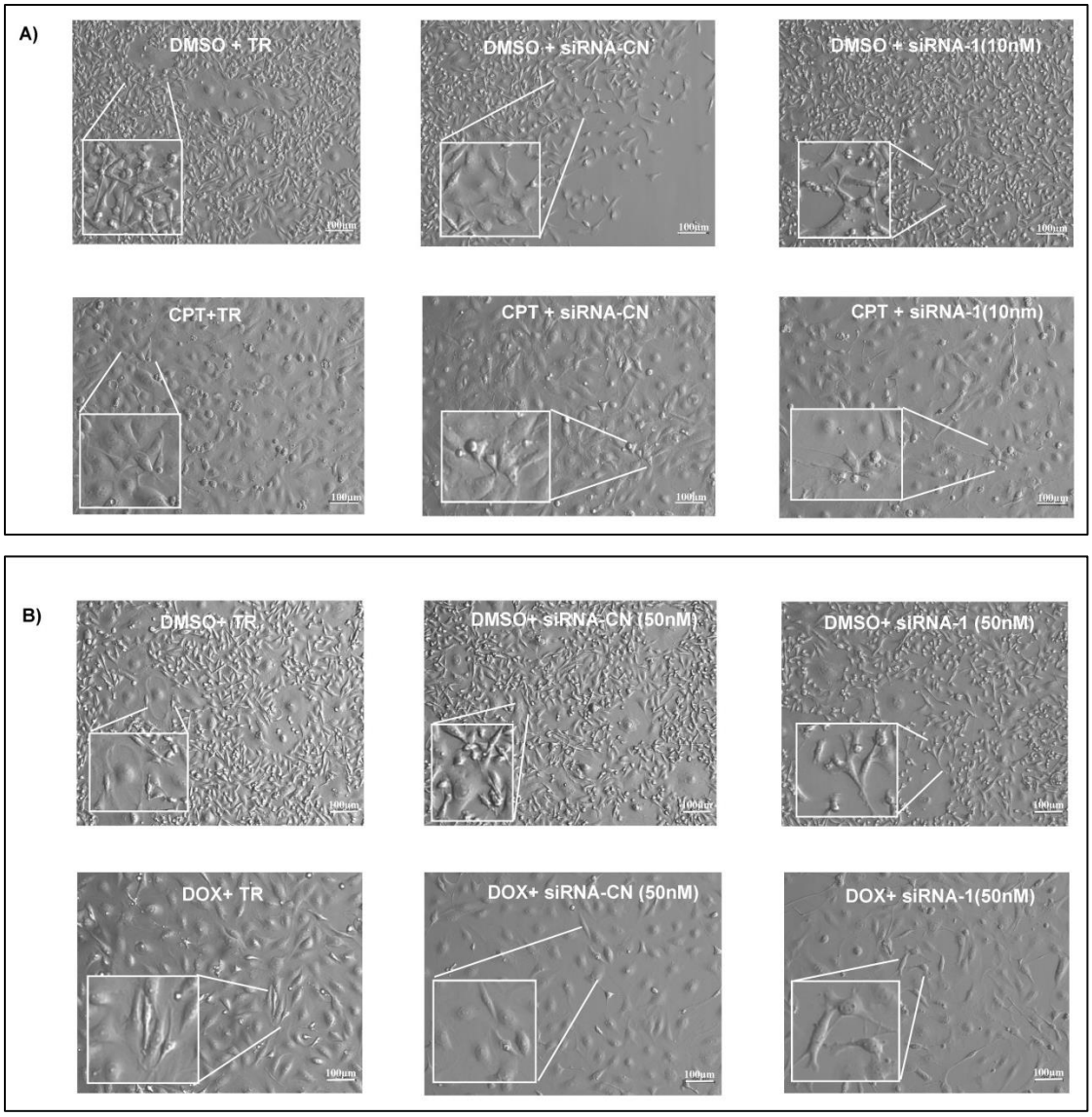


**Figure 3.14**: **Microscopy images of MDA-MB-231 cells. A)** Effect of CPT (0.015μM) along with siRNA-1 (10nM) in comparison to their corresponding control groups on MDA-MB-231 cells' phenotype. **B)** Effect of DOXO (0.06μM) along with siRNA-1(10nM) in comparison to their corresponding control groups in MDA-MB-231 cells.

With western blotting same proteins were examined in this panel as well. With the addition of TOPO inhibitors, CHRNA5 levels had tendency to be decreased yet they were not significant (Figure 3.15A-B). Unlike BT-20 cells, CPT (0.015μM) or DOXO (0.06) treatments along with siRNA-1 (50nM) treatments, CHEK1 levels were significantly downregulated (Figure 3.15 A). Within CPT and DOXO treated samples, siRNA-

1exhibited additive effect in terms of decreasing CHEK1 levels compared to their siRNA-CN control, confirming the previous observation at mRNA level where siRNA-1 alone also significantly downregulated CHEK1 level (Figure 3.7A). Similar with BT-20 cells, in MDA-MB-231 cells CPT treatment resulted in increases in pCHEK1 levels ($p<0.1$), (Figure 3.14C). In comparison to this, DOXO treatment significantly increased pCHEK1 levels regardless of siRNA-1 presence (Figure 3.15D). Despite pH2AX level had tendency to be increased upon CPT treatment, yet both of the drugs, as well as siRNA-1 did not significantly alter pH2AX levels (Figure 3.15C and D).

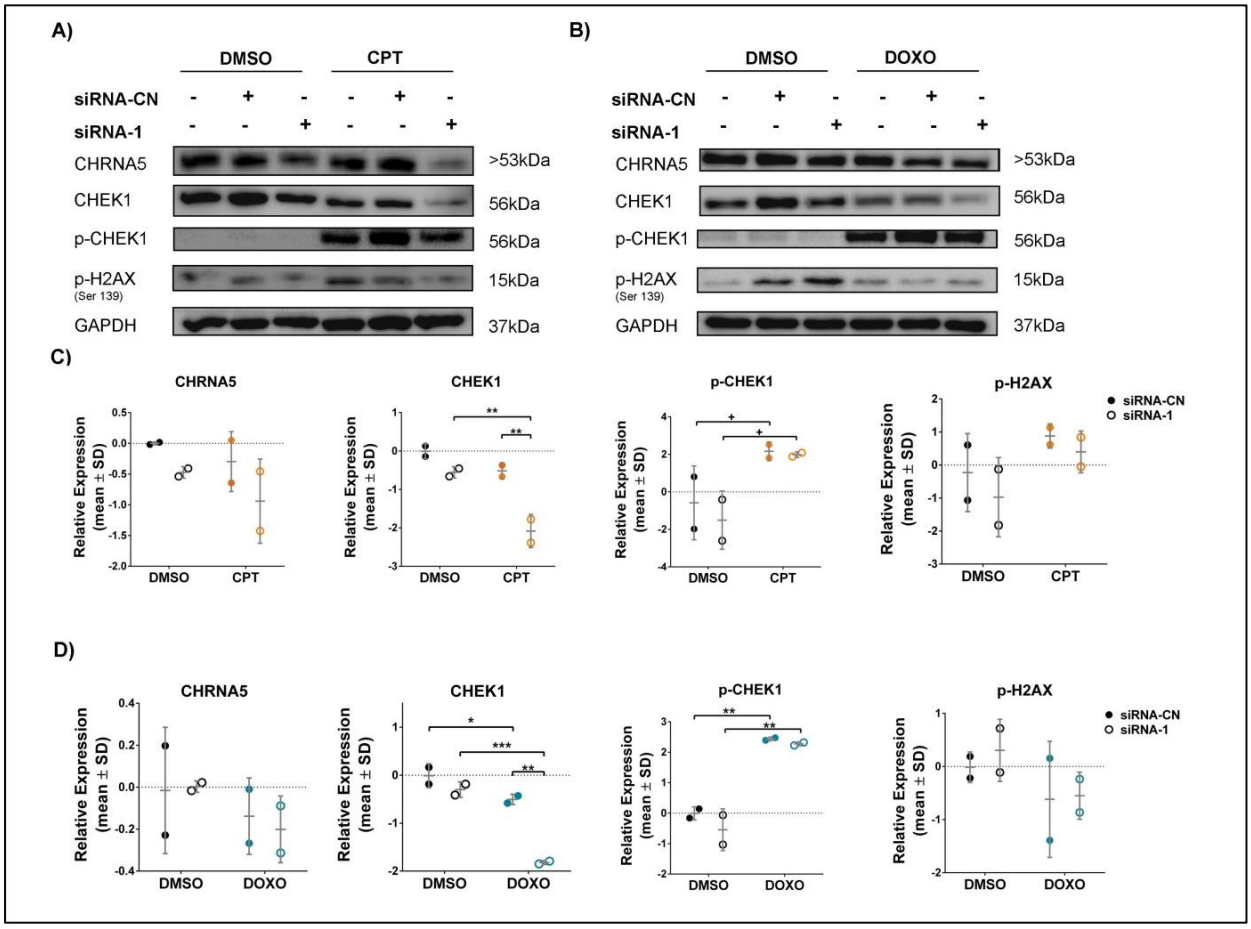


**Figure 3.15: Effects of CHRNA5 RNAi along with TOPO inhibitors on DDR proteins in MDA-MB-231 cells**. Western Blot results of MDA-MB-231 cells with CPT (0.015 μM) **(A)**, and DOXO (0.06 μM) **(B)**, treatments along with siRNA-1(50nM) and siRNA-CN (50nM). Densitometry results with statistical analysis of CPT (**C**) and DOXO (**D**) with or without siRNA-1. (n=2 per group). Two-Way ANOVA was used (+ :$p<0.1$, * :$p< 0.05$, **: $p<0.01$, ***:$p<0.001$).

## 3.8 How CHRNA5 variants and the genes affected by CHRNA5 depletion are modulated upon mir-15a, mir-15b, and mir-16 mimic treatment?

CHRNA5 has been studied with various cancer types such as gastric and lung cancers, however there is not much knowledge in the context of breast cancer so far. Moreover, its regulation with other molecules such as miRNAs has not been studied as well. In this part of the study, I have tried to address the regulation of CHRNA5 variants by miR-15 family which has been shown to participate in tamoxifen [190] resistance in MCF7 cells**.**

miR-15a, miR-15b and miR-16 are the three of the miRNAs belonging to miR-15 family. According to the bioinformatics tools '*Targetscan*' [288] and '*mirna.org'* [191], these three miRNAs have predicted binding sites in 3'UTR of CHRNA5. Before starting any overexpression or inhibition experiments, basal expression levels of these miRNAs were checked in MCF7 cells which were treated with CHRNA5 targeting siRNA-1(10nM) and siRNA-CN (10nM) for 72h. According to the RT-qPCR results, although all three miRNAs had tendency to exhibit decreased expression levels, among them the most downregulated one was miR-15a having p value 0.05 (Figure 3.16). Downregulation of miR-15a upon depletion of CHRNA5 indicates a possible feedback mechanism between CHRNA5 RNAi machinery and miR-15a.

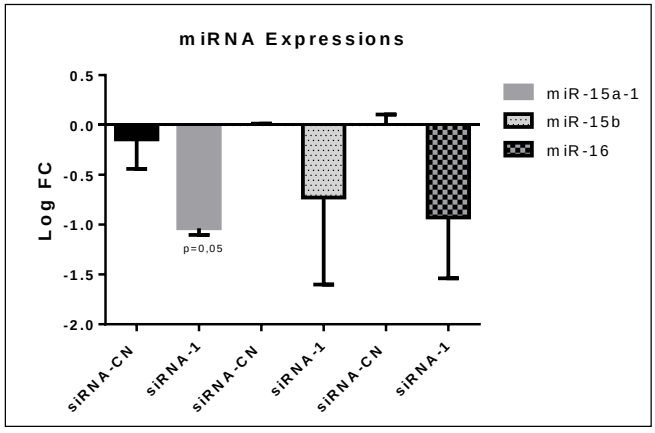

**Figure 3.16: Expression levels of mir-15/16 family members upon 72h of CHRNA5 siRNA-1 treatment in MCF7 cells.** One-Way ANOVA followed by Tukey's multiple test correction is used.

As explained in materials and methods section, in order to overexpress these miRNAs, MCF7 cells were treated synthetic miRNA mimics specific to each of the miRNA molecules. All three miRNAs were successfully upregulated which were confirmed with RT-qPCR (Figure 3.17A, B and C)

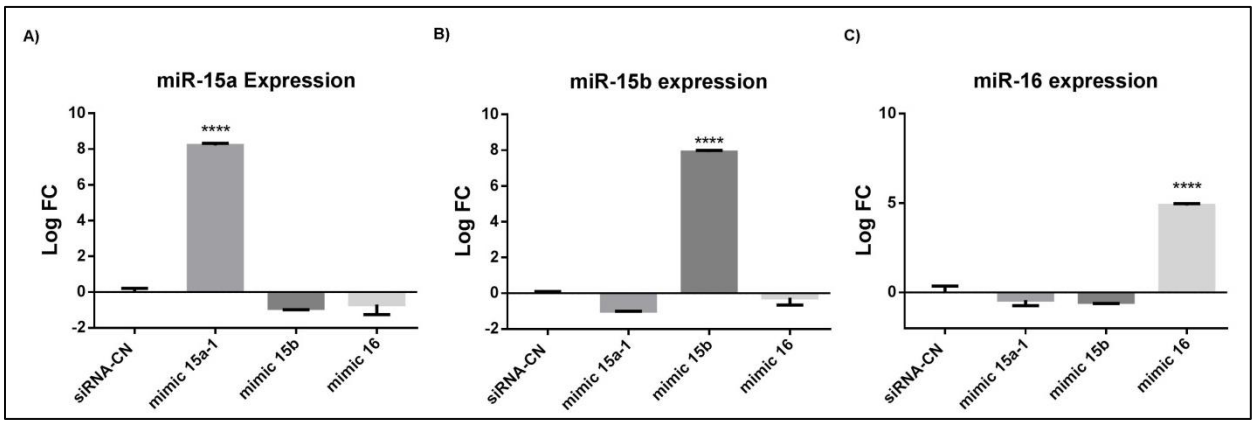


**Figure 3.17: Specific miRNA mimic treatments for 72h**. **A)** Upregulation of miRNA-15a upon miRNA-15a mimic (5nM) treatment, **B)** Upregulation of miRNA-15b (5nM) upon miRNA-15b mimic treatment, **C)** Upregulation of miRNA-16 upon miRNA-16 mimic (5nM) treatment in MCF7 cells, (n=2 per group). Each sample normalized with siRNA-CN group and One-Way ANOVA followed by Tukey's multiple test correction is used. (*:p< 0.05, **: p<0.01, ***:p<0.001, ****:p< 0.0001).

Followed by miRNA overexpression experiments, the expressions of CHRNA5 splice variants were investigated as well. Except CHRNA5_V1 (p=0.06), all four CHRNA5 variants were significantly downregulated upon miRNA by all or some of the mimic treatments while the most effective mimic treatment was found to be miR-15a-1 (Figure 3.18).

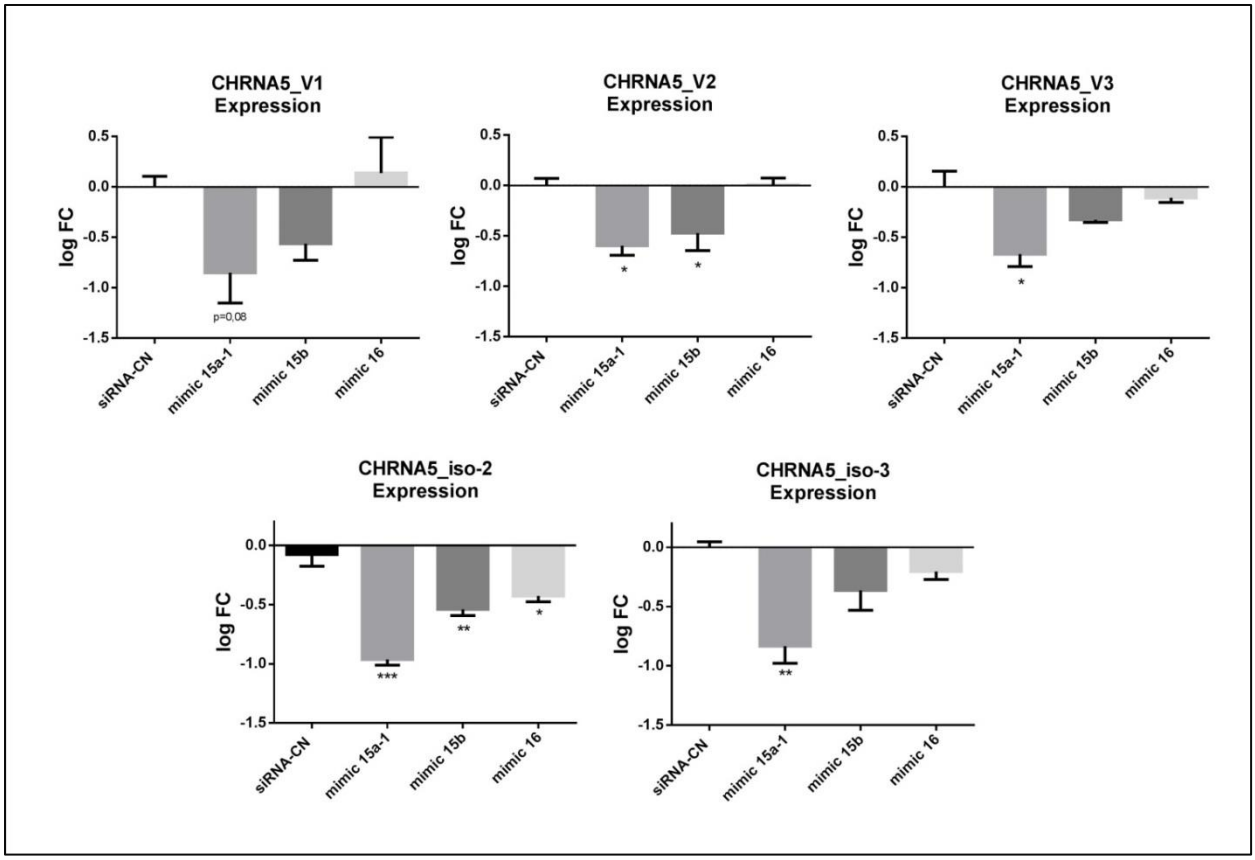


**Figure 3.18: Expression levels of CHRNA5 variants upon 72 h of miRNA specific mimic (5nM) treatments**. One-Way ANOVA followed by Tukey's multiple test correction is used. (*:p< 0.05, **: p<0.01, ***:p<0.001).

Expression levels of the genes analyzed in the previous section, i.e, the proteins regulating TP53 signaling, cell cycle and cytoskeletal arrangement, were checked with these samples in order to reveal whether these miRNAs act similar to CHRNA5 RNAi molecules. In addition, known targets of these mimics were studied using mirnet tool [289] and target scan and literature analysis. Among them CASK (*Calcium/Calmodulin Dependent Serine Protein Kinase)* having a binding site for miR-15a and miR-16 exhibited a significant reduced expression levels upon overexpression of miR-15a and miR-16 (Figure 3.19A). One of the most important genes related with TP53 signaling is GADD45A (*Growth Arrest and DNA-damage Inducible Alpha)* [290] was marginally downregulated upon three of the miRNA mimic treatments (Figure 3.19B). WDHD1 (*WD Repeat and HMG-Box DNA Binding Protein 1)* which is one of the downstream molecules in PI3K/AKT signaling pathway [291] was significantly downregulated upon miR-15a mimic treatment,

yet not affected by other miRNA mimic treatments (Figure 3.19C). One of the representative genes belonging to connexin gene family, GJA1 (Gap Junction Protein Alpha 1) participates in gap junction formation [292], had tendency to be increased upon miR-16 mimic treatment (Figure 3.19D). A major component of tight junction, CLDN1 (Claudin1), which was upregulated upon CHRNA5 depletion (Figure 3.2), was also significantly upregulated upon miR-15a and miR-16 mimic treatments (Figure 3.19E).

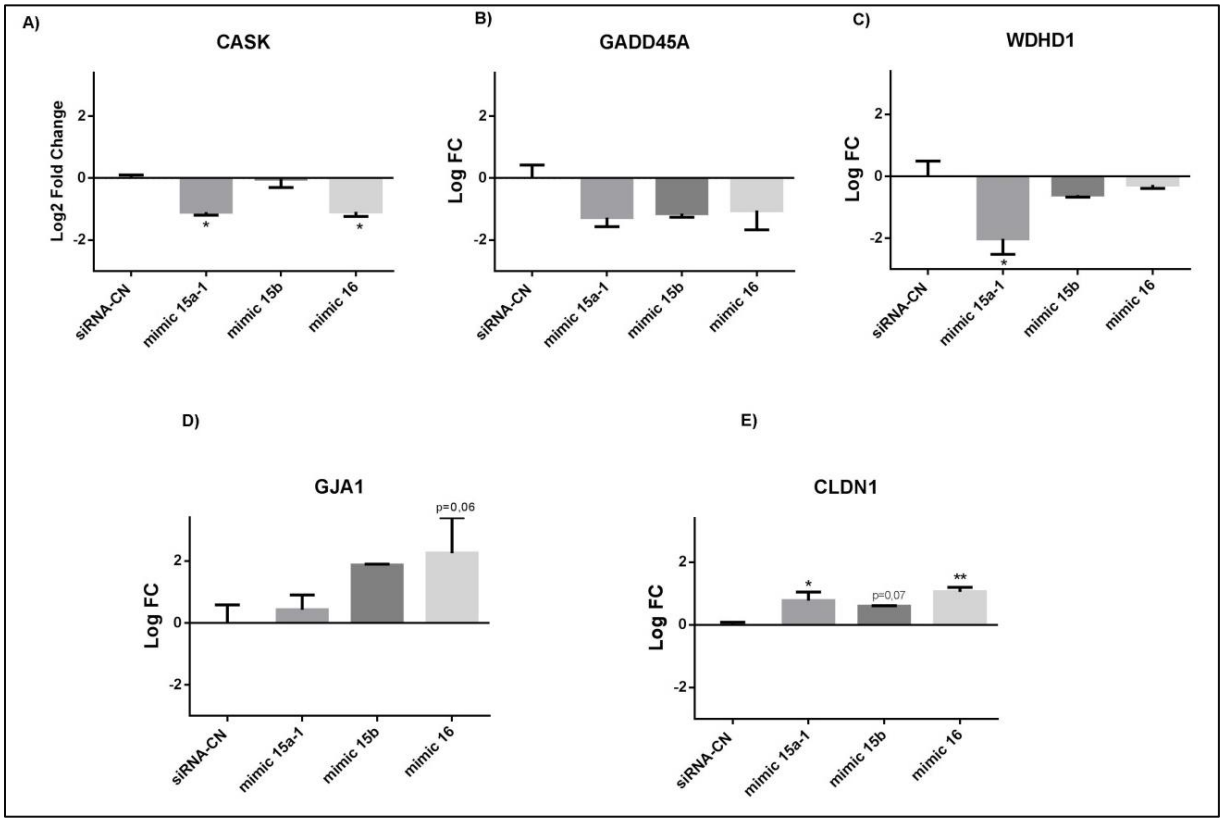


**Figure 3.19**: **RT-qPCR results of the selected genes known to be modulated by CHRNA5 depletion along with 72 h of mir-15/16 family mimic treatments.** CASK **(A),** GADD45A **(B**), WDHD1 **(C)**, GJA1 **(D)**, CLDN1 **(E)**. (n=2 per group). One-way ANOVA was used for statistical analysis. (*: p< 0.05, **: p<0.01).

## 3.9 Does CHRNA5 RNAi affect microRNA expression profile?

Based on the findings obtained so far, the depletion of CHRNA5 in MCF7 cells not only affected wide range of the genes but also affected global microRNA expression profile as well. There has been limited number of studies investigating the interaction between

miRNA and siRNA molecules together, yet there is no study investigating the effects of CHRNA5 depletion on microRNA expression profile in breast cancer. Hence, in this part of the thesis I aimed to reveal the interactions between microRNAs and mRNAs whether they acted additively in MCF7 cells by using various molecular tools.

Consistent with the results from previous sections, significant downregulation of CHRNA5 was again achieved with all three of the siRNA molecules using 5 different samples using a different RNA extraction methodology so that the same samples can be used for both mRNA and microRNA quantification (Figure 3.20A and B; in collaboration with Mehtap Yilmaz Tezcan and Basak Ozgursoy).

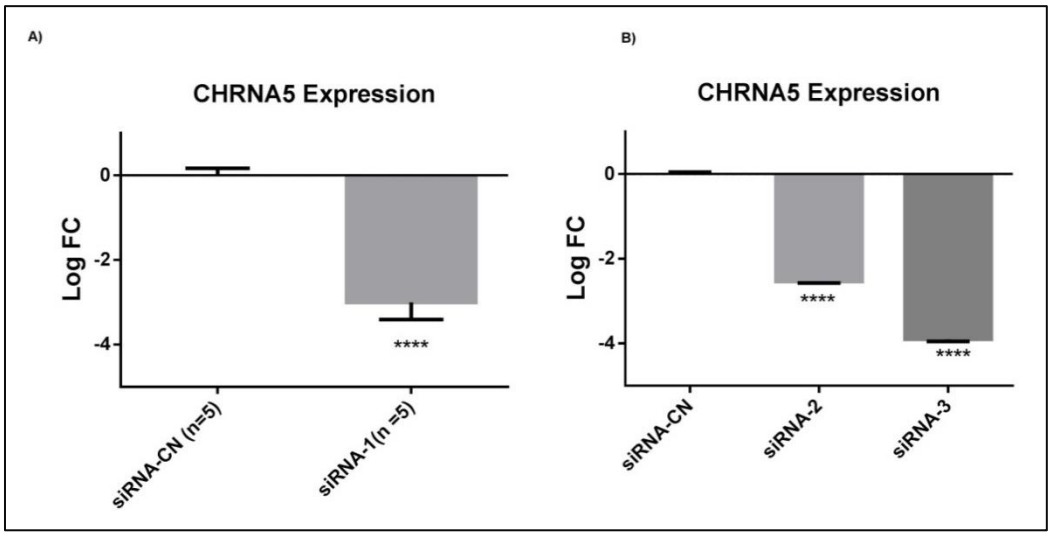


**Figure 3.20: Expression of CHRNA5 levels upon siRNA treatments**. CHRNA5 expressions upon 72h of siRNA-1 (10nM) **(A)** and siRNA-2 (50nM) and siRNA-3(50nM) **(B)** treatments in MCF7 cells. (n=5 for siRNA-1 and siRNA-CN; n=2 for siRNA-CN (50nM), siRNA-2 and siRNA-3). Student's t-test was applied for A, and One-Way ANOVA was used for B (****: p< 0.0001).

Among five of siRNA-CN and five of siRNA-1 treated samples, two samples from each group) having RIN (RNA Integrity Number) values higher than 9 over 10 (Figure 3.21) were chosen and used for microRNA array (GeneChip miRNA 4.0) study.

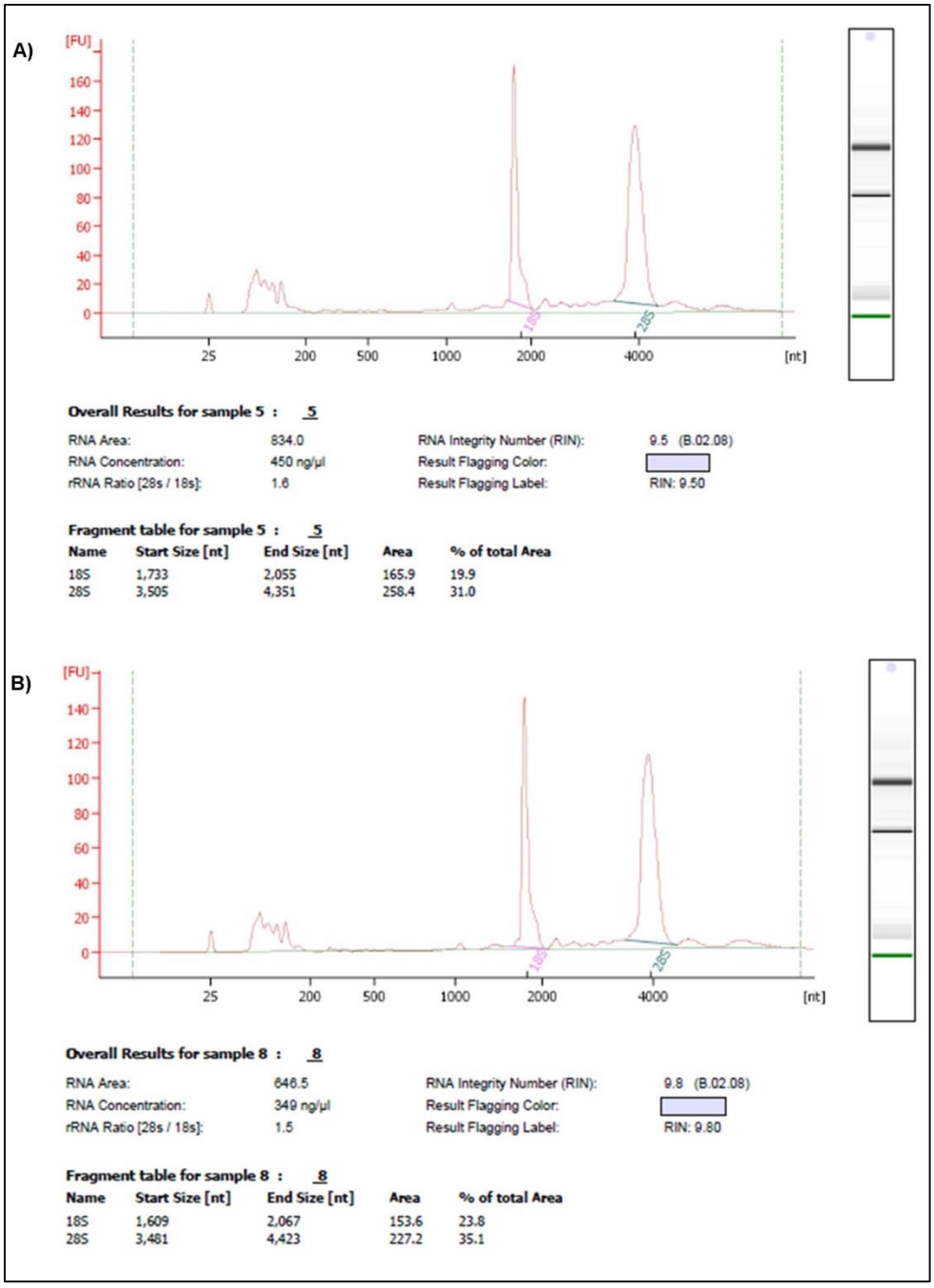


**Figure 3.21: RNA quality and Agilent values of RNAs**. Representative values of RNA samples **A)** for siRNA-CN, **B)** for siRNA-1used in microRNA Array study (n=2 for siRNA-CN and siRNA-1).

When the results of the logarithmically transformed fold changes (logFC) from two miRNA array pairs (siRNA-CN vs siRNA-1) were plotted, a group of miRNAs came into

prominence as such that they were significantly downregulated upon CHRNA5 depletion. Among these miRNAs, a group of them was found to be clustered on chromosome 14q32.31 region (Figure 3.22). As mentioned before, miRNAs encoded from this region are shown to be deregulated in many of the cancer types such as glioblastoma [293] and neuroblastoma [294].

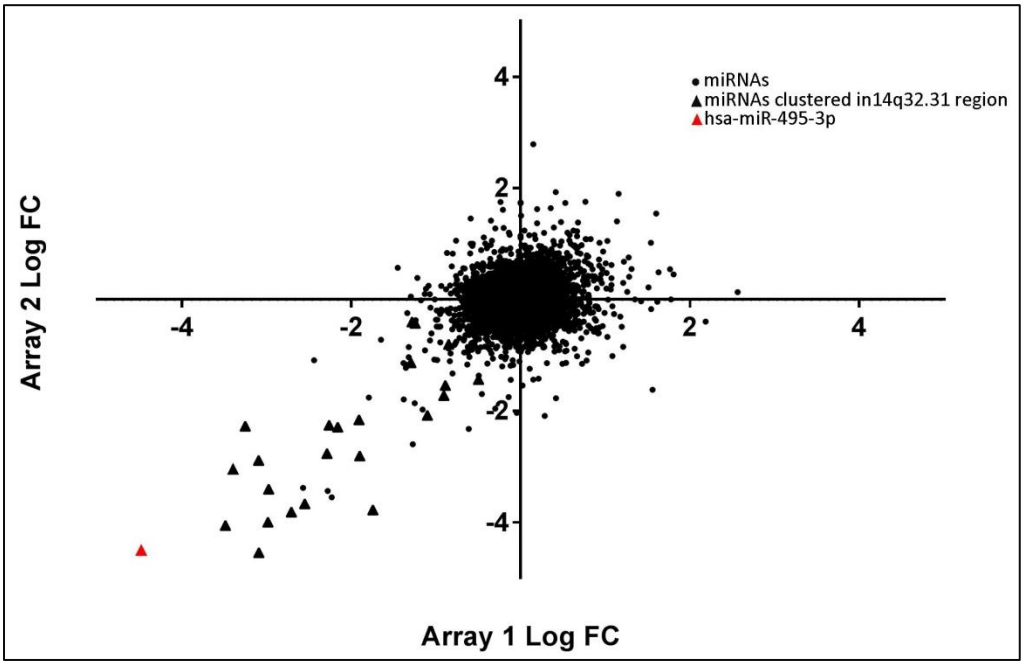


**Figure 3.22: Scatter plot of two miRNA arrays.** CHRNA5 depletion resulted in global changes in miRNA expression profile. The most downregulated miRNAs clustered in 14q32.31 region shown with black triangle, among them the most downregulated one was has-miR-495-3p shown with red triangle.

When the top downregulated miRNAs were listed, hsa-miR-495-3p came in the first rank upon CHRNA5 depletion (Figure 3.22 and Table 3.1). This observation was further confirmed with three siRNA molecules by RT-qPCR (Figure 3.23A and B). Therefore, in this part of the thesis, I have focused on the interactions between CHRNA5 and hsa-miR-495-3p by using siRNA-1 and miRNA mimic-495 together.

**Table 3-1.** Top 10 most affected microRNAs (p< 0.05)

| Probe Set ID | Transcript ID | siRNA-CN1-1 | siRNA-CN1-2 | siRNA1-1 | siRNA1-2 | LFC | P value |
|---|---|---|---|---|---|---|---|
| 20503805 | hsa-miR-495-3p | 6,149546 | 6,123086 | 1,669941 | 1,628936 | -4,4868775 | 8,38E-07 |
| 20502456 | hsa-miR-409-3p | 6,543813 | 6,702369 | 3,454337 | 2,147751 | -3,822047 | 0,000692402 |
| 20504421 | hsa-miR-654-3p | 5,07644 | 5,198967 | 1,590907 | 1,132692 | -3,775904 | 1,87E-05 |
| 20501244 | hsa-miR-379-5p | 5,801826 | 5,84653 | 2,8189 | 1,841176 | -3,49414 | 0,000319436 |
| 20502445 | hsa-miR-329-3p | 5,240331 | 5,290051 | 2,53389 | 1,464056 | -3,266218 | 0,000601522 |
| 20501239 | hsa-miR-376a-3p | 4,753608 | 4,492746 | 1,358125 | 1,456866 | -3,2156815 | 1,09E-05 |
| 20504218 | hsa-miR-487b-3p | 6,12861 | 6,43547 | 3,154359 | 3,022147 | -3,193787 | 1,61E-05 |
| 20503108 | hsa-miR-487a-3p | 3,76394 | 4,402591 | 1,215416 | 0,7250268 | -3,1130441 | 0,000252651 |
| 20501250 | hsa-miR-382-5p | 5,464757 | 5,643095 | 2,370719 | 2,746343 | -2,995395 | 3,59E-05 |
| 20502437 | hsa-miR-431-5p | 5,34937 | 5,753108 | 2,780229 | 2,373163 | -2,974543 | 9,52E-05 |

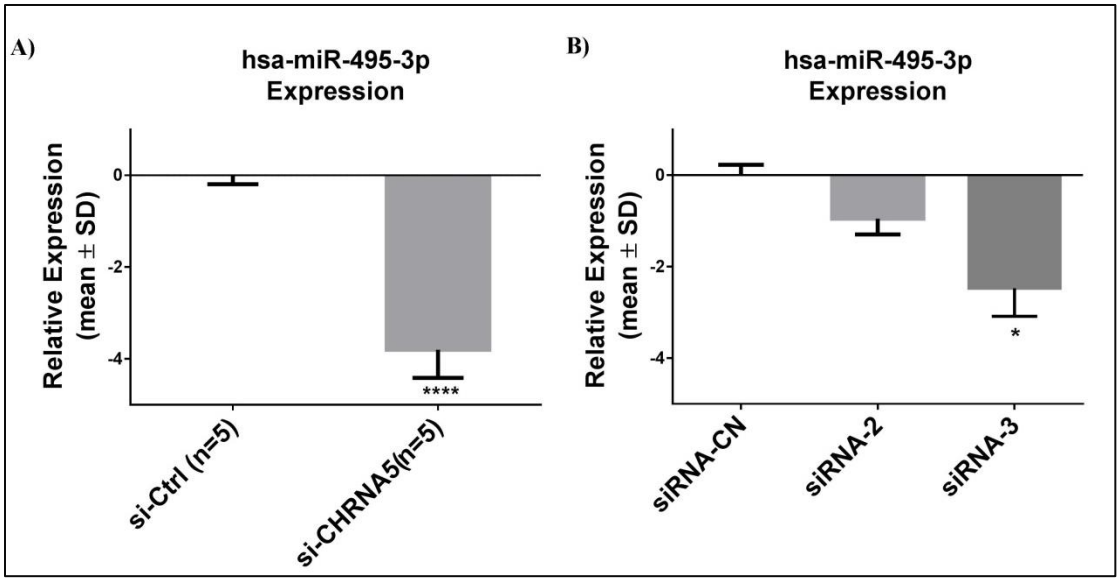


**Figure 3.23: RT-qPCR validation of the hsa-miR-495-3p expression levels upon CHRNA5 depletion**. Results with siRNA-1 (n=5) (A); with siRNA-2 and siRNA-3 (n=2) (B). Student's t-test was applied for A, and One-Way ANOVA was used for B, (*:p< 0.05, ****: p< 0.0001).

## 3.10 Does transcriptional profile of CHRNA5 RNAi correlate with that of mimic miR-495 based on comparative transcriptomics plots (log fold change vs. log fold change)?

In order to study possible synergistic and/or antagonistic effects of CHRNA5 depletion together with miR-495 overexpression on gene expression profile, MCF7 cells were treated with CHRNA5 siRNAs and miRNA mimic-495 alone or together as explained in materials and methods section. Firstly, depletion of CHRNA5 and overexpression of miR-

495 were confirmed by RT-qPCR. Cells treated with siRNA-1 showed significant downregulation of CHRNA5 (Figure 3.24A-B), while the cells treated with miR-495 mimic exhibited significant upregulation of miR-495 (Figure 3.24 C-D). This confirmation allowed us to conduct mRNA array study (Affymetrix HGU133 plus 2) with these samples in order to investigate the expression profile of the genes participating in various signaling pathways to reveal the additive or opposite action these two molecules.

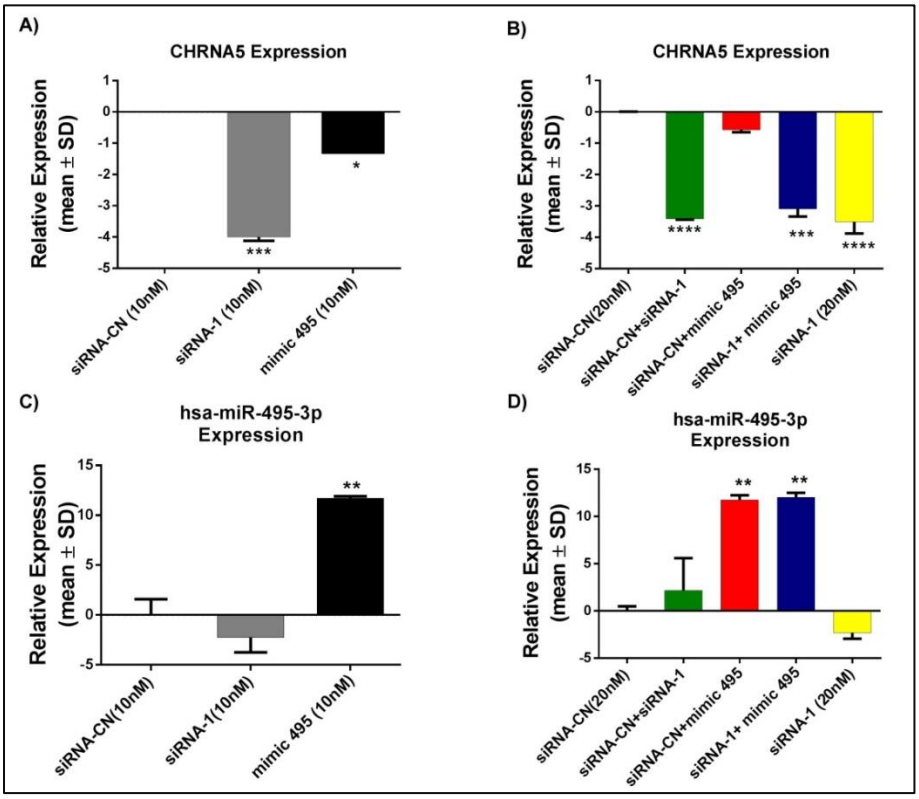


**Figure 3.24: Examination of CHRNA5 and hsa-miR-495-3p expression levels by RT-qPCR.** Validation of the decrease in CHRNA5 expression **(A** and **B)**; increase in hsa-mir-495-3p levels upon miR-495 mimic application **(C** and **D)**. (n=2 per group). One-way ANOVA was conducted as statistical analysis (*: $p<0.05$, **: $p<0.01$).

After successful validation of CHRNA5 depletion and increase in miR-495 expression, the samples treated with siRNA-1 (10nM) and miR-495 mimic (10nM) together, the sample treated with miR-495 mimic (10nM) and siRNA-CN (10nM) together, and the sample

treated siRNA-CN (20nM) alone were chosen to conduct mRNA array study. When the log fold changes resulted from siRNA CHRNA5 and siRNA-CN versus miR-mimic 495 and siRNA-CN experiments were plotted together, a group of genes were discovered to be similarly downregulated by both siRNA-1 and miR-495 mimic treatments (Figure 3.25, red circled area). Moreover, there also appeared a group of genes, in which siRNA-1 and miR-495 mimic acted on oppositely (Figure 3.25, blue circled area).

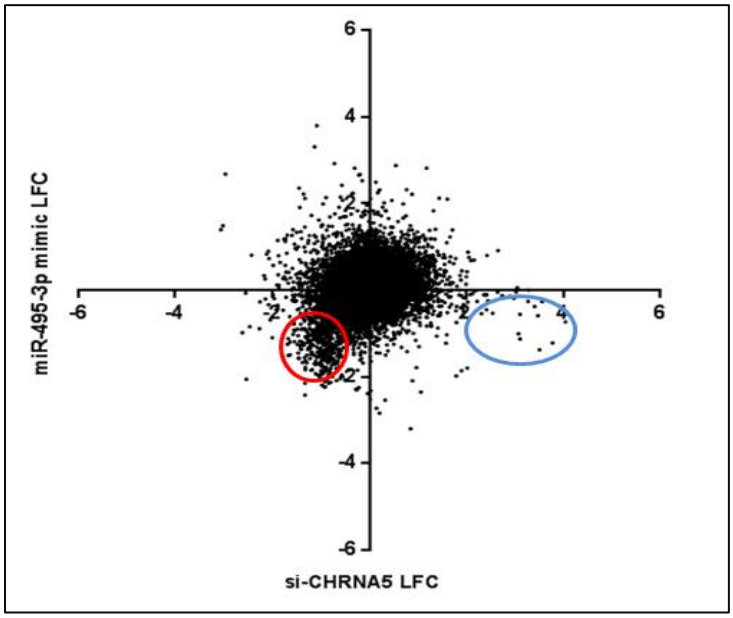


**Figure 3.25: The scatterplot of log fold changes obtained from CHRNA5 siRNA microarray study (Ermira Jahja, PhD Thesis, GSE89333) against those obtained from mir-495 mimic microarray study**. Red circled area represented the genes in which siRNA-1 and miR-495 mimic acted additively; whereas in blue circled area represented the genes in which siRNA-1 and miR-495 mimic acted oppositely.

Among the altered miRNAs, top 10 upregulated and top 10 downregulated genes upon only miR-495 treatment and their modulation by the addition of siRNA-1 are shown in the table 3.2.

**Table 3-2:** Top Upregulated and Downregulated Genes by miRN-495 alone and miR-495+siRNA-1

| Top Up Regulated Genes | miR-495 mimic | siRNA1+miR-495 mimic |
|---|---|---|
| CSTA | 3,798 | 2,514 |
| SEPP1 | 2,923 | -0,238 |
| LRRN1 | 2,818 | 3,308 |
| SNAP25 | 2,681 | -0,799 |
| RUNDC3B | 2,669 | 1,417 |
| AOX1 | 2,655 | -0,397 |
| IL1R1 | 2,528 | 1,092 |
| PMP22 | 2,419 | 1,796 |
| CEACAM6 | 2,317 | 2,646 |
| ST8SIA4 | 2,249 | 1,462 |

| Top Down Regulated Genes | miR-495 mimic | siRNA1+miR-495 mimic |
|---|---|---|
| EGR3 | -1,543 | -3,204 |
| AKR1C2 | -1,208 | -2,844 |
| AKR1C1 | -1,109 | -2,523 |
| AKR1C3 | -0,211 | -2,391 |
| AREG | 0,025 | -2,356 |
| IL24 | -1,13 | -2,287 |
| LBR | -1,373 | -2,255 |
| DEPDC1B | -2,372 | -2,24 |
| DLGAP5 | -2,481 | -2,234 |
| GGH | -2,168 | -2,151 |

Moreover, the pathways were either upregulated or downregulated by miR-495 mimic alone treatments were investigated with KEGG. One of the pathways significantly upregulated was ‘pathways in cancer’ whereas the most of the pathways which were downregulated belonged to cell cycle progression, DNA replication and P53 signaling.

**Table 3-3:** The list of KEGG pathways modulated by mir-495 mimic alone for A) upregulated B) downregulated genes

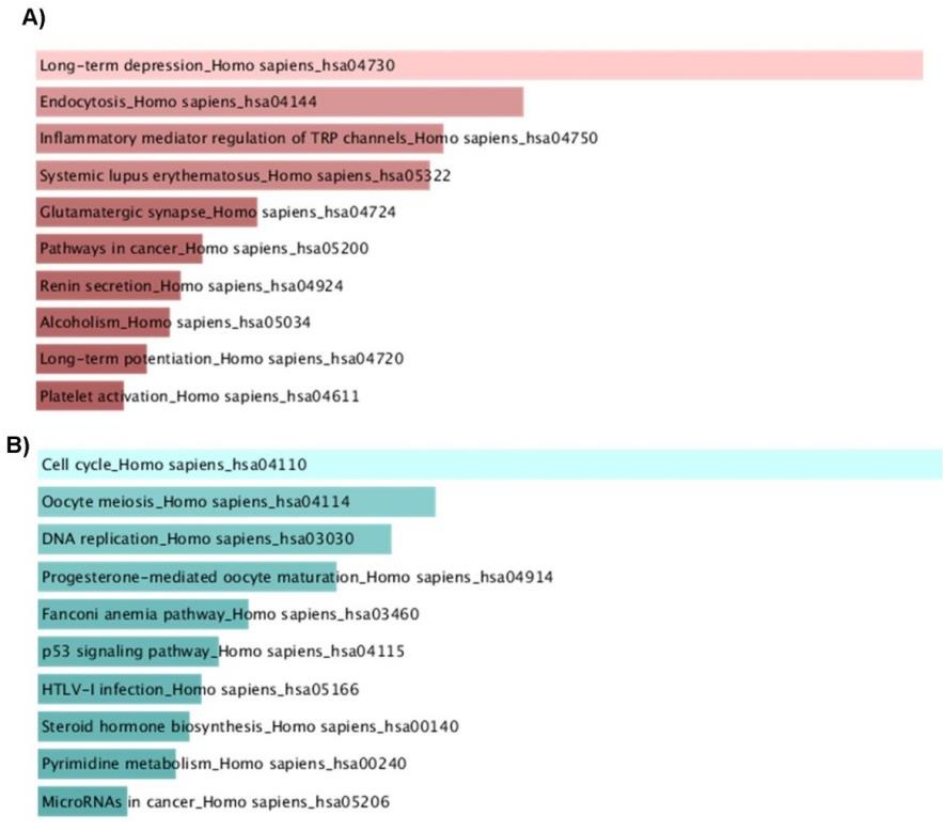


## 3.12 Ingenuity Pathway Analysis (IPA) of the additively or inversely affected pathways upon CHRNA5 siRNA-1 along with mimic miR-495 treatments based on microarray analysis.

The microarray expression profile obtained with siRNA-1 and miRNA mimic-495 was also analyzed with IPA (Ingenuity Pathway Analysis, QIAGEN Inc.) package. First 'Core Analysis' was performed, and the changes in the canonical pathways were ordered according to p-value (Figure 3.26A). Here, the darker the color the significant the pathway affected. As an example, 'Role of CHEK proteins in cell cycle regulation' was significantly affected in each of the treatment, but the significance had an increased tendency when

CHRNA5 depleted and miR-495 overexpressed both (3rd row in Figure 3.26A). Similarly, cyclins and cell cycle regulation, cell cycle: G1/S checkpoint regulation was also exhibited the same trend.

In addition to Canonical pathway analysis, 'Diseases and Bio Functions' analysis was also performed in order to reveal which disease came in prominence due to the affected canonical pathways. According to this, the functions promoting cancer cell proliferation (cell proliferation of tumor cell lines, M phase of tumor cells, entry into S phase, etc) were inhibited by CHRNA5 depletion alone and miR-495 overexpression alone, and this inhibition was further enhanced with the combination of CHRNA5 depletion and miR-495 overexpression together (Figure 3.26B). Compared to the inhibited pathways which were mainly associated with the promotion of cancer cells, the pathways related with DNA damage, chromosome instability and invasion of the cells were activated upon both CHRNA5 depletion and miR-495 overexpression (Figure 3.26B).

Based on these analysis and anti-proliferative effects of CHRNA5 depletion as mentioned in the previous sections, among the affected pathways 'Cell cycle: G1/S check point regulation' was investigated further and a detailed network was generated (Figure 3.26C). Increased level of CDKN1A (p21), whose upregulation upon CHRNA5 depletion was confirmed with microarray and RT-qPCR analysis in the previous sections (Figure 3.2), was observed (Figure 3.26C). Consistent with its role in promoting G1/S arrest by inhibiting CDK2 and CDK4 [295], decreased levels these molecules were appeared in the pathway analysis as well (Figure 3.26C). Moreover, decreased levels RB and E2F levels also strongly pointed to G1-S arrest.

**A)**


Canonical Pathway
-log(p-value)
0,1
7,6
Si_495
Mimic_495
Simimic_495
Role of BRCA1 in DNA Damage Response
Cell Cycle Control of Chromosomal Replication
Role of CHK Proteins in Cell Cycle Checkpoin...
Mitotic Roles of Polo-Like Kinase
Hereditary Breast Cancer Signaling
Cell Cycle: G2/M DNA Damage Checkpoint R...
p53 Signaling
Molecular Mechanisms of Cancer
Mismatch Repair in Eukaryotes
ATM Signaling
Sumoylation Pathway
Protein Ubiquitination Pathway
Pancreatic Adenocarcinoma Signaling
TGF-β Signaling
DNA Double-Strand Break Repair by Homolo...
GADD45 Signaling
Cell Cycle Regulation by BTG Family Proteins
Estrogen-mediated S-phase Entry
Cyclins and Cell Cycle Regulation
Chronic Myeloid Leukemia Signaling
Cell Cycle: G1/S Checkpoint Regulation
Interferon Signaling
Glioblastoma Multiforme Signaling
UVA-Induced MAPK Signaling
PTEN Signaling
Germ Cell-Sertoli Cell Junction Signaling
HER-2 Signaling in Breast Cancer
Breast Cancer Regulation by Stathmin1
Glioma Signaling
Role of NFAT in Cardiac Hypertrophy
Aryl Hydrocarbon Receptor Signaling
Ephrin Receptor Signaling
Prostate Cancer Signaling
PI3K/AKT Signaling
IL-8 Signaling
Death Receptor Signaling
Colorectal Cancer Metastasis Signaling
Semaphorin Signaling in Neurons
Myc Mediated Apoptosis Signaling
NGF Signaling
B Cell Receptor Signaling
Rac Signaling
HGF Signaling
IGF-1 Signaling
Antiproliferative Role of TOB in T Cell Signaling
Actin Nucleation by ARP-WASP Complex
Integrin Signaling
Small Cell Lung Cancer Signaling
Inhibition of Angiogenesis by TSP1
ILK Signaling

**B)**


Diseases and Bio Functions
Activation z-score
-3.650
3.373
siA5
mimic_495
siA5+mimic495
proliferation of cells
homologous recombination
death of embryo
cytokinesis
cell proliferation of tumor cell lines
association of chromosome components
association of chromatin
chromosomal aberration
M phase of tumor cell lines
M phase
quantity of microtubules
entry into interphase
chromosomal congression of chromosomes
metabolism of DNA
alignment of chromosomes
cytokinesis of tumor cell lines
interphase of gonadal cells
checkpoint control
differentiation of cells
senescence of cells
organization of cytoskeleton
organization of cytoplasm
interphase
tumorigenesis of reproductive tract
female genital neoplasm
M phase of cervical cancer cell lines
segregation of chromosomes
cycling of centrosome
DNA replication
formation of mitotic spindle
entry into interphase of oocytes
entry into S phase
microtubule dynamics
DNA damage
chromosomal instability
cytokinesis of cervical cancer cell lines
interphase of connective tissue cells
respiratory system tumor
repair of DNA
invasion of cells
lymphocytic cancer
interphase of tumor cell lines
incidence of tumor
exchange of sister chromatids
sister chromatid exchange of tumor cell lines
cell death of cervical cancer cell lines
S phase of tumor cell lines
quantity of gonad
lung tumor
meiosis I of female germ cells

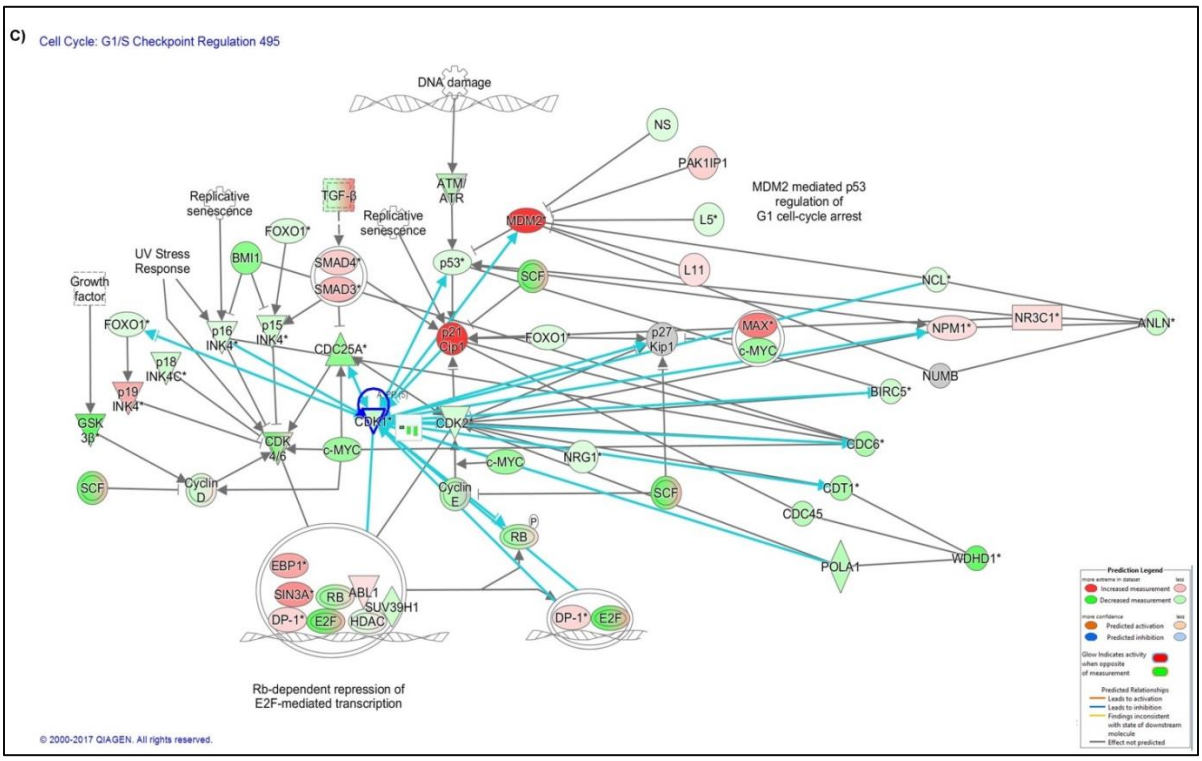


**Figure 3.26: IPA upon CHRNA5 depletion and miR-495 overexpression**. The effects of each 3 treatments (i.e only siRNA-1, only miR-495 mimic and siRNA-1 + miR-495 mimic) in canonical pathways **(A)**, in diseases and bio functions (blue indicates inhibition, orange indicates activation) **(B)**, in G1-S cell cycle arrest (**C**).

Since the majority of the downregulated miRNAs were clustered in 14q32.31 region, I, in collaboration with Said Tiryaki, also wanted to further address what kind of biological functions and diseases that these miRNAs involved in by using IPA (first core analysis of miRNA targets). As illustrated in Figure 3.27, these miRNAs mostly associated with cell growth and survival mechanisms. Among them, 'cellular growth and proliferation' ranked in the 5th place and analyzed further (Figure 3.27 A). According to the number of molecules involved in 'cellular growth and proliferation' category, the top three downregulated functions appaeredd as follows: 'proliferation of tumor cells', 'cell proliferation of breast cancer cell lines' and ' proliferation of cancer cells'. Then, those clustered miRNAs along with the genes both interacting with these miRNAs and the ones affected by CHRNA5 depletion were mapped around these three functions. Overall,

divergent and/or convergent effect of these signalling cascades pointed to inhibited proliferation of breast cancer cell lines (Figure 3.27 B).

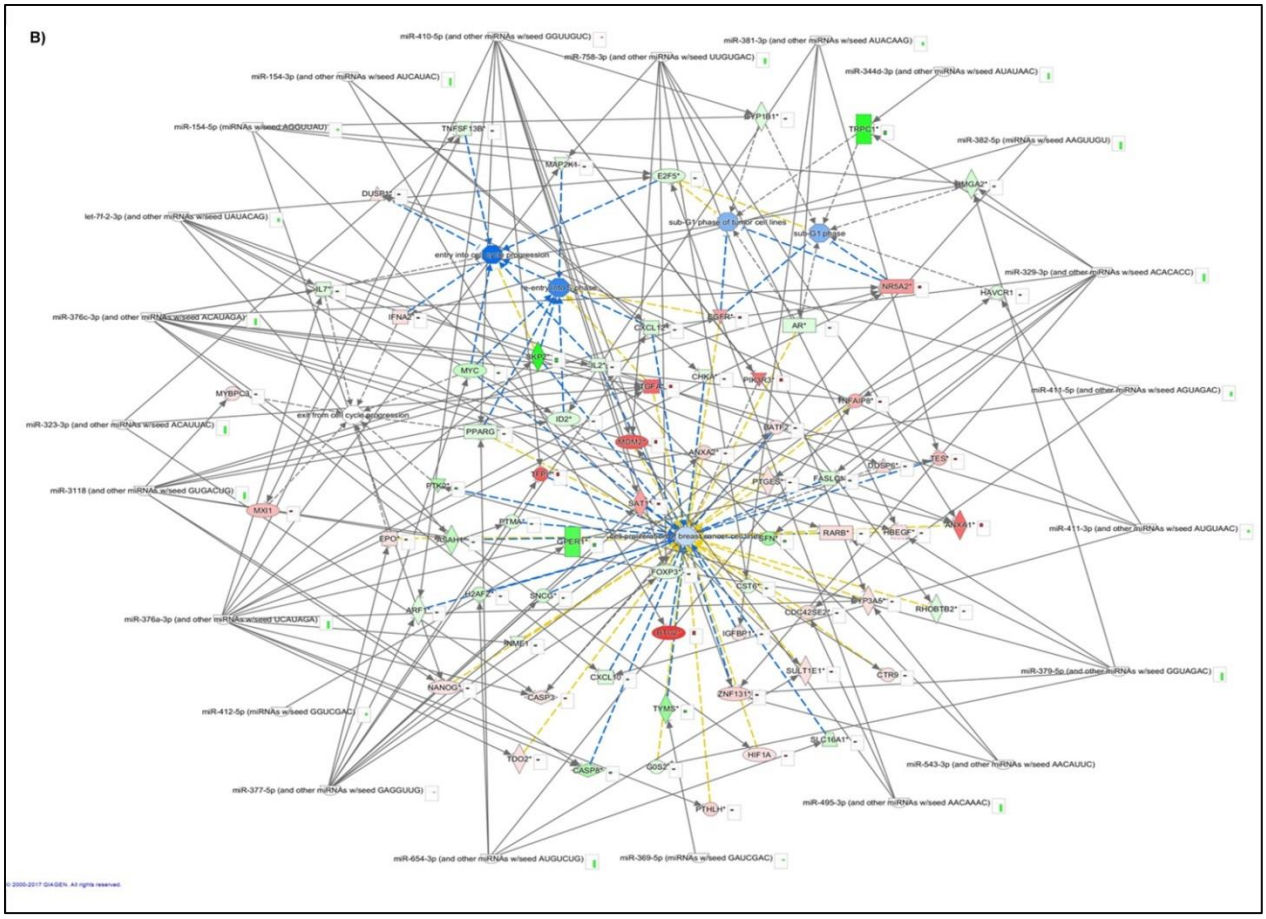


**Figure 3.27: IPA of miRNAs clustered in 14q32.31 region**. Top 10 diseases and bio functions related with miRNAs from 14q32.31 region **(A)**. Detailed map of the affected genes upon CHRNA5 depletion analyzed with the clustered miRNAs at 14q32.31 region **(B)**.

## 3.13 Does use of CHRNA5 RNAi or mimic mir-495 alone or together with each other affect cell viability and cell cycle distributions?

In the beginning of the study, anti-proliferative effects of siRNAs targeting CHRNA5 were well demonstrated (Figure 3.3). In order to observe the effects of siRNA-1 and miRNA-mimic 495 together, MTT assay was carried out. The group having siRNA-1+siRNA-CN (green bar in Figure 3.28) exhibited the effect of CHRNA5 depletion, and in the same manner siRNA-CN+miRNA-mimic 495 (red bar in Figure 3.28) exhibited the effect of

mimic miR-495. Therefore both molecules resulted in decreased cell viability. When these two molecules were given to the cells (blue bar in Figure 3.28), cell viability decreased as much as siRNA-1 (20nM) treatment showing the additive effect of siRNA-1 and mimic miR-495 in terms of reducing in cell viability (Figure 3.28).

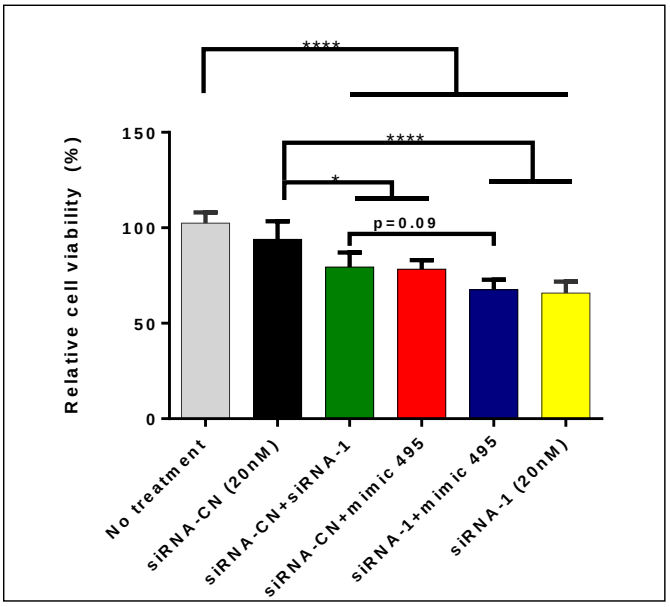


**Figure 3.28: MTT assay to investigate the effects of CHRNA5 depletion and miR-495 mimic treatment on cell viability of MCF7 cells** One-Way ANOVA followed by Tukey's multiple test correction were used for statistical analysis (*: p <0.05, ****: p<0.0001)

To further address the effects of CHRNA5 depletion together with miR-495 overexpression on cell cycle distribution in MCF7 cells, Propidium Iodide (PI) staining was conducted. For this, samples were treated either with siRNA-1 or miR-495 mimic alone or together for 72h. Through FACS analysis, cell cycle distribution of MCF7 cells were observed to be significantly enriched in G1-phase when the cells treated with siRNA-1+siRNA-CN (green bar) or mimic miR-495+siRNA-CN (red bar) compared to siRNA-CN control (black bar). Moreover, the combinatorial effect of siRNA-1 and mimic miR-495 (blue bar) had further resulted in increased number of cells in G1 phase (p=0,055) compared to siRNA-1+siRNA-CN (black bar). This result pointed that enrichment of G1 population upon CHRNA5 depletion could be further enhanced with the additive effect of miR-495 overexpression in MCF7 cells (Figure 3.29).

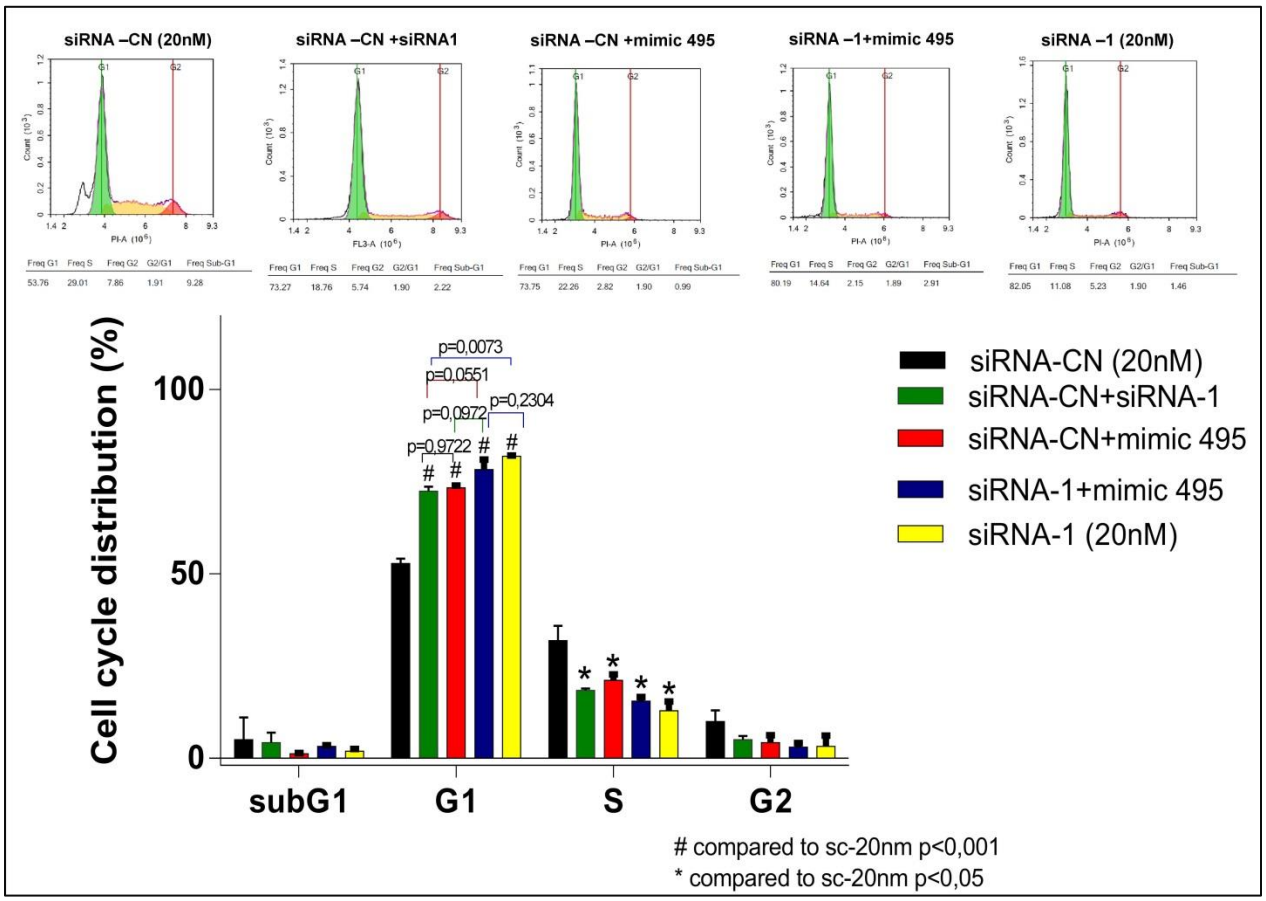


**Figure 3.29: PI staining of MCF7 cells treated with combinations of siRNA-1 and miR-495 mimic.** Treatments were held with either siRNA-1 alone or miR-495 mimic alone and together with siRNA-1 and miR-495 mimic in MCF7 cells for 72h, (n=2 per group). One-Way ANOVA followed by Tukey's multiple test correction were used for statistical analysis. (#: p< 0.001; *: p<0.05 and compared to siRNA-CN (20nM).

In order to well differentiate the cells during cell cycle progression upon CHRNA5 depletion along with miR-495 upregulation, 7-AAD/BrDU staining was also performed with the same treatment groups. Similar to the PI staining, this method also assesses cell proliferation, cell cycle distribution and apoptosis as well. Despite percentage of S phases of all treatment groups were lower than expected; still we could observe enrichment of the cells in G1 phases (Figure 3.30). For example, siRNA-1+miR-495 mimic treated group had more cells enriched in G1 phase compared to siRNA-CN+miR-495 mimic treated group, by supporting the additive effects of these two molecules in terms of induction of G1/S arrest (Figure 3.30).

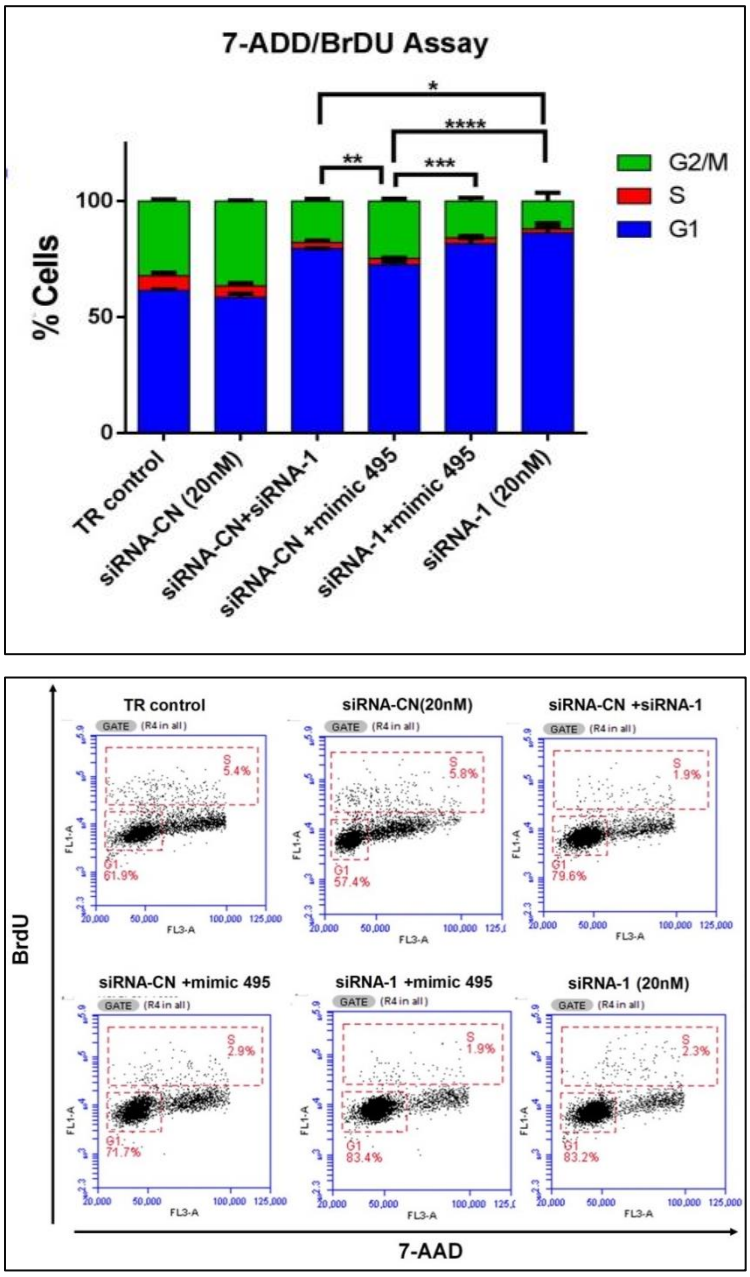


**Figure 3.30: 7-AAD/BrDU staining of MCF7 cells treated with miR-495 mimic alone or together with siRNA-1 in MCF7 cells.** (In the graph, only the statistical analyses in between groups were shown for 'G1' phase. *: p< 0.05, **: p<0.01, ***: p<0.001, ****: p< 0.0001. Two-Way ANOVA was used for statistical analysis and all treatment groups; siRNA-CN+siRNA-1, siRNA-CN+mimic-495, siRNA-1+mimic-495 were significantly different than siRNA-CN and TR control at the same significance level p<0.0001).

## 3.14 Does use of CHRNA5 RNAi or mimic mir-495 alone or together have effects on DNA damage and apoptosis?

In order to reveal the mechanism behind additive action of siRNA-1 and miR-495 mimic on decreased proliferation levels (Figure 3.28) and enrichment of the cells at G1 phase (Figure 3.29 and 3.30), western blotting was performed to examine the proteins that might participate this observed phenotype. MCF7 cells were treated with siRNA-1(10nM) and miR-495 mimic (10nM) alone or in combination as mentioned before. Cells were visualized with DIC microscopy just before protein collection (Figure 3.31). Depletion of CHRNA5 resulted in the same lunate structure as observed before. However, the addition of mimic miR-495 did not enhance this structure, rather acted in between siRNA-CN and siRNA-1 exposed phenotype (Figure 3.31).

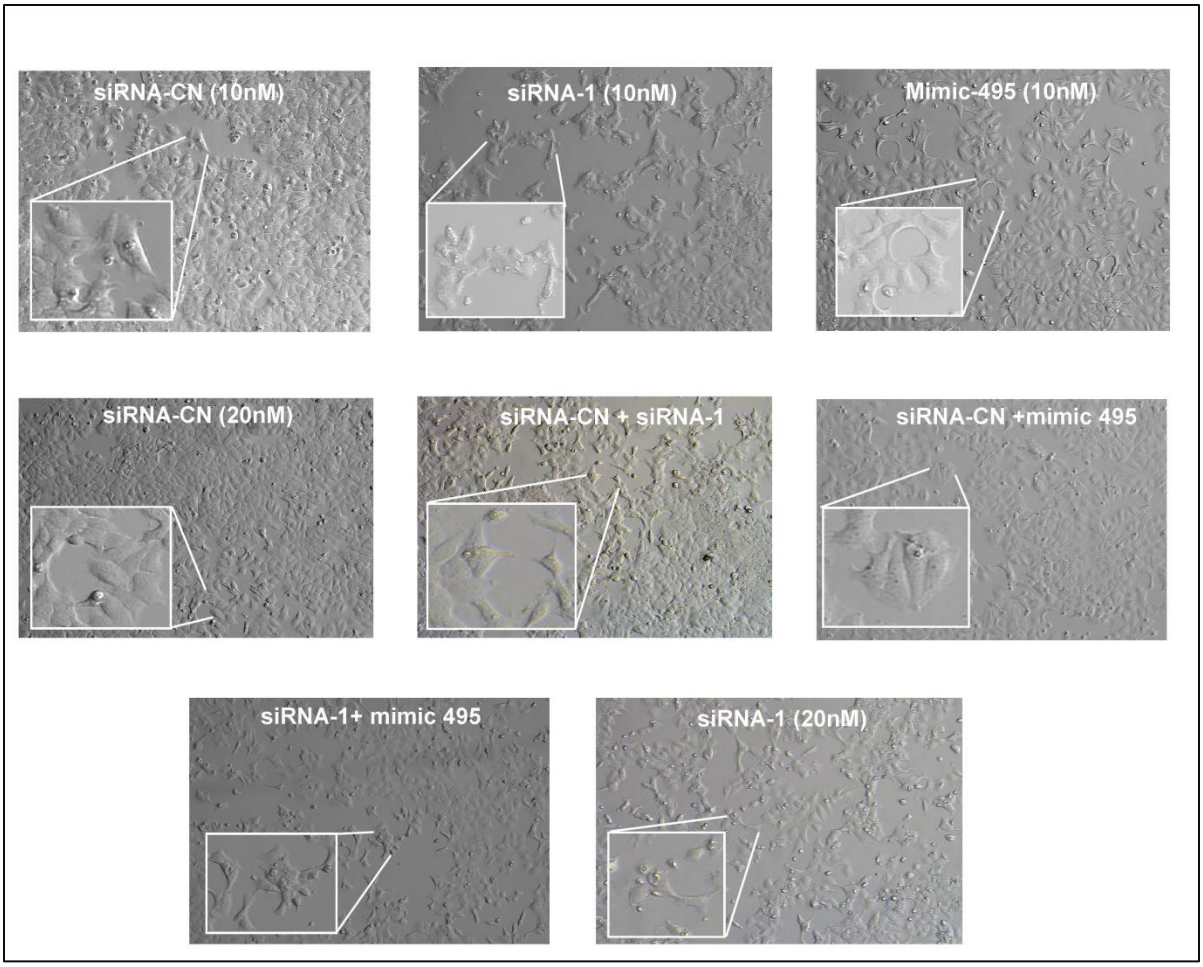


**Figure 3.31: Effects of siRNA-1 and /or mir-495 mimic treatments on MCF7 cells' phenotype.** Images were taken at the end 72h of treatments**.**

With Western blot study, in addition to the proteins checked with the CHRNA5 siRNA study (pRB, BCL2, BAX, p-chek1, γH2AX), proteins involved in cell cycle progression such as CDK2, CDKN1A (p21) were studied as well (Figure 3.32A and B). Depletion of CHRNA5 was confirmed with siRNA-1 alone or mimic miR-495 exposures (Figure 3.32A). The increased level of CDKN1A at mRNA level, which plays an essential role in DNA Damage response by inducing cell cycle arrest [295], was also observed at the protein level upon CHRNA5 depletion as well. However, miR-495 mimic alone or in combination with siRNA-1 did not result in further increases; rather they acted antagonistically on CDKN1A levels (Figure 3.32A). On the other hand, CHRNA5 depletion alone as well as together with miR-495 overexpression diminished the levels of pRB. This was also

compatible with decreased CDK2 levels upon siRNA-1 and mimic miR-495, which is required for the phosphorylation of RB during cell cycle progression [296],(Figure 3.32A).

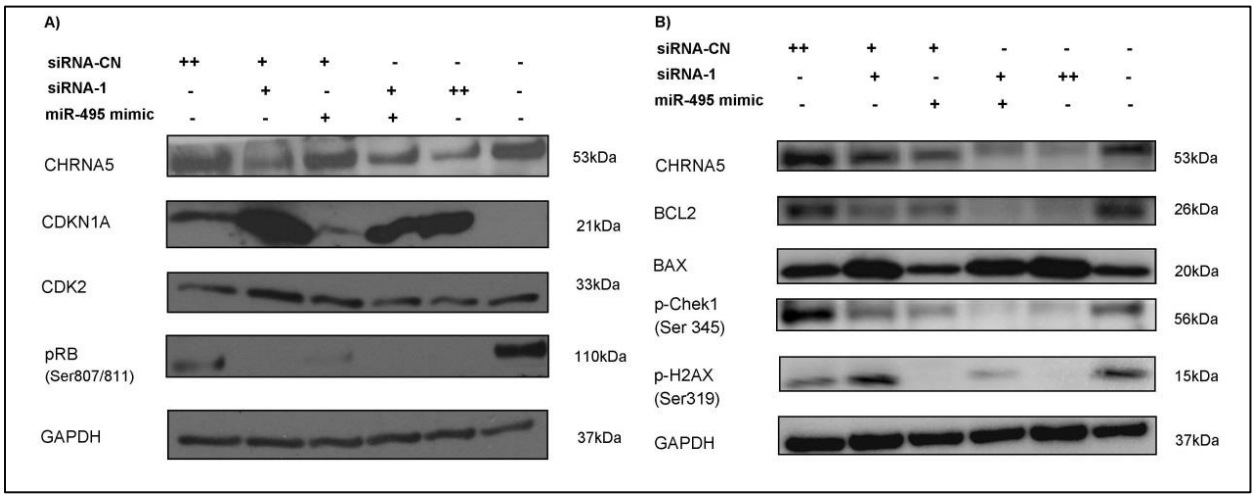


**Figure 3.32: Effects of CHRNA5 depletion and miR-495 overexpression on proteins in MCF7 cells.** Images of CHRNA5, CDKN1A, CDK2, pRB1 proteins **(A)** and BCL2, BAX, p-CHEK1 and γH2AX proteins **(B)** at the end of 72 h treatment with mimic miR-495 alone or together with siRNA-1 in MCF7 cells. GAPDH was used as a loading control.

As observed previously, depletion of CHRNA5 resulted in decreased pCHEK1 levels and this decrease was further enhanced with the addition of miR-495 mimic. In accordance to this, the increased levels of pH2AX (Ser139) was only recorded upon CHRNA5 depletion alone (Figure 3.32B). Increased BAX and decreased BCL2 levels were again observed as expectedly upon CHRNA5 depletion. Despite BAX levels did not further increase with the addition of miR-495 mimic, siRNA-1 and miR-495 mimic together downregulated BCL2 levels even more; implementing a high BAX/BCL2 ratio compared to the control groups (Figure 3.32B).

## 3.15 What are the genes that siRNA-1 and miR-495 mimic act either additively or inversely based on microarray analysis and can they be validated by qPCR?

The genes investigated upon CHRNA5 depletion were also analyzed upon siRNA-1 and miR-495 mimic treatments in order to reveal in which pathways these two molecules acted on additively or inversely.

siRNA-1 and mimic miR-495 acted in similar direction on the genes associated with cell cycle regulation. Those three genes, WDHD1, BIRC5 and ANLN exhibited a decreased expression trend when only siRNA-1 or only mimic miR-495 was given to the cells whereas given together, they significantly resulted in downregulation of each gene (Figure 3.33A). This result was also compatible with the microarray data (Figure 3.33A).

CCND1, one of the modulators of E2F signaling, levels were checked with RT-qPCR and it was not significantly affected by siRNA-1 alone; however, miR-495 mimic significantly downregulated its expression and this effect was still in the same trend when siRNA-1 and miR-495 mimic were given together supporting the microarray data (Figure 3.33B). In accordance with these, CCNE2 and CDC6, other modulators of E2F signaling, were also downregulated upon CHRNA5 depletion; however, they were not affected by miR-495 mimic treatment alone. Upon given together with siRNA-1, they additively downregulated these genes which were at the same time compatible with the microarray data (Figure 3.33B).

As mentioned before, DDR was one of the most significantly affected pathways upon CHRNA5 depletion. Among the key players of this pathway, CHEK1 was examined in previous sections and downregulation of CHEK1 was recorded with three siRNA molecules (Figure 3.5A). Here, CHEK1 again exhibited the same trend upon CHRNA5 depletion however mimic miR-495 did not affect its expression (Figure 3.33C). MDM2, which is the negative regulator of TP53 by inducing its degradation [297], was also

examined in the context of siRNA-1 and miR-495 mimic treatments. MDM2 was significantly downregulated by siRNA-1 however it was not significantly affected by miR-495 mimic treatment alone. When they were given together, the effect of siRNA-1 on MDM2 expression dominated over miR-495 mimic hence the same decreased level was observed (Figure 3.33C).

In addition to the negative regulator of TP53, targets of TP53 signaling pathway were checked in this concept, since CHRNA5 depletion itself resulted in upregulation of TP53 targets (Figure 3.2). Among them, GADD45A, one of the downstream targets of TP53 upon DNA damage which stabilized TP53 [290], was upregulated when CHRNA5 depleted. When miR-495 mimic was given to MCF7 cells, it did not affect the expression level of GADD45A. However, when siRNA-1 and miR-495 mimic were given together, they had tendency to act antagonistically but still the effect of siRNA-1 on upregulating GADD45A levels was prominent (Figure 3.33D). Similarly, another TP53 target gene, CDKN1A (p21) also exhibited the same trend with GADD45A (Figure 3.33D). Another TP53 target GPNMB was also significantly upregulated upon CHRNA5 depletion consistent with previous observations (Figure 3.2). In the case of miR-495 mimic treatment, it marginally downregulated GPNMB levels, in other words acted in opposite direction of siRNA-1. Upon given together, GPNMB had tendency to be increased, however it was not significant. miR-495 mimic treatment opposed siRNA-1 effect on GPNMB expression levels (Figure 3.33D).

Genes in the context of cytoskeletal arrangement were also examined. CLDN1 and MAP1B were significantly upregulated upon CHRNA5 depletion alone and miR-495 mimic treatment alone as well. Furthermore, upon exposure to both siRNA and mimic molecules the expressions of these genes were upregulated even more (Figure 3.33E).

Finally, the genes associated with apoptosis which were checked in the previous sections, were also investigated in this part of the study as well. Unlike previous findings, both siRNA-1 and miR-495 did not affect expressions of BAX at mRNA level (Figure 3.33F), which could be due to feedback mechanism since we were able to observe increased

BAX at protein level (Figure 3.32B). BCL2 had tendency to be downregulated upon CHRNA5 depletion alone or miR-495 mimic treatment alone and with their combinatorial treatments, yet not significantly. However, this trend can still have biological relevance. One of the most important molecules induced during apoptosis is FAS, whose upregulation at both mRNA (Figure 3.5A) and protein levels (Ermira Jahja, PhD thesis, 2017) were recorded in the context of CHRNA5 depletion study, examined in this part of the thesis as well. As expectedly, CHRNA5 depletion resulted in significantly high expression levels of FAS, however miR-495 mimic treatment alone significantly downregulated its expression (Figure 3.33F). When siRNA-1 and miRNA-495 mimic were given together, FAS levels were upregulated but a lesser degree compared to siRNA-1 alone treatment. This result implied the antagonism between siRNA-1 and miR-495 molecules on FAS regulation (Figure 3.33F).

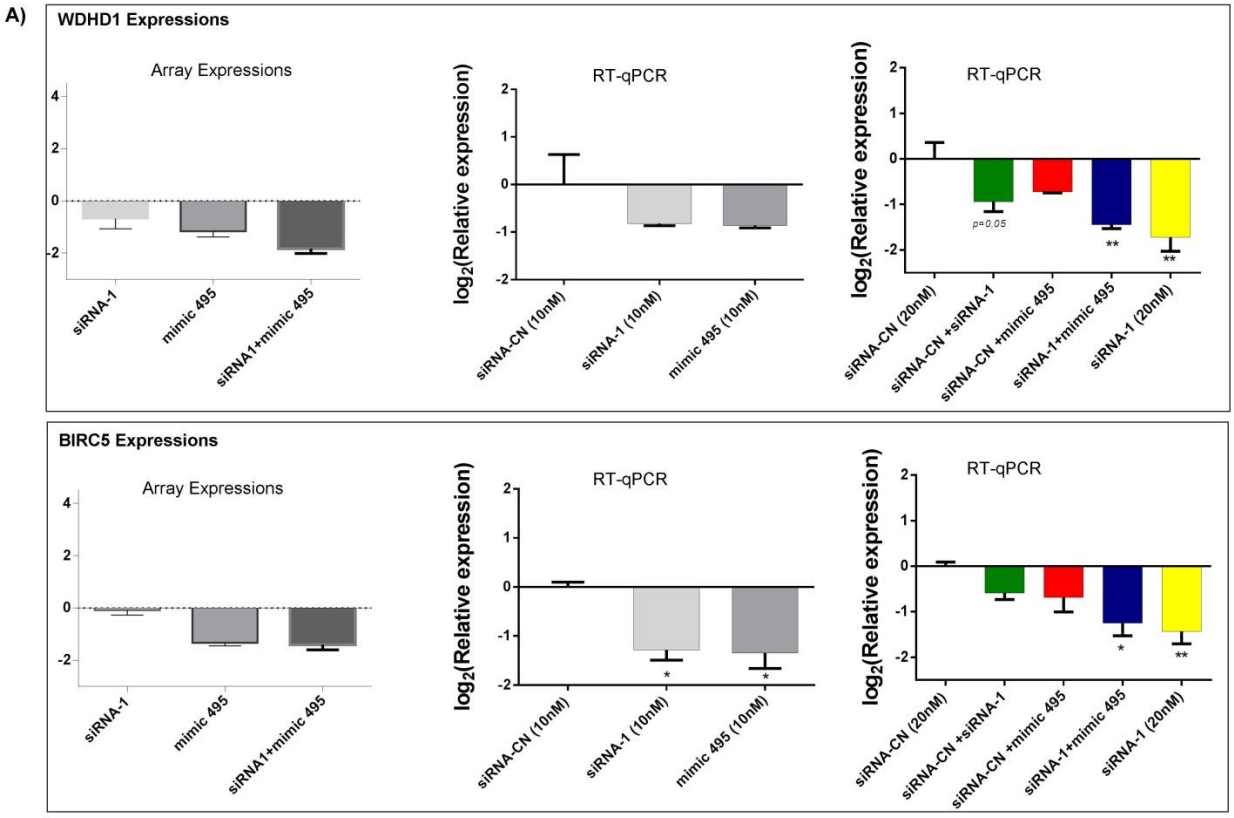

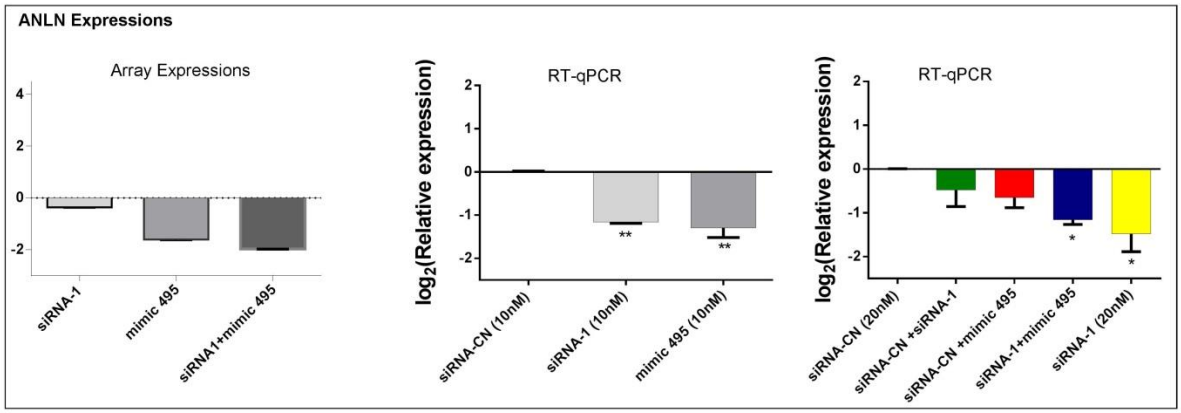
ANLN Expressions
Array Expressions
siRNA-1
mimic 495
siRNA1+mimic 495
RT-qPCR
log2(Relative expression)
siRNA-CN (10nM)
siRNA-1 (10nM)
mimic 495 (10nM)
RT-qPCR
log2(Relative expression)
siRNA-CN (20nM)
siRNA-CN +siRNA-1
siRNA-CN +mimic 495
siRNA-1+mimic 495
siRNA-1 (20nM)

B)

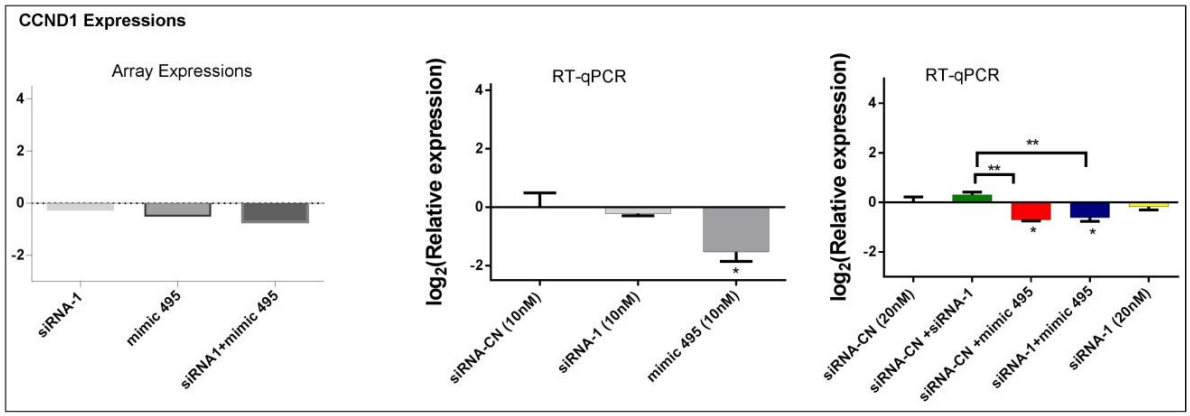
CCND1 Expressions
Array Expressions
siRNA-1
mimic 495
siRNA1+mimic 495
RT-qPCR
log2(Relative expression)
siRNA-CN (10nM)
siRNA-1 (10nM)
mimic 495 (10nM)
RT-qPCR
log2(Relative expression)
siRNA-CN (20nM)
siRNA-CN +siRNA-1
siRNA-CN +mimic 495
siRNA-1+mimic 495
siRNA-1 (20nM)

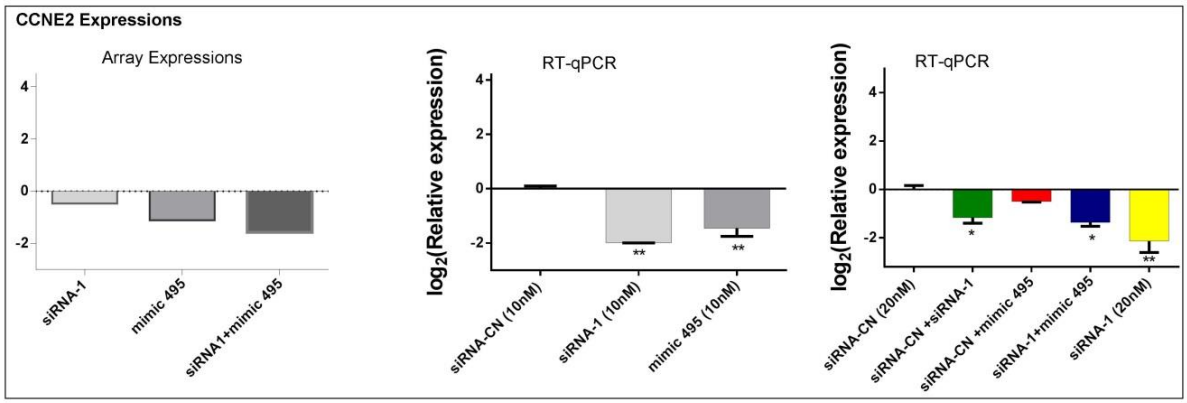
CCNE2 Expressions
Array Expressions
siRNA-1
mimic 495
siRNA1+mimic 495
RT-qPCR
log2(Relative expression)
siRNA-CN (10nM)
siRNA-1 (10nM)
mimic 495 (10nM)
RT-qPCR
log2(Relative expression)
siRNA-CN (20nM)
siRNA-CN +siRNA-1
siRNA-CN +mimic 495
siRNA-1+mimic 495
siRNA-1 (20nM)

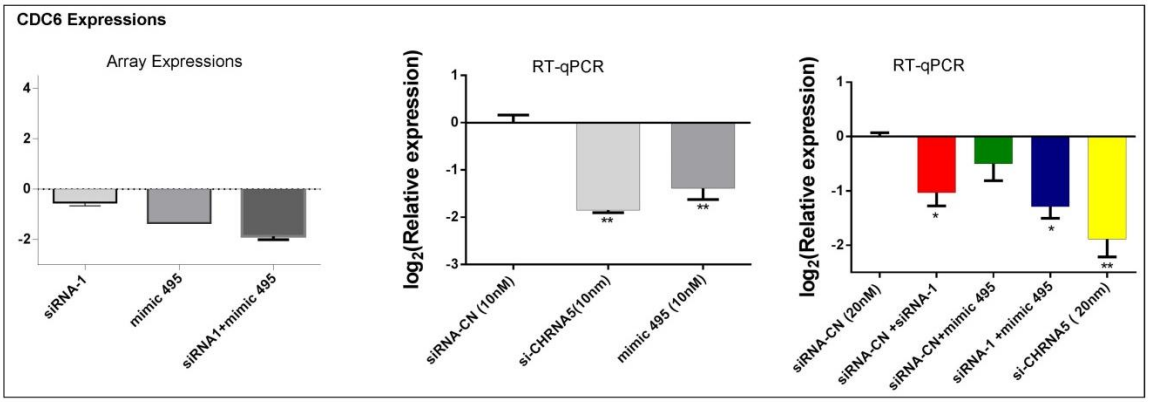
CDC6 Expressions
Array Expressions
siRNA-1
mimic 495
siRNA1+mimic 495
RT-qPCR
log2(Relative expression)
siRNA-CN (10nM)
si-CHRNA5(10nm)
mimic 495 (10nM)
RT-qPCR
log2(Relative expression)
siRNA-CN (20nM)
siRNA-CN +siRNA-1
siRNA-CN+mimic 495
siRNA-1 +mimic 495
si-CHRNA5 ( 20nm)

C)

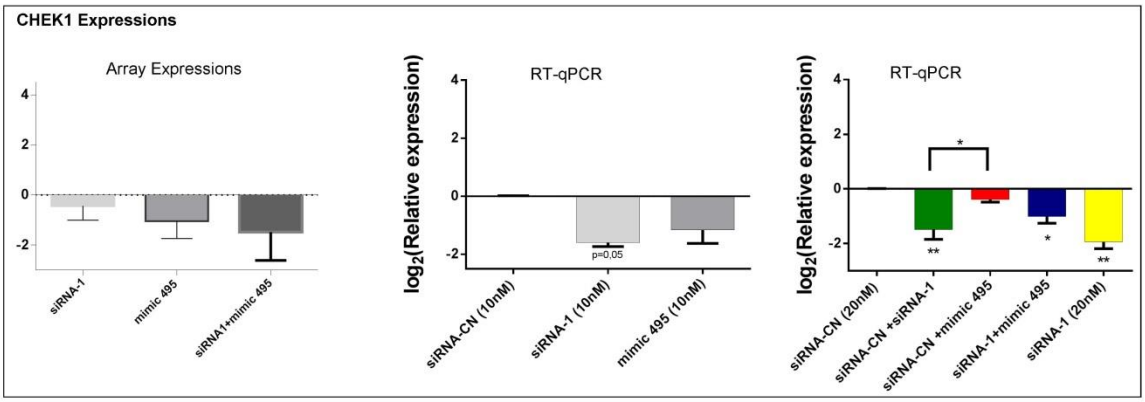
CHEK1 Expressions
Array Expressions
siRNA-1
mimic 495
siRNA1+mimic 495
RT-qPCR
log2(Relative expression)
p=0,05
siRNA-CN (10nM)
siRNA-1 (10nM)
mimic 495 (10nM)
RT-qPCR
log2(Relative expression)
siRNA-CN (20nM)
siRNA-CN +siRNA-1
siRNA-CN +mimic 495
siRNA-1+mimic 495
siRNA-1 (20nM)

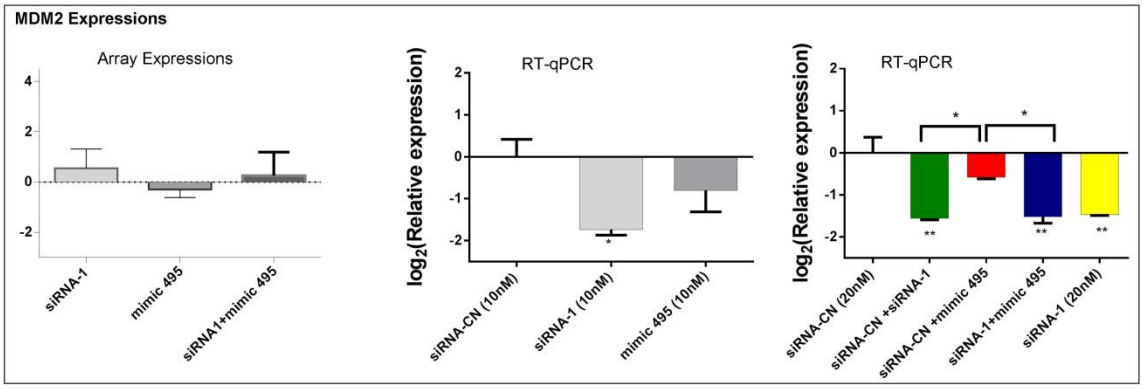
MDM2 Expressions
Array Expressions
siRNA-1
mimic 495
siRNA1+mimic 495
RT-qPCR
log2(Relative expression)
siRNA-CN (10nM)
siRNA-1 (10nM)
mimic 495 (10nM)
RT-qPCR
log2(Relative expression)
siRNA-CN (20nM)
siRNA-CN +siRNA-1
siRNA-CN +mimic 495
siRNA-1+mimic 495
siRNA-1 (20nM)

D)

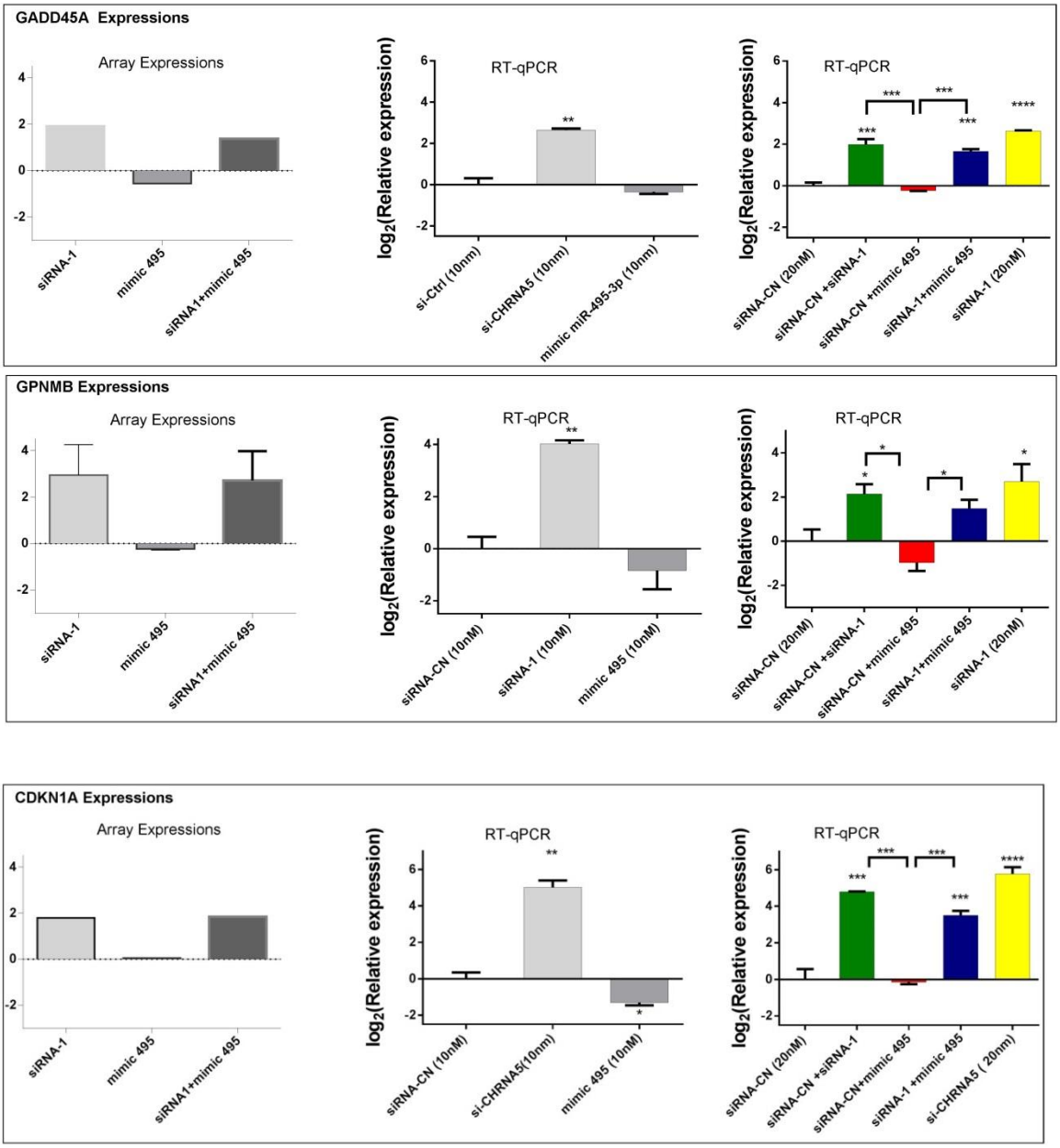
GADD45A Expressions
Array Expressions
siRNA-1
mimic 495
siRNA1+mimic 495
RT-qPCR
log2(Relative expression)
si-Ctrl (10nm)
si-CHRNA5 (10nm)
mimic miR-495-3p (10nm)
siRNA-CN (20nM)
siRNA-CN +siRNA-1
siRNA-CN +mimic 495
siRNA-1+mimic 495
siRNA-1 (20nM)
GPNMB Expressions
siRNA-CN (10nM)
siRNA-1 (10nM)
mimic 495 (10nM)
CDKN1A Expressions
si-CHRNA5(10nm)
siRNA-CN +siRNA-1
siRNA-CN+mimic 495
siRNA-1 +mimic 495
si-CHRNA5 ( 20nm)

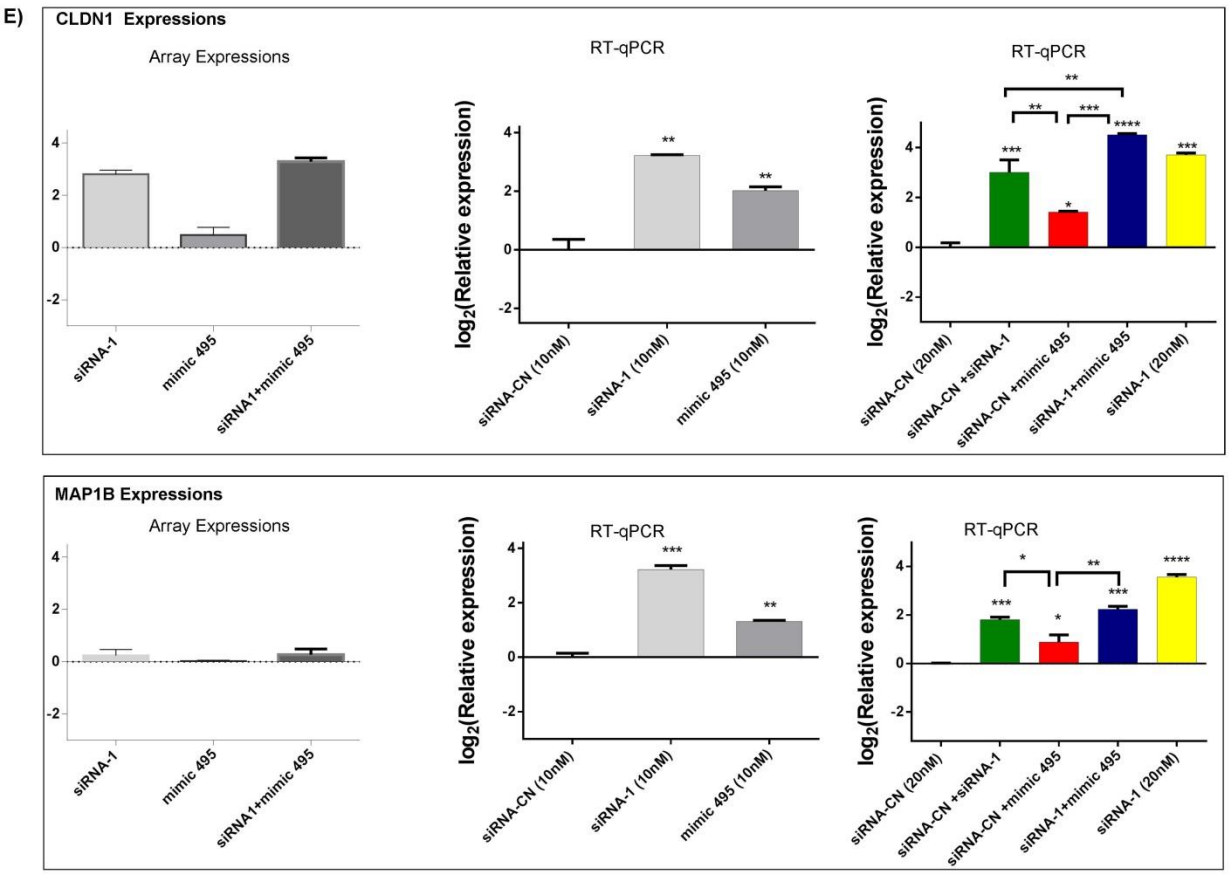


**Figure 3.33**: **RT-qPCR validation of additively or inversely affected genes from miR-495 microarray study**. On the left sides the results from miR-495 array is shown. RT-qPCR results for two groups having different concentrations are shown in the middle and on the right side. **A)** WDHD1, BIRC5 and ANLN. **B)** CCND1, CCNE2 and CDC6. **C)** CHEK1 and CDC6. **D)** GADD45A, GPNMB, CDKN1A. **E)** MAP1B and CLDN1. **F)** BAX, BCL2, FAS. (n=2 per group for RT-qPCR results). One-Way ANOVA followed by Tukey's multiple test correction were used for statistical analysis. (*: p<0.05, **: p<0.01; ***: p<0.001; ****: p<0.0001).

# CHAPTER 4: CONCLUSIONS AND DISCUSSION

## 4.1 Key Findings of the thesis

Cholinergic Receptor Nicotinic Alpha 5 (CHRNA5) is one of the subunits of pentameric cholinergic receptors with important roles in regulation of cellular signaling therefore its dysregulation can result in pathologies including cancer. RNAi is one of the methodologies that can help decipher the role of a gene in the cell while it can also be a treatment modality.

1) In the present thesis I have investigated the role of multiple siRNAs against CHRNA5 on apoptosis markers BAX/BCL2 mRNA and protein ratio and caspase 7 activation, cell proliferation marker RB phosphorylation (pRB) and CCNE2 mRNA expression levels, as well as a series of DNA damage response markers such as CHEK1 at mRNA and protein levels, levels of phosphorylated CHEK1 and H2AX proteins in breast cancer cells. The findings indicated a strong apoptotic response in MCF7 cells in response to CHRNA5 RNAi while cell proliferation was significantly reduced in association with reduced pRB levels and CCNE2 mRNA by at least two of the three siRNA molecules tested in MCF7 cells. I have found that CASP7 and pH2AX exhibited variable levels.

2) I also tested whether topoisomerase inhibitors synergized with CHRNA5 RNAi using MTT and Western blotting and showed lower cell viability at a concentration and cell line dependent manner when TOPO inhibitors combined with CHRNA5 RNAi. Interestingly, both BT-20 and MDA-MB-231 exhibited increased pCHEK1 levels in response to TOPO+CHRNA5 RNAi while MDA-MB-231 exhibited significantly lower CHEK1 levels.

3) One of the most important findings of this thesis is therefore the association between CHRNA5 RNAi and reduced CHEK1 levels, which is an indicator of increased drug sensitivity.

4) In this thesis I also investigated the association of microRNAs with CHRNA5 depletion.
    a. I first showed that miR15a/16, predicted to target CHRNA5, resulted in significant decreases in CHRNA5 expression when using mimics while showing similar changes in some of the CHRNA5 modulated transcripts. Future studies are needed to validate the binding of miR15a/16 on CHRNA5.
    b. I also discovered and validated that miR-495-3p was one of the most downregulated microRNAs upon CHRNA5 depletion in MCF7 cells which was checked with microarrays and validated with RT-qPCR as well. Moreover, along with CHRNA5 depletion, it exhibited anti-proliferative effects which were detected by using MTT, FACS as well as Western blotting and RT-qPCR analyses. Applying CHRNA5 RNAi together with miR-495-3p overexpression, which is known to act as tumor suppressor, resulted in accentuation of the inhibition of cell proliferation.
    c. Microarray and IPA analysis together with RT-qPCR validations revealed the genes that might have played roles in anti-proliferative effects of miR-495-3p. Several genes were discovered as being additively or antagonistically affected by miR-495-3p and CHRNA5 RNAi application.

In summary, I have identified CHRNA5 with important roles in modulation of apoptotic, cell proliferation, and DNA damage inducing pathways and also shown that the anticancer activity of CHRNA5 RNAi can be enhanced using DNA damaging drugs as well as other molecules such as microRNAs, miR-15a/16 and miR-495-3p.

## 4.2 Effect of CHRNA5 depletion on apoptosis, DNA damage and drug sensitivity in cancer cells

Despite there are many studies examining the roles of nAChRs in a variety of cancer types, there are limited number of studies which examine the role of CHRNA5 in cancers and yet there is no study investigating the role of CHRNA5 in breast cancer. In this thesis,

I aimed to reveal the downstream effects of CHRNA5 depletion on apoptosis, DNA damage response and drug sensitivity in MCF7, BT-20, and MDA-MB-231 breast cancer cell lines using different approaches. Complementing the previous findings in our lab, one of which was the successful downregulation of CHRNA5 at mRNA levels with two siRNA molecules (siRNA-1 and siRNA-3, Ermira Jahja, PhD Thesis, 2017), here I also showed downregulation of all five variants of CHRNA5 at mRNA levels with siRNA-2 and siRNA-3 molecules as well. This has made our findings more reliable suggesting the effects we observed are CHRNA5 specific. Indeed, in the literature use of multiple siRNAs are recommended [298]. Moreover, I supported this result at the mRNA level with significant downregulation of CHRNA5 at protein levels with three of the siRNA molecules.

Based on the previously done mRNA microarray study with 72h of siRNA-1 treated MCF7 cells (Ermira Jahja, PhD Thesis, 2017), here I also supported the alterations in the genes examined in siRNA-1 treated cells with siRNA-2 and siRNA-3 treated MCF7 cells. The significant downregulation of cell cycle related genes such as ANLN, BIRC5 and WDHD1 were also confirmed with 72h siRNA-2 and siRNA-3 treated MCF7 cells. Moreover, the upregulation of TP53 pathway related genes such as GADD45A, GPNMB and most importantly CDKN1A (p21) were also further verified with siRNA-2 and siRNA-3 treated samples implying the fact that these changes occurred due to specific targeting of these three siRNA CHRNA5 targeting molecules.

Compared to TP53 wild type MCF7 cells, the TP53 mutant BT-20 and MDA-MB-231 cells were also examined in the context of CHRNA5 depletion study. The longest isoform of CHRNA5 (CHRNA5_V1) levels in these TP53 mutant cells were effectively downregulated by siRNA-1 yet not as significant as in MCF7 cells (Ermira Jahja, PhD Thesis, 2017). In addition to the transcriptomic changes that occurred upon CHRNA5 depletion in these three cell lines, I also checked how phenotypes of these cells altered upon CHRNA5 depletion. Upon 72h of CHRNA5 depletion in MCF7 cells, they lost their typical spherical structure and became sparser with more branched phenotype. This kind of changes were not observed with the other TP53 mutant cell lines which might imply

these phenotypical changes occurred upon CHRNA5 depletion may be dependent on TP53 status of the cells.

One of the contributions of this study is revealing the molecular associations with the anti-proliferative effect of CHRNA5 depletion we observed in breast cancer cells. Moreover, with pathway analysis, alterations in TP53 signaling pathways and the pathways related with cell cycle regulation were found (Ermira Jahja, PhD Thesis, 2017). This finding was also consistent with the one observed with CHRNA5 depleted A549 lung cancer cell line [299]. Moreover, with MTT assay held with three of the siRNA molecules, I further supported the anti-proliferative effect of CHRNA5 depletion in MCF7 cells.

Due to the observation of increased percentage of in sub-G1 population as well as decreases in cell proliferation upon CHRNA5 depletion, further prompted me to examine the several key molecules participating in cell cycle progression, apoptosis and DDR with Western blotting. Decreased levels of pRB in MCF7 cells treated either one of the three siRNA molecules for 72h with two or more independently performed biological replicates strongly supported the molecular explanation of the observed G1/S arrest. Moreover, increased levels of CDKN1A (p21) at mRNA levels observed upon CHRNA5 depletion can further explain the reason behind decreased levels of pRB, since CDKN1A inhibits the phosphorylation of RB [300]. The decreased CCNE2 levels observed both with three of the siRNA molecules at mRNA levels by RT-qPCR as well as with the microarray study could also contribute to the decreased levels of pRB, since CCNE2 activated CDK2 to phosphorylate RB [301],[106].

Reductions in pRB levels result in not only G1/S arrest but also can induce apoptosis through dissociation from BAX [302]. With western blotting I detected increased expression levels of pro-apoptotic protein BAX together with reductions in anti-apoptotic BCL2 levels, pointing to significantly increased levels of BAX/BCL2 ratio with all of the siRNA molecules in MCF7 cells. Since increased BAX/BCL2 ratio is one of the predictive markers for [170] the apoptosis, we further examined the other molecules participating in apoptosis. Upon CHRNA5 depletion in MCF7 cells, three siRNA molecules resulted in

increased levels of FAS at mRNA levels, which is the molecule responsible for the induction of caspase cascade upon complexed with its ligand (FASL) [303]. Despite I observed significantly higher levels of cleaved capase-7/total caspase-7 ratio only with siRNA-1 treated MCF7 cells, prolonged depletion of CHRNA5 with 120h siRNA-1 treatment further implied that the end point of CHRNA5 depletion in MCF7 cells could be apoptosis.

Another important finding of this this study was that depletion CHRNA5 resulted in inhibition of CHEK1 phosphorylation. CHEK1 inhibitors have gained importance in cancer treatment [304], since they also enhance the chemosensitivity of cancer cells [123]. As stated in the literature decreased levels of CHEK1 lead to interruptions in DDR [305]. The contribution of this thesis at this point is, upon CHRNA5 depletion, the observed downregulation of CHEK1 phosphorylation along with total CHEK1 at protein levels supporting the increased sensitivity of cancer cells yet with cell type and dose specific manner.

To further identify the relationship between CHRNA5 depletion and CHEK1 inhibition together, I checked the levels of both CHEK1 and pCHEK1 levels in BT-20 and MDA-MB-231 cells treated with CPT and/or DOXO along with siRNA-1 treatments. Interestingly, those cells exhibited high levels of pCHEK1 upon TOPO treatments as opposed to MCF7 cells. This could be due to the intact DDR mechanism that these cells have [306]. Moreover, whereas CHRNA5 depletion enhanced the sensitivity of MCF7 cells to TOPO inhibitors at much lower doses, this was not the case for TP53 mutant BT20 cells probably due to increased pCHEK1 levels.

The major upstream players of CHEK1 activation in DDR are ATM and ATR [307], which are mostly activated upon double strand break and single strand break or stalled replication forks, respectively. ATR-CHEK1 signaling is important for genomic stability. Moreover, in the literature it was found high association between ATR and pCHEK1 levels in terms of prognosis of breast cancer [304] .Despite we did not examine these molecules in this study in detail, in our microarray analysis performed with siRNA1 and its control,

mild but significant reduction was observed in ATR levels (LFC=-0.3; p value=0.007). Therefore, in the future studies, changes that we observed in CHEK1 and pCHEK1 levels upon CHRNA5 depletion, should be also examined with regard to ATR as well.

Overall, in this part of the study I for the first time showed that CHRNA5 depletion resulted in inhibition of total CHEK1 in TP53 independent manner which interrupts DDR mechanism resulting in enhanced sensitivity against TOPO inhibitors. However there existed differences among cell lines with respect to TP53 status in pCHEK1 levels. Moreover, since CHRNA5 depletion also resulted in increased BAX/BCL2 ratio together with downregulation of cell cycle genes, in a TP53 dependent manner it is possible to say the result of these treatments clearly pointed to regulation of apoptosis.

## 4.3 Effect of CHRNA5 depletion on miR-15/16 family in MCF7 cells

RNAi mediated alterations in CHRNA5 and the resultant cellular consequences that were have observed in Konu lab, prompted me to investigate other molecules that could modulate CHRNA5 expression. One of them is miRNA family which are the small non-coding endogenous molecules participate in transcriptional or post-transcriptional regulation of target genes [308]. For this, I examined the expression levels of miR-15a family in CHRNA5 depleted cells, since they have predicted binding sites in 3'UTR of CHRNA5 based on targetscan prediction [288]. Previously it was shown that low level of miR-15a expression is highly associated with poor prognosis in breast cancer patients due to the tumor suppressor property of this miRNA [309]. Moreover, based on the findings in the literature such as the role of miR-15 family in doxorubicin sensitization in osteosarcoma [216] and tamoxifen sensitization in breast cancer [190] further led me to check the interactions between miR-15 family and CHRNA5 in MCF7 cells.

Although miR-15 family members of miRNAs generally act as anti-proliferative or apoptosis inducers [310], there also exist disease types where they act in the opposite direction [311]. To reveal the expression pattern of these miRNAs in MCF7 cells, first I

checked their expression levels in CHRNA5 depleted MCF7 cells. Since their expression levels were decreased upon CHRNA5 depletion and by knowing the fact that introduction of miR-15a increases the tamoxifen resistance [190], induces apoptosis through targeting of anti-apoptotic protein BCL-2 [192] and inhibits proliferation through reductions in CCND1 levels [196], I also overexpressed miR-15 family expression using miRNA mimics in MCF7 cells.

miR-15a mimicking acted similarly to CHRNA5 RNAi since it resulted in consistent and significant downregulation of five of the CHRNA5 variants in MCF7 cells. This led me to ask whether this mimicking would also affect the genes in the same direction that siRNA CHRNA5 did. First, I checked the expression of CASK which has putative binding sites for miR-15 family based on *targetscan* results [288]. Significant downregulation of CASK with of miR-15a and miR-16 mimic treatments confirmed the effectiveness of the miRNA mimics and the methodology of this study. Therefore, I checked the expression of representative genes from cytoskeleton structure, as well as cell cycle regulation. Among them, CLDN1, which is one of the major components of tight junctions [312], significantly was upregulated by miR-15a overexpression similar to the CHRNA5 RNAi (significant increases in CLDN1 with three of the siRNA molecules). Since low levels of CLDN1 in triple negative breast cancer is highly associated with high risk of death and recurrence [313], in the case of combinatorial treatment with siRNA CHRNA5 and miR-15a may result in increased upregulation of CLDN1 compared to siRNA alone or miR-15a mimic alone treatments and warrants further study.

Another gene examined in this concept was WDHD1 which is an important molecule in centromere function during cell division [314]. Consistent with CHRNA5 depletion results, miR-15a mimicking also resulted in significant downregulation of WDHD1.

Overall these results suggested that some of miR-15 family members may exert similar effects on cancer signaling pathways as CHRNA5 depletion; this could be due to the possibility mir15a/16 conducts some of its downstream effects through inhibition of CHRNA5 which can be tested by overexpression of CHRNA5 levels in the presence of

miR15a/16 mimics. In addition, combinatorial treatment with miR-15a/16 mimics might boost the anti-proliferative effects that we observed with CHRNA5 depletion.

## 4.4 Effect of CHRNA5 depletion on global miRNA changes and restoration of hsa-miR-495-3p levels in MCF7 cells

The findings that we have observed with miR-15a/16 mimics and the massive effects of CHRNA5 depletion on various cancer signaling pathways has led me to investigate whether this intervention also affected miRNA regulation in MCF7 cells as well. t
Although there exists studies examining the relationship between miRNAs and nAChRs such as downregulation of nAChR β4 subunit upon miR-138 overexpression [315], to our knowledge there is no study in the literature examining the interaction between CHRNA5 and miRNAs. One of the strongest parts of my study came from our *in silico* findings with respect to the effects of siRNA-1 on mRNA and microRNA expression profiles. Microarray technology is an important biological tool since it provides a large amount of information about the changes in gene expression profiles upon certain treatment conditions [316]. By this way, altered genes can be clustered with the aid of other biological tools which can also further help to classify the disease more precisely and can have impacts on prognosis and diagnosis of the diseases.

Therefore, in this part of the thesis, I aimed to investigate the possible genes and biological pathways which can be altered by the interaction between siRNA and miRNA mimic studies. The combinatorial application of siRNA and miRNA mimicking raised attention recently, since this kind of targeting of an oncogene can boost the expected outcome. For example, in a recent study, it was revealed that the effect of TP53 targeted tumor suppressor miR-34a overexpression together with Kras (Kristen rat sarcoma viral oncogene homolog) silencing using an siRNA improved the chemotherapeutic response in lung cancer when compared to the either miR-34a mimic alone or Kras-RNAi treatments [317]. Moreover in another study it was demonstrated that, downregulation of the anti-apoptotic BCL2 protein levels with siRNA along with mimicking the expression of

miR-15a, which also targets BCL2, resulted in increased apoptosis in Raji cells [318] in comparison to BCL2 RNAi or miR-15a mimic treatments alone. Therefore, by taking into account the advantage of using siRNA and miRNA mimics together and based on the other cancer studies, here I aimed to boost the anti-proliferative effect of CHRNA5 depletion upon restoring the expression of the most downregulated miRNA miR-495 by using miRNA mimics in order to identify pathways that could be targeted by both or uniquely.

By knowing the fact that, miR-495 mostly act as a tumor suppressor miRNA (references presented in the introduction section), overexpression of miR-495 by using miR-495 specific mimic along with CHRNA5 RNAi treatments thus allowed for identifying the mRNAs uniquely or commonly affected by the two different treatments (siRNA vs mimic or siRNA+mimic).

With ingenuity pathway analysis (IPA), most of the canonical signaling pathways which were significantly and additively affected by siRNA-1 and miR-495 mimic treatments belonged to the ones related to cell cycle progression. Moreover, among the most affected diseases and biofunctions, I observed enhanced inhibition of proliferation of the cells as well as attenuated levels of cells entering S phase upon combinatorial siRNA-1 and miR-495 mimic treatments. This further promoted me to validate these observations with molecular tools as well, such as MTT, PI staining, 7-AAD/BrDU staining, Western blotting and RT-qPCR. Interestingly TP53 downstream responder CKDN1A was not affected by miR-495 mimic while it was by CHRNA5 siRNA-1. Previous studies have shown that miR-495 could act as an oncogene through its inhibition of PTEN and CDKN1A and use of siRNAs with the mimic can overcome this feedback mechanism [249],[250]. The combinatorial treatment increased antiproliferative activity was also confirmed using MTT assay, PI staining as well.

7-AAD/BrDU staining gives information about actively dividing cells via the incorporation of BrdU into newly synthesized DNA as well as viable cells by the exclusion of 7-AAD which is a membrane impermeable dye [319]. In the literature the effects of combinatorial treatments have been tested with similar methodologies [320]. Future studies should

involve use of *in vivo* zebrafish models when siRNA+mimic were used together as well as *in silico* studies that can test prognostic effects of miR-495 overexpression and CHRNA5 depletion in cancer patients using datasets such as TCGA [321].

The results of cell proliferation assays were also confirmed with western blotting by checking the most important proteins involved in cell cycle progression. Among them is CDKN1A (p21) whose expression is tightly controlled by TP53 [322]. Upon DNA damage, its expression is increased which in turn inhibits cyclinD/CDK4 or cyclinE/CDK2 complexation resulting in inhibition of RB phosphorylation hence leading to G1/S arrest [323]. While CHRNA5 depletion resulted in upregulation of CDKN1A levels, it was downregulated by miR-495 mimic treatment as expectedly since in the literature it was stated that CDKN1A is one of the targets of miR-495 [258]. However, as also seen in the western blot results, the effect of siRNA-1 boosted over miR-495 inhibitory effect which could be the reason for the presence of CDKN1A and this might contributed to G1/S arrest seen with PI staining [237]. Despite miR-495 had negative effect on cell cycle arrest by inhibiting CDKN1A, it can still propagate the G1/S arrest by targeting other molecules which negatively affects G1-S transition such as with the inhibition of Bmi-1 by miR-495 in breast cancer cell lines [245].

Consistent with the finding that restoration of miR-495 in glioblastoma cells resulted in decreased pRB levels [242], similar to this, in MCF7 cells, I also observed inhibitory effect of miR-495 on pRB along with CHRNA5 depletion as well. Therefore, decreased pRB levels by those two molecules might contribute to the anti-proliferation of MCF7 cells that I observed with MTT, PI staining and 7-AAD/BrDU staining.

The anti-apoptotic protein BCL2 is also targeted by miR-495 and lead to inhibition of cell proliferation in osteosarcoma [251]. Similar to this, in MCF7 cells, I also observed decreased levels of BCL2 at protein levels upon miR-495 restoration. Similar to the study done with Raji cells where BCL-2 was targeted by another miRNA (miR-15a) along with BCL2 RNAi [318], here miR-495 overexpression along with the use of CHRNA5 RNAi also exhibited the same trend.

Since one of the most important finding of this thesis is the inhibitory effect of CHRNA5 depletion on decreased CHEK1 phosphorylation levels, I also examined pCHEK1 in the context of miR-495 study as well. Interestingly, as there is no study in the literature related with CHRNA5 depletion and pCHEK1 expression. Therefore, we can state that, as CHRNA5 RNAi is a potential CHEK1 inhibitor, so as miR-495 can also potentially be one as well. Future studies should focus on total CHEK1 levels along with pCHEK1 and repetition of the Western blotting experiments when mimic and siRNA were given together or alone should be performed as well.

All these observations might suggest that the final phenotype that we observed with the depletion of CHRNA5 together with the restoration of miR-495 levels could achieve overall additive effects of these to molecules. This could be due the fact that one miRNA can target many mRNAs and one mRNA can be targeted by many miRNAs as well [324].

## 4.4 Proposed Mechanism

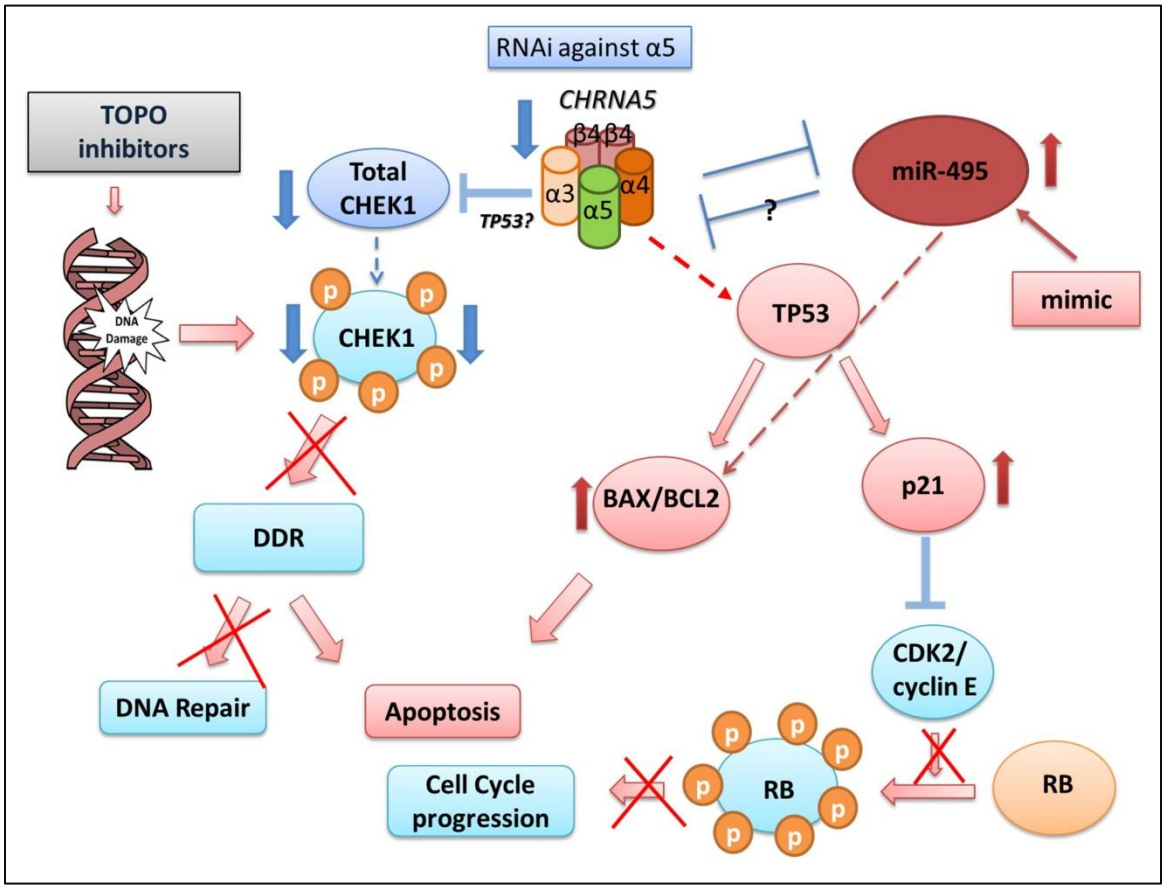


**Figure 4.1 Proposed Mechanism of action for CHRNAi and miR-495 mimic**.

I have also proposed a potential working mechanism which future studies can help decipher in detail how CHRNA5 RNAi works in accord with miR-495, each complementing the other's actions while restoring feedback mechanisms (Figure 4.1).

## 4.5 Future Perspectives

Future studies stemmed from the findings from this thesis can be as followed:

- In order to clarify whether the changes occurred upon CHRNA5 depletion such as cell cycle arrest, DNA damage, apoptosis and drug sensitivity is

indeed related with TP53 status of the cells, the experiments held for MCF7 cells should be also performed in isogenic cell line which does not express wild type TP53.

- The experiments held for MCF7 cells could be confirmed with another cell line having the similar genotype with MCF7, such as T47D.

- To clearly identify if the DNA damage occurred upon CHRNA5 depletion and TOP treatments, in addition to the pH2AX levels, total H2AX levels should be checked at protein level as well as its cellular localization should be identified by IHC.

- Examination of ATR levels with RT-qPCR and Western blotting can further enlighten at which step CHRNA5 depletion affects the total CHEK1 and pCHEK1 levels.

- In addition to the pRB levels, detection of total RB would be helpful whether the changes upon CHRNA5 depletion occurred at transcriptional or post-transcriptional levels.

- In this study, the cellular consequences of CHRNA5 depletion were identified. However, the mechanism behind how alteration of this receptor resulted in such changes remains to be elucidated. For this, intracellular Ca+ levels can be measured in the presence or absence of CHRNA5. For this, examining of the proteins such as calmodulin or the transcription factors which are responsive to the levels of Ca+ can help our understanding in CHRNA5 depletion and the resultant phenotype.

- The observed changes upon CHRNA5 depletion on miRNAs were examined with mature miRNAs. However, CHRNA5 depletion might also

exert its effect prior to or during miRNA processing. Therefore, it is crucial to examine the levels of pre-miRNAs upon CHRNA5 depletion as well.

- Most importantly, the changes occurred in chromosomal region 14q32.31 should be investigated further whether these changes occur with hypermethylation of this region or loss of heterozygocity in the context of CHRNA5 depletion. Moreover, a detailed interaction network of this clustered miRNAs can provide information whether these miRNAs altogether result in convergent or divergent biological functions.

# APPENDIX A

## A1: Preliminary studies for co-culturing

In order to obtain stably EGFP or EBFP expressing MCF7 cells to be used in siRNA and miRNA mimic competition studies, several optimization steps were held as explained in detail in materials and methods section. Firstly, different volumes of attractane transfection reagent in combination with either 0.4 µg/µL or 0.6 µg/µL DNA were used (A) together with their corresponding control groups (B and C). Secondly, two other transfection reagents, Lipofectamine (2000) and PEI, were used (D). Next,due to the observation of toxicity, after using Lipofectamine (2000) and attractane transfection reagents,media changes were also held (E and F).At the end of all these trials, cells transfected with 0.25 µg/µL DNA complexed with 0,5 µL Lipofectamine exhibited the least toxicity upon changing the transfection media 6 h post-transfection. Polyclonal MCF7 cells either expressing EGFP or EBFP were further processed to obtain monoclonal MCF7 cells by Said Tiryaki (MSc Thesis, 2018).

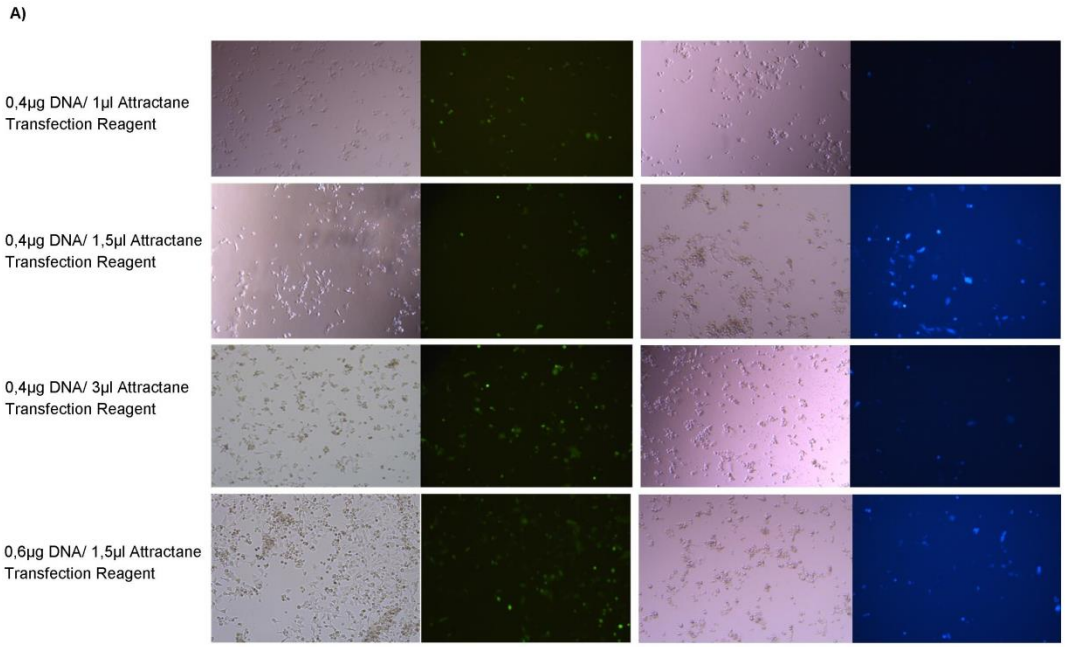

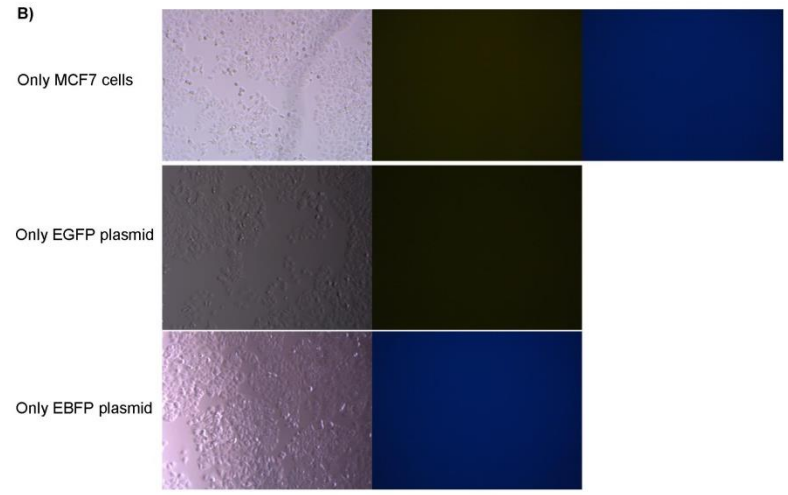
B)
Only MCF7 cells
Only EGFP plasmid
Only EBFP plasmid

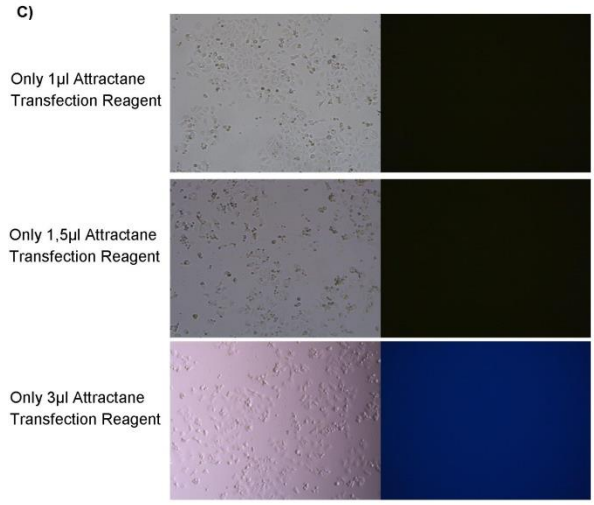
C)
Only 1µl Attractane Transfection Reagent
Only 1,5µl Attractane Transfection Reagent
Only 3µl Attractane Transfection Reagent

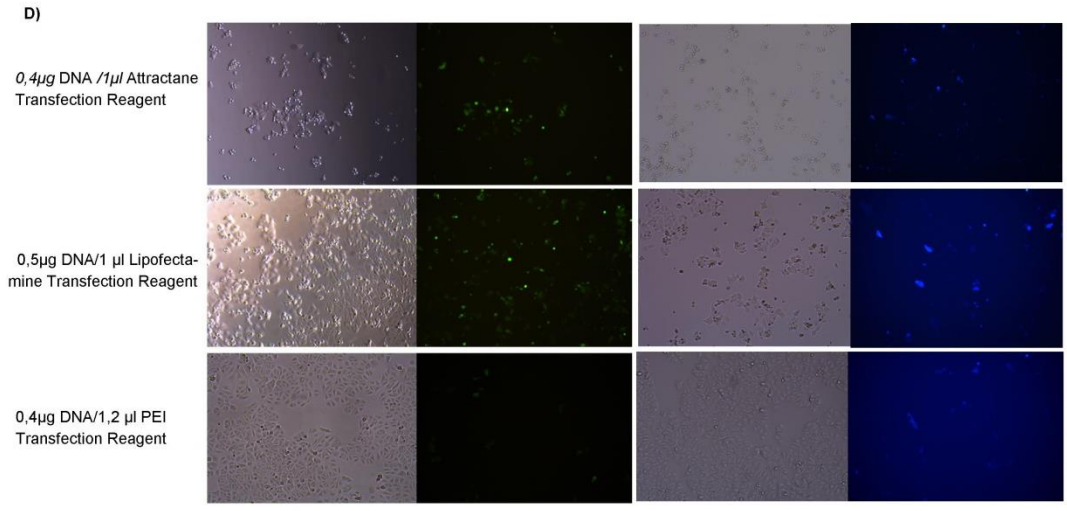
D)
0,4µg DNA /1µl Attractane Transfection Reagent
0,5µg DNA/1 µl Lipofecta-mine Transfection Reagent
0,4µg DNA/1,2 µl PEI Transfection Reagent

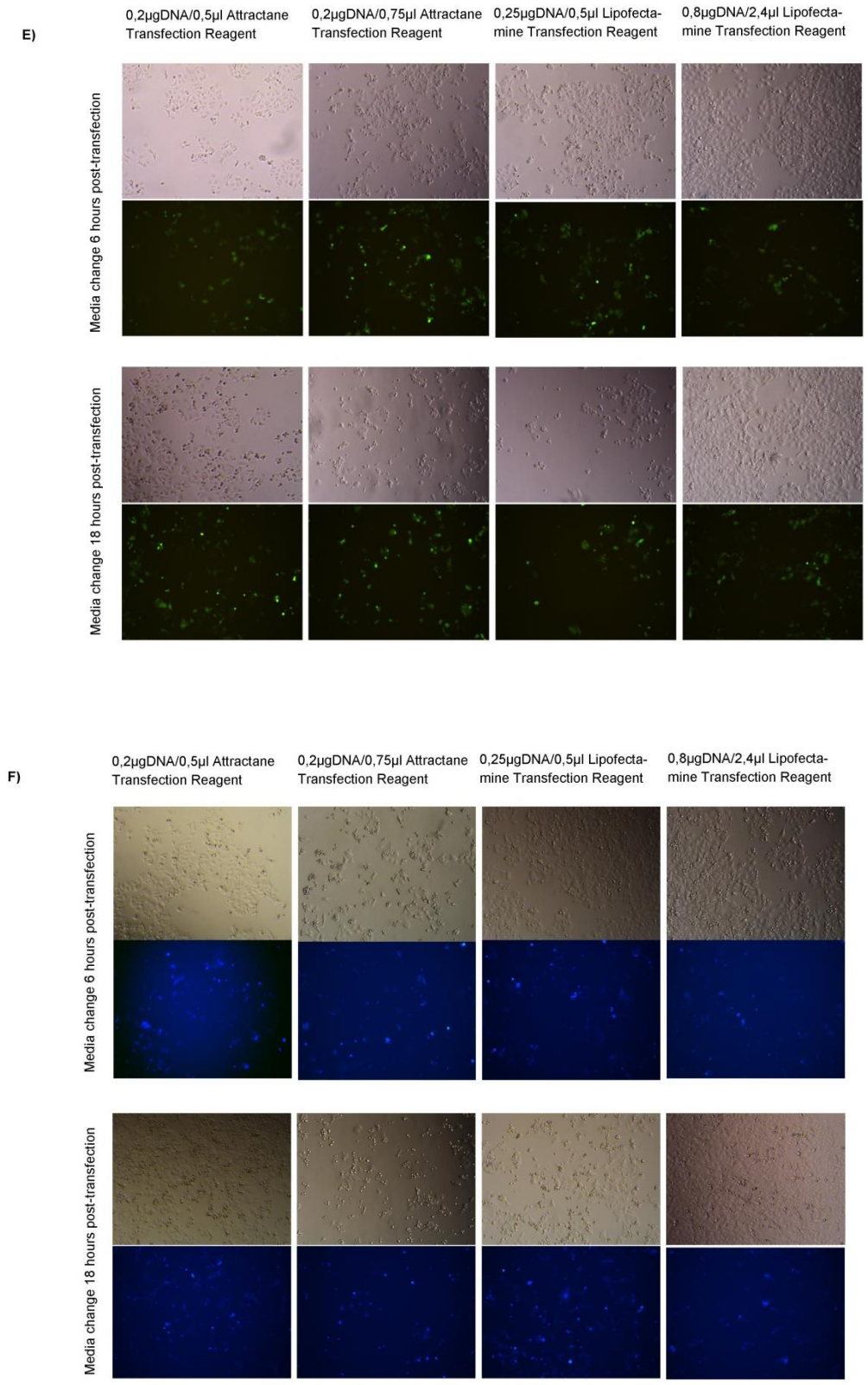


**Figure Appendix A 1**: Generation of stable EGFP and EBFP expressing MCF7 cells.

# A2: Preliminary Studies for the generation of shCHRNA5 Expressed MCF7 cells

As explained in Materials and Methods section, after the isolation of shCHRNA5 expressing plasmids, MCF7 cells were transfected with them together with negative control. Among different clones of shRNA molecules at least three of them showed varying degress of inhibition with respect to shRNA-CN and can be further pursued in the upcoming studies.

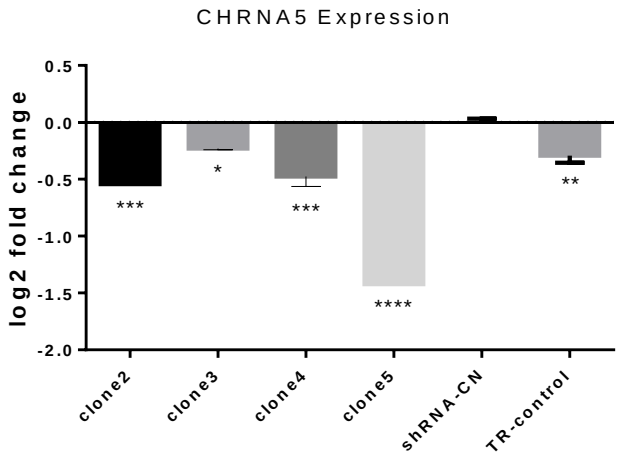


**Figure Appendix A 2**: CHRNA5 Expression levels. Optimization studies for the generation shCHRNA5 in MCF7 cells.

# REFERENCES


[1] M. Ghoncheh, Z. Pournamdar, and H. Salehiniya, “Incidence and Mortality and Epidemiology of Breast Cancer in the World,” *Asian Pacific J. Cancer Prev.*, 2016.

[2] A. G. Rivenbark, S. M. O’Connor, and W. B. Coleman, “Molecular and cellular heterogeneity in breast cancer: Challenges for personalized medicine,” *Am. J. Pathol.*, 2013.

[3] K. J. B. GS, “Breast cancer epidemiology. TT -,” *CANCER Res.*, 1988.

[4] P. Van Der Groep, E. Van Der Wall, and P. J. Van Diest, “Pathology of hereditary breast cancer,” *Cell. Oncol.*, 2011.

[5] Glueck, A. Monterro, and M. Kittane, “Molecular Profiling for Breast Cancer: A Comprehensive Review,” *Biomark. Cancer*, 2013.

[6] K. Polyak, “Heterogeneity in breast cancer,” *Journal of Clinical Investigation*. 2011.

[7] A. J. Darlington, “Anatomy of the breast,” in *Digital Mammography: A Holistic Approach*, 2015.

[8] J. L. Inman, C. Robertson, J. D. Mott, and M. J. Bissell, “Mammary gland development: cell fate specification, stem cells and the microenvironment,” *Development*, 2015.

[9] C. W. Daniel and G. H. Smith, “The mammary gland: a model for development.,” *Journal of mammary gland biology and neoplasia*. 1999.

[10] A. H. Sims, A. Howell, S. J. Howell, and R. B. Clarke, “Origins of breast cancer subtypes and therapeutic implications,” *Nature Clinical Practice Oncology*. 2007.

[11] S. R. Wellings and H. M. Jensen, “On the origin and progression of ductal carcinoma in the human breast,” *J. Natl. Cancer Inst.*, 1973.

[12] D. C. Allred, “Ductal carcinoma in situ: Terminology, classification, and natural history,” *J. Natl. Cancer Inst. - Monogr.*, 2010.

[13] Y. Myal, E. Leygue, and A. A. Blanchard, “Claudin 1 in breast tumorigenesis: Revelation of a possible novel ‘claudin high’ subset of breast cancers,” *Journal of Biomedicine and Biotechnology*. 2010.

[14] E. A. Perez, “Breast Cancer Management: Opportunities and Barriers to an Individualized Approach,” *Oncologist*, 2011.

[15] Z. Hu *et al.*, “The molecular portraits of breast tumors are conserved across microarray platforms,” *BMC Genomics*, 2006.

[16] A. Prat and C. M. Perou, “Deconstructing the molecular portraits of breast cancer,” *Molecular Oncology*. 2011.

[17] J. Baselga, “Adjuvant Trastuzumab: A Milestone in the Treatment of HER-2-Positive Early Breast Cancer,” *Oncologist*, 2006.

[18] S. Loi *et al.*, “Definition of clinically distinct molecular subtypes in estrogen receptor-positive breast carcinomas through genomic grade,” *J. Clin. Oncol.*, 2007.

[19] M. C. U. Cheang *et al.*, “Ki67 index, HER2 status, and prognosis of patients with luminal B breast cancer,” *J. Natl. Cancer Inst.*, 2009.

[20] T. Sorlie *et al.*, “Repeated observation of breast tumor subtypes in independent gene expression data sets,” *Proc. Natl. Acad. Sci.*, 2003.

[21] C. M. Perou *et al.*, “Molecular portraits of human breast tumours.,” *Nature*, 2000.

[22] M. F. Rimawi *et al.*, “Multicenter phase II study of neoadjuvant lapatinib and trastuzumab with hormonal therapy and without chemotherapy in patients with human epidermal growth factor receptor 2–overexpressing breast cancer: TBCRC 006,” *J. Clin. Oncol.*, 2013.

[23] E. de Azambuja *et al.*, “Lapatinib with trastuzumab for HER2-positive early breast cancer (NeoALTTO): survival outcomes of a randomised, open-label, multicentre, phase 3 trial and their association with pathological complete response,” *Lancet. Oncol.*, 2014.

[24] K. Gelmon, R. Dent, J. R. Mackey, K. Laing, D. Mcleod, and S. Verma, “Targeting triple-negative breast cancer: Optimising therapeutic outcomes,” *Annals of Oncology*. 2012.

[25] L. A. Carey, “Targeted chemotherapy? Platinum in BRCA1-dysfunctional breast cancer,” *Journal of Clinical Oncology*, 2010.

[26] A. Prat *et al.*, “Phenotypic and molecular characterization of the claudin-low intrinsic subtype of breast cancer.,” *Breast Cancer Res.*, vol. 12, no. 5, p. R68, 2010.

[27] X. Dai *et al.*, “Breast cancer intrinsic subtype classification, clinical use and future trends,” *American Journal of Cancer Research*. 2015.

[28] X. Dai, H. Cheng, Z. Bai, and J. Li, “Breast cancer cell line classification and Its

relevance with breast tumor subtyping," *Journal of Cancer*. 2017.

[29] A. M. Saito, M. Landrum, B. A. Neville, J. Z. Ayanian, and C. C. Earle, "The effect on survival of continuing chemotherapy to near death," *BMC Palliat. Care*, 2011.

[30] H. Zahreddine and K. L. B. Borden, "Mechanisms and insights into drug resistance in cancer," *Frontiers in Pharmacology*. 2013.

[31] F. S. Liu, "Mechanisms of Chemotherapeutic Drug Resistance in Cancer Therapy-A Quick Review," *Taiwanese Journal of Obstetrics and Gynecology*. 2009.

[32] D. B. Longley and P. G. Johnston, "Molecular mechanisms of drug resistance," *Journal of Pathology*. 2005.

[33] C. Swanton, "Intratumor heterogeneity: Evolution through space and time," *Cancer Research*. 2012.

[34] C. Holohan, S. Van Schaeybroeck, D. B. Longley, and P. G. Johnston, "Cancer drug resistance: An evolving paradigm," *Nature Reviews Cancer*. 2013.

[35] J. L. Hartman IV, B. Garvik, and L. Hartwell, "Cell Biology: Principles for the buffering of genetic variation," *Science*. 2001.

[36] N. G. Bush, K. Evans-Roberts, and A. Maxwell, "DNA Topoisomerases.," *EcoSal Plus*, 2015.

[37] J. E. Deweese, M. A. Osheroff, and N. Osheroff, "DNA topology and topoisomerases: Teaching A 'knotty' subject," *Biochemistry and Molecular Biology Education*. 2009.

[38] H. Ulukan and P. W. Swaan, "Camptothecins: A review of their chemotherapeutic potential," *Drugs*. 2002.

[39] J. A. Holden, "DNA topoisomerases as anticancer drug targets: from the laboratory to the clinic.," *Curr. Med. Chem. Anticancer. Agents*, 2001.

[40] J. L. Delgado, C.-M. Hsieh, N.-L. Chan, and H. Hiasa, "Topoisomerases as anticancer targets," *Biochem. J.*, 2018.

[41] C. B. Jones, M. K. Clements, S. Wasi, and S. S. Daoud, "Sensitivity to camptothecin of human breast carcinoma and normal endothelial cells," *Cancer Chemother. Pharmacol.*, 1997.

[42] Y. H. Hsiang and L. F. Liu, "Identification of mammalian dna topoisomerase i as an intracellular target of the anticancer drug camptothecin," *Cancer Res.*, 1988.

[43] D. Strumberg, A. A. Pilon, M. Smith, R. Hickey, L. Malkas, and Y. Pommier, “Conversion of topoisomerase I cleavage complexes on the leading strand of ribosomal DNA into 5’-phosphorylated DNA double-strand breaks by replication runoff,” *Mol. Cell. Biol.*, 2000.

[44] M. T. Tomicic and B. Kaina, “Topoisomerase degradation, DSB repair, p53 and IAPs in cancer cell resistance to camptothecin-like topoisomerase I inhibitors,” *Biochimica et Biophysica Acta - Reviews on Cancer*. 2013.

[45] J. L. Nitiss, “Targeting DNA topoisomerase II in cancer chemotherapy,” *Nature Reviews Cancer*. 2009.

[46] W. K. Kaufmann, “Human Topoisomerase II Function, Tyrosine Phosphorylation and Cell Cycle Checkpoints,” *Proc. Soc. Exp. Biol. Med.*, 1998.

[47] C. Carvalho *et al.*, “Doxorubicin: The Good, the Bad and the Ugly Effect,” *Curr. Med. Chem.*, 2009.

[48] O. Tacar, P. Sriamornsak, and C. R. Dass, “Doxorubicin: An update on anticancer molecular action, toxicity and novel drug delivery systems,” *Journal of Pharmacy and Pharmacology*. 2013.

[49] P. B. Jensen *et al.*, “Antagonistic Effect of Aclarubicin on the Cytotoxicity of Etoposide and 4′-(9-Acridinylamino)methanesulfon-m-anisidide in Human Small Cell Lung Cancer Cell Lines and on Topoisomerase II-mediated DNA Cleavage,” *Cancer Res.*, 1990.

[50] H. Sun and X. Ma, “α5-nAChR modulates nicotine-induced cell migration and invasion in A549 lung cancer cells,” *Exp. Toxicol. Pathol.*, 2015.

[51] S. A. Grando, “Connections of nicotine to cancer,” *Nature Reviews Cancer*. 2014.

[52] S. Kispert and J. McHowat, “Recent insights into cigarette smoking as a lifestyle risk factor for breast cancer,” *Breast Cancer: Targets and Therapy*. 2017.

[53] S. S. Hecht, “Tobacco smoke carcinogens and lung cancer,” *Curr. Cancer Res.*, 2011.

[54] T. Nakada *et al.*, “Lung tumorigenesis promoted by anti-apoptotic effects of cotinine, a nicotine metabolite through activation of PI3K/Akt pathway,” *J. Toxicol. Sci.*, 2012.

[55] S. S. Hecht, “Research opportunities related to establishing standards for tobacco

products under the family smoking prevention and tobacco control act," *Nicotine and Tobacco Research*. 2012.

[56] S. S. Hecht, "Biochemistry, biology, and carcinogenicity of tobacco-specific N-nitrosamines," *Chemical Research in Toxicology*. 1998.

[57] T. Nishioka, H. S. Kim, L. Y. Luo, Y. Huang, J. Guo, and C. Yan Chen, "Sensitization of epithelial growth factor receptors by nicotine exposure to promote breast cancer cell growth," *Breast Cancer Res.*, 2011.

[58] F. Di Cello *et al.*, "Cigarette smoke induces epithelial to mesenchymal transition and increases the metastatic ability of breast cancer cells," *Mol. Cancer*, 2013.

[59] R. Davis *et al.*, "Nicotine promotes tumor growth and metastasis in mouse models of lung cancer," *PLoS One*, 2009.

[60] C. H. Wu, C. H. Lee, and Y. S. Ho, "Nicotinic acetylcholine receptor-based blockade: Applications of molecular targets for cancer therapy," *Clinical Cancer Research*. 2011.

[61] J. A. Dani and D. Bertrand, "Nicotinic Acetylcholine Receptors and Nicotinic Cholinergic Mechanisms of the Central Nervous System," *Annu. Rev. Pharmacol. Toxicol.*, 2007.

[62] N. M. Nathanson, "Muscarinic Acetylcholine Receptors," in *Encyclopedia of Biological Chemistry: Second Edition*, 2013.

[63] J. P. Changeux and S. J. Edelstein, "Allosteric mechanisms in normal and pathological nicotinic acetylcholine receptors," *Curr. Opin. Neurobiol.*, 2001.

[64] V. Itier and D. Bertrand, "Neuronal nicotinic receptors: From protein structure to function," in *FEBS Letters*, 2001.

[65] H. M. Schuller, "Is cancer triggered by altered signalling of nicotinic acetylcholine receptors?," *Nature Reviews Cancer*. 2009.

[66] C. H. Lee, C. H. Wu, and Y. S. Ho, "From smoking to cancers: Novel targets to neuronal nicotinic acetylcholine receptors," *Journal of Oncology*. 2011.

[67] H. M. Schuller, "Cell type specific, receptor-mediated modulation of growth kinetics in human lung cancer cell lines by nicotine and tobacco-related nitrosamines," *Biochem. Pharmacol.*, 1989.

[68] J. P. Cooke, "Angiogenesis and the role of the endothelial nicotinic acetylcholine

receptor," *Life Sci.*, 2007.

[69] P. L. Wei *et al.*, "Tobacco-specific carcinogen enhances colon cancer cell migration through ??7-nicotinic acetylcholine receptor," *Ann. Surg.*, 2009.

[70] A. Paliwal *et al.*, "Aberrant DNA methylation links cancer susceptibility locus 15q25.1 to apoptotic regulation and lung cancer," *Cancer Res.*, 2010.

[71] C. Schaal and S. P. Chellappan, "Nicotine-Mediated Cell Proliferation and Tumor Progression in Smoking-Related Cancers," *Mol. Cancer Res.*, 2014.

[72] P. Dasgupta and S. P. Chellappan, "Nicotine-mediated cell proliferation and angiogenesis: New twists to an old story," *Cell Cycle*. 2006.

[73] M. R. Improgo, A. R. Tapper, and P. D. Gardner, "Nicotinic acetylcholine receptor-mediated mechanisms in lung cancer," in *Biochemical Pharmacology*, 2011.

[74] S. A. Grando, "Cholinergic control of epidermal cohesion," *Experimental Dermatology*. 2006.

[75] N. Le Novere and J. P. Changeux, "Molecular evolution of the nicotinic acetylcholine receptor: An example of multigene family in excitable cells," *J. Mol. Evol.*, 1995.

[76] P. Dasgupta *et al.*, "Nicotine induces cell proliferation by β-arrestin-mediated activation of Src and Rb-Raf-1 pathways," *J. Clin. Invest.*, 2006.

[77] P. Dasgupta *et al.*, "ARRB1-mediated regulation of E2F target genes in nicotine-induced growth of lung tumors," *J. Natl. Cancer Inst.*, 2011.

[78] M. Xin and X. Deng, "Nicotine inactivation of the proapoptotic function of Bax through phosphorylation," *J Biol Chem*, 2005.

[79] H. Mai, W. S. May, F. Gao, Z. Jin, and X. Deng, "A functional role for nicotine in Bcl2 phosphorylation and suppression of apoptosis," *J. Biol. Chem.*, 2003.

[80] P. Dasgupta, R. Kinkade, B. Joshi, C. DeCook, E. Haura, and S. Chellappan, "Nicotine inhibits apoptosis induced by chemotherapeutic drugs by up-regulating XIAP and survivin," *Proc. Natl. Acad. Sci.*, 2006.

[81] R. J. Chen, Y. S. Ho, H. R. Guo, and Y. J. Wang, "Long-term nicotine exposure-induced chemoresistance is mediated by activation of Stat3 and downregulation of ERK1/2 via nAChR and beta-adrenoceptors in human bladder cancer cells," *Toxicol. Sci.*, 2010.

[82] J. K. Cataldo, S. Dubey, and J. J. Prochaska, “Smoking cessation: An integral part of lung cancer treatment,” *Oncology*. 2010.

[83] L. T. Nordquist, G. R. Simon, A. Cantor, W. M. Alberts, and G. Bepler, “Improved survival in never-smokers vs current smokers with primary adenocarcinoma of the lung,” *Chest*. 2004.

[84] S. A. Mousa, H. R. Arias, and P. J. Davis, “Role of non-neuronal nicotinic acetylcholine receptors in angiogenesis modulation,” in *Angiogenesis Modulations in Health and Disease: Practical Applications of Pro- and Anti-angiogenesis Targets*, 2013.

[85] P. CARMELIET and D. COLLEN, “Molecular Basis of Angiogenesis: Role of VEGF and VE-Cadherin,” *Ann. N. Y. Acad. Sci.*, 2006.

[86] W. Risau, “Mechanisms of angiogenesis,” *Nature*. 1997.

[87] J. P. Cooke and Y. T. Ghebremariam, “Endothelial Nicotinic Acetylcholine Receptors and Angiogenesis,” *Trends in Cardiovascular Medicine*. 2008.

[88] C. Heeschen, M. Weis, A. Aicher, S. Dimmeler, and J. P. Cooke, “A novel angiogenic pathway mediated by non-neuronal nicotinic acetylcholine receptors,” *J. Clin. Invest.*, 2002.

[89] M. J. Jarzynka, P. Gou, I. Bar-Joseph, B. Hu, and S. Y. Cheng, “Estradiol and nicotine exposure enhances A549 bronchioloalveolar carcinoma xenograft growth in mice through the stimulation of angiogenesis,” *Int. J. Oncol.*, 2006.

[90] P. Dasgupta *et al.*, “Nicotine induces cell proliferation, invasion and epithelial-mesenchymal transition in a variety of human cancer cell lines,” *Int. J. Cancer*, 2009.

[91] K. A. West *et al.*, “Rapid Akt activation by nicotine and a tobacco carcinogen modulates the phenotype of normal human airway epithelial cells,” *J. Clin. Invest.*, 2003.

[92] S. P. Arneric, M. Holladay, and M. Williams, “Neuronal nicotinic receptors: A perspective on two decades of drug discovery research,” *Biochem. Pharmacol.*, 2007.

[93] C. I. Amos *et al.*, “Genome-wide association scan of tag SNPs identifies a susceptibility locus for lung cancer at 15q25.1,” *Nat. Genet.*, 2008.

[94] R. J. Hung *et al.*, “A susceptibility locus for lung cancer maps to nicotinic acetylcholine receptor subunit genes on 15q25,” *Nature*, 2008.

[95] T. E. Thorgeirsson *et al.*, “A variant associated with nicotine dependence, lung cancer and peripheral arterial disease,” *Nature*, 2008.

[96] A. Tammimäki *et al.*, “Impact of human D398N single nucleotide polymorphism on intracellular calcium response mediated by α3β4α5 nicotinic acetylcholine receptors,” *Neuropharmacology*, 2012.

[97] J. Ramirez-Latorre, C. R. Yu, X. Qu, F. Perin, A. Karlin, and L. Role, “Functional contributions of α5 subunit to neuronal acetylcholine receptor channels,” *Nature*, 1996.

[98] G. Lassi *et al.*, “The CHRNA5–A3–B4 Gene Cluster and Smoking: From Discovery to Therapeutics,” *Trends in Neurosciences*. 2016.

[99] M. Hopkins, J. J. Tyson, and B. Novák, “Cell-cycle transitions: a common role for stoichiometric inhibitors,” *Mol. Biol. Cell*, 2017.

[100] G. H. Williams and K. Stoeber, “The cell cycle and cancer,” *Journal of Pathology*. 2012.

[101] Kato, “ Induction of S phase by G1 regulatory factors,” *J. . Front Biosci*, 1999.

[102] A. Zetterberg and O. Larsson, “Kinetic analysis of regulatory events in G1 leading to proliferation or quiescence of Swiss 3T3 cells.,” *Proc. Natl. Acad. Sci.*, 1985.

[103] M. Malumbres and M. Barbacid, “Is Cyclin D1-CDK4 kinase a bona fide cancer target?,” *Cancer Cell*. 2006.

[104] Z. A. Stewart, M. D. Westfall, and J. A. Pietenpol, “Cell-cycle dysregulation and anticancer therapy,” *Trends in Pharmacological Sciences*. 2003.

[105] E. A. Nigg, “Mitotic kinases as regulators of cell division and its checkpoints,” *Nat. Rev. Mol. Cell Biol.*, 2001.

[106] C. Giacinti and A. Giordano, “RB and cell cycle progression,” *Oncogene*. 2006.

[107] V. A. J. Smits and R. H. Medema, “Checking out the G2/M transition,” *Biochimica et Biophysica Acta - Gene Structure and Expression*. 2001.

[108] D. M. Koepp, J. W. Harper, and S. J. Elledge, “How the cyclin became a cyclin: Regulated proteolysis in the cell cycle,” *Cell*. 1999.

[109] A. G. Paulovich, D. P. Toczyski, and L. H. Hartwell, “When checkpoints fail,” *Cell*.

1997.

[110] L. Zheng and W. H. Lee, “The retinoblastoma gene: A prototypic and multifunctional tumor suppressor,” *Experimental Cell Research*. 2001.

[111] M. A. Ozbun and J. S. Butel, “Tumor suppressor p53 mutations and breast cancer: a critical analysis.,” *Adv. Cancer Res.*, 1995.

[112] J. Momand, D. Jung, S. Wilczynski, and J. Niland, “The MDM2 gene amplification database,” *Nucleic Acids Research*. 1998.

[113] A. Ghelli Luserna Di Rora, I. Iacobucci, and G. Martinelli, “The cell cycle checkpoint inhibitors in the treatment of leukemias,” *Journal of Hematology and Oncology*. 2017.

[114] S. P. Jackson and J. Bartek, “The DNA-damage response in human biology and disease,” *Nature*. 2009.

[115] M. F. Lavin, “ATM and the Mre11 complex combine to recognize and signal DNA double-strand breaks,” *Oncogene*. 2007.

[116] D. Cortez, S. Guntuku, J. Qin, and S. J. Elledge, “ATR and ATRIP: Partners in checkpoint signaling,” *Science (80-. ).*, 2001.

[117] L. Busino, M. Chiesa, G. F. Draetta, and M. Donzelli, “Cdc25A phosphatase: Combinatorial phosphorylation, ubiquitylation and proteolysis,” *Oncogene*. 2004.

[118] C. Y. Peng, P. R. Graves, R. S. Thoma, Z. Wu, A. S. Shaw, and H. Piwnica-Worms, “Mitotic and G2 checkpoint control: Regulation of 14-3-3 protein binding by phosphorylation of Cdc25c on serine-216,” *Science (80-. ).*, 1997.

[119] Z. Qiu, N. L. Oleinick, and J. Zhang, “ATR/CHK1 inhibitors and cancer therapy,” *Radiother. Oncol.*, 2017.

[120] M. J. O’Connor, “Targeting the DNA Damage Response in Cancer,” *Molecular Cell*. 2015.

[121] J. Bartkova *et al.*, “DNA damage response as a candidate anti-cancer barrier in early human tumorigenesis,” *Nature*, 2005.

[122] M. Sun *et al.*, “Activation of the ATM-Snail pathway promotes breast cancer metastasis,” *J. Mol. Cell Biol.*, 2012.

[123] S. Grabauskiene *et al.*, “CHK1 levels correlate with sensitization to pemetrexed by CHK1 inhibitors in non-small cell lung cancer cells,” *Lung Cancer*, 2013.

[124] R. Boutros, V. Lobjois, and B. Ducommun, “CDC25 phosphatases in cancer cells: Key players? Good targets?,” *Nature Reviews Cancer*. 2007.

[125] H. Maacke *et al.*, “DNA repair and recombination factor Rad51 is over-expressed in human pancreatic adenocarcinoma,” *Oncogene*, 2000.

[126] R. Brosh and V. Rotter, “When mutants gain new powers: News from the mutant p53 field,” *Nature Reviews Cancer*. 2009.

[127] A. S. Coutts, C. J. Adams, and N. B. La Thangue, “p53 ubiquitination by Mdm2: A never ending tail?,” *DNA Repair*. 2009.

[128] S. Angèle, I. Treilleux, A. Brémond, P. Tanière, and J. Hall, “Altered expression of DNA double-strand break detection and repair proteins in breast carcinomas,” *Histopathology*, 2003.

[129] L. Ai *et al.*, “Ataxia-Telangiectasia-Mutated (ATM) Gene in Head and Neck Squamous Cell Carcinoma: Promoter Hypermethylation with Clinical Correlation in 100 Cases,” *Cancer Epidemiol. Biomarkers Prev.*, 2004.

[130] J. Bartkova *et al.*, “Aberrations of the MRE11-RAD50-NBS1 DNA damage sensor complex in human breast cancer: MRE11 as a candidate familial cancer-predisposing gene,” *Mol. Oncol.*, 2008.

[131] D. S. Kim *et al.*, “Epigenetic inactivation of checkpoint kinase 2 gene in non-small cell lung cancer and its relationship with clinicopathological features,” *Lung Cancer*, 2009.

[132] C. S. Sørensen *et al.*, “Chk1 regulates the S phase checkpoint by coupling the physiological turnover and ionizing radiation-induced accelerated proteolysis of Cdc25A,” *Cancer Cell*, 2003.

[133] M. H. Lam, Q. Liu, S. J. Elledge, and J. M. Rosen, “Chk1 is haploinsufficient for multiple functions critical to tumor suppression,” *Cancer Cell*, 2004.

[134] H. Takai *et al.*, “Aberrant cell cycle checkpoint function and early embryonic death in Chk1(-/-) mice,” *Genes Dev.*, 2000.

[135] F. Bertoni, A. M. Codegoni, D. Furlan, M. G. Tibiletti, C. Capella, and M. Broggini, “CHK1 frameshift mutations in genetically unstable colorectal and endometrial cancers,” *Genes Chromosom. Cancer*, 1999.

[136] A. Menoyo, H. Alazzouzi, S. Schwartz, E. Espín, M. Armengol, and H. Yamamoto,

"Somatic mutations in the DNA damage-response genes ATR and CHK1 in sporadic stomach tumors with microsatellite instability," *Cancer Res.*, 2001.

[137] V. Vassileva, A. Millar, L. Briollais, W. Chapman, and B. Bapat, "Genes involved in DNA repair are mutational targets in endometrial cancers with microsatellite instability," *Cancer Res.*, 2002.

[138] L. M. Tho, S. Libertini, R. Rampling, O. Sansom, and D. A. Gillespie, "Chk1 is essential for chemical carcinogen-induced mouse skin tumorigenesis," *Oncogene*, 2012.

[139] L. Verlinden *et al.*, "The E2F-regulated Gene Chk1 is highly expressed in triple-negative estrogen receptor-/progesterone receptor-/HER-2- breast carcinomas," *Cancer Res.*, 2007.

[140] R. Thompson and A. Eastman, "The cancer therapeutic potential of Chk1 inhibitors: How mechanistic studies impact on clinical trial design," *Br. J. Clin. Pharmacol.*, 2013.

[141] L. Carrassa and G. Damia, "Unleashing Chk1 in cancer therapy," *Cell Cycle*. 2011.

[142] N. Bucher and C. D. Britten, "G2 checkpoint abrogation and checkpoint kinase-1 targeting in the treatment of cancer," *Br. J. Cancer*, 2008.

[143] M. D. Garrett and I. Collins, "Anticancer therapy with checkpoint inhibitors: What, where and when?," *Trends Pharmacol. Sci.*, 2011.

[144] R. G. Shao, C. X. Cao, T. Shimizu, P. M. O'Connor, K. W. Kohn, and Y. Pommier, "Abrogation of an S-phase checkpoint and potentiation of camptothecin cytotoxicity by 7-hydroxystaurosporine (UCN-01) in human cancer cell lines, possibly influenced by p53 function," *Cancer Res.*, 1997.

[145] K. K. Flatten *et al.*, "The role of checkpoint kinase 1 in sensitivity to topoisomerase I poisons.," *J. Biol. Chem.*, 2005.

[146] A. N. Tse *et al.*, "CHIR-124, a novel potent inhibitor of Chk1, potentiates the cytotoxicity of topoisomerase I poisons in vitro and in vivo," *Clin. Cancer Res.*, 2007.

[147] M. I. Walton *et al.*, "The Preclinical Pharmacology and Therapeutic Activity of the Novel CHK1 Inhibitor SAR-020106," *Mol. Cancer Ther.*, 2010.

[148] M. Patil, N. Pabla, and Z. Dong, "Checkpoint kinase 1 in DNA damage response and cell cycle regulation," *Cellular and Molecular Life Sciences*. 2013.

[149] J. M. Vicencio *et al.*, “Senescence, apoptosis or autophagy? When a damaged cell must decide its path - A mini-review,” *Gerontology*, 2008.

[150] M. Hassan, H. Watari, A. Abualmaaty, Y. Ohba, and N. Sakuragi, “Apoptosis and molecular targeting therapy in cancer,” *BioMed Research International*. 2014.

[151] L. Duprez, E. Wirawan, T. Vanden Berghe, and P. Vandenabeele, “Major cell death pathways at a glance,” *Microbes Infect.*, 2009.

[152] S. Shalini, L. Dorstyn, S. Dawar, and S. Kumar, “Old, new and emerging functions of caspases,” *Cell Death and Differentiation*. 2015.

[153] L. Portt, G. Norman, C. Clapp, M. Greenwood, and M. T. Greenwood, “Anti-apoptosis and cell survival: A review,” *Biochimica et Biophysica Acta - Molecular Cell Research*. 2011.

[154] S. Gupta, G. E. N. Kass, E. Szegezdi, and B. Joseph, “The mitochondrial death pathway: A promising therapeutic target in diseases,” *Journal of Cellular and Molecular Medicine*. 2009.

[155] S. Yuan and C. W. Akey, “Apoptosome structure, assembly, and procaspase activation,” *Structure*. 2013.

[156] C. Wang and R. J. Youle, “The Role of Mitochondria in Apoptosis,” *Annu. Rev. Genet.*, 2009.

[157] A. Letai, “The control of mitochondrial apoptosis by the BCL-2 family,” in *Apoptosis: Physiology and Pathology*, 2011.

[158] J. C. Reed, J. M. Jurgensmeier, and S. Matsuyama, “Bcl-2 family proteins and mitochondria,” *Biochimica et Biophysica Acta - Bioenergetics*. 1998.

[159] D. S. Ziegler, A. L. Kung, and M. W. Kieran, “Anti-apoptosis mechanisms in malignant gliomas,” *Journal of Clinical Oncology*. 2008.

[160] S. Fulda, “Tumor resistance to apoptosis,” *International Journal of Cancer*. 2009.

[161] D. Hanahan and R. A. Weinberg, “The hallmarks of cancer,” *Cell*. 2000.

[162] D. L. Vaux, S. Cory, and J. M. Adams, “Bcl-2 gene promotes haemopoietic cell survival and cooperates with c-myc to immortalize pre-B cells,” *Nature*. 1988.

[163] J. E. Chipuk and D. R. Green, “How do BCL-2 proteins induce mitochondrial outer membrane permeabilization?,” *Trends in Cell Biology*. 2008.

[164] M. Landriscina, M. R. Amoroso, A. Piscazzi, and F. Esposito, “Heat shock proteins,

cell survival and drug resistance: The mitochondrial chaperone TRAP1, a potential novel target for ovarian cancer therapy," *Gynecologic Oncology*. 2010.

[165] S. Fulda, A. M. Gorman, O. Hori, and A. Samali, "Cellular stress responses: Cell survival and cell death," *International Journal of Cell Biology*. 2010.

[166] S. Takayama, J. C. Reed, and S. Homma, "Heat-shock proteins as regulators of apoptosis," *Oncogene*. 2003.

[167] H. Sharma, S. Sen, L. Lo Muzio, M. A. Mariggiò, and N. Singh, "Antisense-mediated downregulation of anti-apoptotic proteins induces apoptosis and sensitizes head and neck squamous cell carcinoma cells to chemotherapy," *Cancer Biol. Ther.*, 2005.

[168] S. H. Wei *et al.*, "Inducing apoptosis and enhancing chemosensitivity to Gemcitabine via RNA interference targeting Mcl-1 gene in pancreatic carcinoma cell," *Cancer Chemother. Pharmacol.*, 2008.

[169] J. Yang *et al.*, "Prevention of apoptosis by Bcl-2: Release of cytochrome c from mitochondria blocked," *Science (80-. ).*, 1997.

[170] J. J. Liu *et al.*, "Expression of survivin and bax/bcl-2 in peroxisome proliferator activated receptor-γ ligands induces apoptosis on human myeloid leukemia cells in vitro," *Ann. Oncol.*, 2005.

[171] H. Matsumoto, T. Wada, K. Fukunaga, S. Yoshihiro, H. Matsuyama, and K. Naito, "Bax to Bcl-2 ratio and Ki-67 index are useful predictors of neoadjuvant chemoradiation therapy in bladder cancer," *Jpn. J. Clin. Oncol.*, 2004.

[172] K. Vucicevic *et al.*, "Association of Bax Expression and Bcl2/Bax Ratio with Clinical and Molecular Prognostic Markers in Chronic Lymphocytic Leukemia," *J. Med. Biochem.*, 2016.

[173] M. Lamkanfi, W. Declercq, M. Kalai, X. Saelens, and P. Vandenabeele, "Alice in caspase land. A phylogenetic analysis of caspases from worm to man," *Cell Death Differ.*, 2002.

[174] K. M. Boatright *et al.*, "A unified model for apical caspase activation," *Mol. Cell*, 2003.

[175] J. G. Walsh, S. P. Cullen, C. Sheridan, A. U. Luthi, C. Gerner, and S. J. Martin, "Executioner caspase-3 and caspase-7 are functionally distinct proteases," *Proc.*

*Natl. Acad. Sci.*, 2008.

[176] S. A. Lakhani *et al.*, “Caspases 3 and 7: Key mediators of mitochondrial events of apoptosis,” *Science (80-. ).*, 2006.

[177] R. U. Jänicke, M. L. Sprengart, M. R. Wati, and A. G. Porter, “Caspase-3 is required for DNA fragmentation and morphological changes associated with apoptosis,” *J. Biol. Chem.*, 1998.

[178] S. Shaw, M. Bencherif, and M. B. Marrero, “Janus kinase 2, an early target of α7 nicotinic acetylcholine receptor-mediated neuroprotection against Aβ-(1-42) amyloid,” *J. Biol. Chem.*, 2002.

[179] R. R. Resende, A. S. Alves, L. R. G. Britto, and H. Ulrich, “Role of acetylcholine receptors in proliferation and differentiation of P19 embryonal carcinoma cells,” *Exp. Cell Res.*, 2008.

[180] R. R. Resende, K. N. Gomes, A. Adhikari, L. R. G. Britto, and H. Ulrich, “Mechanism of acetylcholine-induced calcium signaling during neuronal differentiation of P19 embryonal carcinoma cells in vitro,” *Cell Calcium*, 2008.

[181] R. Zeidler, K. Albermann, and S. Lang, “Nicotine and apoptosis,” *Apoptosis*, 2007.

[182] R. R. Resende and A. Adhikari, “Cholinergic receptor pathways involved in apoptosis, cell proliferation and neuronal differentiation,” *Cell Communication and Signaling*. 2009.

[183] D. P. Bartel, “MicroRNAs: Genomics, Biogenesis, Mechanism, and Function,” *Cell*. 2004.

[184] D. Lenkala, B. LaCroix, E. R. Gamazon, P. Geeleher, H. K. Im, and R. S. Huang, “The impact of microRNA expression on cellular proliferation,” *Hum. Genet.*, 2014.

[185] M. Garofalo, G. L. Condorelli, C. M. Croce, and G. Condorelli, “MicroRNAs as regulators of death receptors signaling,” *Cell Death and Differentiation*. 2010.

[186] J. Zhang and L. Ma, “MicroRNA control of epithelial-mesenchymal transition and metastasis,” *Cancer Metastasis Rev.*, 2012.

[187] J. Winter, S. Jung, S. Keller, R. I. Gregory, and S. Diederichs, “Many roads to maturity: MicroRNA biogenesis pathways and their regulation,” *Nature Cell Biology*. 2009.

[188] L.-A. MacFarlane and P. R. Murphy, “MicroRNA: Biogenesis, Function and Role in

Cancer," *Curr. Genomics*, 2010.

[189] T. G. Hullinger *et al.*, "Inhibition of miR-15 protects against cardiac ischemic injury," *Circ. Res.*, 2012.

[190] J. Chu *et al.*, "E2F7 overexpression leads to tamoxifen resistance in breast cancer cells by competing with E2F1 at miR-15a/16 promoter.," *Oncotarget*, 2015.

[191] D. Betel, M. Wilson, A. Gabow, D. S. Marks, and C. Sander, "The microRNA.org resource: Targets and expression," *Nucleic Acids Res.*, 2008.

[192] J. Tang, Z. Wang, L. Chen, G. Huang, and X. Hu, "Gossypol acetate induced apoptosis of pituitary tumor cells by targeting the BCL-2 via the upregulated microRNA miR-15a," *Int. J. Clin. Exp. Med.*, 2015.

[193] A. Fesler, H. Liu, and J. Ju, "Modified miR-15a has therapeutic potential for improving treatment of advanced stage colorectal cancer through inhibition of BCL2, BMI1, YAP1 and DCLK1," *Oncotarget*, 2018.

[194] W. Lu *et al.*, "MIR 15a induces cell apoptosis by targeting BCL2L2 and BCL2 in HPV-positive hypopharyngeal squamous cell carcinoma," *Oncol. Rep.*, 2016.

[195] Y. Zhang, F. Huang, J. Wang, L. Peng, and H. Luo, "MiR-15b mediates liver cancer cells proliferation through targeting BCL-2," *Int. J. Clin. Exp. Pathol.*, 2015.

[196] G. Reid *et al.*, "Restoring expression of miR-16: A novel approach to therapy for malignant pleural mesothelioma," *Ann. Oncol.*, 2013.

[197] Z. Lv, Y. Wei, D. Wang, C. Y. Zhang, K. Zen, and M. Li, "Argonaute 2 in cell-secreted microvesicles guides the function of secreted miRNAs in recipient cells," *PLoS One*, 2014.

[198] P. Gao, J. Si, B. Yang, and J. Yu, "Upregulation of MicroRNA-15a Contributes to Pathogenesis of Abdominal Aortic Aneurysm (AAA) by Modulating the Expression of Cyclin-Dependent Kinase Inhibitor 2B (CDKN2B)," *Med. Sci. Monit.*, 2017.

[199] G. Cutrona *et al.*, "Effects of miRNA-15 and miRNA-16 expression replacement in chronic lymphocytic leukemia: Implication for therapy," *Leukemia*, 2017.

[200] I. Venza, M. Visalli, C. Beninati, S. Benfatto, D. Teti, and M. Venza, "IL-10Rα expression is post-transcriptionally regulated by MIR-15a, MIR-185, and MIR-211 in melanoma," *BMC Med. Genomics*, 2015.

[201] J. Xiao, L. Liu, Z. Zhong, C. Xiao, and J. Zhang, "Mangiferin regulates proliferation

and apoptosis in glioma cells by induction of microRNA-15b and inhibition of MMP-9 expression," *Oncol. Rep.*, 2015.

[202] L. Xing and B. F. Boyce, "Regulation of apoptosis in osteoclasts and osteoblastic cells," *Biochemical and Biophysical Research Communications*. 2005.

[203] A. Druz, Y. C. Chen, R. Guha, M. Betenbaugh, S. E. Martin, and J. Shiloach, "Large-scale screening identifies a novel microRNA, miR-15a-3p, which induces apoptosis in human cancer cell lines," *RNA Biol.*, 2013.

[204] K. Zhu *et al.*, "MicroRNA-15a Inhibits Proliferation and Induces Apoptosis in CNE1 Nasopharyngeal Carcinoma Cells," *Oncol. Res. Featur. Preclin. Clin. Cancer Ther.*, 2016.

[205] G. Sun *et al.*, "MiR-15b targets cyclin D1 to regulate proliferation and apoptosis in glioma cells," *Biomed Res. Int.*, 2014.

[206] E. A. Ye, L. Liu, and J. J. Steinle, "miR-15a/16 inhibits TGF-beta3/VEGF signaling and increases retinal endothelial cell barrier proteins," *Vision Res.*, 2017.

[207] E. Dejean *et al.*, "Hypoxia-microRNA-16 downregulation induces VEGF expression in anaplastic lymphoma kinase (ALK)-positive anaplastic large-cell lymphomas," *Leukemia*, 2011.

[208] A. Braza-Boïls *et al.*, "Peritoneal fluid modifies the microRNA expression profile in endometrial and endometriotic cells from women with endometriosis," *Hum. Reprod.*, 2015.

[209] H. Wang, Y. Zhang, Q. Wu, Y. Bin Wang, and W. Wang, "MIR-16 mimics inhibit TGF-β1-induced epithelial-Tomesenchymal transition via activation of autophagy in non-small cell lung carcinoma cells," *Oncol. Rep.*, 2018.

[210] H. Wang, Y. Zhan, J. Jin, C. Zhang, and W. Li, "MicroRNA-15b promotes proliferation and invasion of non-small cell lung carcinoma cells by directly targeting TIMP2," *Oncol. Rep.*, 2017.

[211] Y. Singh, O. A. Garden, F. Lang, and B. S. Cobb, "MicroRNA-15b/16 Enhances the Induction of Regulatory T Cells by Regulating the Expression of Rictor and mTOR," *J. Immunol.*, 2015.

[212] F. Andriani *et al.*, "MiR-16 regulates the pro-tumorigenic potential of lung fibroblasts through the inhibition of HGF production in an FGFR-1- and MEK1-dependent

manner," *J. Hematol. Oncol.*, 2018.

[213] J. Long, C. Jiang, B. Liu, S. Fang, and M. Kuang, "MicroRNA-15a-5p suppresses cancer proliferation and division in human hepatocellular carcinoma by targeting BDNF," *Tumor Biol.*, 2016.

[214] W. Renjie and L. Haiqian, "MiR-132, miR-15a and miR-16 synergistically inhibit pituitary tumor cell proliferation, invasion and migration by targeting Sox5," *Cancer Lett.*, 2015.

[215] Z. Mei, T. Su, J. Ye, C. Yang, S. Zhang, and C. Xie, "The miR-15 Family Enhances the Radiosensitivity of Breast Cancer Cells by Targeting G $_2$ Checkpoints," *Radiat. Res.*, 2015.

[216] Z. Duan *et al.*, "miR-15b modulates multidrug resistance in human osteosarcoma in vitro and in vivo," *Mol. Oncol.*, 2017.

[217] P. Utaijaratrasmi *et al.*, "The microRNA-15a-PAI-2 axis in cholangiocarcinoma-associated fibroblasts promotes migration of cancer cells," *Mol. Cancer*, 2018.

[218] B. Liu *et al.*, "MiR-15a suppresses hepatocarcinoma cell migration and invasion by directly targeting cMyb," *Am. J. Transl. Res.*, 2017.

[219] L. O. Sousa *et al.*, "Lymph node or perineural invasion is associated with low miR-15a, miR-34c and miR-199b levels in head and neck squamous cell carcinoma," *BBA Clin.*, 2016.

[220] H. Zhao, A. Kalota, S. Jin, and A. M. Gewirtz, "Autoregulatory feedback loop in human hematopoietic cells the c-myb proto-oncogene and microRNA-15a comprise an active," *Blood*, 2009.

[221] L. Sun *et al.*, "MiR-200b and miR-15b regulate chemotherapy-induced epithelial-mesenchymal transition in human tongue cancer cells by targeting BMI1," *Oncogene*, 2012.

[222] S. Vimalraj, N. C. Partridge, and N. Selvamurugan, "A positive role of microRNA-15b on regulation of osteoblast differentiation," *J. Cell. Physiol.*, 2014.

[223] E. A. Ye *et al.*, "miR-15a/16 reduces retinal leukostasis through decreased pro-inflammatory signaling," *Journal of Neuroinflammation*. 2016.

[224] X. Wang *et al.*, "miR-15a/16 are upreuglated in the serum of neonatal sepsis patients and inhibit the LPS-induced inflammatory pathway," *Int. J. Clin. Exp. Med.*,

2015.

[225] X. Liang *et al.*, “MicroRNA-16 suppresses the activation of inflammatory macrophages in atherosclerosis by targeting PDCD4,” *Int. J. Mol. Med.*, 2016.

[226] N. Shanmugam, M. A. Reddy, and R. Natarajan, “Distinct roles of heterogeneous nuclear ribonuclear protein K and microRNA-16 in cyclooxygenase-2 RNA stability induced by S100b, a ligand of the receptor for advanced glycation end products,” *J. Biol. Chem.*, 2008.

[227] S. C. Kao *et al.*, “Tumor Suppressor microRNAs Contribute to the Regulation of PD-L1 Expression in Malignant Pleural Mesothelioma,” *J. Thorac. Oncol.*, 2017.

[228] H.-G. Moon, J. Yang, Y. Zheng, and Y. Jin, “miR-15a/16 Regulates Macrophage Phagocytosis after Bacterial Infection,” *J. Immunol.*, 2014.

[229] L. L. Sun, B. G. Jiang, W. T. Li, J. J. Zou, Y. Q. Shi, and Z. M. Liu, “MicroRNA-15a positively regulates insulin synthesis by inhibiting uncoupling protein-2 expression,” *Diabetes Res. Clin. Pract.*, 2011.

[230] M. Chu *et al.*, “miR-15b negatively correlates with lipid metabolism in mammary epithelial cells,” *Am. J. Physiol. Physiol.*, 2018.

[231] E. A. Ye and J. J. Steinle, “miR-15b/16 protects primary human retinal microvascular endothelial cells against hyperglycemia-induced increases in tumor necrosis factor alpha and suppressor of cytokine signaling 3,” *J. Neuroinflammation*, 2015.

[232] P. Cai, T. Yang, X. Jiang, M. Zheng, G. Xu, and J. Xia, “Role of miR-15a in intervertebral disc degeneration through targeting MAP3K9,” *Biomed. Pharmacother.*, 2017.

[233] B. Zhu, X. xia Wei, T. bao Wang, Y. cai Zhou, A. min Liu, and G. wen Zhang, “Increased miR-16 expression induced by hepatitis C virus infection promotes liver fibrosis through downregulation of hepatocyte growth factor and Smad7,” *Arch. Virol.*, 2015.

[234] J. Wang *et al.*, “miR-15b Inhibits the Progression of Glioblastoma Cells Through Targeting Insulin-like Growth Factor Receptor 1,” *Horm. Cancer*, 2017.

[235] A. Formosa *et al.*, “MicroRNAs, miR-154, miR-299-5p, miR-376a, miR-376c, miR-377, miR-381, miR-487b, miR-485-3p, miR-495 and miR-654-3p, mapped to the

14q32.31 locus, regulate proliferation, apoptosis, migration and invasion in metastatic prostate cancer cells," *Oncogene*, 2013.

[236] P. Mu, J. Zhou, X. Ma, G. Zhang, and Y. Li, "Expression, regulation and function of MicroRNAs in endometriosis," *Pharmazie*. 2016.

[237] C. Wang, Z. Yun, T. Zhao, X. Liu, and X. Ma, "MIR-495 is a Predictive Biomarker that Downregulates GFI1 Expression in Medulloblastoma," *Cell. Physiol. Biochem.*, 2015.

[238] H. Yang *et al.*, "MicroRNAs regulate methionine adenosyltransferase 1A expression in hepatocellular carcinoma," *J. Clin. Invest.*, 2013.

[239] X. Jiang *et al.*, "miR-495 is a tumor-suppressor microRNA down-regulated in MLL-rearranged leukemia," *Proc. Natl. Acad. Sci.*, 2012.

[240] H. Chu *et al.*, "MiR-495 regulates proliferation and migration in NSCLC by targeting MTA3," *Tumor Biol.*, 2014.

[241] Z. Li *et al.*, "MiR-495 and miR-551a inhibit the migration and invasion of human gastric cancer cells by directly interacting with PRL-3," *Cancer Lett.*, 2012.

[242] S. M. Chen *et al.*, "MicroRNA-495 inhibits proliferation of glioblastoma multiforme cells by downregulating cyclin-dependent kinase 6," *World J. Surg. Oncol.*, 2013.

[243] W. W. Hwang-Verslues *et al.*, "MiR-495 is upregulated by E12/E47 in breast cancer stem cells, and promotes oncogenesis and hypoxia resistance via downregulation of E-cadherin and REDD1," *Oncogene*, 2011.

[244] M. Cao *et al.*, "MicroRNA-495 induces breast cancer cell migration by targeting JAM-A," *Protein Cell*, 2014.

[245] L. Wang *et al.*, "Downregulated MIR-45 Inhibits the G1-S Phase Transition by Targeting Bmi-1 in Breast Cancer," *Med. (United States)*, 2015.

[246] S. Mishra, A. K. Srivastava, S. Suman, V. Kumar, and Y. Shukla, "Circulating miRNAs revealed as surrogate molecular signatures for the early detection of breast cancer," *Cancer Lett.*, 2015.

[247] Y. Chen, D. Luo, W. Tian, Z. Li, and X. Zhang, "Demethylation of miR-495 inhibits cell proliferation, migration and promotes apoptosis by targeting STAT-3 in breast cancer," *Oncol. Rep.*, 2017.

[248] Y. Y. Xu, J. Tian, Q. Hao, and L. R. Yin, "MicroRNA-495 downregulates FOXC1

expression to suppress cell growth and migration in endometrial cancer," *Tumor Biol.*, 2016.

[249] M. Tan *et al.*, "microRNA-495 promotes bladder cancer cell growth and invasion by targeting phosphatase and tensin homolog," *Biochem. Biophys. Res. Commun.*, 2017.

[250] Y. Lu *et al.*, "LncRNA UCA1 promotes renal cell carcinoma proliferation through epigenetically repressing p21 expression and negatively regulating miR-495," *Tumor Biol.*, 2017.

[251] W. Jiang, J. Zheng, T. Yu, and J. Wang, "Overexpression of microRNA-495 suppresses the proliferation and invasion and induces the apoptosis of osteosarcoma cells by targeting high-mobility group nucleosome-binding domain 5," *Oncol. Rep.*, 2017.

[252] J. W. Eun *et al.*, "MicroRNA-495-3p functions as a tumor suppressor by regulating multiple epigenetic modifiers in gastric carcinogenesis," *J. Pathol.*, 2018.

[253] G. Chen and Y. Xie, "MiR-495 inhibits proliferation, migration, and invasion and induces apoptosis via inhibiting PBX3 in melanoma cells," *Onco. Targets. Ther.*, 2018.

[254] Y. Ye *et al.*, "MicroRNA-495 suppresses cell proliferation and invasion of hepatocellular carcinoma by directly targeting insulin-like growth factor receptor-1," *Exp. Ther. Med.*, 2018.

[255] Z. Bai *et al.*, "The MiR-495/Annexin A3/P53 Axis Inhibits the Invasion and EMT of Colorectal Cancer Cells," *Cell. Physiol. Biochem.*, 2018.

[256] L. Yan, J. Yao, and J. Qiu, "miRNA-495 suppresses proliferation and migration of colorectal cancer cells by targeting FAM83D," *Biomed. Pharmacother.*, 2017.

[257] X. Q. Chu, J. Wang, G. X. Chen, G. Q. Zhang, D. Y. Zhang, and Y. Y. Cai, "Overexpression of microRNA-495 improves the intestinal mucosal barrier function by targeting STAT3 via inhibition of the JAK/STAT3 signaling pathway in a mouse model of ulcerative colitis," *Pathol. Res. Pract.*, 2018.

[258] S. H. Lee, Y. D. Jung, Y. S. Choi, and Y. M. Lee, "Targeting of RUNX3 by miR-130a and miR-495 cooperatively increases cell proliferation and tumor angiogenesis in gastric cancer cells," *Oncotarget*, 2015.

[259] C. Lv, Z. Bai, Z. Liu, P. Luo, and J. Zhang, “MicroRNA-495 suppresses human renal cell carcinoma malignancy by targeting SATB1,” *Am. J. Transl. Res.*, 2015.

[260] B. Zhang *et al.*, “Hsa-miR-495 acts as a tumor suppressor gene in glioma via the negative regulation of MYB,” *Mol. Med. Rep.*, 2016.

[261] H. Wang, Z. Jiang, H. Chen, X. Wu, J. Xiang, and J. Peng, “MicroRNA-495 Inhibits Gastric Cancer Cell Migration and Invasion Possibly via Targeting High Mobility Group AT-Hook 2 (HMGA2),” *Med. Sci. Monit.*, 2017.

[262] W. Li *et al.*, “MicroRNA-495 regulates starvation-induced autophagy by targeting ATG3,” *FEBS Lett.*, 2016.

[263] J. Z. Li, Z. L. Wang, W. H. Xu, Q. Li, L. Gao, and Z. M. Wang, “MicroRNA-495 Regulates Migration and Invasion in Prostate Cancer Cells Via Targeting Akt and mTOR Signaling,” *Cancer Invest.*, 2016.

[264] Y. Mao, L. Li, J. Liu, L. Wang, and Y. Zhou, “MiR-495 inhibits esophageal squamous cell carcinoma progression by targeting Akt1,” *Oncotarget*, 2016.

[265] M. Ye *et al.*, “TSPAN12 promotes chemoresistance and proliferation of SCLC under the regulation of miR-495,” *Biochem. Biophys. Res. Commun.*, 2017.

[266] T. Wei *et al.*, “miR-495 promotes the chemoresistance of SCLC through the epithelial-mesenchymal transition via Etk/BMX,” *Am. J. Cancer Res.*, 2017.

[267] Z. Zou *et al.*, “miR-495 sensitizes MDR cancer cells to the combination of doxorubicin and taxol by inhibiting MDR1 expression,” *J. Cell. Mol. Med.*, 2017.

[268] D. Adams *et al.*, “Patisiran, an RNAi Therapeutic, for Hereditary Transthyretin Amyloidosis,” *N. Engl. J. Med.*, 2018.

[269] S. Y. Wu, G. Lopez-Berestein, G. A. Calin, and A. K. Sood, “RNAi therapies: Drugging the undruggable,” *Science Translational Medicine*. 2014.

[270] Y. Nakata, T. K. Kim, S. Shetzline, and A. M. Gewirtz, “Nucleic acid modulation of gene expression: approaches for nucleic acid therapeutics against cancer.,” *Crit Rev Eukaryot Gene Expr*, 2005.

[271] J. K. W. Lam, M. Y. T. Chow, Y. Zhang, and S. W. S. Leung, “siRNA versus miRNA as therapeutics for gene silencing,” *Molecular Therapy - Nucleic Acids*. 2015.

[272] M. Ha and V. N. Kim, “Regulation of microRNA biogenesis.,” *Nat. Rev. Mol. Cell Biol.*, 2014.

[273] G. A. Calin *et al.*, “Human microRNA genes are frequently located at fragile sites and genomic regions involved in cancers,” *Proc. Natl. Acad. Sci.*, 2004.

[274] J. E. Zuckerman and M. E. Davis, “Clinical experiences with systemically administered siRNA-based therapeutics in cancer,” *Nature Reviews Drug Discovery*. 2015.

[275] A. de Fougerolles, H. P. Vornlocher, J. Maraganore, and J. Lieberman, “Interfering with disease: A progress report on siRNA-based therapeutics,” *Nat. Rev. Drug Discov.*, 2007.

[276] T. L. Yuan *et al.*, “Development of siRNA payloads to target KRAS-Mutant cancer,” *Cancer Discov.*, 2014.

[277] S. Y. Wu *et al.*, “2′-OMe-phosphorodithioate-modified siRNAs show increased loading into the RISC complex and enhanced anti-tumour activity,” *Nat. Commun.*, 2014.

[278] J. Wang, Z. Lu, M. G. Wientjes, and J. L.-S. Au, “Delivery of siRNA Therapeutics: Barriers and Carriers,” *AAPS J.*, 2010.

[279] P. Barata, A. K. Sood, and D. S. Hong, “RNA-targeted therapeutics in cancer clinical trials: Current status and future directions,” *Cancer Treatment Reviews*. 2016.

[280] K. B. Reddy, “MicroRNA (miRNA) in cancer,” *Cancer Cell International*. 2015.

[281] C. Kutter and P. Svoboda, “miRNA, siRNA, piRNA: Knowns of the unknown,” in *RNA Biology*, 2008.

[282] R. Rupaimoole and F. J. Slack, “MicroRNA therapeutics: Towards a new era for the management of cancer and other diseases,” *Nature Reviews Drug Discovery*. 2017.

[283] H. Ling, M. Fabbri, and G. A. Calin, “MicroRNAs and other non-coding RNAs as targets for anticancer drug development,” *Nature Reviews Drug Discovery*. 2013.

[284] C. Bryant, R. Rawlinson, and A. J. Massey, “Chk1 Inhibition as a novel therapeutic strategy for treating triple-negative breast and ovarian cancers,” *BMC Cancer*, 2014.

[285] C. Bryant, K. Scriven, and A. J. Massey, “Inhibition of the checkpoint kinase Chk1 induces DNA damage and cell death in human Leukemia and Lymphoma cells,”

*Mol. Cancer*, 2014.

[286] M. M. Al-Kaabi *et al.*, “Checkpoint kinase1 (CHK1) is an important biomarker in breast cancer having a role in chemotherapy response,” *Br. J. Cancer*, 2015.

[287] N. J. Curtin, “DNA repair dysregulation from cancer driver to therapeutic target,” *Nature Reviews Cancer*. 2012.

[288] V. Agarwal, G. W. Bell, J. W. Nam, and D. P. Bartel, “Predicting effective microRNA target sites in mammalian mRNAs,” *Elife*, 2015.

[289] Y. Fan, K. Siklenka, S. K. Arora, P. Ribeiro, S. Kimmins, and J. Xia, “miRNet - dissecting miRNA-target interactions and functional associations through network-based visual analysis,” *Nucleic Acids Res.*, 2016.

[290] S. Jin *et al.*, “Gadd45a contributes to p53 stabilization in response to DNA damage,” *Oncogene*, 2003.

[291] N. Sato *et al.*, “Activation of WD repeat and high-mobility group box DNA binding protein 1 in pulmonary and esophageal carcinogenesis,” *Clin. Cancer Res.*, 2010.

[292] C. L. Grek, J. M. Rhett, J. S. Bruce, G. S. Ghatnekar, and E. S. Yeh, “Connexin 43, breast cancer tumor suppressor: Missed connections?,” *Cancer Letters*. 2016.

[293] T. Shahar *et al.*, “Expression level of miRNAs on chromosome 14q32.31 region correlates with tumor aggressiveness and survival of glioblastoma patients,” *J. Neurooncol.*, 2016.

[294] C. H. Gattolliat *et al.*, “Expression of miR-487b and miR-410 encoded by 14q32.31 locus is a prognostic marker in neuroblastoma,” *Br. J. Cancer*, 2011.

[295] O. Cazzalini, A. I. Scovassi, M. Savio, L. A. Stivala, and E. Prosperi, “Multiple roles of the cell cycle inhibitor p21CDKN1Ain the DNA damage response,” *Mutation Research - Reviews in Mutation Research*. 2010.

[296] T. Akiyama, T. Ohuchi, S. Sumida, K. Matsumoto, and K. Toyoshima, “Phosphorylation of the retinoblastoma protein by cdk2 ,” *Proc. Natl. Acad. Sci.* , 1992.

[297] S. Nag, X. Zhang, K. S. Srivenugopal, M.-H. Wang, W. Wang, and R. Zhang, “Targeting MDM2-p53 Interaction for Cancer Therapy: Are We There Yet?,” *Curr. Med. Chem.*, 2014.

[298] Y. K. Oh and T. G. Park, “siRNA delivery systems for cancer treatment,” *Advanced*

*Drug Delivery Reviews*. 2009.

[299] H. J. Sun, Y. F. Jia, and X. L. Ma, “Alpha5 nicotinic acetylcholine receptor contributes to nicotine-induced lung cancer development and progression,” *Front. Pharmacol.*, 2017.

[300] J. Wade Harper, G. R. Adami, N. Wei, K. Keyomarsi, and S. J. Elledge, “The p21 Cdk-interacting protein Cip1 is a potent inhibitor of G1 cyclin-dependent kinases,” *Cell*, 1993.

[301] T. Otto and P. Sicinski, “Cell cycle proteins as promising targets in cancer therapy,” *Nature Reviews Cancer*. 2017.

[302] L. A. Antonucci, J. V. Egger, and N. A. Krucher, “Phosphorylation of the Retinoblastoma protein (RB) on serine-807 is required for association with Bax,” *Cell Cycle*, 2014.

[303] E. Volpe, M. Sambucci, L. Battistini, and G. Borsellino, “Fas-fas ligand: Checkpoint of t cell functions in multiple sclerosis,” *Frontiers in Immunology*. 2016.

[304] T. M. A. Abdel-Fatah *et al.*, “Untangling the ATR-CHEK1 network for prognostication, prediction and therapeutic target validation in breast cancer,” *Mol. Oncol.*, 2015.

[305] C. J. Norbury and B. Zhivotovsky, “DNA damage-induced apoptosis,” *Oncogene*. 2004.

[306] C. Q. X. Yeo *et al.*, “P53 Maintains Genomic Stability by Preventing Interference between Transcription and Replication,” *Cell Rep.*, 2016.

[307] A. Maréchal and L. Zou, “DNA damage sensing by the ATM and ATR kinases,” *Cold Spring Harb. Perspect. Biol.*, 2013.

[308] K. C. D. S. Oliveira *et al.*, “Role of miRNAs and their potential to be useful as diagnostic and prognostic biomarkers in gastric cancer,” *World Journal of Gastroenterology*. 2016.

[309] Y. Shinden *et al.*, “Diminished expression of MiR-15a is an independent prognostic marker for breast cancer cases,” *Anticancer Res.*, 2015.

[310] Y. Pekarsky and C. M. Croce, “Role of miR-15/16 in CLL,” *Cell Death and Differentiation*. 2015.

[311] B. Zhang, C. F. Chen, A. H. Wang, and Q. F. Lin, “MiR-16 regulates cell death in

Alzheimer's disease by targeting amyloid precursor protein," *Eur. Rev. Med. Pharmacol. Sci.*, 2015.

[312] T. Hoevel, R. Macek, O. Mundigl, K. Swisshelm, and M. Kubbies, "Expression and targeting of the tight junction protein CLDN1 in CLDN1-negative human breast tumor cells," *J. Cell. Physiol.*, 2002.

[313] F. Ma *et al.*, "A CLDN1-negative phenotype predicts poor prognosis in triple-negative breast cancer," *PLoS One*, 2014.

[314] C. L. Hsieh *et al.*, "WDHD1 modulates the post-transcriptional step of the centromeric silencing pathway," *Nucleic Acids Res.*, 2011.

[315] X. Gallego, R. J. Cox, J. R. Laughlin, J. A. Stitzel, and M. A. Ehringer, "Alternative CHRNB4 3′-UTRs Mediate the Allelic Effects of SNP rs1948 on Gene Expression," *PLoS One*, 2013.

[316] K. Kaliyappan, M. Palanisamy, R. Govindarajan, and J. Duraiyan, "Microarray and its applications," *J. Pharm. Bioallied Sci.*, 2012.

[317] W. Xue *et al.*, "Small RNA combination therapy for lung cancer," *Proc. Natl. Acad. Sci.*, 2014.

[318] X. Hu *et al.*, "The effect of Bcl-2 siRNA combined with miR-15a oligonucleotides on the growth of Raji cells," *Med. Oncol.*, 2013.

[319] X. Liu, H. Chen, and D. J. Patel, "Solution structure of actinomycin-DNA complexes: Drug intercalation at isolated G-C sites," *J. Biomol. NMR*, 1991.

[320] E. Morelli *et al.*, "Selective targeting of IRF4 by synthetic microRNA-125b-5p mimics induces anti-multiple myeloma activity in vitro and in vivo," *Leukemia*, 2015.

[321] J. N. Weinstein *et al.*, "The cancer genome atlas pan-cancer analysis project," *Nature Genetics*. 2013.

[322] E. V. Broude *et al.*, "p21 (CDKN1A) is a negative regulator of p53 stability," *Cell Cycle*, 2007.

[323] A. Karimian, Y. Ahmadi, and B. Yousefi, "Multiple functions of p21 in cell cycle, apoptosis and transcriptional regulation after DNA damage," *DNA Repair*. 2016.

[324] S. Lin and R. I. Gregory, "MicroRNA biogenesis pathways in cancer," *Nature Reviews Cancer*. 2015.

# Permissions to the Copyrighted Materials

## COPYRIGHT PERMISSIONS

***For Figure 1.1:***

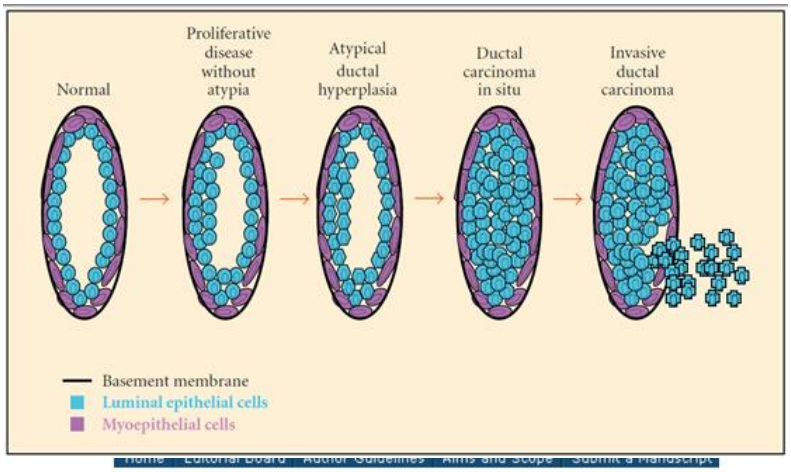




J Biomed Biotechnol. 2010; 2010: 956897.
Published online 2010 May 13. doi: [10.1155/2010/956897]
PMCID: PMC2871677
PMID: 20490282

Claudin 1 in Breast Tumorigenesis: Revelation of a Possible Novel "Claudin High" Subset of Breast Cancers

Yvonne Myal,[1, 2*] Etienne Leygue,[3] and Anne A. Blanchard[1, 2]



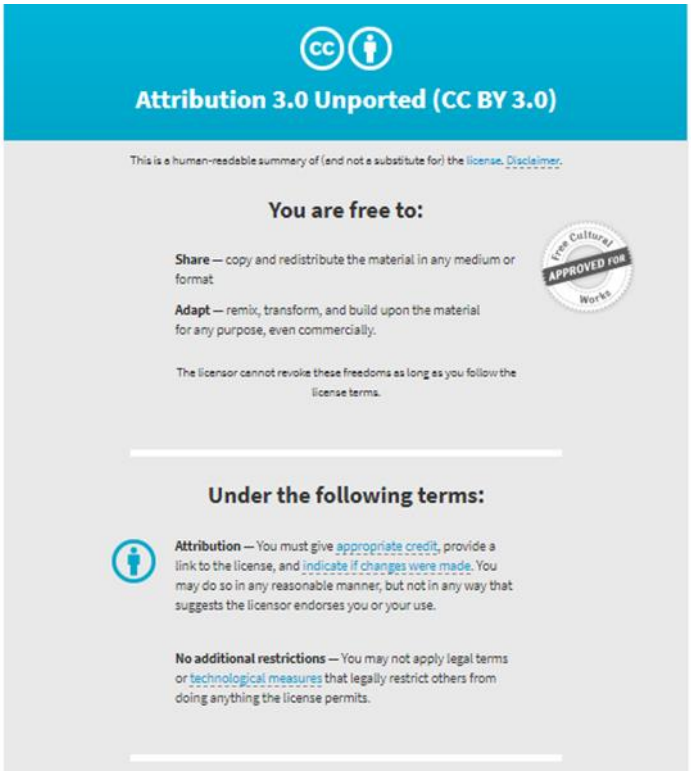

***For Figure 1.2:***

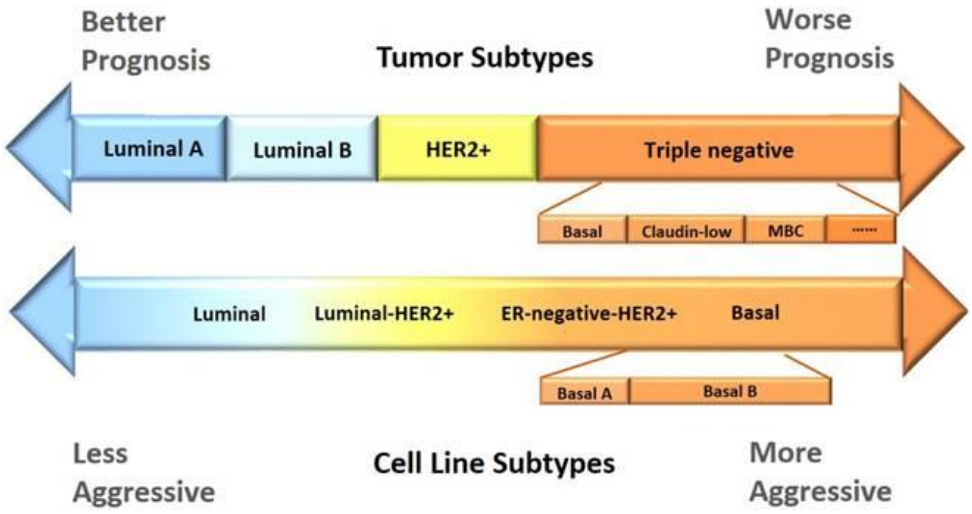


***For Figure 1.3 and 1.4:***

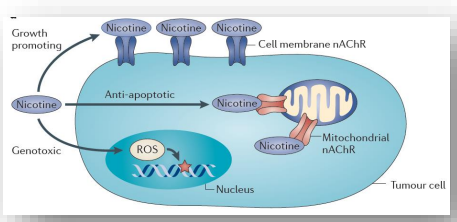


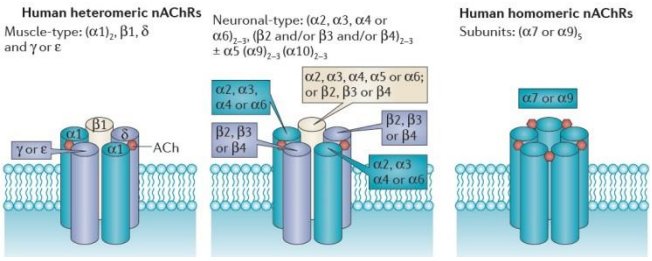


Copyright Clearance Center RightsLink®

My Orders | My Library | My Profile | Welcome sahika.cingir@bilkent.edu.tr Log out | Help

My Orders > Orders > All Orders

## License Details

This Agreement between Mrs. sahika cingir koker ("You") and Springer Nature ("Springer Nature") consists of your license details and the terms and conditions provided by Springer Nature and Copyright Clearance Center.

Print Copy

| | |
|---|---|
| License Number | 4487160216099 |
| License date | Dec 13, 2018 |
| Licensed Content Publisher | Springer Nature |
| Licensed Content Publication | Nature Reviews Cancer |
| Licensed Content Title | Connections of nicotine to cancer |
| Licensed Content Author | Sergei A. Grando |
| Licensed Content Date | May 15, 2014 |
| Licensed Content Volume | 14 |
| Licensed Content Issue | 6 |
| Type of Use | Thesis/Dissertation |
| Requestor type | non-commercial (non-profit) |
| Format | print and electronic |
| Portion | figures/tables/illustrations |
| Number of figures/tables/illustrations | 2 |
| High-res required | no |
| Will you be translating? | no |
| Circulation/distribution | <501 |
| Author of this Springer Nature content | no |
| Title | PhD student |
| Institution name | Bilkent University |
| Expected presentation date | Dec 2018 |
| Portions | Figure 1a and Figure 2a |
| Requestor Location | Mrs. sahika cingir koker<br>Bilkent university<br><br>Ankara, 06800<br>Turkey<br>Attn: Mrs. sahika cingir koker |
| Billing Type | Invoice |
| Billing address | Mrs. sahika cingir koker<br>Bilkent university<br><br>Ankara, Turkey 06800<br>Attn: Mrs. sahika cingir koker |
| Total | 0.00 USD |

***For Figure 1.5:***

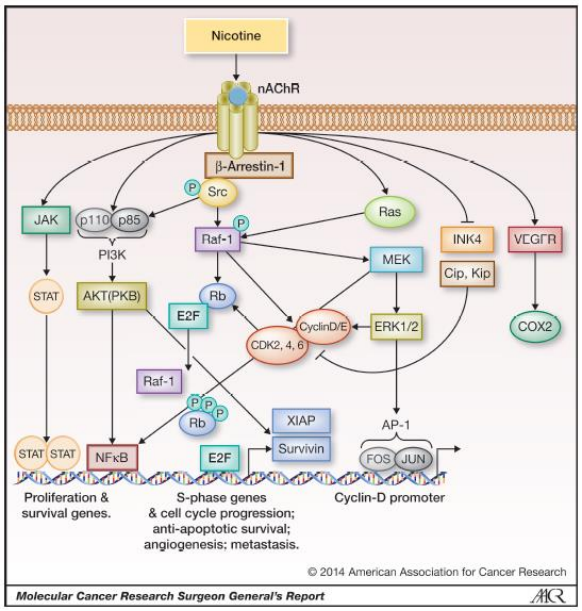


Copyright Clearance Center RightsLink®

My Orders | My Library | My Profile | Welcome sahika.cingir@bilkent.edu.tr Log out | Help

My Orders > Orders > All Orders

## License Details

This Agreement between Mrs. sahika cingir koker ("You") and American Association for Cancer Research ("American Association for Cancer Research") consists of your license details and the terms and conditions provided by American Association for Cancer Research and Copyright Clearance Center.

Print Copy

| | |
|---|---|
| License Number | 4487160885032 |
| License date | Dec 13, 2018 |
| Licensed Content Publisher | American Association for Cancer Research |
| Licensed Content Publication | Molecular Cancer Research |
| Licensed Content Title | Nicotine-Mediated Cell Proliferation and Tumor Progression in Smoking-Related Cancers |
| Licensed Content Author | Courtney Schaal,Srikumar P. Chellappan |
| Licensed Content Date | Jan 1, 2014 |
| Licensed Content Volume | 12 |
| Licensed Content Issue | 1 |
| Type of Use | Thesis/Dissertation |
| Requestor type | academic/educational |
| Format | print and electronic |
| Portion | figures/tables/illustrations |
| Number of figures/tables/illustrations | 1 |
| Will you be translating? | no |
| Circulation | 1 |
| Territory of distribution | Worldwide |
| Title of your thesis / dissertation | PhD student |
| Expected completion date | Dec 2018 |
| Estimated size (number of pages) | 1 |
| Requestor Location | Mrs. sahika cingir koker<br>Bilkent university<br><br>Ankara, 06800<br>Turkey<br>Attn: Mrs. sahika cingir koker |
| Billing Type | Invoice |
| Billing address | Mrs. sahika cingir koker<br>Bilkent university<br><br>Ankara, Turkey 06800<br>Attn: Mrs. sahika cingir koker |
| Total | 0.00 USD |

***For Figure 1.6:***

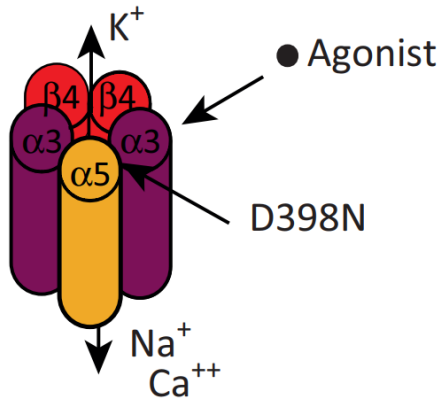

***For Figure 1.7:***

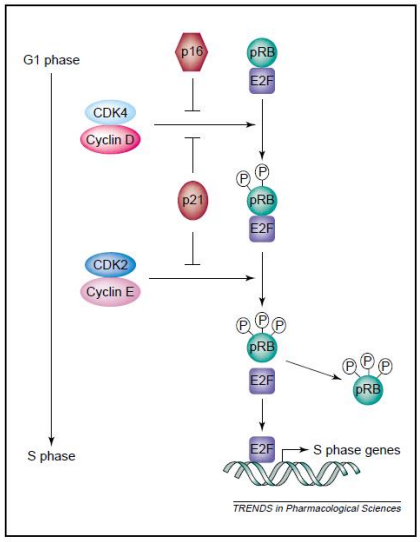


Copyright Clearance Center RightsLink®

My Orders | My Library | My Profile | Welcome sahika.cingir@bilkent.edu.tr | Log out

My Orders > Orders > All Orders

## License Details

This Agreement between Mrs. sahika cingir koker ("You") and Elsevier ("Elsevier") consists of your license details and the terms and conditions provided by Elsevier and Copyright Clearance Center.

Print Copy

| | |
|---|---|
| License Number | 4490711193284 |
| License date | Dec 16, 2018 |
| Licensed Content Publisher | Elsevier |
| Licensed Content Publication | Trends in Pharmacological Sciences |
| Licensed Content Title | Cell-cycle dysregulation and anticancer therapy |
| Licensed Content Author | Zoe A Stewart,Matthew D Westfall,Jennifer A Pietenpol |
| Licensed Content Date | Mar 1, 2003 |
| Licensed Content Volume | 24 |
| Licensed Content Issue | 3 |
| Licensed Content Pages | 7 |
| Type of Use | reuse in a thesis/dissertation |
| Portion | figures/tables/illustrations |
| Number of figures/tables/illustrations | 1 |
| Format | both print and electronic |
| Are you the author of this Elsevier article? | No |
| Will you be translating? | No |
| Original figure numbers | Figure 1 |
| Title of your thesis/dissertation | PhD student |
| Publisher of new work | Bilkent University |
| Expected completion date | Dec 2018 |
| Estimated size (number of pages) | 1 |
| Requestor Location | Mrs. sahika cingir koker<br>Bilkent university<br><br>Ankara, 06800<br>Turkey<br>Attn: Mrs. sahika cingir koker |
| Publisher Tax ID | GB 494 6272 12 |
| Total | **0.00 USD** |

***For Figure 1.8:***

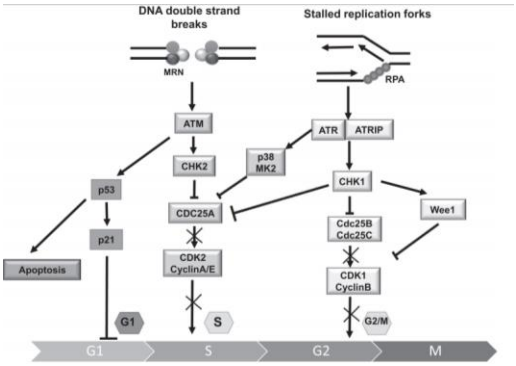


---

Copyright Clearance Center RightsLink®

My Orders | My Library | My Profile | Welcome sahika.cingir@bilkent.edu.tr Log out | H

My Orders > Orders > All Orders

## License Details

This Agreement between Mrs. sahika cingir koker ("You") and Elsevier ("Elsevier") consists of your license details and the terms and conditions provided by Elsevier and Copyright Clearance Center.

Print Copy

| | |
|---|---|
| License Number | 4490720913271 |
| License date | Dec 16, 2018 |
| Licensed Content Publisher | Elsevier |
| Licensed Content Publication | Radiotherapy and Oncology |
| Licensed Content Title | ATR/CHK1 inhibitors and cancer therapy |
| Licensed Content Author | Zhaojun Qiu,Nancy L. Oleinick,Junran Zhang |
| Licensed Content Date | Mar 1, 2018 |
| Licensed Content Volume | 126 |
| Licensed Content Issue | 3 |
| Licensed Content Pages | 15 |
| Type of Use | reuse in a thesis/dissertation |
| Portion | figures/tables/illustrations |
| Number of figures/tables/illustrations | 1 |
| Format | both print and electronic |
| Are you the author of this Elsevier article? | No |
| Will you be translating? | No |
| Original figure numbers | Figure1 |
| Title of your thesis/dissertation | PhD student |
| Publisher of new work | Bilkent University |
| Expected completion date | Dec 2018 |
| Estimated size (number of pages) | 1 |
| Requestor Location | Mrs. sahika cingir koker<br>Bilkent university<br><br>Ankara, 06800<br>Turkey<br>Attn: Mrs. sahika cingir koker |
| Publisher Tax ID | GB 494 6272 12 |
| Total | 0.00 USD |

BACK

***For Figure 1.9:***

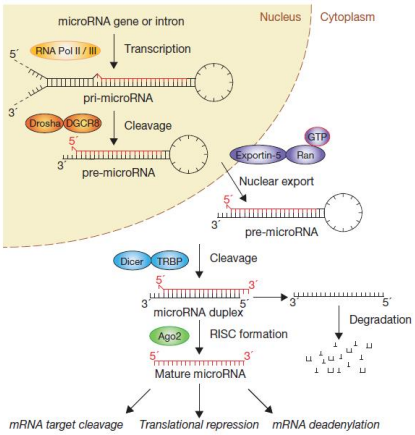




## License Details

This Agreement between Mrs. sahika cingir koker ("You") and Springer Nature ("Springer Nature") consists of your license details and the terms and conditions provided by Springer Nature and Copyright Clearance Center.

Print | Copy

| | |
|---|---|
| License Number | 4487170124632 |
| License date | Dec 13, 2018 |
| Licensed Content Publisher | Springer Nature |
| Licensed Content Publication | Nature Cell Biology |
| Licensed Content Title | Many roads to maturity: microRNA biogenesis pathways and their regulation |
| Licensed Content Author | Julia Winter, Stephanie Jung, Sarina Keller, Richard I. Gregory, Sven Diederichs |
| Licensed Content Date | Mar 1, 2009 |
| Licensed Content Volume | 11 |
| Licensed Content Issue | 3 |
| Type of Use | Thesis/Dissertation |
| Requestor type | academic/university or research institute |
| Format | print and electronic |
| Portion | figures/tables/illustrations |
| Number of figures/tables/illustrations | 1 |
| High-res required | no |
| Will you be translating? | no |
| Circulation/distribution | <501 |
| Author of this Springer Nature content | no |
| Title | PhD student |
| Institution name | Bilkent University |
| Expected presentation date | Dec 2018 |
| Portions | Figure 1 |
| Requestor Location | Mrs. sahika cingir koker<br>Bilkent university<br><br>Ankara, 06800<br>Turkey<br>Attn: Mrs. sahika cingir koker |
| Billing Type | Invoice |
| Billing address | Mrs. sahika cingir koker<br>Bilkent university<br><br>Ankara, Turkey 06800<br>Attn: Mrs. sahika cingir koker |
| Total | 0.00 USD |

All copyrights:

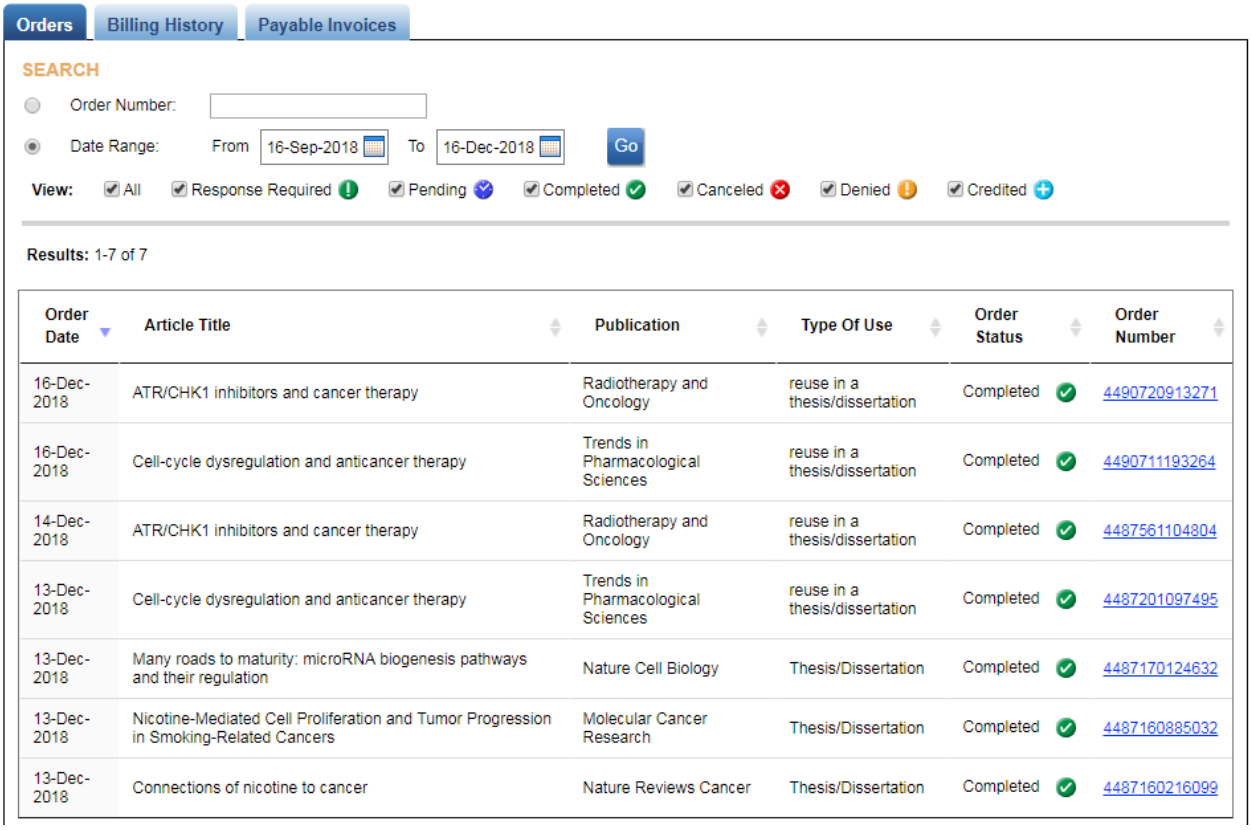

Orders | Billing History | Payable Invoices

SEARCH

Order Number:

Date Range: From 16-Sep-2018 To 16-Dec-2018 Go

View: All | Response Required | Pending | Completed | Canceled | Denied | Credited

**Results:** 1-7 of 7

| Order Date | Article Title | Publication | Type Of Use | Order Status | Order Number |
|---|---|---|---|---|---|
| 16-Dec-2018 | ATR/CHK1 inhibitors and cancer therapy | Radiotherapy and Oncology | reuse in a thesis/dissertation | Completed | 4490720913271 |
| 16-Dec-2018 | Cell-cycle dysregulation and anticancer therapy | Trends in Pharmacological Sciences | reuse in a thesis/dissertation | Completed | 4490711193264 |
| 14-Dec-2018 | ATR/CHK1 inhibitors and cancer therapy | Radiotherapy and Oncology | reuse in a thesis/dissertation | Completed | 4487561104804 |
| 13-Dec-2018 | Cell-cycle dysregulation and anticancer therapy | Trends in Pharmacological Sciences | reuse in a thesis/dissertation | Completed | 4487201097495 |
| 13-Dec-2018 | Many roads to maturity: microRNA biogenesis pathways and their regulation | Nature Cell Biology | Thesis/Dissertation | Completed | 4487170124632 |
| 13-Dec-2018 | Nicotine-Mediated Cell Proliferation and Tumor Progression in Smoking-Related Cancers | Molecular Cancer Research | Thesis/Dissertation | Completed | 4487160885032 |
| 13-Dec-2018 | Connections of nicotine to cancer | Nature Reviews Cancer | Thesis/Dissertation | Completed | 4487160216099 |